

**Investigating the effects of human cytomegalovirus infection in
the adult brain**

Hannah Beaumont

Submitted in accordance with the requirements for the degree of Doctor of
Philosophy in Medicine

The University of Leeds

October, 2022

The candidate confirms that the work submitted is her own and that appropriate credit has been given where reference has been made to the work of others.

This copy has been supplied on the understanding that it is copyright material and that no quotation from the thesis may be published without proper acknowledgement.

Acknowledgements

First and foremost, I'd like to thank Steve for the opportunity to work on such an exciting project. Thank you for your encouragement and optimism throughout this project, particularly for the support, patience and understanding during difficult health issues. Thank you for believing in me, without you I would have quit, several times over. Thank you to Heiko and his Stem Cell and Brain Tumours Research Group for their patient teaching, incredible knowledge and generosity of both time and resources. I'm extremely grateful to Matt for answering my endless questions, problem solving my failed experiments and never saying no to coffee. Thank you to Peter for always going above and beyond as my PGR tutor, it is greatly appreciated. Special thanks go to Jenny and Lynette for their encyclopaedic knowledge of how to do absolutely everything in the lab and always being patient and helpful. I'd also like to thank all the past and current members of the Griffin group from 2015 to 2022, we have celebrated wins, commiserated failures, laughed and cried, had the best nights out and collectively kept the hospital Costa Coffee in business. I know some of you will be my friends for life, especially Emma and Alex. I'd like to acknowledge every single member of the 9 am coffee club and the LIMM café lunch gang for their scientific input, emotional support, fun and laughter. You guys brightened up so many of the hard days.

Outside of the lab, I'd firstly like to thank my mum for her endless support, not letting me give up, looking after me through my illness and feeding me Michelin star worthy dinners every Friday. I honestly wouldn't have made it through without you, though I'd likely be several pounds lighter! Special thanks go to my personal chiropractor, early morning workout buddy and talented mixologist, Simon. You always know how to cheer me up (usually with viennoiseries). Thank you also to Sam, for listening to my lab problems even when you had no idea what I was talking about, reminding me to have fun and understanding when I had to spend weekends in cell culture and thesis writing. A special thank you to Dr Kaye who quite frankly changed my life. I'm eternally grateful for your amazing brain, care, empathy and compassion with a healthy dose of wicked humour. A big thank you to Johnathon for being my unpaid IT support and constant supplier of dog pictures and hilarious memes.

A few other people who deserve a big thank you for contributing significantly to my health, happiness and surviving this PhD are The Greenhalghs, The Turners, The Beaumonts, The Shaws, Linda, Raks, Lenny, Tim, Susie, and Sophie. I'm so lucky to have such wonderful people in my life!

And finally, thank you to my partner in crime, snuggle buddy and unofficial emotional support dog, Cooper.

Abstract

The relationship between human cytomegalovirus (HCMV) and glioblastoma (GBM) remains highly controversial. Consensus regarding both detection of HCMV and any potential oncogenic role within tumours has yet to be reached. Nevertheless, HCMV-directed immunotherapy can lead to GBM clearance, supporting a direct link.

Detection of HCMV in GBM is predominantly within CD133+ stem-like cells, although infectious virus is seemingly absent. Adult neural progenitor cells (NP) are a likely cell of origin for GBM, yet unlike foetal and iPSC-derived neural progenitors, the behaviour of HCMV within genuine adult NP is unknown.

Here I have shown that HCMV can infect adult NP cells *in vitro*, with virus detected up to 100 days post infection. Initial infection of adult NP's *in vitro* results in lytic gene expression without infectious virion production. However, application of an *in vitro* differentiation protocol leads to detectable secreted infectivity. HCMV infection perturbs the differentiation seen in uninfected controls with cells retaining progenitor morphology rather than developing neuronal features. Additionally, infection post-differentiation appears to de-differentiate these cells as they lose their neuronal processes and regain PCNA and Ki67 expression.

This work shows that several pathways associated with gliomagenesis are dysregulated during HCMV infection of NP including modulation of cell cycle, MAPK and PI3K-Akt, with TERT expression increased in HCMV+ NP post-differentiation compared to a non-infected control. HCMV induces a stem cell phenotype in NP, including inducing expression of GBM stem cell marker CD133 and stem cell factor KLF4. This is significant as these changes are all known to occur in GBM.

HCMV appears to unlock phenotypic plasticity as it both impairs and seemingly reverses NP differentiation, consistent with a potential direct oncogenic role during GBM pathogenesis. This may be important in understanding the role of HCMV in GBM, specifically during gliomagenesis.

Table of Contents

| | |
|--|-----------|
| Chapter 1 – Introduction | 1 |
| 1.1 Herpesviruses | 1 |
| 1.1.1 <i>Herpesviridae</i> | 1 |
| 1.1.2 Latency and reactivation of herpesviruses | 1 |
| 1.1.3 Herpes viruses in cancer..... | 5 |
| 1.2 Human Cytomegalovirus | 10 |
| 1.2.1 Prevalence and transmission | 10 |
| 1.2.2 Genome and structure | 13 |
| 1.2.3 HCMV lytic life cycle..... | 14 |
| 1.2.4 HCMV latency and reactivation | 20 |
| 1.2.5 HCMV and host immune response | 23 |
| 1.2.6 HCMV immune evasion | 23 |
| 1.2.7 HCMV therapy..... | 24 |
| 1.3 The brain | 28 |
| 1.3.1 Brain anatomy and function..... | 28 |
| 1.3.2 Brain development | 29 |
| 1.3.3 Cell types of the brain | 30 |
| 1.3.4 HCMV infection of the brain | 33 |
| 1.4 Glioblastoma | 35 |
| 1.4.1 Background and features | 35 |
| 1.4.2 Glioblastoma subtypes..... | 35 |
| 1.4.3 GBM stem cells | 36 |
| 1.4.4 GBM origins | 37 |
| 1.4.5 Signalling pathways in GBM..... | 37 |
| 1.4.6 Current GBM treatments | 40 |
| 1.5 HCMV in glioblastoma | 40 |
| 1.5.1 Detection of HCMV in GBM..... | 40 |
| 1.5.2 Potential oncogenic or oncomodulatory effects of HCMV in GBM..... | 42 |
| 1.5.3 HCMV targeted therapeutics in the treatment of GBM | 45 |
| 1.6 Project rationale | 46 |
| Chapter 2 – Materials and methods..... | 48 |
| 2.1 Tissue culture maintenance and cell lines | 48 |

| | | |
|---|--|-----------|
| 2.2 | Generation of Merlin-IE2-GFP stocks..... | 48 |
| 2.3 | Determination of virus titre..... | 49 |
| 2.3.1 | Supernatant titre by focus forming assay | 49 |
| 2.3.2 | Intracellular titre by focus forming assay | 50 |
| 2.3.3 | Infectious centre assay | 50 |
| 2.4 | Western Blotting | 50 |
| 2.5 | Immunofluorescence (IF)..... | 51 |
| 2.6 | Differentiation of neural progenitor cells | 52 |
| 2.6.1 | Serum titration..... | 52 |
| 2.6.2 | Differentiation using DMSO..... | 52 |
| 2.6.3 | Differentiation using BMP4..... | 52 |
| 2.6.4 | Differentiation using Walton <i>et al.</i> , (2006) protocol..... | 53 |
| 2.7 | RNA extraction | 53 |
| 2.7.1 | RNeasy extraction..... | 53 |
| 2.7.2 | TRizol extraction | 54 |
| 2.8 | Real-time quantitative polymerase chain reaction (RT-qPCR) | 54 |
| 2.8.1 | Generation of cDNA by reverse transcription | 54 |
| 2.8.2 | SYBR Green | 55 |
| 2.8.3 | TaqMan..... | 55 |
| 2.9 | RNA sequencing | 56 |
| 2.9.1 | Novogene RNA sequencing..... | 56 |
| Chapter 3 - Characterising HCMV infection of adult neural progenitor cells <i>in vitro</i> | | 58 |
| 3.1 | Introduction..... | 58 |
| 3.2 | Establishing HCMV culture and detection protocols..... | 60 |
| 3.3 | Characterising HCMV infection of adult neural progenitor cells..... | 61 |
| 3.3.1 | Infection of NP1 with HCMV..... | 61 |
| 3.4 | Are adult neural progenitor cells fully permissive to the complete HCMV replication cycle? | 64 |
| 3.4.1 | Production of infectious HCMV particles from NP1 cells..... | 65 |
| 3.4.2 | Is the lack of virion production in HCMV infected NP1 due to lack of assembly compartment (AC) formation?..... | 67 |
| 3.5 | Chronic infection of NP1 cells with HCMV..... | 68 |
| 3.5.1 | Isolation of individual HCMV infected cell clones | 71 |
| 3.6 | Discussion | 74 |

| | |
|---|------------|
| Chapter 4 - The effects of HCMV infection on neural progenitor cell differentiation..... | 78 |
| 4.1 Introduction..... | 78 |
| 4.2 Establishing an in vitro model of neural progenitor cell differentiation | 79 |
| 4.3 HCMV infection perturbs <i>in vitro</i> differentiation of NP1 | 84 |
| 4.3.1 HCMV infection inhibits the development of neuronal morphology and disrupts neurite outgrowth during differentiation..... | 84 |
| 4.3.2 The effect of HCMV infection on differentiation markers | 88 |
| 4.4 CD133 expression is induced within HCMV infected NP1 during differentiation | 91 |
| 4.5 Effects of differentiation on virus production..... | 94 |
| 4.5.1 HCMV gene expression during NP1 differentiation | 97 |
| 4.6 Infection of pre-differentiated NP1 | 98 |
| 4.6.1 Effects of HCMV infection post differentiation in NP1 cells . | 100 |
| 4.6.2 Does infection of differentiated NP1 with HCMV lead to productive infection? | 102 |
| 4.7 Differentiation of colony 2 | 103 |
| 4.8 Discussion | 108 |
| Chapter 5 – RNAseq analysis of the effects of HCMV on the differentiation of neural progenitor cells..... | 116 |
| 5.1 RNAseq experimental design and quality control | 116 |
| 5.2 RNAseq correlation | 118 |
| 5.3 RNAseq distribution..... | 120 |
| 5.4 RNAseq analysis of neural progenitor differentiation markers..... | 123 |
| 5.5 Enrichment analysis of differentially expressed genes | 130 |
| 5.6 RNAseq co-expression analysis..... | 139 |
| 5.7 Effects of differentiation on viral gene expression | 146 |
| 5.8 Discussion | 151 |
| Chapter 6 – Final discussion | 157 |

List of figures

- Figure 1.1 Summary of EBV latent antigens associated with B cell lymphoma development
- Figure 1.2 EBV driven B cell lymphomas and their associated EBV latency program
- Figure 1.3 Estimates of mean HCMV seroprevalence by different World Health Organisation regions
- Figure 1.4 HCMV genome structure
- Figure 1.5 HCMV virion structure
- Figure 1.6 Figure 1.6 Tegument proteins assist in delivering capsids to the host cell nucleus
- Figure 1.7 Summary of HCMV life cycle
- Figure 1.8 Adult brain anatomy
- Figure 1.9 Neural progenitor cell lineage cell types
- Figure 1.10 Summary of HCMV infection of brain
- Figure 1.11 Summary of HCMV proteins with oncogenic effects
- Figure 1.12 Graphical summary project rationale and potential origin of glioblastoma
- Figure 2.1 SYBR green melt curve protocol
- Figure 2.2 Novogene RNA sequencing method summary
- Figure 3.1 HCMV infection of human foetal foreskin fibroblast cells
- Figure 3.2.1 HCMV infection adult neural progenitor cells *in vitro*
- Figure 3.2.2 Immediate early, early and late protein expression in HCMV infection of adult neural progenitor cells *in vitro*
- Figure 3.3.1 Detection of HCMV infectivity from HCMV infected NP1
- Figure 3.3.2 Localisation of pp65 in HCMV infected HFFF2 and NP1
- Figure 3.3.3 Immunofluorescence of pp28 and gB in HCMV infected NP1 cells
- Figure 3.4 Long term HCMV infection of NP1
- Figure 3.5.1 Isolation, expansion and longitudinal tracking of a chronically HCMV infected NP1 colony

Figure 3.5.2 Immunofluorescence of colony 2 cells at 60 d.p.i stained for HCMV IE, pp52 and pp65

Figure 3.5.3 GFP expression in Colony 2 cells following freeze-thaw

Figure 4.1 Phase images of NP1 treated with BMP4

Figure 4.2 GFAP immunofluorescence of NP1 treated with BMP4

Figure 4.3 Serum starvation of NP1 cells

Figure 4.4 Summary of neural progenitor neuronal differentiation protocol

Figure 4.5 Neuronal differentiation of NP1

Figure 4.6 Comparison of GFAP and β -III-tubulin immunofluorescence in neuronal differentiation of NP1 cells

Figure 4.7 Differentiation of HCMV and mock infected NP1 showing virus driven GFP expression

Figure 4.8 F-actin staining of Mock and HCMV infected NP1

Figure 4.9 Neurite outgrowth at day 5 of differentiation in mock and HCMV infected NP1

Figure 4.10 Protein expression during neural progenitor cell differentiation in HCMV infected NP1 cells

Figure 4.11 Ki67 expression in HCMV infected NP1 during differentiation

Figure 4.12 CD133 expression in HCMV infected NP1 cells during differentiation

Figure 4.13 Supernatant titre from differentiation of HCMV infected NP1

Figure 4.14 HCMV IE and pp65 expression during differentiation of HCMV infected NP1

Figure 4.15 NP1 cells +/- HCMV at day 5 of differentiation stained for TGN46 and pp65

Figure 4.16 HCMV gene expression during differentiation of NP1

Figure 4.17 HCMV infection of differentiated NP1

Figure 4.18 Ki67 expression in NP1 infected with HCMV at day 5 of differentiation

Figure 4.19 PCNA expression in NP1 infected with HCMV post differentiation

Figure 4.20 Immunofluorescence of CD133 in NP1 infected with HCMV post-differentiation

Figure 4.21 Supernatant titre of NP1 infected with HCMV post-differentiation

Figure 4.22 HCMV pp65 immunofluorescent staining in NP1 cells differentiated and infected with HCMV post differentiation.

Figure 4.23 GFP expression during differentiation of colony 2

Figure 4.24 HCMV protein expression during differentiation of colony 2

Figure 4.25 HCMV gene expression during differentiation of colony 2

Figure 4.26 HCMV supernatant titres in differentiation of colony 2

Figure 4.27 Expression of differentiation markers GFAP and PCNA in differentiation of colony 2

Figure 4.28 CD133 protein expression during differentiation of colony 2

Figure 5.1 Experimental design for RNAseq analysis

Figure 5.2 RNA sample quality control

Figure 5.3 3D Principal component analysis (PCA)

Figure 5.4 Pearson correlation between RNA samples

Figure 5.5 Violin plot of RNAseq sample FPKM distribution

Figure 5.6 Heirarchical Clustering Heatmap of RNA-seq

Figure 5.7 Volcano plots of RNAseq data

Figure 5.8 RNAseq FPKM of differentiation markers

Figure 5.9 qPCR for differentiation markers

Figure 5.10 Neuronal marker differential gene expression

Figure 5.11 Astrocyte marker differential gene expression

Figure 5.12 KEGG enrichment analysis of differentially expressed genes between NP1_5 and NP1_0

Figure 5.13 KEGG enrichment analysis of differentially expressed genes between HCMV_0 and NP1_0

Figure 5.14 KEGG enrichment analysis of differentially expressed genes between HCMV_5 and HCMV_0

Figure 5.15 KEGG enrichment analysis of differentially expressed genes between HCMV_5 and NP1_5

Figure 5.16 Differentially expressed calcium signalling genes in HCMV_0 v NP1_0

Figure 5.17 Differentially expressed PI3K-Akt genes between HCMV_0 v NP1_0

Figure 5.18 Differentially expressed axon guidance genes between HCMV_0 v NP1_0 and HCMV_5 v NP1_5

Figure 5.19 Venn diagram of RNAseq co-expression data

Figure 5.20 KEGG enrichment analysis of genes exclusive to NP1_0, NP1_5, HCMV_0 and HCMV_5

Figure 5.21 KEGG enrichment analysis of genes exclusively co-expressed in HCMV_0 and HCMV_5 and genes exclusively co-expressed in NP1_0 and NP1_5

Figure 5.22 Expression of MAPK signalling pathway genes identified as expressed in HCMV_0 and HCMV_5, but not in NP1_0 or NP1_5

Figure 5.23 Expression of genes associated with signalling pathways regulating pluripotency of stem cells, co-expressed in HCMV_0 and HCMV_5, but not in NP1_0 or NP1_5

Figure 5.24 Expression of differentially expressed genes associated with signalling pathways regulating pluripotency of stem cells.

Figure 5.25 Differential expression of TERT

Figure 5.26 Average FPKM of all HCMV genes in HCMV_0

Figure 5.27 Average FPKM of all HCMV genes in HCMV_5

Figure 5.28 Differentially expressed HCMV genes during differentiation of HCMV infected NP1

Abbreviations

- AC - Assembly compartment
- ADU - Arbitrary densitometry units
- AIDS - Acquired immunodeficiency syndrome
- Akt - Protein kinase B
- ANS - Autonomic nervous system
- APC - Antigen-presenting cell
- ATF5 - Activating transcription factor 5
- ATP - Adenosine triphosphate
- BCA - Bicinchoninic acid
- BCL-2 - B-cell lymphoma 2
- BET - Bromodomain and extraterminal
- BMP4 - Bone morphogenetic protein 4
- BSA - Bovine serum albumin
- BST - Bone marrow stromal antigen
- CACNB1 - calcium voltage-gated channel auxiliary subunit beta 1
- cAMP - Cyclic adenosine monophosphate
- CDK - Cyclin-dependent kinase
- cDNA - Complementary DNA
- CDV – Cidofovir
- cHL - Classical Hodgkin's lymphoma
- CNS - Central nervous system
- COX-2 - Cyclooxygenase 2
- CPE - Cytopathic effect
- CREB - Cyclic adenosine monophosphate response element-binding protein
- CSC - Cancer stem cell
- CTL - Cytotoxic T lymphocytes
- CT - Cycle threshold
- DC - Dendritic cell

DLBCL - Diffuse large B-cell lymphoma
DMEM - Dulbecco's modified eagle's medium
DMSO - dimethyl sulfoxide
DNA - Deoxyribonucleic acid
eBL - Endemic Burkitt's lymphoma
EBNA - Epstein-Barr nuclear antigen
EBV - Epstein-Barr virus
ECL - Enhanced chemiluminescence reagent
EDTA - Ethylenediaminetetraacetic acid
EGF - Epidermal growth factor
eGFP - Enhanced green fluorescent protein
EGFR - Epidermal growth factor receptor
ER - Endoplasmic reticulum
ERK - Extracellular signal-regulated kinases
ESC - Embryonic stem cell
FACT - Facilitates chromatin transcription
FBS - Foetal bovine serum
FDR - False discovery rate
FFU - Focus forming unit
FGF - Fibroblast growth factor
FLICE - Fas-associated death domain-like interleukin-1 β -converting enzyme
FPKM - Fragments per kilobase of exon per million mapped fragments
GABA - gamma-aminobutyric acid
GABRA1 - Gamma-Aminobutyric Acid Type A Receptor Subunit Alpha1
GAPDH - Glyceraldehyde 3-phosphate dehydrogenase
gB - Glycoprotein B
GBM - Glioblastoma
GCV - Ganciclovir
GPCR - G protein-coupled receptor
GSC - Glioblastoma stem cell

GFAP - Glial fibrillary acidic protein
GFP - Green fluorescent protein
GLUL - glutamate-ammonia ligase
GO - Gene ontology
GPM6A - Glycoprotein M6A
HAART - Highly active antiretroviral therapy
HCMV - Human cytomegalovirus
HDACi - Histone deacetylase inhibitor
HFFF - Human foetal foreskin fibroblast
HHV-6A - Human herpesvirus 6A
HHV-6B - Human herpesvirus 6B
HHV-7 - Human herpesvirus 7
HIF1 α - Hypoxia-inducible factor 1 α
HMEC - Human mammary epithelial cells
HPV - Human papilloma virus
HSV - Herpes simplex virus
I-BET - Inhibitors of bromodomain and extraterminal
IBMX - 3-isobutyl-1-methylxanthine
IDH1 - Isocitrate dehydrogenase
IE - Immediate early
IF - Immunofluorescence
IFN – Interferon
IHC - Immunohistochemistry
IL - Interleukin
IP - Intermediate progenitor
iPSC - Induced pluripotent stem cell
IQGAP1 - IQ Motif Containing GTPase Activating Protein 1
IRES - Internal ribosome entry site
IRL - Internal repeat long
IRS - Internal repeat short

ISH - In situ hybridisation

JAK - Janus kinase

JARID2 - Jumonji And AT-Rich Interaction Domain Containing 2

JNK - c-Jun N-terminal kinases pathway

KAP1 - Krüppel-associated box-associated protein 1

KEGG - Kyoto Encyclopaedia of Genes and Genomes

KLF4 - Krüppel-Like Factor 4

KSHV - Kaposi's sarcoma-associated herpes virus

LANA - Latency-associated nuclear antigen

LANA-1 - latency-associated nuclear antigen 1

LAT - Latency associated transcripts

LL- Latency locus

LMP - Latent membrane protein

LMP2A - Latent membrane protein 2A

LUNA - Latency unique natural antigen

MAP2 - Microtubule associated protein 2

MAPK - Mitogen-activated protein kinase

MCD - Multicentric Castleman disease

MCP - Major capsid protein

MCMV - Murine cytomegalovirus

MIEP - Major immediate early promoter

MHC - Major histocompatibility complex

MOI - Multiplicity of infection

MRP-1 - Multidrug resistance-associated protein 1

mTOR - Mammalian target of rapamycin

mTORC - Mammalian target of rapamycin complex

MYC - Cellular myelocytomatosis oncogene

ND10 - Nuclear domain 10

NEC - Nuclear egress complex

NES - Nestin

NF1 - Neurofibromatosis type 1
NFACT1 - Nuclear factor of activated T cells 1
NF κB - Nuclear factor kappa-light-chain-enhancer of activated B cells
NGF - Nerve growth factor
NGFR - Nerve growth factor receptor
NIEP - Non-infectious enveloped particles
NK - Natural killer cell
NOS - Not otherwise specified
NP - Neural progenitor
Nrp2 - Neuropilin-2
NSC - Neural stem cell
OCT4 - Octamer-binding transcription factor 4
OLIG2 - Oligodendrocyte transcription factor 2
OPC - Oligodendrocyte progenitor cells
ORF – Open reading frame
oriLyt – Lytic origins of replication
PAL - Pyothorax-associated lymphoma
PBS - Phosphate buffered saline
PCA - Principal component analysis
PCNA - Proliferating cell nuclear antigen
PCR - Polymerase chain reaction
PDGF - Platelet-derived growth factor
PDGFR α - Platelet derived growth factor alpha
PDL1 - Programmed death-ligand 1
PE - Pseudomonas exotoxin
PEL - Primary effusion lymphoma
PFA - Paraformaldehyde
PGCC - Polyploid giant cancer cell
PKC - Protein Kinase C
PKM2 - Pyruvate kinase M2

PI3K - phosphatidylinositide 3'-OH kinase
PRR - Pattern recognition receptors
PTEN - Phosphatase and tensin homolog
RAF - Rapidly accelerated fibrosarcoma
RAS - Rat sarcoma
RBFOX3 - RNA Binding Fox-1 Homolog 3
RG - Radial glia
RIPA - Radioimmunoprecipitation assay
RNA - Ribonucleic acid
RPKM - Reads per kilobase of exon model per million mapped read
RTA - Replication and transcription activator
S100B - S100 calcium binding protein B
sBL - Sporadic Burkitt's lymphoma
SCP - Smallest capsid protein
SDS-PAGE - Sodium dodecyl sulphate – poly acrylamide gel electrophoresis
SGK - Serum/glucocorticoid regulated kinase
SGZ - Subgranular zone
SHH - Sonic hedgehog
SLC12A5 - Solute carrier family 12 member 5
SLC1A2 - Solute Carrier Family 1 Member 2
SLC1A3 - Solute Carrier Family 1 Member 3
SOX2 - Sex determining region Y box 2
SREBP1c - Sterol regulatory binding element protein 1C
STAT - Signal transducer and activator of transcription
STING - Stimulator of interferon genes
SVZ - Subventricular zone
SYP - Synaptophysin
SYT1 - Synaptotagmin 1
TAM - Tumour associated macrophages
TAZ - Transcriptional coactivator with PDZ-binding motif

TBS-T - Tris-buffered saline with 0.1 % (v/v) Tween 20

TERT - Telomerase reverse transcriptase

TGN - *Trans*-Golgi network

TLR - Toll like receptor

TNF - Tumour necrosis factor

TPA - 12-O-tetradecanoylphorbol-13-acetate

Tri1 - Triplex monomer

Tri2 - Triplex dimer

TRL - Terminal repeat long

TRS - Terminal repeat short

TTF - Tumour treating fields

TUBB3 - β -III-tubulin

UL - Unique long

US - Unique short

VEGF - Vascular endothelial growth factor

vFLIP - Viral Fas-associated death domain-like interleukin-1 β -converting enzyme inhibitory protein

VGCV - Valganciclovir

VZ - Ventricular zone

VZV - Varicella-zoster virus

WB - Western blot

Chapter 1 – Introduction

1.1 Herpesviruses

1.1.1 *Herpesviridae*

The *Herpesviridae* are a family of DNA viruses that infect and often cause disease in an array of hosts, including humans and are species specific. Of over 100 known herpes viruses, nine primarily infect humans, leading to persistence for the lifetime of the host in a state known as latency during which the viral genome is maintained in cells, but viral gene expression is restricted and infectious particle production halts. However, particle production can be reactivated under specific conditions as further explained in section 1.2.4 (Whitley, 1996, Ding, 2008).

The herpes viruses specific to humans are; herpes simplex virus 1 and 2 (HSV-1 and HSV-2), varicella-zoster virus (VZV), Epstein-Barr virus (EBV), human herpes virus 6A and B (HHV-6A and HHV-6B), human herpesvirus 7 (HHV-7), Kaposi's sarcoma herpes virus (KSHV/HHV-8) and human cytomegalovirus (HCMV). Herpes viruses can be categorised into three main groups; α herpesviruses, β herpesviruses and γ herpesviruses. The α herpesviruses include HSV-1, HSV-2 and VZV, which are primarily distinguished from the other groups by their comparatively short replication cycles of several hours in culture, rapid destruction of host cells and the broad range of host cell types that are permissive to replication. HCMV, HHV-6 and HHV-7, belong to the β herpesvirus group. In contrast to the α herpesviruses, β herpesviruses have long replicative cycles over a number of days as opposed to hours. They have a restricted host range and characteristically cause cytomegaly, which is exemplified in HCMV infection. EBV and KSHV are γ herpesviruses, which have a more limited host cell range including B cells and epithelial cells, or epithelial cells, endothelial cells, B cells and monocytes, respectively (Sathiyamoorthy *et al.*, 2016, Chakraborty *et al.*, 2012).

1.1.2 Latency and reactivation of herpesviruses

Establishment of latency with the ability to reactivate is a hallmark of herpesviruses and results in lifelong infection of the host. Three widely accepted principles distinguish latency from both persistent and abortive infection (Weidner-Glunde *et al.*, 2020). Firstly, during latency the entire viral genome persists. In herpesvirus infection this is via multiple circularised episomes maintained in host cell nuclei, except HHV-6, which integrates its genome into

the telomeres of host cell chromosomes (Arbuckle *et al.*, 2010). Secondly, viral gene expression is limited and particle production ceases. Thirdly, the lytic cycle and particle production can be restored through a process known as reactivation. Whilst some aspects of latency are common to all herpesviruses, the mechanisms governing latency and reactivation vary between each virus. Several herpesviruses such as HCMV, KSHV, and EBV establish latency in dividing cells such as haematopoietic progenitor cells and thus tether their circular episomes to the host cell genome, ensuring the episomes are maintained in the daughter cells post-division (De Leo *et al.*, 2019). The γ -herpesviruses encode origin binding proteins (OBPs) which tether the episomes through interacting with specific viral DNA sequences whilst simultaneously binding host cell chromatin binding proteins (Edwards *et al.*, 1998). A similar mechanism has been shown to exist in the prototypic β -herpesvirus HCMV, though the specifics of this remain poorly understood (Mauch-Mücke *et al.*, 2020). Conversely, α -herpesviruses establish latency in terminally differentiated, non-dividing neuronal cells and so tethering to the genome is not required for maintenance of latency. Many human herpesviruses express a set of non-coding RNAs that play a role in the establishment of latency, for example α -herpesviruses express anti-sense transcripts of lytic specific RNAs that contribute to the establishment of latency (Cohen, 2020). Both γ and β -herpesviruses also express several non-coding RNA's involved in establishing latency.

The most comprehensively understood latency mechanisms are those of the γ -herpesviruses. EBV infects naïve B cells and establishes latency during differentiation of these cells to memory B lymphocytes (Hatton *et al.*, 2014). EBV has several distinct latency programs that have been shown to be specific to the different stages of B cell differentiation. Each of these is characterised by the expression of a specific viral transcriptional program. EBV induced tumours have also been shown to have specific latency gene expression programs specific to the tumour type. Epstein–Barr nuclear antigen 1 (EBNA1) tethers the episome and recruits host cell replication machinery to the viral genome, whilst other EBNA proteins are responsible for regulating expression of latency transcripts and proteins (Frappier, 2012). EBV also expresses up to three latent membrane proteins (LMP) during latency, including LMP-1, which belongs to the tumour necrosis factor (TNF) family of proteins and binds NF- κ B, increasing NF- κ B signalling, and LMP-2a which increases survival signalling in B cells through interaction with B cell receptors (BCR) (Jean-Pierre *et al.*, 2021, Weidner-Glunde *et al.*, 2020).

KSHV can establish latency in a broader array of cell types including B cells, spindle cells and vascular endothelial cells (Chakraborty *et al.*, 2012). KSHV has

its own distinct latency associated gene expression profile, however unlike EBV is not believed to have multiple latency programs. KSHV latency proteins are expressed from four open reading frames (ORF). ORF73, encodes latency-associated nuclear antigen (LANA) and is required to tether the viral episome and ensure latent replication (Sun *et al.*, 2014). LANA contributes to latency establishment and maintenance through several mechanisms, mainly by hijacking host epigenetic machinery, including recruiting host cell DNA methyltransferases to methylate and so silence large regions of the viral genome (Shamay *et al.*, 2006). LANA also binds another transcriptional repressor, Krüppel-associated box-associated protein 1 (KAP1) which inhibits lytic gene transcription (Sun *et al.*, 2014). ORF72 encodes a KSHV viral cyclin (vCyclin), which is a homologue of the cellular cyclin D2 (Chang *et al.*, 1996). A viral Fas-associated death domain-like interleukin-1 β -converting enzyme (FLICE) inhibitory protein (vFLIP) is transcribed from ORF71 (Ballon *et al.*, 2011). This is a homologue of human cFLIP. Both promote cellular survival through inhibition of caspase 8 and induction of NF- κ B signalling. Finally, ORF K12 encodes kaposins A, B and C (Sadler *et al.*, 1999). Kaposin A has been shown to induce cellular transformation through interaction with guanine nucleotide exchange factor cytohesin-1, which activates multiple signalling pathways (Yan *et al.*, 2019). Kaposin B increases the levels of multiple cytokines by preventing specific mRNA degradation and also regulates microRNA's known to interact with c-Myc.

Latency of α -herpesviruses is established in sensory nerve ganglia. All α -herpesviruses encode latency associated transcripts (LATs), in HSV these originate from the ICP0 region of the viral genome and the other α -herpesviruses express LATs from their ICP0 homologue regions (Depledge *et al.*, 2018). LATs include short non-coding RNAs and long non-coding RNAs which contribute to latency establishment through repressing lytic gene expression (Kwiatkowski *et al.*, 2009). Additionally, LATs have been shown to inhibit apoptosis of host cells (Ahmed *et al.*, 2002). During HSV latency, the chromatin associated with the viral genome becomes progressively repressed, but despite this repressive state, a very low level of lytic gene expression is maintained throughout (Sawtell and Thompson, 2021).

Reactivation from latency is exhibited by all herpesviruses and can be triggered by a variety of physiological and environmental stimuli. For instance, γ -herpesviruses can be triggered to reactivate through infection with other herpesviruses and other pathogens (Grinde, 2013). EBV is known to be periodically reactivated when latently infected B cells differentiate into plasma cells, infecting nearby resting B cells and once again establishing latency in a perpetual cycle of latency and reactivation (Hatton *et al.*, 2014). EBV is also

known to be reactivated through B cell receptor activation during co-infection of the host with other pathogens and can also be reactivated through toll like receptor (TLR) activation (Murata *et al.*, 2013). EBV reactivation is mediated by two immediate early (IE) proteins, known as Rta and Zta, which together lead to re-induction of the full lytic cascade of EBV gene expression (Li *et al.*, 2016). Rta and Zta can activate both their own and each other's promoters, leading to amplification of their effects on lytic gene transcription. The induction of Rta and Zta can occur through interaction with several host cell pathways including protein kinase C (PKC), phosphatidylinositide 3'-OH kinase (PI3K) and mitogen-activated protein kinase (MAPK).

KSHV reactivation is dependent on the expression of replication and transcription activator (RTA), which is the master switch for initiating lytic gene expression in latent infection. RTA is a transactivator of over 30 lytic genes and outcompetes LANA to bind its major cofactor, recombination signal binding protein for immunoglobulin kappa J (RBP- κ) (Guito and Lukac, 2015). The suppression of LANA's transcriptional repressive effects contributes to reactivation, along with transactivated RTA's ability to induce continually increasing levels of lytic gene expression through a feed forward loop (Broussard and Damania, 2020). KSHV is also known to be reactivated through host pro-inflammatory cytokines released in response to other infections, which stimulate RTA activation (Chang *et al.*, 2000). Additionally, hypoxia is known to reactivate latent KSHV through RTA activation and a similar response is seen in EBV (Davis *et al.*, 2001, Jiang *et al.*, 2006). Several chemical stimuli can reactivate latent herpesviruses in cell culture models. For example, histone deacetylase inhibitors (HDAC) such as sodium butyrate can be used to reactivate HCMV, KSHV and EBV and reactivate lytic expression through reduction of histone deacetylation. Phorbol ester 12-O-tetradecanoylphorbol-13-acetate (TPA) reactivates KSHV and EBV through its ability to activate a broad range of host cell signalling pathways, which in turn stimulate viral reactivation (Gao *et al.*, 2001).

Reactivation of β -herpesviruses is mediated by immune response, cytokine stimulation and host cell differentiation. These mechanisms are exemplified by HCMV and discussed further in section 1.2.4. HCMV, HHV-6 and HHV-7 can also be reactivated in cell culture through treatment with TPA (Prasad *et al.*, 2013). Clinical reactivation of the α -herpesvirus HSV can occur in response to several stimuli and can occur repeatedly for some of those infected. Sunlight, UV and local injury can all contribute to clinical HSV reactivation and the emergence of cold sores (Wilson *et al.*, 2012). In neuronal cell culture models of latency, withdrawal of neuronal growth factor (NGF), dexamethasone and cyclic

adenosine monophosphate (cAMP) can also lead to reactivation of HSV (Camerena *et al.*, 2010, Suzich and Cliffe, 2018). In these models, reactivation begins with a “relaxing” of chromatin structure, followed by transcription of lytic genes. VZV tends to clinically reactivate far less frequently than HSV and can be stimulated through immunosuppression, UV radiation and emotional stress (Lasserre *et al.*, 2012). Similarly to VZV, lytic gene expression can be restored through disruption of NGF signalling (Cohrs and Gildea, 2003).

1.1.3 Herpes viruses in cancer

Currently two herpesviruses are recognised as being directly oncogenic in humans, namely, EBV and KSHV. Several other herpesviruses have been shown to have potential oncogenic effects, but there is currently no consensus on whether these viruses are truly oncogenic. Herpesviruses associated with cancer proposed to have potentially oncogenic effects include HCMV, VZV, HHV-6, HHV-7, HSV-1 and HSV-2 (Cobbs *et al.*, 2002, Eliassen *et al.*, 2016, Alibek *et al.*, 2014).

EBV was the first human tumour virus to be discovered and is associated with a several cancers, including malignant lymphoma, nasopharyngeal carcinoma and gastric cancer (Epstein *et al.*, 1964, Teow *et al.*, 2017, Chen *et al.*, 2015). In the immunocompetent host, EBV establishes latency in naïve memory B cells in a non-pathogenic state, however if the host becomes immunocompromised, latent EBV infection can trigger oncogenesis in both epithelial and lymphoid cell types. EBV driven oncogenesis of the immunocompromised host is exemplified in the development of several types of B cell lymphoma in immunosuppressed transplant recipients and those infected with HIV. The type of lymphoma that develops is highly dependent on the latent transcriptional programme employed by EBV and, as discussed in section 1.1.2, the latency programme is determined by the stage of B cell differentiation/activation. The oncogenic effects of EBV can be recapitulated *in vitro*, where EBV infection can directly transform and immortalise human B lymphocytes, which cause lymphoma when grafted into immunodeficient mice (Dai *et al.*, 2012, Zhang *et al.*, 2016). The pathogenesis of EBV driven cancers is complex and varied, with an intricate interplay between the host immune landscape, viral gene expression and virus-induced cellular genetic changes contributing to oncogenesis. Just five EBV latency antigens are required for the efficient transformation of B cells, namely EBNA2, EBNA1, EBNA3A, EBNA3B, and EBNA3C, however several other viral antigens and RNAs can contribute to oncogenesis (Summarised in figure 1.1) (Saha and Robertson, 2019). EBNA2 is a key viral transcription factor expressed immediately upon B

cell infection and throughout latency. Expression of EBNA2 contributes to oncogenesis by transcriptionally activating over 300 cellular genes, notably including proto-oncogene myelocytomatosis oncogene (MYC). Similarly to EBNA2, Epstein-Barr virus nuclear antigen leader protein (EBNALP), another EBV transcription factor, is also expressed immediately upon infection and throughout latency. EBNALP is a key co-activator of EBNA-2s transcriptional activity, which crucially enhances MYC expression (Portal *et al.*, 2013). The EBNA3 family are also viral transcription factors that are known to regulate host cell transcription and B cell proliferation, particularly in the immunosuppressed (Bhattacharjee *et al.*, 2016). EBNA3A and EBNA3C have been shown to interact with an array of host cell proteins, notably including RBP-Jk, a key downstream regulator of notch signalling which is essential for growth. All EBNA3 proteins are powerful transcriptional repressors, with EBNA3A repressing genes essential for B cell differentiation and epigenetically repressing proapoptotic BIM, senescence inducing p14, p15, p16, and a key regulator of B cell differentiation, p18 (Saha and Robertson, 2019). EBNA3C directly binds tumour suppressor p53 and is thought to inhibit its transactivation, transcriptional activities which subsequently inhibits apoptosis (Yi *et al.*, 2009).

EBV is known to activate oncogenes including B-cell lymphoma 2 (BCL-2) and cellular MYC, as well as modulating cell cycle progression including promoting G1/S phase transition and inhibiting apoptosis (summarised in figure 1.2)(Yin *et al.*, 2018, Dheekollu *et al.*, 2017). Several signalling pathways have been linked with EBV induced cell cycle modulation and oncogenesis including activation of Janus kinase/signal transducer and activator of transcription (JAK/STAT) and PI3K- protein kinase B (PI3K-Akt), all of which can be activated through direct interaction with LMP1 (Vaysberg *et al.*, 2010, Chen 2012). EBV tegument protein BGLF2 is also known to contribute to cell cycle dysregulation and G1/S arrest through inducing p21 (Palladino *et al.*, 2014).

| EBV latent protein | Function related to B-cell lymphomagenesis |
|--------------------|---|
| EBNA1 | Regulates viral DNA replication and transcription of a number of viral and cellular genes; facilitates p53 degradation and thereby promotes overall oncogenesis |
| EBNA2 | One of the key viral transcription factors; in association with EBNA1P, EBNA2 regulates transcription of several viral and cellular gene expression levels; essential for B-cell transformation |
| EBNA1P | Transcriptional coactivator of EBNA2-mediated transcription of both viral and cellular genes; bypasses cell innate immune response; essential for B-cell transformation |
| EBNA3A | Along with EBNA3C, represses BIM and p14, p15, p16, and p18 gene transcription through epigenetic regulation; inhibits B-cell-to-plasma cell differentiation; essential for B-cell transformation |
| EBNA3B | Virus-encoded tumour suppressor protein |
| EBNA3C | Along with EBNA3A, represses BIM and p14, p15, p16, and p18 gene transcription through epigenetic regulation; facilitates G ₁ -S and G ₂ -M transitions of cell cycle; hijacks ubiquitin-proteasome pathway; inhibits p53-, E3F1-, and Bim-mediated apoptosis; activates autophagy; essential for B-cell transformation |
| LMP1 | Functionally mimics CD40 signaling pathway; one of the major transcriptional regulators; constitutively activates NF- κ B, JAK/STAT, ERK MAPK, IRF, and Wnt signaling pathways; stimulates bcl-2 and a20 expression to block apoptosis; essential for B-cell transformation |
| LMP2A | Functionally mimics BCR signaling pathway; blocks apoptosis; EBV latency regulation |
| LMP2B | Regulates LMP2A functions |
| EBERs | Most abundant noncoding viral RNAs present in all form of latency programs; affects innate immune response and gene expression; blocks PKR-dependent apoptosis |
| miRNAs | Transcribed from BART and BHRF1 loci; maintains latently infected B cells through blocking cellular apoptosis |

Figure 1.1 Summary of EBV latent antigens associated with B cell lymphoma development

Table of latently expressed EBV antigens that have been shown to be associated with development of B cell lymphomas and their function in relation to oncogenesis (Table adapted from Saha and Robertson, 2019).

| Genes in latent expression | Latency program | |
|---|--|---------------|
| Posttransplant B-lymphoproliferative disorder | EBNA1, EBNA2, EBNA3A, EBNA3B, EBNA3C, EBNALP, LMP1, LMP2A, LMP2B, EBER1, EBER2, and BHRF1 and BART miRNAs | III |
| HIV-linked B-lymphoproliferative disorder | EBNA1, EBNA2, EBNA3A, EBNA3B, EBNA3C, EBNALP, LMP1, LMP2A, LMP2B, EBER1, EBER2, and BHRF1 and BART miRNAs | III |
| Primary central nervous system lymphoma | EBNA1, EBNA2, EBNA3A, EBNA3B, EBNA3C, EBNALP, LMP1, LMP2A, LMP2B, EBER1, EBER2, and BHRF1 and BART miRNAs | III |
| eBL | EBNA1, EBER1, EBER2, and BART miRNAs | I |
| sBL | EBNA1, EBER1, EBER2, and BART miRNAs | I |
| HIV-linked Burkitt's lymphoma | EBNA1, EBER1, EBER2, and BART miRNAs | I |
| cHL | EBNA1, LMP1, LMP2A, EBER1, EBER2, and BART miRNAs | II |
| HIV-linked Hodgkin's lymphoma | EBNA1, LMP1, LMP2A, EBER1, EBER2, and BART miRNAs | II |
| DLBCL, NOS | EBNA1, LMP1, LMP2A, EBER1, EBER2, and BART miRNAs or all transcripts | II or III |
| DLBCL, PAL | EBNA1, EBNA2, EBNA3A, EBNA3B, EBNA3C, EBNALP, LMP1, LMP2A, LMP2B, EBER1, EBER2, and BHRF1 and BART miRNAs | III |
| DLBCL, HIV linked | EBNA1, EBER1, EBER2, and BART miRNAs or EBNA1, LMP1, LMP2A, EBER1, EBER2, and BART miRNAs or all transcripts | I, II, or III |
| PEL | EBNA1, EBER1, EBER2, and BART miRNAs | I |
| Plasmablastic lymphoma | EBNA1, EBER1, EBER2, and BART miRNAs | I |

Figure 1.2 EBV driven B cell lymphomas and their associated EBV latency program

Summary of EBV driven B cell lymphomas and their associated latency gene expression program. eBL, endemic Burkitt's lymphoma; sBL, sporadic Burkitt's lymphoma; cHL, classical Hodgkin's lymphoma (cHL); DLBCL, diffuse large B-cell lymphoma; NOS, not otherwise specified; PAL, pyothorax-associated lymphoma; PEL, primary effusion lymphoma (table adapted from Saha and Robertson, 2019).

KSHV is the aetiological agent of Kaposi's sarcoma (KS), an angioproliferative neoplasm, originating in endothelial cells, with lesions usually found in the skin and visceral organs (Cesarman *et al.*, 2019). Incidence of KSHV is increased in immunosuppressed transplant recipients (iatrogenic KS), and in individuals with human immunodeficiency virus (HIV) viraemia, particularly with worsening acquired immunodeficiency syndrome (AIDS) (Chang *et al.*, 1994). Treatment

with antiretroviral therapies that reduce HIV viraemia dramatically reduce KS incidence via restoration of CD4+ cells (Portsmouth *et al.*, 2003). Additionally, treatment using highly active antiretroviral therapy (HAART) can lead to clinical remission in AIDS-related KS, with suppression of HIV replication essential for this effect. KSHV infection can also lead to a rare B cell malignancy called primary effusion lymphoma (PEL) and multicentric Castleman disease (MCD), a lymphoproliferative disorder. KSHV modulates many of the same host cell signalling pathways as EBV, including activation of nuclear factor kappa-light-chain-enhancer of activated B cells (NF- κ B), PI3K-Akt and mammalian target of rapamycin (mTOR) to promote host cell proliferation and survival (Grossman *et al.*, 2006, Tomlinson and Damania, 2004, Chang and Ganem, 2013). Similar to EBV, KSHV promotes oncogenesis through its ability to induce proliferation and prevent apoptosis of infected B cells, whilst evading the immune system (Goncalves *et al.*, 2018).

The KSHV latency locus (LL) includes several latently expressed viral products, including LANA, vCyclin, vFLIP and viral microRNAs (miRNAs) (Bravo-Cruz and Damania, 2019). The LL is under control of a single B-cell-specific promoter and the genes of this region are constitutively expressed. KSHV encoded LANA has a range of oncogenic properties that impact cell cycle progression, proliferation, and apoptosis and can transform primary cells *in vitro*. LANA binds and suppresses tumour suppressor protein 53 kDa, (p53) decreasing its transcriptional activity (Friborg *et al.*, 1999). Additionally, LANA has been shown to lower the threshold for B cell activation, inducing continuous activation (Sin *et al.*, 2010). Expression of KSHV vCyclin occurs in both lytic and latent KSHV infection and interacts with multiple host cyclin-dependent kinases (CDKs), including CDK6. Complexes formed with vCyclin and CDK's have an increased number of substrates compared to CDK's alone and are known to dysregulate cell cycle progression including through phosphorylation of retinoblastoma protein (Rb) (Godden-Kent *et al.*, 1997). Additionally, vCyclin modulates both p53 and BCL-2 and induces the DNA damage response (Bravo-Cruz and Damania, 2019). Although expression of vCyclin is not essential for KSHV induced oncogenesis, it enhances it through preventing contact inhibition (Jones *et al.*, 2014). KSHV also encodes a viral FLIP (as does EBV), which is expressed in PEL and KS and stimulates activation of NF- κ B. KSHV vFLIP also inhibits apoptosis through preventing recruitment of caspase 8 (Sturzl *et al.*, 1999). *In vivo* studies have shown vFLIP contributes to KSHV induced lymphomagenesis (Chugh *et al.*, 2005, Ballon *et al.*, 2011). Several KSHV lytic proteins have also been shown to have oncogenic effects, though lytic products are detected in far fewer cells within tumours than latent products, which are detected in all cells

(Cesarman *et al.*, 2019). For example, the pro-inflammatory KSHV viral interleukin 6 (vIL6), which induces vascular endothelial growth factor (VEGF) expression can be detected in the sera of patients with KS, PEL and MCD (Aoki *et al.*, 2001). KSHV G protein-coupled receptor (vGPCR), a homologue of a human chemokine transmembrane receptor, can induce constitutive activation of host cell signalling pathways, increasing VEGF and platelet-derived growth factor (PDGF) (Cavallin *et al.*, 2018). The increase in such inflammatory and angiogenic factors is thought to contribute to development of KS. In mouse models, expression of KSHV vGPCR in a small number of cells is sufficient to induce vascular lesions (Cesarman *et al.*, 2000).

Whilst EBV and KSHV are considered directly oncogenic, other herpes viruses have been linked with cancer, though their potential role in oncogenesis is less clear. A 2017 study showed that seropositivity for HSV-2 is an independent predictor of cervical cancer (Wen and Li, 2017). Co-infection with HSV-2 has been shown to increase the oncogenic potential of human papilloma virus (HPV), increasing the risk of HPV induced cervical squamous cell carcinoma by 60 times (Smith *et al.*, 2002). Similarly, HHV-6 has also been proposed to act as an enhancing co-factor to other oncogenic viruses, including HPV and EBV, with both HHV-6A and HHV-6B identified in an array of tumours, including glioma, oral cancer, cervical cancer, adrenocortical tumours, gastrointestinal cancer and lymphomas (Eliassen *et al.*, 2018). It is currently unclear whether HHV-6A and HHV-6B are directly oncogenic. As with other viruses found in cancers, the high prevalence of infection makes it difficult to discern whether this is an associative, causative or modulatory relationship. Finally, HCMV has been detected in over 90 % of epithelial cancers, including, but not limited to glioma, breast, colon, salivary gland, ovarian and prostate cancers (Cobbs *et al.*, 2002, Harkins *et al.*, 2010, Samanta *et al.*, 2003, Harkins *et al.*, 2002, Rådestad *et al.*, 2018). Whether or not HCMV is directly oncogenic remains controversial. The potential oncogenic effects of HCMV are discussed in section 1.5.2.

1.2 Human Cytomegalovirus

1.2.1 Prevalence and transmission

HCMV is highly prevalent throughout the global human population, with estimates of seroprevalence ranging from 50 up to 100 % (figure 1.3) (Manicklal *et al.*, 2013, Schottstedt *et al.*, 2010). Socioeconomic environment is the most powerful predictive influence over prevalence, which is much higher in lower income countries (Mustakangas *et al.*, 2000).

| Regions | General Population | Women of Reproductive Age | Blood and Organ Donors |
|------------------------------|--------------------|---------------------------|------------------------|
| European region | 66 (56-74) | 70 (63-76) | 69 (61-77) |
| Region of the Americas | 75 (64-84) | 79 (69-87) | 78 (67-87) |
| South-east Asian region | 86 (77-93) | 89 (82-94) | 88 (81-94) |
| African region | 88 (80-93) | 90 (85-94) | 90 (84-94) |
| Western Pacific region | 88 (81-93) | 91 (86-94) | 90 (85-94) |
| Eastern Mediterranean region | 90 (85-94) | 92 (88-95) | 92 (87-95) |
| Global | 83 (78-88) | 86 (83-89) | 86 (82-89) |

Figure 1.3 Estimates of mean HCMV seroprevalence by different World Health Organisation regions

Estimates of mean HCMV seroprevalence % and 95 % uncertainty interval by different World Health Organisation regions, stratified by general population, women of reproductive age and blood and organ donors. Taken from Zahair *et al.* (2019).

HCMV can be transmitted via several routes, including through contact with bodily fluids such as urine, saliva, cervical secretions, semen, breast milk and tears from infected individuals that are shedding virus (Cannon, Hyde and Schmid, 2011). HCMV can also be transmitted by blood, haematopoietic stem cell or organ transplantation and crucially through vertical transmission from mother to neonate either *in utero* or during delivery (Atabani *et al.*, 2012). Infection of immunocompetent hosts is usually asymptomatic, accounting for over 90 % of primary infections (Whitley, 1996). However, HCMV infection of the immunocompromised and neonates leads to significant disease resulting in considerable morbidity and mortality (Emery, 2001, Peckham *et al.*, 1987). In primary and recurrent infection of immunocompetent hosts, the immune system plays a key role in suppressing viral replication. HCMV elicits one of the largest cellular immune responses documented in humans, stimulating both adaptive and innate immune response (Rosa and Diamond, 2012). In contrast, if the host immune system is compromised, such as in individuals with HIV or immunosuppressed organ transplant recipients, HCMV can replicate more effectively, leading to high viral loads and more severe pathology (Griffiths and Reeves, 2021).

Mother to child transmission of HCMV can occur through *in utero* transmission via the placenta, during delivery where the neonate comes into contact with maternal blood and cervical fluid, and also through breast milk (Stagno *et al.*, 1986). *In utero* HCMV infection can occur by primary maternal infection during pregnancy, infection with a second strain or reactivation of latent maternal HCMV

infection. All three scenarios can lead to mother to foetus transmission via the placenta, yet primary HCMV infection carries a much higher risk of mother to foetus transmission and ensuing detrimental effects upon the developing foetus (Fowler *et al.*, 1992). The transmission rate from infected mother to foetus increases with gestational age. The incidence in primary maternal infection being transmitted to the foetus for infection acquired at 3-12 weeks preconception, is 9%, rising to 30% for infection in the first, 38% in the second and 72% in the third trimesters of pregnancy (Revello *et al.*, 2001, Enders *et al.*, 2011).

Whilst the adult brain is usually protected from HCMV infection by the blood brain barrier, during neonatal infection, HCMV can infect the developing brain, which is susceptible to viral penetration due to its immature blood brain barrier. The magnitude of effect and subsequent neurological sequelae vary greatly depending on the gestational stage at which infection occurs, with the most detrimental sequelae correlating with infection in early stages of gestation, namely conception and first trimester (Buxmann *et al.*, 2017).

Mothers who are HCMV seropositive prior to conception can develop a secondary HCMV infection through reactivation of pre-existing latent virus or through reinfection with a different viral strain. Whilst the majority of secondary infections are asymptomatic for both mother and foetus, a small percentage (0.2 – 2 %) of infants born to such mothers display congenital HCMV sequelae (Boppana *et al.*, 2001). Although symptomatic congenital HCMV infection has been well characterised, it is estimated that around 90 % of congenital infections are clinically asymptomatic at birth (Ronchi *et al.*, 2019). A 2019 study by Ronchi *et al.* found that 56 % of infants initially classified as asymptomatic should be reclassified as symptomatic after a more in-depth examination. Of those tested, 45 % showed abnormalities of the brain by cranial ultrasound. In light of these findings, it is difficult to estimate how many cases of congenital HCMV infection go undiagnosed each year.

HCMV infection in the first and second trimester of pregnancy is a leading cause of congenital neurological disability such as mental retardation, cerebral palsy, seizures, chorioretinitis and sensorineural hearing loss (Foulon *et al.*, 2008). Damage to the brain and central nervous system during *in utero* HCMV infection is irreversible (Cheeran *et al.*, 2009). Several regions and cell types of the developing brain are permissive to HCMV infection, including neural stem and progenitor cells (NSC, NPC) located within in the subventricular zone (SVZ) (Odeberg *et al.*, 2006). HCMV infection of various cell types of the brain is further discussed in section 1.3.4.

1.2.2 Genome and structure

HCMV is a large double stranded DNA (dsDNA) virus, maintained as an episome leading to lifelong infection of the host as further discussed in section 1.2.4. The HCMV genome is approximately 235 kb encoding over 200 proteins, making it the largest genome of the human herpesviruses (Dolan *et al.*, 2004). The HCMV genome contains two unique regions known as the unique long (UL) and unique short (US) regions, which encode viral proteins. These two domains are flanked by a pair of non-coding inversely repeated sequences which facilitate genome isomerisation, in a configuration known as TRL-UL-IRL-IRS-US-TRS



Figure 1.4 HCMV genome structure

HCMV genomic structure depicting the following regions: terminal repeat long (TRL), unique long (UL), unique short (US), internal repeat long (IRL), internal repeat short (IRS), terminal repeat short (TRS), and internal repeat (IR).

HCMV virions are enveloped and measure approximately 200 nm in diameter. The HCMV genome is encapsulated by an icosahedral capsid comprising 60 asymmetrical subunits with a triangulation number of 16 (figure 1.5) (Chen *et al.*, 1999). The capsid is surrounded by tegument, consisting of an array of diverse tegument proteins and RNAs, which are unlikely to form a definitive structure (Wang and Zhao, 2020, Greijer, Dekker and Middlesdorp, 1999). Components of the tegument layer are delivered directly to the cytoplasm and include proteins such as pp65, pp71, pp150 and pp28 among many others, which have diverse effects on the host cellular environment. The tegument is encased in a lipid envelope, which is acquired when budding through host Golgi derived vacuole compartments and is studded with viral envelope proteins (Homman-Loudiyi, 2003). Envelope proteins are primarily involved in binding host cells, viral entry and are also implicated in immune evasion by sequestering human chemokines (Frascaroli *et al.*, 2006, Frascaroli *et al.*, 2018).

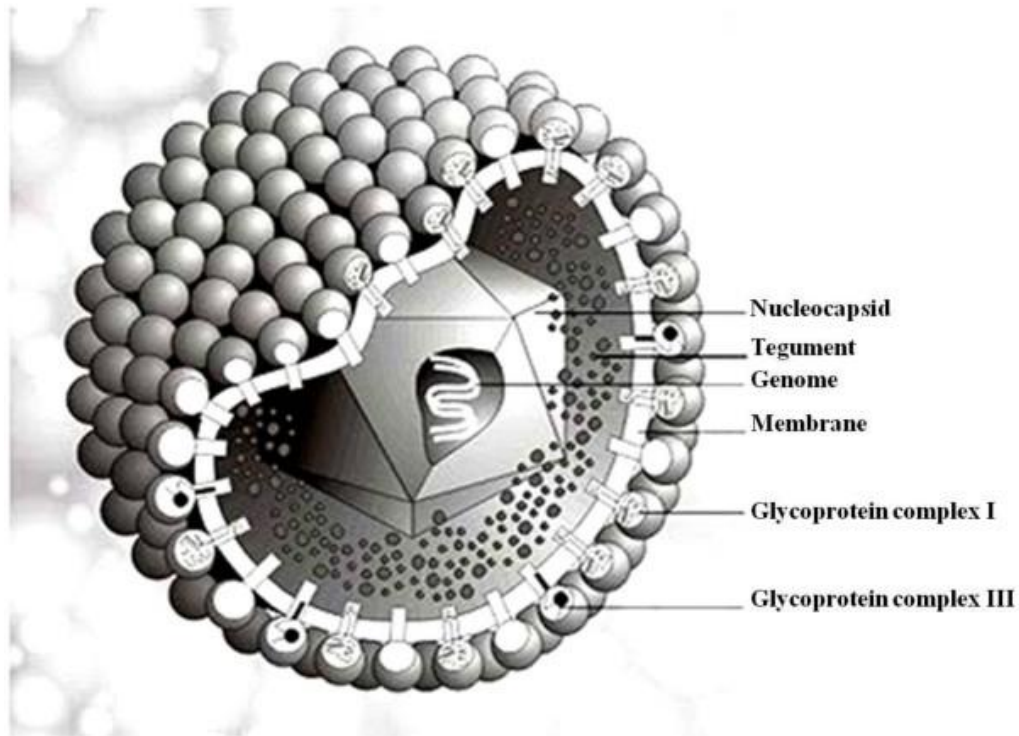


Figure 1.5 HCMV virion structure

Illustration of a HCMV virion showing the double stranded DNA genome inside the nucleocapsid, surrounded by the tegument layer and encapsulated by the viral envelope covered with glycoprotein complexes. Image taken from Tomtishen (2012).

1.2.3 HCMV lytic life cycle

As is characteristic of all herpes viruses, HCMV has both a lytic and latent life cycle. The lytic phase is characterised by the production of infectious virions, whilst in the latent phase, virion production ceases and viral gene expression is limited. The first step of the HCMV lytic life cycle is virus entry into host cells. The core entry membrane fusion machinery consists of surface glycoprotein complex gH/gL and gB (Vanarsdall and Johnson, 2012). HCMV gB has been shown to act as a viral fusogen as well as a host cell receptor binding protein, whilst gH/gL is thought to trigger gB membrane fusion, though the mechanism for this is unclear (Wille *et al.*, 2013). The gH/gL glycoprotein complex exists both in isolation and forms two distinct complexes with other glycoproteins to assist viral entry. One of these complexes is a trimer consisting of gH/gL/gO. The second complex is pentameric and consists of gH/gL/UL128/UL130/UL131. The pentameric complex promotes a form of cell-cell infectivity that resists neutralisation by host cell antibodies, whereas the trimer is required for cell free infectivity (Zhou *et al.*, 2015). The presence of the pentameric complex dramatically expands the cell tropism of the virus and permits entry into epithelial and endothelial cell types in addition to fibroblasts (Wang and Shenk, 2005a,

Wang and Shenk, 2005b). It has also been shown that HCMV modulates its gH/gL complexes depending on the type of cell in which virions are produced.

Multiple host cellular factors have been implicated as HCMV receptors, or as mediating entry, including; epidermal growth factor receptor (EGFR), integrins, platelet derived growth factor alpha (PDGFR α), bone marrow stromal antigen/tetherin (BST/tetherin), and neuropilin-2 (Nrp2) (Wang *et al.*, 2003, Soroceanu *et al.*, 2008, Viswanathan *et al.*, 2011, Martinez-Martin *et al.*, 2018). PDGFR α has been identified as a receptor for trimer, whereas Nrp2 is a known receptor for the pentamer (Kabanova *et al.*, 2018, Martinez-Martin *et al.*, 2018). EGFR and PDGFR α both bind gB. It is thought that the use of the EGFR receptor and integrins for entry primes CD34+ haematopoietic progenitor cells for the establishment of latency before the virus has even entered the cell through initiation of downstream signalling (Collins-McMillen *et al.*, 2018). HCMV entry in fibroblasts occurs by pH independent fusion at the plasma cell membrane leading to micropinocytosis (Hetzenecker *et al.*, 2016). However, for pentameric entry into epithelial and endothelial cells, acidification of endosomes is required and entry in to these cell types is mediated by genes from UL128 – UL150 (Ryckman *et al.*, 2006).

Following fusion, viral capsids and free tegument proteins are deposited into the host cell cytoplasm. A subset of non-capsid bound tegument proteins including pp65 and pp71 migrate independently to the nucleus (Kalejta, 2008). It is thought that other tegument proteins such as pUL47, pUL48 and potentially pp150 remain tightly bound to the genome containing viral capsids and play a role in manipulating host microtubule machinery to transport them into the nucleus (summarised in figure 1.6) (Bechtel and Shenk, 2002, Ogawa-Koto, 2002, Ogawa-Koto, 2003). HCMV pUL48 is a large tegument protein that is conserved across several herpesviruses. In HSV-1, pUL36 (HCMV pUL48 homologue) is essential for targeting the nuclear pore complex and proteolytic cleavage of pUL36 is required to release viral DNA from the capsid into the nucleus (Abaitua *et al.*, 2012). HSV-1 UL36 deletion mutants are incapable of replication as the viral genome cannot enter the nucleus and capsids accumulate in the cytoplasm (Desai, 2000).

Evidence suggests that pUL48 plays a very similar role in targeting capsids to the nucleus and releasing the viral genome (Brock *et al.*, 2013). The immune adaptor protein stimulator of interferon genes (STING) is also required for HCMV nuclear entry, without it the interaction between the capsid and the nuclear pore complex is defective (Hong *et al.*, 2021). Deposited viral genomes localise to nuclear domain 10 (ND10) bodies.

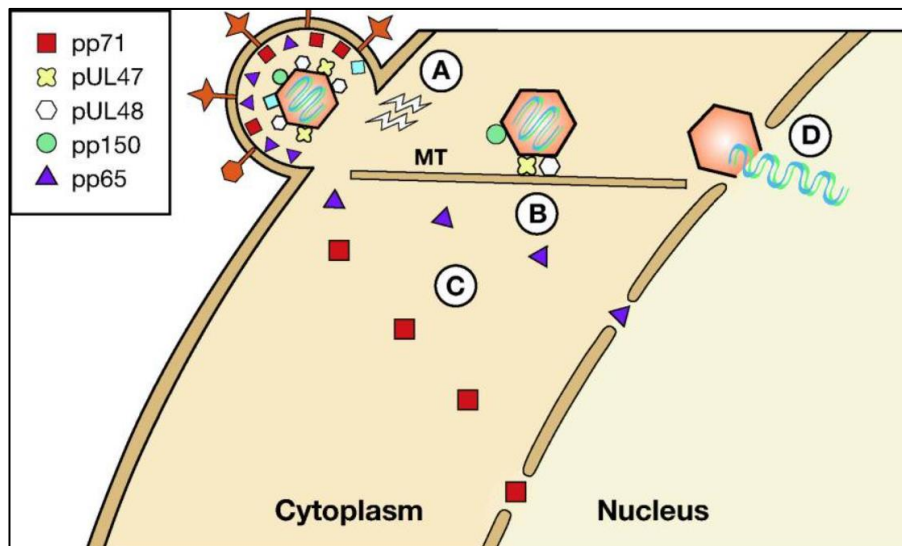


Figure 1.6 Tegument proteins assist in delivering capsids to the host cell nucleus

During entry and translocation to the nucleus HCMV tegument proteins have several functions. A) capsids and free tegument proteins are released into the cytoplasm. B) pUL47, pUL48 and pp150 remain tightly bound to the capsid to direct them along host cell microtubules towards nuclear pore complexes. C) Free tegument proteins such as pp71 and pp65 independently migrate to the nucleus. D) pUL48 assists in capsid docking to nuclear pores and release of viral genomes into the nucleus. Adapted from Kalejta *et al.*, 2008.

During lytic infection HCMV genes are expressed as a tightly regulated temporal cascade. This begins with immediate early (IE), gene expression under control of the major immediate early promoter (MIEP). Expression of genes under control of the MIEP is essential for lytic infection. In cells such as CD34+ progenitor cells, which only support latent infection, the MIEP is silenced through transcriptional repressors and co-repressors which induce inhibitory chromatin structure including extensive histone acetylation (Murphy *et al.*, 2002). The MIEP drives expression of a number of differentially spliced IE proteins acting primarily as transcriptional regulators (Awasthi *et al.*, 2004). Hence, IE proteins play a vital role in controlling the subsequent expression of the early and late genes (Marchini *et al.*, 2001). The MIE locus consists of five exons, IE proteins including exon four are known as IE1 (four have been identified) and those containing exon five are collectively known as IE2 (five have been identified).

By far the two most abundant and arguably most important IE proteins are pp72, from now on referred to as IE1, and pp86, from now on referred to as IE2 (Akrigg *et al.*, 1985). These two nuclear phosphoproteins share an identical region of 85 amino acids at the amino terminus, but have different carboxyterminal structures; both are potent transcriptional regulators of HCMV early genes (Fortunato *et al.*, 1997). IE2 is a transcription factor that is a powerful transactivator of both human

genes, including several interleukin genes, *myc* and *fos* and also HCMV early and late genes which are essential for viral replication (Arend *et al.*, 2016). IE2 has several mechanisms for transcriptional regulation, including directly binding DNA, protein-protein interactions and blocking chain elongation during transcription (Ball *et al.*, 2022). Whilst IE2 expression has been shown to be essential for progression of the virus life cycle and production of infectious virus particles, IE1-null viruses have been shown to replicate effectively *in vitro* at high multiplicity of infection (MOI) (Mocarski *et al.*, 1996). However, replication of IE1-null viruses is significantly diminished at low MOI. IE1 promotes viral gene expression as it inhibits HDACs which would otherwise limit the transcription of HCMV lytic genes through formation of repressive chromatin structure (Nevels *et al.*, 2004).

Additionally, both IE1 and IE2 have been shown to inhibit the expression of host genes with antiviral functions (Paulus and Nevels, 2009). IE1 does this through interacting with host cell STAT proteins. Whilst IE2 can be a powerful activator of many early and late HCMV genes, it also has repressive functions. By binding core promotor regions, IE2 can block transcription through preventing formation of preinitiation complexes, whereas binding nearby, but not directly to promoters can lead to transcriptional activation (Ball *et al.*, 2022). Importantly, IE2 can negatively autoregulate its own promoter, the MIEP, through direct association with nucleosomes and TATA-binding protein, which is important for efficient production of virions as excessive IE2 is cytotoxic and therefore reduces viral production. IE2 has been shown to block interferon production and expression of some host chemokines. Whilst IE2 has the ability bind DNA directly in a sequence specific manner, IE1 has not been shown to directly bind DNA, but does interact with host cell chromatin (Macias and Stinski, 2003, Reinhardt *et al.*, 2005).

Early gene expression requires expression of IE1 and IE2 to initiate transcription and early genes primarily code for proteins required for viral DNA replication (Isomura *et al.*, 2011). Viral DNA synthesis is initiated from around 24 hr post infection (h.p.i), after early gene expression, but before late gene expression (Ishov and Maul, 1996). Replication of herpesvirus DNA begins at a lytic origins of replication (*oriLyt*) site, which in HCMV is located upstream of UL57, a gene encoding a single stranded DNA binding protein (Borst and Messerle, 2005). The HCMV *oriLyt* is notable for its large size and complexity and its obvious lack of homology to other viral DNA replication origins. UL84, UL83, IRS1 and IE2 are known to interact with *oriLyt*, though the full mechanism of the initiation of replication is poorly understood (Kagele *et al.*, 2012). Viral replication machinery is recruited to the DNA replication compartment, which is formed from ND10.

This replication machinery includes a viral DNA processivity subunit, pp52, which interacts with cellular nucleolin and viral pUL114, and TRS1 to co-ordinate DNA replication (Strang *et al.*, 2010). Viral pp52 forms a homodimer that can wrap around DNA to tether the catalytic subunit of the viral DNA polymerase encoded by UL54, to allow continuous elongation of the synthesised strand (Weiland *et al.*, 1994). UL57, the single-stranded DNA binding protein downstream of oriLyt, pUL70 a primase, pUL102 a primase-associated factor, and pUL105 a viral helicase completes the DNA replication machinery.

Newly synthesised HCMV genomes are tightly wrapped and packaged into capsids. The nucleocapsids are formed via interactions between the four main capsid components; the major capsid protein (MCP), the triplex dimer (Tri2), the triplex monomer (Tri1), and the smallest capsid protein (SCP) (Li *et al.*, 2021). The nuclear egress complex (NEC), is a heterodimer formed of pUL50 and pUL53 which is responsible for transporting the nucleocapsids from the nucleus into the cytoplasm. Viral pUL97, a protein kinase, phosphorylates components of the nuclear lamina, disrupting the structure to allow emergence of the capsid from the inner nuclear membrane (Sharma *et al.*, 2014). As the nucleocapsid passes through the inner nuclear membrane facilitated by a nuclear egress complex comprising pUL53 and pUL50, it acquires a primary envelope, which is subsequently shed as it passes through the outer nuclear membrane. The process of nucleocapsid envelopment and the ensuing de-envelopment are essential for successful nuclear egress (Mettenleiter, 2002). Viral proteins pUL96 and pp150 cooperate to stabilise nucleocapsids as they translocate to the viral assembly compartment (AC). The AC is a juxtannuclear structure where final tegumentation and acquisition of the viral envelope occur to complete the formation of mature virions (Sanchez *et al.*, 2000). The HCMV AC is a structure often as large as the cell nucleus, formed from multiple membranous elements derived from the host cell. The nature of formation of the HCMV AC remains unclear, though studies from MCMV indicate that rearrangement of Golgi as being the first step and is initiated as early as 6 h.p.i (Lucin *et al.*, 2020). The AC also acts as a microtubule-organizing center, with HCMV promoting microtubule formation through recruitment of end binding proteins such as EB3 to the AC (Procter *et al.*, 2018). As the AC forms it distorts the enlarged host cell nucleus, with microtubules pulling it around the AC into a distinctive kidney shape (Alwine, 2012). Studies of the HCMV AC by electron microscopy have identified the displacement of Golgi stacks into a vacuolar ring surrounding an accumulation of aggregated vesicular, vacuolar, and tubular membranous structures. Immunofluorescent staining of the AC has revealed the presence of components derived from Golgi, early endosomes, and recycling endosomes (Homman-

Loudiyi, 2003, Cepeda *et al.*, 2010). Both pUL48 and pUL103 are thought to be key players in rearranging the cellular infrastructure to optimise virion production, in the absence of these proteins formation of the Golgi rings and the specific localisation of markers of early and recycling endosomes to the centre of these rings is impaired (Das *et al.*, 2014). HCMV pUL94 assists the localisation and accumulation of pp28 in the AC, a late protein essential for viral envelopment (Phillips *et al.*, 2012). In order for envelopment to take place, a threshold amount of pp28 must accumulate and multimerise within the AC (Seo and Britt, 2008). The process of tegumentation and envelopment at the AC remains poorly understood, though pUL71, which contains a basic leucine zipper-like domain is thought to be important for efficient envelope acquisition. In the absence of pUL71, capsids accumulate at the AC, but very few obtain their envelope and go on to egress (Schauflinger *et al.*, 2011). Within the AC vesicular membranes wrap around the capsid to form the viral envelope, in a process termed budding. This is followed by membrane scission, which results in the enveloped capsid contained within a vesicle. The complete assembled virions are then released into the extracellular space via fusion with the plasma membrane (Close *et al.*, 2018). During lytic infection, as well as production of infectious virions, two types of non-infectious particles are also produced. Dense bodies are the most common and are capsidless, non-infectious particles filled mainly with pp65 (Tandon and Mocarski, 2012). Non-infectious enveloped particles (NIEP) are produced when particles that do have capsids, but lack viral genomes mature. The HCMV lytic life cycle is summarised in Figure 1.7.

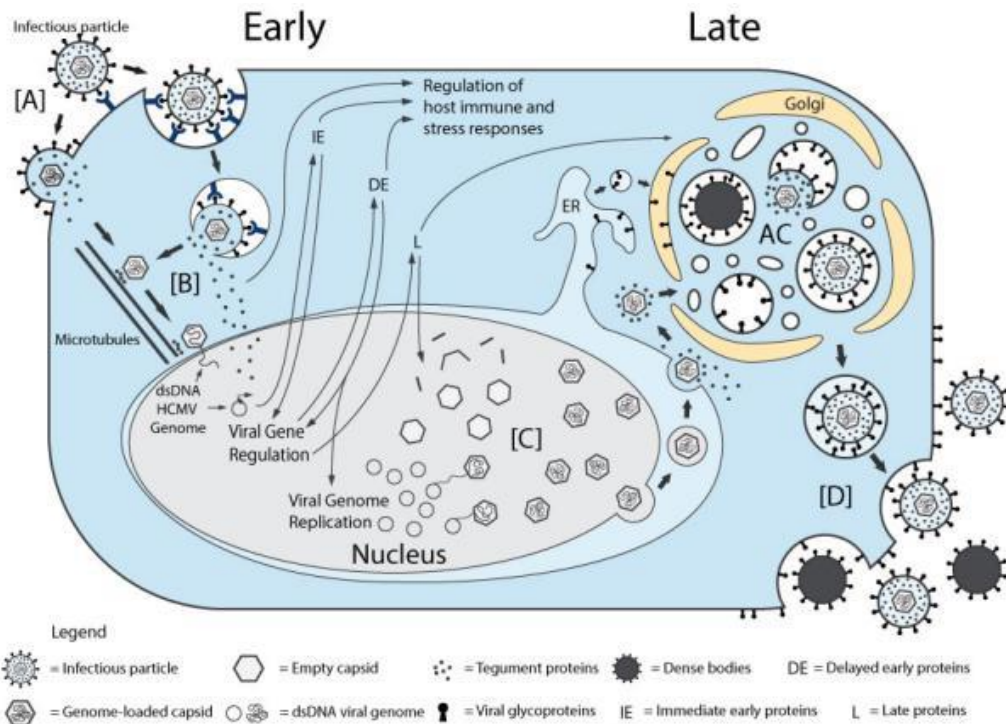


Figure 1.7 Summary of HCMV life cycle

Summary of HCMV life cycle showing viral entry mediated through virion glycoprotein interaction with host cell receptors and fusion at the plasma cell membrane. HCMV tegument proteins are released into the cytoplasm and capsids are transported to the nucleus through hijacking of host cell microtubules. Viral genome replication occurs in the nucleus, before being packaged into capsids and obtaining a primary envelope as it passes through the inner nuclear membrane, but is shed during passage through the outer membrane. Capsids translocate to the viral assembly compartment, where they undergo final tegumentation, acquire the viral envelope through budding from the assembly compartment and are subsequently contained within a vesicle. Complete virions are released into the extracellular space through fusion with the viral membrane. Image taken from Beltran and Christea, 2014.

1.2.4 HCMV latency and reactivation

The life cycle of HCMV is largely dependent on the type of cell that is infected. Whilst some cell types, such as fibroblasts are highly permissive to viral replication and therefore support a highly productive lytic infection, other infectable cell types are not. Some endothelial and epithelial cell types support a more “smouldering” chronic infection, in which low levels of virus are shed over several months or years (Jarvis and Nelson, 2007, Adler and Sinzger, 2009). The factors leading to chronic low-level virus production instead of highly productive lytic infection remain poorly understood.

Infection of haematopoietic stem cells and cells of the myeloid lineage leads to latent HCMV infection (Mendelson *et al.*, 1996, von Laer *et al.*, 1995, Forte *et al.*, 2020). In these cells, there is an initial burst of productive, lytic gene expression,

before a significant decrease in transcription of viral genes via chromatin remodelling and histone acetylation, particularly of the MIEP (Reeves *et al.*, 2005). Latency is defined as the state where HCMV replication competent genomes are present, but no virions are produced. During latency, HCMV genomes are maintained as closed, circular episomes in the nuclei of infected cells. A recent study has shown that HCMV episomes tether to the host chromosomes, facilitating nuclear retention (Mauch-Mücke *et al.*, 2020). This is reminiscent of episome tethering in the two oncogenic human γ -herpesviruses, EBV and KSHV (Chiu and Sugden, 2018). Early studies suggested that during latency viral gene expression was almost completely repressed through heterochromatinisation of HCMV DNA (Reeves *et al.*, 2005).

Transcriptional analysis of latently infected cells found that several HCMV transcripts, including UL138 and latency unique nuclear antigen (LUNA) could be detected in the absence of IE expression (Goodrum *et al.*, 2007, Bego *et al.*, 2005). UL138 has been shown to repress IE expression in CD34+ myeloid progenitor cells by enhancing the repressive methylation of H3K9 at the MIEP although interestingly, UL138 fails to repress IE expression in terminally differentiated cells (Lee *et al.*, 2015). Several transcripts expressed during lytic infection have also been widely detected during latency. These transcripts include: UL111A, which encodes a viral homologue of the immunosuppressive human interleukin, IL-10; US28, a G protein-coupled receptor that interacts with both CC and CX(3)C chemokines; transcripts from the IE region; and non-coding RNAs 2.7 and 4.9 (Jenkins, Abedroth and Slobedman, 2004, Beisser *et al.*, 2001, Kondo and Mocarski, 2006, Forte *et al.*, 2020). Recent studies utilising sensitive, high throughput, and unbiased analysis of the HCMV viral transcriptome have revealed that in fact, many lytic genes are transcribed at low levels during latency with no current consensus on a unique latency specific transcriptional profile (Cheng *et al.*, 2017, Schwartz and Stern-Ginossar, 2019). Single cell analysis of infected monocytes showed a high level of heterogeneity in the cellular response to HCMV infection and revealed that many cells do express lytic genes in a similar pattern to late lytic infection in the absence of virus production (Shnayder *et al.*, 2018, Shnayder *et al.*, 2020). However, the number of viral genes expressed per cell decreased over time, consistent with an increase in transcriptional repression. Whilst it is difficult to determine exactly what constitutes a latent transcriptional profile, several studies have looked at relative expression of IE genes to latency genes (eg. LUNA, UL138) to determine latency (Krishna *et al.*, 2019, Buheller *et al.*, 2019).

Although symptomatic disease usually only occurs in those in the acute phase of HCMV infection or in reactivation of latent infection in the immunosuppressed,

there is a wealth of evidence supporting frequent cellular reactivation of latent infection in healthy immunocompetent hosts, which is rapidly suppressed by T-cell response (Wylie *et al.*, 2014, Boeckh *et al.*, 2003). It is important to differentiate between clinical reactivation, which is characterised by the recurrence of detectable viraemia, whereas cellular reactivation is the re-initiation of viral replication within latently infected cells. Clinical reactivation of HCMV often occurs in patients with T-cell immunodeficiency and lymphopenia, which is common in recipients of solid organ or haematopoietic stem cell transplants. CD34+ myeloid progenitors of the bone marrow are known to be a reservoir for latent HCMV infection *in vivo* (Hahn *et al.*, 1998). *In vitro*, reactivation of latent HCMV occurs upon differentiation of these progenitors into mature dendritic cells (DC) (Taylore-Wiederman *et al.*, 1994). This reactivation is associated with a significant increase in viral gene expression, in part due to chromatin remodelling (Reeves *et al.*, 2005, Dupont *et al.*, 2019). One of the drivers of this remodelling, a protein complex known as “facilitates chromatin transcription” (FACT), increases the accessibility of heterochromatin to RNA polymerase by repositioning histones. FACT binds to the MIE locus, both during latency and post-reactivation, and so is thought to be important for re-establishing sufficient IE expression for viral replication (O’Conner *et al.*, 2016).

Expression of viral proteins, UL7, UL135 and certain isoforms of UL136 are required for reactivation to take place (Umashankar *et al.*, 2014, Caviness *et al.*, 2016, Rak *et al.*, 2018). HCMV encoded miRNA’s have also been implicated in reactivation, due to their modulation of host cell signalling pathways (Mikell *et al.*, 2019). Changes in levels of host cell transcription factors and modulation of their binding to the MIE region have also been associated with initiating reactivation. This is exemplified by host cAMP-response element binding protein (CREB), which drives expression of IE1 and IE2 during differentiation mediated HCMV reactivation from latency in both monocytes and Ntera2, a pluripotent human embryonal carcinoma cell line (Kew *et al.*, 2014, Yuan *et al.*, 2015). Recent findings support a model where IE expression in latently infected CD34+ haematopoietic progenitor cells is restored via switching to intronic MIE promoters, rather than de-repression of the MIEP (Collins-McMillen *et al.*, 2019). However, in CD14+ monocytes treated with phorbol ester and other *in vitro* models of differentiation induced reactivation, MIEP driven IE expression is restored, suggesting HCMV may have multiple mechanisms for restoring IE expression (Mason *et al.*, 2020).

1.2.5 HCMV and host immune response

The severity of disease caused by HCMV infection is determined early in the initial infection, when a rapid host innate immune response is key. HCMV is detected through pattern recognition receptors (PRRs) including Toll-like receptors (TLRs), triggering an inflammatory response through release of pro-inflammatory factors, including type 1 interferons (IFN), tumour necrosis factor alpha (TNF- α) and interleukin-6 (IL-6) (Boehme *et al.*, 2006). Induction of an array of IFNs and cytokines leads to the nuclear translocation of NF- κ B, an important regulator of host innate immune response which further upregulates production of inflammatory cytokines, subsequently recruiting and activating dendritic cells and natural killer (NK) cells (Babic *et al.*, 2011). Neutrophils also play a role in the response to early HCMV infection (Jackson *et al.*, 2019). The initial innate immune response dampens viral replication and primes for the host adaptive immune response, which plays a key role in the control of long-term HCMV infection (Isaacson *et al.*, 2008).

Once HCMV infection is established, virus particles and dense bodies are processed by antigen-presenting cells (APCs), stimulating a subsequent adaptive antigen specific response, which is one of the strongest ever-documented in human hosts (Rosa and Diamond, 2012). Antibodies for several HCMV proteins are detected during primary infection, including tegument proteins with a structural function such as pp65, envelope glycoproteins (particularly gB, gH and gH/gL complexes), and non-structural proteins including IE1 (Gerna *et al.*, 2008). This humoral response is important for restricting viral dissemination, particularly through neutralisation with antibodies specific to the gH/gL complexes. The magnitude of the T-cell response to HCMV is particularly notable, with HCMV-specific T-cell numbers much higher than those observed for many other viruses, including other herpesviruses (Sylwester *et al.*, 2005). Interestingly, although HCMV-specific CD4+ and CD8+ T-cells comprise around 10 % of the memory T-cells in seropositive individuals, this is seemingly not essential for protection from symptomatic disease as individuals with minimal T-cell response can still be asymptomatic.

1.2.6 HCMV immune evasion

Whilst in the immunocompetent host, primary HCMV infection is often asymptomatic due to a robust initial innate and adaptive immune response, this is still insufficient to clear HCMV infection or prevent it from establishing latency and persisting for the lifetime of the host. HCMV has evolved a number of strategies to modulate and evade the host immune response, contributing to both

the establishment of infection and dissemination. HCMV encodes several proteins that modulate host NK cell activity, including UL135, UL141, UL142, UL148, UL18 and UL40 which all contribute to NK cell inhibition (Patel *et al.*, 2018). HCMV US2 and US11 have been shown to target the host major histocompatibility complex (MHC) class I molecules for degradation and US3 and US6 inhibit translocation of MHC, which may diminish T-cell response (Gabor *et al.*, 2020). HCMV infection decreases the transcription of MHC class II gene, HLA-DR, although the mechanism for this has not been elucidated (Sandhu and Buchkovic, 2020). This decrease in MHC class II transcription could potentially blunt the CD4⁺ T-cell response.

Several virus-encoded human cytokine homologues and cytokine receptors are expressed during HCMV infection. Amongst the most important for host immune response modulation is UL111A. UL111A encodes a HCMV vIL-10 homologue, which mimics many of the functions of human IL-10 including inhibiting production of pro-inflammatory TNF- α and IL-6 (Nachtwey and Spencer, 2008). Additionally, vIL-10 also decreases MHC class I and II expression in monocytes, and inhibits DC maturation, amongst other immunosuppressive effects (Chang *et al.*, 2004). HCMV US28 encodes a G-coupled receptor that has an array of pleiotropic functions, including immunomodulatory effects as well and being proposed as a potential oncogene. US28 binds several chemokines including RANTES/CCL5, MCP-1/CCL2, MCP-3/CCL7, MIP-1 α /CCL3, MIP-1 β /CCL4 and CX3CL1 (McSharry *et al.*, 2012). Studies suggest that US28 binds and internalises a range of chemokines, limiting their effects on immune cells in the immediate environment and thus acting as an immunovasin (Bodaghi *et al.*, 1998).

HCMV encodes a number of proteins known to block apoptosis in infected host cells. IE1 and IE2 both inhibit apoptosis through their effects on the host cellular kinase Akt-mediated pathway (Lukac and Alwine, 1999). UL36 encodes a protein that prevents apoptosis through binding to the pro-domain of caspase-8, inhibiting its activation (Skaletskaya *et al.*, 2001). Additionally, HCMV pUL37x1 sequesters the pro-apoptotic protein Bax and pUL38 also has anti-apoptotic effects (Arnoult *et al.*, 2004, Terhune *et al.*, 2007).

1.2.7 HCMV therapy

Whilst immunocompetent individuals with HCMV rarely require treatment, current gold standard treatment of immunocompromised patients is with intravenous antiviral ganciclovir (GCV) or its bioavailable orally administered derivative, valganciclovir (VGCV). VGCV can also be used as a prophylactic in

recipients of solid organ transplant (Lischker and Zimmerman, 2008). Both GCV and VGCV are nucleoside analogues that, when phosphorylated, preferentially inhibit the viral DNA polymerase UL54 inducing chain termination in viral DNA replication (Mar *et al.*, 1985). The effects of GCV and VGCV are specific to HCMV infected cells due to their requirement of phosphorylation by a virus-encoded serine/threonine kinase, UL97 (Biron *et al.*, 1985). Dosage with GCV and VGCV is limited by cytotoxic side effects, which can lead to neutropenia and thrombocytopenia, putting patients at higher risk of bacterial and fungal infection (Nichols *et al.*, 2002). Resistance to GCV and VGCV often develops through mutation in viral DNA polymerase pUL54 and the viral kinase UL97, which is essential for activation of these drugs (Limaye, 2002). Second-line antivirals against HCMV include cidofovir (CDV) and foscarnet, both of which inhibit viral replication by preferentially binding HCMV DNA polymerase over cellular polymerase (Lischker and Zimmerman, 2008). Acyclovir also requires UL97 for phosphorylation and terminates HCMV DNA replication through inhibiting its DNA polymerase.

As CDV, foscarnet and acyclovir all target the same viral DNA polymerase as GCV and VGCV, acquired resistance to one of these drugs through UL54 mutation usually leads to cross resistance of the other drugs in this category (Chaer *et al.*, 2016). Due to this cross-resistance, the development of effective new antivirals with pUL54 independent activity is desperately needed. Letermovir inhibits pUL56, a key component of the HCMV terminase complex (pUL51, pUL56 and pUL89) which is responsible for packaging viral genomes into capsids (Goldner *et al.*, 2011). As there is no human homologue of this target, its effects are virus specific and so fewer side-effects have been reported than with other HCMV antivirals (Kim, 2018). Resistance to Letermovir has been reported due to acquired mutations in UL56 (Marty *et al.*, 2017). The HCMV pUL97 inhibitor Maribavir has shown promising results in clinical trials and has been shown to have activity in some GCV resistant strains with mutated UL97 (Maertens *et al.*, 2019, Drew *et al.*, 2006). One of the major limitations with use of all these antivirals is that they all target viral DNA replication and so are unable to treat latent HCMV infections.

The ability to reduce the number of latently HCMV infected cells could provide great clinical benefit, particularly in transplant recipients. A potential treatment for latent HCMV infection is the tubulin inhibitor vincristine which has antimetabolic effects and is used in the treatment of various cancers (Škubník *et al.*, 2021). In uninfected cells, vincristine is rapidly transported out of cells by multidrug resistance-associated protein 1 (MRP-1), however in latently HCMV infected cells, viral UL138 downregulates MRP-1 making cells susceptible to vincristine

cytotoxicity (Weekes *et al.*, 2013). However, the toxicity of this drug may limit its suitability as a HCMV treatment, particularly in transplant recipients. A fusion toxin protein called F49A-FTP consists of the pseudomonas exotoxin (PE) fused to the soluble region of fractalkine (CX3CL1), a human chemokine that regulates inflammation and chemotaxis (Spiess *et al.*, 2015). The fractalkine moiety allows binding to the latently expressed HCMV encoded chemokine receptor pUS28, which localises to the cell surface and internalises F49A-FTP. Following internalisation PE is cleaved and inhibits translation, inducing cell death. Unfortunately, HCMV does become resistant to F49A-FTP, through US28 mutations, but this could be a promising treatment for combination use with other traditional HCMV antivirals such as GCV. The main advantage of this drug is its ability to target latently infected cells, although potential off-target effects upon the immune and nervous system may prohibit its clinical use.

Another area of research with potential for treating latent HCMV infection is the so-called “shock and kill” method. Transcriptional repression of the MIEP is a key factor in maintaining HCMV latency. In contrast, reactivation from latency occurs in response to de-repression of the MIEP, which allows for transcription of lytic viral genes (Reeves *et al.*, 2005). Histone deacetylase inhibitors (HDACi) can effectively reverse histone deacetylation of the MIEP, restoring lytic infection through MIEP de-repression and subsequent IE transcription (Krishna *et al.*, 2016). This restoration of lytic gene expression constitutes the “shock” portion of the shock and kill method. Lytic gene expression provides a target for circulating HCMV-specific cytotoxic T cells to “kill”. In healthy HCMV+ individuals it is estimated that ~10 % of peripheral blood cytotoxic T lymphocytes (CTLs) are specific to HCMV lytic antigens and effectively target cells with lytic HCMV infection (Sylwester *et al.*, 2005). However, T-cell immunodeficiency would likely affect the efficacy of this treatment, which may make it unsuitable for many immunocompromised patients. Groves *et al.*, (2021) recently showed that inhibitors of bromodomain and extraterminal (BET) proteins (I-BETs) may provide a more clinically useful option as a “shock” agent than HDACi. I-BET GSK726 was shown to have a more potent effect in restoring IE1 and IE2 expression than HDACi in latently infected monocytes, without full reactivation of lytic HCMV infection, which is advantageous by minimising risk of viraemia patients. Expression of late proteins such as pp65 was also detected in the absence of viral DNA replication, showing that GSK726 initiates an alternative programme of lytic gene expression that does not follow the classical temporal cascade. Expression of immunogenic HCMV antigens such as pp65 and gB are particularly useful for stimulating the “kill” effect as ~70 % of neutralising antibodies in seropositive individuals target gB and pp65 is targeted by ~80 % of

HCMV specific CTLs (Britt and Mach, 1996, Wills *et al.*, 1996). Further research is needed to determine if I-BET may be a viable treatment for latent HCMV infection as I-BETs have potentially broad off target effects.

HCMV has previously been designated as the second highest priority for vaccine development by the Centers for Disease Control (CDC) due to its widespread prevalence, high disease burden and the limited success of currently available therapies. Attempts at HCMV vaccine development began in the 1970's, but at present a successful candidate has yet to be identified. Live attenuated vaccines against strains such as Towne and Toledo have been developed, however they have proved unsuccessful in progressing through clinical trials, likely due to the large genetic differences between these laboratory passaged strains and circulating HCMV (Adler *et al.*, 2016). So far, subunit vaccines comprising major HCMV antigens such as gB and pp65 have shown the most promise in clinical trials, eliciting a strong immune response and around 50 % protection. However, they have not yet been licenced for clinical use and antibodies from vaccinated patients have failed to neutralise HCMV *in vitro* (Anderholm *et al.*, 2016). As HCMV has the ability to superinfect an already seropositive, latently infected host, vaccine development remains challenging and it is still unclear what immune response is required to protect against HCMV infection (Hansen *et al.*, 2010).

1.3 The brain

1.3.1 Brain anatomy and function

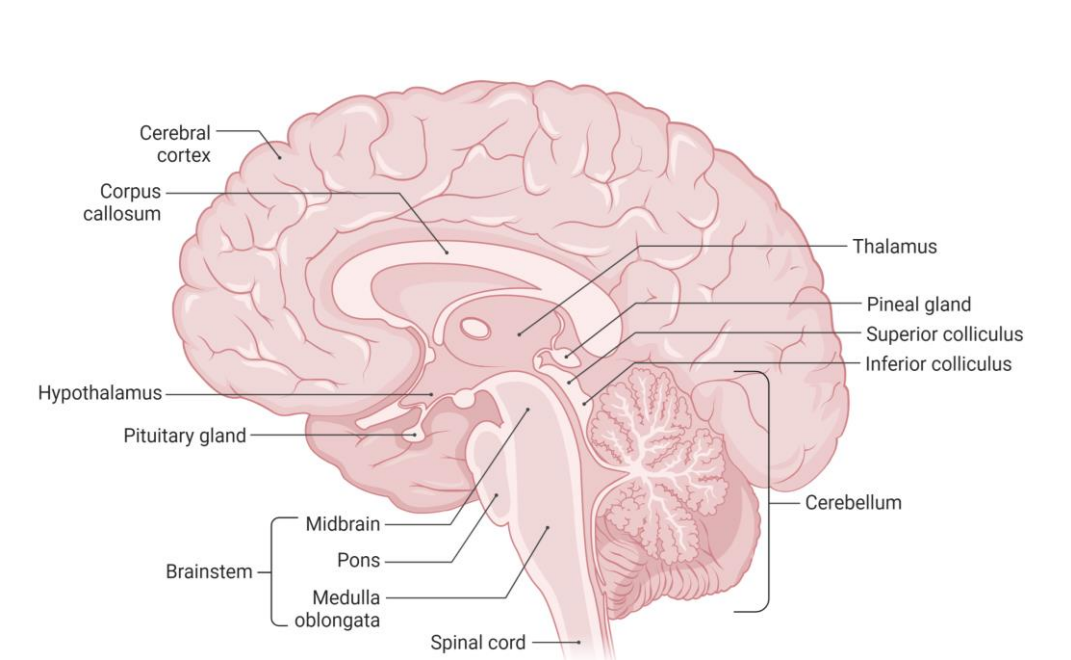


Figure 1.8 Adult brain anatomy

Diagram summarising the structure of the adult brain (created with BioRender.com). The brain is made up of two hemispheres connected by the corpus callosum. The outer surface of the brain is made up of the cerebral cortex, made up of billions of neurons and glia and characterised by its folded appearance. The cerebellum sits at the back of the brain, behind the brainstem (including the midbrain, pons and medulla oblongata), which has the superior and inferior colliculus on its external surface. The pituitary gland is located in front of the midbrain, beneath the hypothalamus. The thalamus and pineal gland are situated in the centre of the brain, above the brainstem.

The brain is one of the largest and most complex organs of the human body. It is responsible for many of the functions of the body, including control of motor function, breathing, vision, thought, temperature control and hunger (Hartmann *et al.*, 1994). The cerebrum is the largest part of the brain and consists of the left and right hemispheres, divided by the great longitudinal fissure (anatomy summarised in figure 1.8). Each of these hemispheres consist of a frontal, temporal, parietal and occipital lobe and the two hemispheres are connected by the corpus callosum, which allows communication across the two sides (Ackerman, 1992). The surface of the cerebrum is made up of billions of neurons and glia which form the cerebral cortex, commonly known as the grey matter. The cerebral cortex is characterised by its folded appearance made up of numerous sulci (small grooves) and fissures (large grooves) on its surface, with the bulges between these grooves known as gyri. The ventricular system consists of four cavities within the brain, known as ventricles. The two lateral

ventricles are located within the cerebral hemispheres and are connected to the third ventricle by the Foramen of Munro. The third ventricle is situated in the middle of the brain and is connected to the fourth ventricle by the Aqueduct of Sylvius. The cerebellum sits under the back of the occipital lobes and serves to fine tune motor functions. The thalamus and hypothalamus sit in the core of the brain, just above the brainstem. The thalamus comprises two oval structures, containing nerve cell bodies, responsible for relaying sensory information to the cerebral cortex. Below the thalamus and just above the pituitary gland sits the hypothalamus, which is the main point of interaction for the CNS and the endocrine system. The hypothalamus also regulates body temperature, hunger, thirst, emotional response and sexual function. The pituitary and pineal glands interact with the hypothalamus to produce hormones. The pituitary gland produces human growth hormone, dopamine and thyroid-stimulating hormone amongst others and the pineal gland produces melatonin, a powerful regulator of the sleep-wake cycle (Zhu *et al.*, 2007, Aulinas, 2019). The brainstem extends from the lower part of the brain, in front of the cerebellum and connects brain to spinal cord. It relays messages between the cerebral cortex and the rest of the body and is responsible for many primitive and essential functions such as breathing and heartbeat (Ackerman, 1992). On the external posterior surface of the brainstem are the superior and inferior colliculi, which function to orient the head and eyes to auditory and visual stimulus.

1.3.2 Brain development

Development of the embryonic brain begins with formation of the neural groove (18 postovulatory days), followed by initiation of neurulation two days later, during which the neural tube, the precursor of the brain and spinal cord, is formed from the neural plate (O’Rahilly and Müller, 1994). The inner cells of the neural tube go on to form the central nervous system (CNS) and the outer cells form the autonomic nervous system (ANS) (Tierney and Nelson, 2009). Once neural tube formation is complete, cells of the inner area of the tube, known as the ventricular zone (VZ) proliferate extensively. This extensive proliferation leads to the new-born brain containing more neurons than an adult brain. Subsequent genetically regulated apoptosis decreases the number of neurons by over 50 % to the number present in the adult brain (Mazarakis *et al.*, 1997). Following proliferation, the resulting cells including neurons and glia migrate from the VZ outwards to form cortical layers (Fritsch and Northcutt, 1993, Herculano-Houzel, 2009). At 25 weeks of gestation the 6 layers of the cortex are formed. Once neurons reach their final destination, they either differentiate to form mature neurons or undergo apoptosis. Once mature neurons have developed

axons and dendrites, synapses form via a process known as synaptogenesis (Molliver *et al.*, 1973).

1.3.3 Cell types of the brain

Neural stem cells

Neural stem cells (NSC) are multipotent progenitor cells that are capable of self-renewal and generation of all types of neurons, astroglia and oligodendrocytes (Kempermann *et al.*, 2015). These cells play a key role in both embryonic neural development and also in adult neurogenesis. There are several types of neural stem, and more committed progenitor, cells present in the developing brain, including neuroepithelial cells of the VZ of the neural tube and radial glia (RG) (Alvarez-Buylla *et al.*, 2001). Both neuroepithelial and RG cells are capable of both symmetrical and asymmetric divisions. Asymmetric division of neuroepithelial NSCs can give rise to a more differentiated NSC such as RG, or a neuron, whereas RG give rise to more differentiated progenitor cells or neurons and are responsible for producing the majority of neurons in the developing brain (Noctor *et al.*, 2008, Shitamukai *et al.*, 2011).

Neural progenitor cells

Neural progenitor (NP) cells reside in both the embryonic and adult brain and give rise to both glial and neuronal cell types. It is thought that embryonic NP's also give rise to adult NP's (lineage summarised in figure 1.9) (Merkle *et al.*, 2004). Embryonic NP cells exist within two distinct niches. The VZ, which appears first during development and is located adjacent to the ventricle (Tramontin *et al.*, 2003). Later in development the subventricular zone (SVZ) forms on the outside of the VZ. The ventricular zone contains RG, which appear through differentiation of the neuroepithelial cells of the neural tube (Aaku-Saraste *et al.*, 1996). RG initially undergo symmetrical division to increase the RG pool, before undergoing asymmetrical division to produce an RG and neuronal daughter cell (Takahashi *et al.*, 1996, Malatesta and Götz). Asymmetric RG division can also produce NP daughter cells known as intermediate progenitors (IP), that migrate to the SVZ before symmetrical division resulting in two neurons (Noctor *et al.*, 2004). IP can be distinguished from bipolar RG by their multipolar morphology and expression of a transcription factor called Tbr2 (Englund *et al.*, 2005). Adult NP cells also exist within two distinct niches, the "adult SVZ", which surrounds the lateral ventricles of the cerebral cortex and the subgranular zone (SGZ) of the dentate gyrus. The adult NP cells of the SGZ have similar properties to those of embryonic RG and are therefore often referred

to as “RG-like” cells or type 1 cells (Martínez-Cerdeño and Noctor, 2018). These cells can give rise to IP cells, which share properties with embryonic IP, including expression of *Trb2*. NP cells of the adult SVZ exhibit astrocytic properties and can differentiate to form glia and neurons (Doetsch *et al.*, 1999). Adult NP cells are responsible for adult neurogenesis, which occurs throughout adulthood and into old age in humans (Eriksson *et al.*, 1998, Kempermann *et al.*, 2018). The stimuli for neurogenesis and neuronal differentiation are vast and complex. Pathways that have been implicated include notch, hedgehog, MAPK, BMP, ERK and FGF among many others (Chuang *et al.*, 2015). Adult human NP cells are highly expandable *in vitro* (Walton *et al.*, 2006).

Neurons

There are an estimated 86 billion neurons in the adult brain, which are responsible for sending and receiving signals within the brain and the rest of the body, through electrical and chemical signalling (Ackerman, 1992, Azevedo *et al.*, 2009). Neurons comprise three distinct structures, the soma (cell body), axon and dendrites. Action potentials are generated from the soma and travel down the long tail like projection of the axon, triggering release of neurotransmitters or electrical transmission across the synapse through direct contact between the pre-synaptic and post-synaptic neuron to perpetuate the signal to the next cell (Debanne *et al.*, 2011). Action potentials are generated and propagated through changes in the cationic gradient across the cell membrane via adenosine triphosphate (ATP)-dependant pumps which transport sodium out of the cell and potassium in (Kole and Stuart, 2012). The opening of voltage gated ion channels allows ions to flow down their electrochemical gradients causing a shift in the neuronal membrane potential. The dendrites of neurons appear like small branches protruding from the soma and their function is to receive signals from nearby axons (Nimchinsky *et al.*, 2002). Neurons are specialised according to their function and can be broadly split into four categories, sensory neurons, motor neurons, interneurons and neurons of the brain. Distinction and categorisation of the neurons within the brain is much more complex, with hundreds of named neuronal cell types within the human brain (Masland, 2004).

Astrocytes

Astrocytes are cells of the glial lineage with branched processes and star-like morphology that outnumber neurons by fivefold in the brain (Nedergaard *et al.*, 2003). Whilst initially it was thought that the role of astrocytes was simply to support neurons, more recent work has shown that they play a more crucial active role in the CNS and are now known to modulate neuronal behaviour as well as providing structural support and contributing to the blood brain barrier

(Halassa *et al.*, 2010). One of the most important functions of astrocytes is the uptake and release of neurotransmitters such as gamma-aminobutyric acid (GABA), which is important for optimising synaptic function (Kinney *et al.*, 2002). Astrocytes also play a key role in reacting to damaged brain tissue, during which time they undergo significant morphological and biochemical changes and are termed “reactive” astrocytes (Wilhelmsson *et al.*, 2006). It is thought that astrocytes are responsible for guiding the neurorepair process, neurogenesis and re-establishment of homeostasis after injury (Acosta *et al.*, 2017). Astrocytes respond to signalling from neurons and can in turn signal to neurons through calcium signalling and calcium dependant glutamate release (Fiacco *et al.*, 2009).

Oligodendrocytes

Oligodendrocytes are the myelinating cells of the CNS and are generated through the migration, proliferation and differentiation of oligodendrocyte progenitor cells (OPC) (Kuhn *et al.*, 2019). Oligodendrocytes are critical for axonal myelination following damage through injury, particularly due to diseases that cause loss of myelin such as multiple sclerosis (Nave, 2010).

Microglia

Microglia account for around 10 % of the cells in the brain and are macrophages that reside throughout the CNS (Pelvig *et al.*, 2008). As well as being the principal immune cells of the brain also play a key role in maintaining normal brain function (Kettenmann *et al.*, 2011). Their functions include nourishing and supporting neurons and clearing cell debris. Resting microglia detect changes in their environment such as trauma, neurodegeneration and infection and respond to this by undergoing rapid changes in gene expression and morphology, resulting in microglial activation (Streit *et al.*, 2004). Microglia detect nearby damage through the identification of neurodegeneration-associated molecular patterns (NAMPs), in a mechanism very similar to that of the peripheral immune system’s pathogen- and damage-associated stress signals (PAMPs and DAMPs)(Deczkowska *et al.*, 2018). Following activation, microglia migrate to the affected site where they undergo proliferation where they can release an array of cytokines depending on the specific stimuli and also perform phagocytosis (Kettenmann *et al.*, 2011).

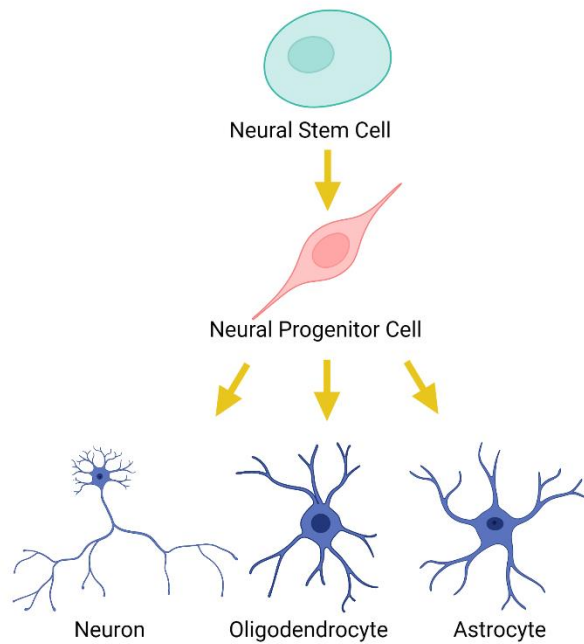


Figure 1.9 Neural progenitor cell lineage

Diagram of neural progenitor cell lineage. Neural stem cells give rise to neural progenitor cells, which can subsequently give rise to neurons, astrocytes and oligodendrocytes through differentiation (created with BioRender.com).

1.3.4 HCMV infection of the brain

HCMV infection profoundly affects the neonatal brain, with resulting structural abnormalities observed as early as 28 weeks of gestation in foetal imaging studies (Barkovich and Girard, 2003, Malingier *et al.*, 2003). Studies of neonatal HCMV CNS infection are mainly restricted to observational and histopathological findings, yet mouse models and clinical data show that the neonatal brain is more susceptible to MCMV and HCMV respectively, than the adult brain (van den Pol *et al.*, 2002). Congenital HCMV infection is disseminated and penetrates the blood-brain barrier through carriage in mononuclear cells (Koontz *et al.*, 2008). However, adult mice are resistant to MCMV invasion of the adult brain following peripheral infection and the same is thought to be true in the adult human brain in immunocompetent individuals, due to the lack of neurological sequelae (Reuter *et al.*, 2004). However, in immunocompromised mice, CNS MCMV infection was observed in multiple cell types. HCMV infection of the adult brain is also seen in immunocompromised humans and is known to be the most frequent opportunistic infection in the CNS of AIDS patients (Setinek *et al.*, 2005). In very rare cases HCMV associated encephalomyelitis has been reported in

immunocompetent adults, though why this occurs is unknown (Daida *et al.*, 2016).

In vitro studies have shown that almost all brain derived cell types are susceptible to HCMV infection. Brain microvascular cells, astrocytes, neurons, oligodendrocytes, microglia, and both neural stem and progenitor cells can all be infected (summarised in figure 1.10) (Fish *et al.*, 1998, Lokensgard *et al.*, 1999, Poland *et al.*, 1990, Spiller, Borysiewicz and Morgan, 1997, Pulliam, Moore and West, 1995, Cheeran *et al.*, 2005, McCarthy, Auger, Whittemore, 2000). The ability to support full viral replication varies between these cell types, with neural stem and progenitor cells being more permissive. In histopathological analysis of acute HCMV infection in the neonatal brain, astrocytes have been found to be the predominant infected cell type and have been shown *in vitro* to be fully permissive and able to support HCMV replication (Teissier *et al.*, 2014, Lokensgard *et al.*, 1999). Brain resident immune cells, microglia, have been shown to be HCMV+ in congenital infection and can also be infected *in vitro* (Lecointe *et al.*, 1999). HCMV+ neurons are detected in infected foetal brain tissue, though HCMV+ neurons are far less common than HCMV+ astrocytes (Gabielli *et al.*, 2012, Teissier *et al.*, 2014). Opposing information about the permissiveness of neurons *in vitro* ranges from zero to fully permissive, with some suggestions that neurons could be a potential reservoir for HCMV latency (Luo *et al.*, 2008, Cheeran *et al.*, 2005). Characterisation of HCMV infection of oligodendrocytes is limited, although human oligodendroglioma cell lines support productive HCMV infection *in vitro* (Spiller and Morgan, 1997). Histopathology of congenitally HCMV infected foetal brains shows HCMV+ ependymal cells (the cells that line the ventricles), and ependymal cell lines are permissive to HCMV infection *in vitro* (Gabielli *et al.*, 2009, Abdi *et al.*, 2018). Foetal NP cells are infected during congenital HCMV infection and are the most infected brain cell type in mouse models of congenital infection (Perlman and Argyll, 1992, Luo *et al.*, 2010). Luo *et al.* (2008) showed that foetal NP cells were also permissive to HCMV *in vitro* and that infection leads to aberrant differentiation. Similarly, HCMV infection of NSCs also leads to abnormal differentiation (Roland *et al.*, 2016). In studies of embryonic stem cell derived NSCs, HCMV infection was non-productive due to a block in transition from IE to early gene expression. Whilst this block was partially reversed through differentiation, infection was still non-productive, suggesting that such cells may be able to support latent infection (Belzile *et al.*, 2014); HCMV genomes were detectable in NSCs for over one month post infection.

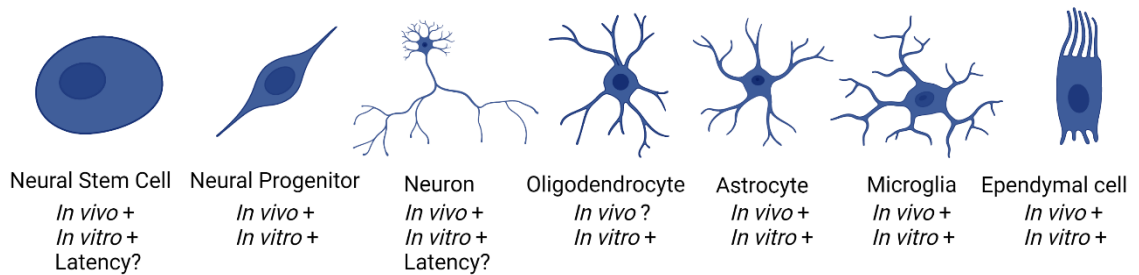


Figure 1.10 Summary of HCMV infection of brain cell types

Summary of HCMV permissiveness of human neural stem cells, neural progenitor cells, neurons, oligodendrocytes, astrocytes, microglia and ependymal cells *in vitro* and *in vivo*.

1.4 Glioblastoma

1.4.1 Background and features

Glioblastoma (GBM) is the most common type of malignant primary brain tumour in the adult population, representing ~45 % of all primary malignant brain tumours (Ostrom *et al.*, 2013). GBM is a World Health Organisation grade IV, highly infiltrative and aggressive form of glioma (tumours derived from neuroglial cells), which is notoriously difficult to treat and no curative therapy is currently available (Louis *et al.*, 2016). Incidence of GBM is rising, with rates in England more than doubling between 1995 and 2015 (Philips *et al.*, 2018). Current survival rates are less than 5 % after five years, with an average survival of 12 – 18 months from diagnosis (Tamimi and Juweid, 2017).

Around 90 % of GBM arise as a primary *de novo* tumour, but can also occur as a secondary tumour developing from a lower grade lesion (Ohgaki and Kleihues, 2012). Secondary GBM often arise through mutations in the IDH1 gene which encodes the metabolic enzyme isocitrate dehydrogenase (Bleeker *et al.*, 2010). IDH1 mutations cause extensive metabolic reprogramming, epigenetic shift and therapeutic resistance (Dang *et al.*, 2009, Grassian *et al.*, 2014). One of the main difficulties in developing effective GBM treatments is the high level of both intra- and inter-tumour heterogeneity.

1.4.2 Glioblastoma subtypes

GBM can be classified into four molecular subtypes, namely: proneural, neural, classical, and mesenchymal (Verhaark *et al.*, 2010). Proneural GBM often exhibit amplification or mutation in PDGFR α , which leads to activation of the phosphoinositide 3-kinases - protein kinase B (PI3K-Akt) and rat sarcoma virus

(RAS) pathways. Mutations in IDH1, as well as the tumour suppressor TP53, are also common in this subtype. Proneural tumours often express high levels of common oligodendrocytic markers such as NK2 Homeobox 2 (NKX2-2) and oligodendrocyte transcription factor 2 (OLIG2). This subtype is also associated with a cell cycle and proliferation gene signature.

Neural GBM tumours express high levels of genes normally present in differentiated cell types, particularly those associated with neurons such as neurofilament light chain (NEFL), gamma-Aminobutyric Acid Type A Receptor Subunit Alpha1 (GABRA1), synaptotagmin 1 (SYT1) and solute carrier family 12 member 5 (SLC12A5). Classical GBM is associated with amplification of chromosome 7 and chromosome 10 loss, with high-level epidermal growth factor receptor (EGFR) amplification and mutation. Classical GBM differ from the other subtypes in that they often lack TP53 mutations. By contrast, the stem cell marker nestin, notch pathway, and sonic hedgehog signalling genes are frequently expressed at high levels in this subtype. Classical GBM are astrocyte-like in overall phenotype. Finally, the mesenchymal GBM subtype regularly display lower neurofibromatosis type 1 NF1 (NF1) expression levels, alongside mutations in this gene. This subtype is characterised by expression of both mesenchymal and astrocytic markers, including genes associated with epithelial to mesenchymal transition. High expression of NF- κ B pathway genes is also associated with this subtype.

1.4.3 GBM stem cells

The cancer stem cell (CSC) model states that cancer cells are hierarchically organised within tumours and that a population of so-called “cancer stem cells” exists, which drives tumour growth and shares properties with normal stem cells (Kreso and Dick, 2014). CSCs have been reported in many common malignancies including leukaemia, breast cancer, colorectal cancer, liver cancer and brain tumours (Uckun *et al.*, 1995, Al-Hajj *et al.*, 2003, O'Brien *et al.*, 2007, Singh *et al.*, 2004). Similar to normal stem cells, CSCs are capable of self-renewal, asymmetric division and differentiation, which is posited to drive intra-tumour heterogeneity (Bao *et al.*, 2013). GBM contains glioblastoma stem cells (GSC) identified via expression of cell surface markers including CD133 and CD44. However, the highly heterogeneous nature of GBM means that there is no universally expressed GSC marker (Clarke *et al.*, 2003).

It is currently unclear whether such cells originate from tissue-resident adult neural stem/progenitor cells, or through the de-differentiation of terminally differentiated cell types, such as astrocytes and oligodendrocytes. GSCs have

been shown to confer resistance to treatments such as chemotherapy and radiotherapy and following escape of such therapies, GSCs drive tumour recurrence, particularly in mesenchymal GBM (Wang *et al.*, 2021). Due to the innate plasticity of GSCs, it is not unusual for recurrent tumours to be distinctly different to the primary tumour, including therapy induced switching of GBM subtype, particularly from proneural to treatment resistant mesenchymal (Wang *et al.*, 2016, Halliday *et al.*, 2014). GBM cells treated with the anti-GBM chemotherapeutic temozolomide *in vitro* acquired CD133 expression and exhibited a phenotypic switch gaining stem cell-like traits (Lee *et al.*, 2016).

1.4.4 GBM origins

The cell of origin for GBM remains unclear, with some studies suggesting NSC in the SVZ and some suggesting OPC as the origin (Llaguno *et al.*, 2009, Liu *et al.*, 2011). Other studies have postulated that gliomagenesis begins in dedifferentiated neurons or astrocytes (Vitucci *et al.*, 2017, Friedmann-Morvinski *et al.*, 2012). Some research has suggested that rather than there being a universal cell of origin for GBM, that different cells of origin may give rise to different pathological subtypes. For example Lei *et al.* (2011) found that GBM originating from inducing transforming genetic lesions to glial progenitors in mouse brains led specifically to proneural GBM. Interestingly, ablation of Olig2 can switch proneural, OPC derived tumours to a classical subtype, whereas over-expression of transcriptional coactivator with PDZ-binding motif (TAZ) or suppression of NF1 causes a switch to the mesenchymal subtype (Lu *et al.*, 2016, Bhat *et al.*, 2011). The process of gliomagenesis remains poorly defined, largely due to the extensive genetic heterogeneity of GBM and the unknown cell of origin. It is likely that gliomagenesis is as heterogeneous as GBM itself, arising from a variety of cell types with many different mutations (Shao and Lieu, 2018).

1.4.5 Signalling pathways in GBM

The highly mutated genomes of GBM result in dysregulation of many signalling pathways that contribute to the aggressive nature of these tumours. Key signalling pathways that are modulated in GBM include those regulating growth, proliferation, survival and apoptosis (Mao *et al.*, 2012).

P53 signalling pathway

The p53 pathway is commonly deregulated during the tumourigenesis of many cancers and is thought to be the most frequently mutated gene across all malignancies (Lawrence *et al.*, 2014). P53 itself is a tumour suppressor that

responds to DNA damage and other cytotoxic stress by initiating cell cycle arrest and apoptosis (Baker *et al.*, 1999). As well as its well characterised role in tumour suppression, p53 also functions as a transcription factor, regulating over 2500 genes; p53 mutations can therefore contribute to tumourigenesis, tumour development and invasion (Sullivan *et al.*, 2013). It is estimated that 85 % of GBM display p53 pathway dysregulation. (Brennan *et al.*, 2013). The frequency of p53 mutations in GBM differs according to molecular subtype, with 54 % of proneural, 32 % of mesenchymal, 21 % of neural and 0 % of classical tumours having p53 mutation (Verhaark *et al.*, 2010). Interestingly, while p53 mutations in primary GBM are varied and widely distributed, p53 mutations that occur in secondary GBM are predominantly located within two codons, namely 248 and 273 (Ohgaki *et al.*, 2007). Several p53 regulators including MDM2, MDM4 and ARF also modulate the p53 signalling pathway in GBM through mechanisms independent of direct p53 mutations (Riemenschneider *et al.*, 1999, Labuhn *et al.*, 2001).

PI3K/Akt/mTOR signalling pathway

The PI3K/Akt/mTOR signalling pathway regulates a variety of cellular functions, including proliferation, differentiation, migration, metabolism and survival (Engelman *et al.*, 2006). PI3K alterations are present in ~70 % of GBM, predominantly through deletion of the tumour suppressive phosphatase and tensin homolog (PTEN). Constitutive pathway activation can also occur via amplification of receptors such as EGFR, vascular endothelial growth factor receptor (VEGFR) and PDGFR (Zhi *et al.*, 2009). Constitutive PI3K activation is thought to play a key role during gliomagenesis, tumour development and is associated with increasing grade of glioma, decreased apoptosis and poor prognosis (Chakravarti *et al.*, 2003). Importantly, PI3K activation dampens the effects of the standard GBM chemotherapeutic temozolomide and promotes therapeutic resistance (Stupp *et al.*, 2005). mTOR functions as both a regulator and downstream effector of PI3K, making it a key pathway in GBM development (Akhavan *et al.*, 2010). The mTOR protein complex itself comprises two sub-complexes, mTORC1 and mTORC2. The oncogenic effects of mTORC1 include driving oncogene translation, autophagy inhibition, upregulation of hypoxia-inducible factor 1 α (HIF1 α) and activation of sterol regulatory binding element protein 1C (SREBP1c). Similarly, mTORC2 also exerts oncogenic effects including stimulating glucose uptake via Akt activation and activating serum/glucocorticoid regulated kinase (SGK), which increases both proliferation and survival (Zoncu *et al.*, 2011).

RAS/MAPK signalling pathway

RAS genes are a related group of transforming oncogenes, belonging to the G-protein family (Hurley *et al.*, 1984). Activated RAS directly binds and activates rapidly accelerated fibrosarcoma (RAF) kinase, which subsequently regulates the downstream MAPK pathway that regulates cell proliferation, differentiation, motility, and survival (Moodie *et al.*, 1993, Cargnello and Roux, 2011). Cellular effects of MAPK signalling are context dependent, with MAPK activation involved in several normal brain functions, including initiation of cortical neurogenesis. Around 88 % of gliomas have dysregulation of the MAPK signalling pathway which leads to a more invasive and proliferative phenotype (Gao *et al.*, 2005). Many GBMs have high levels of phosphorylated MAPK, which correlates with poor overall survival and resistance to radiotherapy (Marwin *et al.*, 2003, Pelloski *et al.*, 2006).

JAK/STAT signalling

The JAK/STAT signalling pathway mediates downstream events including haematopoiesis, immune fitness, tissue repair, inflammation, apoptosis, and adipogenesis (Owen *et al.*, 2019). JAK/STAT signalling is active in many cancers including GBM (Thomas *et al.*, 2015). The STAT family of transcription factors is activated through phosphorylation as a downstream effect of other signalling pathways (Dekker and Kovarik, 2000). Whilst STAT1 was originally deemed a tumour suppressor, recent evidence shows that increased STAT1 signalling is associated with poor prognosis (Thota *et al.*, 2014). STAT1 expression was initially thought to lead to decreased proliferation and increased apoptosis in GBM (Ju *et al.*, 2013). However, other studies present contrasting evidence that STAT1 expression in GBM leads to increased growth, migration, invasion, and mesenchymal transition, suggesting that the effects of STAT1 may be context dependant (Meng *et al.*, 2015, Duarte *et al.*, 2012). STAT5 expression is linked to gliomagenesis, and confers increased proliferation and invasion in GBM (Liang *et al.*, 2009, Cao *et al.*, 2010). STAT3 is the best-known member of the STAT family, due to its oncogenic and immunosuppressive function. Whilst gain of function STAT3 mutations have not been reported in GBM, constitutive EGFR activation is common in GBM and leads to STAT3 signalling dysregulation (Lo *et al.*, 2008). A lack of various negative regulation mechanisms of STAT3 has also been described in GBM (Veeriah *et al.*, 2009, Martini *et al.*, 2008).

1.4.6 Current GBM treatments

Current treatment for GBM is usually a multimodal approach, which most commonly consists of a combination of tumour debulking surgery, chemotherapy and radiotherapy. The standard initial approach is to perform resection to remove as much tumour as it is safe to take out, which is sent for histopathological examination to determine the diagnosis. Upon diagnosis of GBM, resection is followed by 60 gray radiotherapy over a six week period with concomitant chemotherapeutic temozolomide. After the initial six weeks, six subsequent cycles of maintenance temozolomide are given (Tan *et al.*, 2020). Antimitotic tumour treating fields (TTF), a non-invasive treatment, can also be employed alongside temozolomide for patients with disease in the upper parts of the brain and have been shown to prolong survival in eligible patients (Stupp *et al.*, 2017). TTF deliver low intensity, alternating electric fields, which are delivered via transducer arrays applied to the scalp.

After initial treatment, the majority of GBM patients face recurrence, at which point treatment regimens are less well defined, but often consist of alkylating chemotherapeutics such as lomustine and carmustine or rechallenge with temozolomide. Bevacizumab, a monoclonal antibody that targets VEGF is also used in some countries, although its efficacy is unclear due to lack of overall survival increase in clinical trials (Kreisl *et al.*, 2008). Whilst immunotherapy has been successfully employed for many different types of cancer, there is yet to be a widely accepted immunotherapy for GBM despite extensive research (Tan *et al.*, 2020). The CNS has a unique immune environment, making targeted immunotherapy of the brain and therefore GBM more difficult than other tissues and organs. For example, GBM have far lower levels of infiltrating lymphocytes than other tumour types and also exert an immunosuppressive effect within the tumour microenvironment (Li *et al.*, 2016, Heimberger *et al.*, 2007).

1.5 HCMV in glioblastoma

1.5.1 Detection of HCMV in GBM

Cobbs *et al.* (2002) first reported the presence of HCMV in glioma, including GBM, detecting HCMV IE1 in 27 of 27 GBM samples by immunohistochemistry (IHC) and in situ hybridisation (ISH). Following this initial observation, several groups have attempted to recapitulate the findings using a variety of detection methods with disparate results. A study conducted by Scheurer *et al.* (2008) addressed several factors that could attribute the conflicting evidence for the presence of HCMV in glioblastoma to technical variations. Scheurer *et al.* discuss in detail several crucial steps in their optimised IHC and ISH protocols that can

be the difference between a positive and false negative result. The study detected HCMV in 21/21 GBM samples. Interestingly, only GBM samples showed cytoplasmic HCMV IE expression, whereas other low-grade tumours had purely nuclear IE as is expected for IE. One explanation for this is that minor IE isoforms could be present in the cytoplasm of GBM such as IE1x4, a smaller IE1 isoform that has been detected in latently infected haematopoietic progenitors and is associated with viral genome maintenance (Tarrant-Elorza *et al.*, 2014). Ranganathan *et al.* (2012) note that fresh frozen tissue is better for detecting HCMV by polymerase chain reaction (PCR) than paraffin embedded samples which may also explain the disparity in detection of HCMV in GBM in other studies. Low viral copy number and high diversity in clinical specimens of HCMV could also account for high levels of variability in detection rates of HCMV genomes by PCR. Overall, it appears that HCMV protein was reliably detected, whereas detection of HCMV nucleic acids was less reliable. A systematic review by Peredo-Harvey *et al.* (2021) stated that HCMV was detected in 1391 (84.2%) of 1653 samples when studies employed optimised immunohistochemical techniques. Additionally, HCMV DNA and viral proteins have been detected in a multitude of other cancers including breast cancer, colorectal cancer, prostate cancer, mucoepidermoid carcinoma, medulloblastoma, and neuroblastoma, though viral particles have not been detected (Chen *et al.*, 2014, Kumar *et al.*, 2018, Melnick *et al.*, 2012, Baryawno *et al.*, 2011, Wolmer-Solberg *et al.*, 2013). HCMV seropositivity has been shown to be associated with a higher risk of all-cancer mortality. However, the nature of this link remains unclear and may be associated with socioeconomic status or other risk factors rather than direct effects from HCMV infection (Okedele *et al.*, 2020). HCMV positivity in ovarian adenocarcinoma has potential effects on patient survival with patients with HCMV pp65+ tumours having median overall survival of 18.2 months versus 54 months in those with pp65- tumours (Carlson *et al.*, 2018). Similarly, detection of HCMV IE and pp65 is common in epithelial ovarian cancer, with 82 % of tumours IE+ and 97 % pp65+. In benign ovarian tumours in the same study, 36 % were IE+ and 63 % pp65+ suggesting HCMV infection may increase the risk of ovarian cancer. Additionally, high IE expression was shown to indicate poor prognosis (Yin *et al.*, 2020). Meta-analysis of data for 11 studies of HCMV detection in colorectal cancers found a statistically association between HCMV infection and an increased risk of colorectal cancer (Bai *et al.*, 2016).

1.5.2 Potential oncogenic or oncomodulatory effects of HCMV in GBM

Whilst it is now widely accepted that HCMV antigens are present in GBM and other gliomas, its potential role as an oncogenic versus a oncomodulatory agent remains unclear. Oncomodulation is defined as cancer cells acquiring enhanced malignant traits following viral infection, rather than undergoing direct viral transformation (Barami, 2010). The concept of oncomodulation implies that HCMV infects established tumour cells, where it modulates the malignant properties of the cells through effects on survival, proliferation, cell cycle and immunodetection amongst others. Many studies have investigated the role of HCMV in GBM pathogenesis, with an array of potential oncogenic effects identified. One such effect is activation of the PI3K-Akt pathway which is known to be hyperactivated in around 90 % of GBM (Fan *et al.*, 2010). Activation of the PI3K-Akt by HCMV gB binding of EGFR is required initially for viral entry and later sustained activation by IE1 and IE2 is needed for optimal viral gene expression and viral DNA replication (Alwine *et al.*, 2002). In the later stages of infection, activation of EGFR and PI3K by interaction with viral UL135 and UL138 promotes latency (Buehler *et al.*, 2016). Sustained PI3K-Akt activation in HCMV infected monocytes is crucial for their long-term survival (Cojohari *et al.*, 2016). Infection of human astro-glia and glioma cells with HCMV led to rapid activation of the PI3K-Akt pathway and increased migration and invasion (Cobbs *et al.*, 2007).

HCMV US28 encodes a chemokine receptor, which is posited as a potential viral oncogene (Maussang *et al.*, 2006). US28 expression has been detected in around 60 % of GBM samples and it is known to bind multiple human chemokines, including CCL2, CCL5, and CX3CL1 (Slinger *et al.*, 2010). US28 expression promotes tumourigenesis through increased proliferation and angiogenesis in a mouse model (Maussang *et al.*, 2006). This is likely due to the fact that US28 has been shown to constitutively activate NF- κ B, increasing COX-2 expression and activity and also enhances VEGF expression through IL-6 mediated STAT3 activation (Maussang *et al.*, 2009, Slinger *et al.*, 2010). Additionally, activation of hypoxia inducible factor 1alpha/pyruvate kinase M2 (HIF-1alpha/PKM2) by US28 also upregulates VEGF and increase proliferation (de Wit *et al.*, 2016).

HCMV infection has been shown to enhance the stem cell properties of glioma cells (Soroceanu *et al.*, 2015). Soroceanu *et al.* (2015) demonstrated that HCMV IE proteins promote stemness and that HCMV IE is preferentially expressed in the stem-like cells within GBM samples. HCMV IE proteins have been shown to

colocalise with stem cell markers including CD133, nestin and Sox2. Further to this, RNAi against HCMV IE prevented tumoursphere formation, cell cycle progression and survival. The reverse was demonstrated in HCMV negative GBM cells infected with HCMV which increased self-renewal and proliferation. Fornara *et al.* (2016) also found that HCMV infection of GBM cells led to increased expression of stem cell markers Notch1, sex determining region Y box 2 (Sox2), octamer-binding transcription factor 4 (Oct4) and Nestin and reported that high CD133 and HCMV IE expression correlated with poor prognosis in GBM patients. They also found that HCMV infection conferred the ability to form neurospheres to GBM cells, which was prevented through treatment with GCV. Importantly, GBM cells with IE expression failed to differentiate into neurons or astrocytes.

Activation of telomerase by HCMV is potentially oncogenic, as telomerase activation expression through expression of the telomerase reverse transcriptase (TERT) gene is known to lead to immortalisation and transformation of cells (Lee *et al.*, 2004). HCMV infection of TERT negative normal human fibroblasts was shown to induce constitutive TERT expression and subsequent telomerase activity due to IE1 interaction with the TERT promoter region, increasing Sp1 binding (Straat *et al.*, 2009). Further to this, GBM samples showed co-localisation of HCMV IE and TERT, with TERT expression levels correlating with IE levels.

HCMV suppresses apoptosis through increasing the expression of anti-apoptotic protein activating transcription factor 5 (ATF5) (Wang *et al.*, 2014). ATF5 is abundantly expressed in GBM and is essential for glioma cell survival (Sheng *et al.*, 2010). Additionally, it has been shown to inhibit apoptosis in both glioma and breast cancer (Monaco *et al.*, 2007). Several HCMV products have been associated with inhibition of apoptosis, including IE1, IE2, pUL38 and RNA 2.7. The mechanisms through which IE1 and IE2 prevent apoptosis remain unclear, though it is known that they affect several key signalling pathways, particularly activation of PI3k-Akt, which is a well-known pro-survival signalling pathway in glioma (Cobbs *et al.*, 2007). UL38 encodes a cell death inhibitory protein that blocks proteolytic cleavage of caspase 3 and poly(ADP-ribose) polymerase, two key enzymes involved in apoptosis (Terhune *et al.*, 2007). Additionally, UL38 expression can suppress the ER stress response, thus avoiding apoptosis (Qian *et al.*, 2011). Reeves *et al.*, (2005) showed that HCMV RNA β 2.7 prevented apoptosis in HCMV infected neuronal cells. HCMV IE2 inhibits activity of the tumour suppressor p53 (Tsai *et al.*, 1996).

HCMV employs a variety of immune evasion strategies, including inhibition of detection and activation of natural killer (NK) cells and inhibition the MHC class I and II pathways preventing the recognition of CD4+ and CD8+ T-cells (Hewitt, 2003, Krough and Khanna, 2009). HCMV encoded IL-10 (vIL-10) also suppresses T-cell function (Vossen *et al.*, 2002). HCMV has been shown to manipulate the tumour environment, with tumour associated macrophages (TAM) found in several cancers associated with HCMV, including GBM (Mantovani *et al.*, 2017). TAM from HCMV+ GBM display the M2 phenotype, which responds to vIL10 by promoting angiogenesis and enhanced migration (Dziurzynski *et al.*, 2011).

Perhaps the most compelling evidence for an oncogenic role for HCMV comes not from GBM, but from breast cancer. HCMV infection of primary human mammary epithelial cells (HMECs) has been shown to transform them, leading to spheroid formation and development of fast growing triple negative tumours upon transplantation into mice (Kumar *et al.*, 2018). HCMV transformed cells formed tumours with a distinct viral gene signature associated with long noncoding RNA 4.9 (lncRNA 4.9). This finding was supported by the presence of HCMV lncRNA 4.9 in tumour biopsies from breast cancer patients. Nehme *et al.* (2021), found HCMV to be capable of reprogramming HMECs through de-differentiation to generate a polyploid giant cancer cell (PGCC) phenotype. PGCC's exhibit stem cell-like features and are associated with metastasis, recurrence, drug resistance and overall poor prognosis (Zhang *et al.*, 2014). Such cells are highly tumourigenic, with a single PGCC capable of forming a spheroid and subsequent tumour upon transplantation to immunodeficient mice. Notably, PGCC derived tumours are mesenchymal and express high levels of the cancer stem cell markers CD133 and CD44, which are also associated with GSCs. Interestingly, there exist both high and low risk clinical strains of HCMV and whilst infection of HMECs with high risk HCMV strains form tumours *in vivo*, low risk strains do not (Ahmad *et al.*, 2021). High-risk strains confer several oncogenic properties to HMECs increased oncogene expression, cell survival, proliferation, and epithelial-mesenchymal transition.

Whilst HCMV induces an array of oncogenic and oncomodulatory effects in multiple cell and tumour types, other studies have found HCMV infection to have the opposite effect. Notably, HCMV infection of two mesenchymal breast cancer lines, MDA-MB-231 and SUM1315, led to mesenchymal to epithelial transition and decreased migratory capacity (Oberstein and Shenk, 2017). Whilst some studies have suggested that HCMV enhances tumourigenicity in human liver cancer line, HepG2, one study found that HCMV+ HepG2 had less tumourigenic

capacity *in vivo*, than non-infected controls, suggesting HCMV is anti-tumourigenic in this cell type (Kumar *et al.*, 2016).

| HCMV protein | Biological function | Oncogenic effect |
|-----------------|---|--|
| IE1 | Entry into S phase | Cellular proliferation |
| | Suppression of p53 and Rb activity | Evading growth suppressors |
| | Dysregulation of cyclin E expression | Immortality |
| | Activation of telomerase | Inflammation |
| | Induction of IL-1 | Enhanced cell survival |
| | Inhibition of apoptosis | Genome instability and mutation |
| IE2 | Entry into S phase | Cellular proliferation |
| | Binding to p53 | Evading growth suppressors |
| | Activation of PI3K/Akt pathway | Enhanced cell survival |
| | Induction of TGF-beta expression | Increased immune suppression |
| pUS28 | IL-6/JAK/STAT3 activation | Cellular proliferation |
| | Activation of RhoA dependent mobility of U373 cells | Tumor growth |
| | Induction of VEGF expression | Enhanced angiogenesis |
| pUL111A (vIL10) | NF-kB activation | Cellular proliferation, migration and metastasis |
| | STAT3 activation | Telomerase activation |
| | Production of homologs to immunosuppressive cytokines | Increased immune suppression |
| pUL76 | Chromosomal breaks | Genome instability and mutation |
| | Induction of chromosomal aberrations | |
| pUL97 | Phosphorylation and inactivation of pRb | Evading growth suppressors |
| pUL82 (pp71) | Rb downregulation | Evading growth suppressors |
| | Induction of E2F gene expression | Cellular proliferation |
| | Increased mutation frequency | Genomic mutation |
| pUS2 | Inhibition of the major histocompatibility complex class I expression | Escape of immune control |
| pUL16 | Intracellular retention of NKG2D | Escape of immune control |
| pUL83 (pp65) | Increased mutation frequency | Genomic mutation |
| | Antagonizes the NKp30 activating receptor | Escape of immune control |
| pUL36 (vICA) | Inhibits caspase-8 activation and apoptosis | Enhanced cell survival |
| pUL37x1 (vMIA) | Inhibits mitochondrial-mediated apoptosis | Enhanced cell survival |
| lncRNA4.9 | Viral latency, binding to PRC2 | Cellular proliferation and transformation |

Figure 1.11 Summary of HCMV proteins with oncogenic effects

Summary of oncogenic effects attributed to specific HCMV proteins. Table adapted from Herbein *et al.*, (2018).

1.5.3 HCMV targeted therapeutics in the treatment of GBM

Regardless of whether or not HCMV is oncogenic, HCMV is an effective therapeutic target in GBM patients. One study found that patients who received HCMV antiviral VGC as an add-on to standard GBM treatment had improved survival in a small sample group (Stragliotto *et al.*, 2013). However, the study was inadmissible due to the method of post-hoc analysis used and survivorship bias. The authors reanalysed their results to eliminate immortal time bias and still found a survival advantage in those receiving VGC for >6 months (Söderberg-Naucler *et al.*, 2014). Recent investigation of VGC as an add-on treatment specifically in secondary GBM found increased survival of 19.1 versus 12.7 months ($p = 0.0072$) in those receiving the antiviral (Stragliotto *et al.*, 2020). The small cohort and study design of these studies does not make them sufficient for introducing VGC as a treatment for GBM, however further clinical trials for VGC as an add on therapy for GBM patients with a larger cohort are ongoing until

2024 and may provide an answer as to whether VGC should be routinely used in GBM treatment. Whether the mechanism underlying the increased survival in VGC treated GBM patients is HCMV specific remains unclear, with criticism of these studies being used as evidence of HCMV in GBM due to the fact that a significant proportion of the participants were seronegative for HCMV.

Several studies have investigated the use of HCMV targeted immunotherapy as a treatment for GBM. Adoptive T-cell therapy has been one approach used to target HCMV in GBM patients. Crough *et al.* (2012) expanded HCMV pp65 specific T-cells *ex vivo* and then used them for adoptive transfer in a patient with recurrent GBM. Following four infusions, the patient displayed a significant reduction in the degree of enhancing tissue by MRI and remained clinically stable for the 17 months of the study. Schuessler *et al.* (2014) also used autologous T-cell therapy for HCMV to treat recurrent GBM with four out of ten participants remaining progression free for the duration of the study. In addition to T-cell therapies, dendritic cell (DC) therapy targeted to HCMV has shown promise in GBM patients. A clinical trial using pp65 pulsed DC in a vaccine combined with tetanus diphtheria toxoid (which increases lymph node homing and efficiency) showed increased DC migration to draining lymph nodes and significantly increased overall survival of >36.6 months versus 18.5 months (Mitchell *et al.*, 2015). Reap *et al.*, (2018) reported that DC vaccines improved the functionality of adoptively transferred HCMV targeted T-cells, which improved overall survival in a pilot study of GBM patients. It has not yet been determined whether the effects of HCMV targeted therapies for GBM work through a direct or indirect mechanism of action. The direct antigen specific hypothesis suggests that immunotherapies directly target and kill HCMV antigen expressing tumour cells, whereas the indirect targeting hypothesis suggests that in addition to the direct response, a robust activation of host immune response within the tumour microenvironment, including cytokines, NK cells, macrophages etc. also occurs (Rahman *et al.*, 2019).

1.6 Project rationale

There is now an overwhelming amount of evidence that shows HCMV antigen is present in GBM cells, although there has been no definitive evidence that HCMV is oncogenic and causes GBM. The presence of HCMV antigens in GBM in the absence of infectious virus particles suggests that HCMV may be latently infecting cells within the adult brain. Evidence suggests that adult NSCs, NPs, OPC or dedifferentiated neurons or astrocytes are potential cells of origin for GBM (Wang *et al.*, 2021). Whilst there is a wealth of research on the effects of

HCMV on embryonic NP cells, there is a distinct lack of research on HCMV in adult NP cells, which are distinct from embryonic NPs. Therefore, the first objective of this study was to determine whether adult NP cells could be infected with HCMV and to characterise the nature of this infection. Secondly, as neutralisation of differentiation is thought to be an early step in gliomagenesis and HCMV has previously been shown to disrupt the differentiation of embryonic NP cells, it was important to determine if HCMV infection of adult NP would perturb differentiation of NP cells (Hu *et al.*, 2013, Luo *et al.*, 2010). This first involved optimising an *in vitro* protocol for adult NP differentiation. Thirdly, we sought to use RNAseq to analyse gene expression changes associated with HCMV infection of adult NP cells, both before and after differentiation to screen for potentially oncogenic or oncomodulatory changes conferred by infection of these cells.

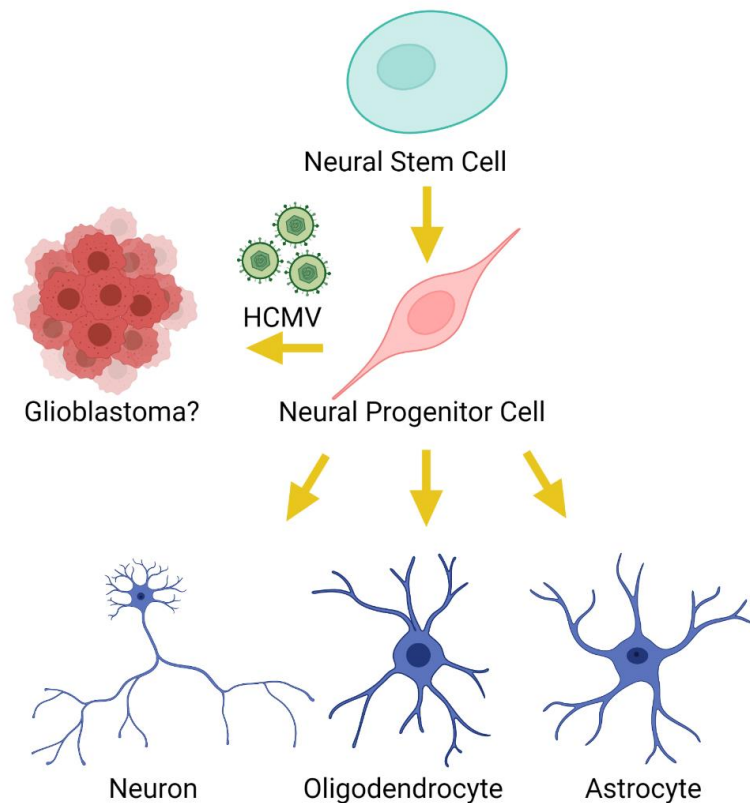


Figure 1.12 Graphical summary project rationale and potential origin of glioblastoma

Graphical summary of project rationale. HCMV antigens are widely found in GBM tumour samples, however the role of HCMV in gliomagenesis is unclear. Adult NP cells are a potential cell of origin for GBM and neutralisation of differentiation is an early step in gliomagenesis. Therefore the aim of this project is to investigate HCMV infection of adult NP cells and the subsequent effects this has on these cells and their ability to differentiate (created with BioRender.com).

Chapter 2 – Materials and methods

2.1 Tissue culture maintenance and cell lines

All cells were cultured in a humidified incubator in the presence of 5 % v/v CO₂ at 37 °C. Cells were maintained in vented cell culture flasks (Corning) of 25 cm², 75 cm² or 150 cm². All passaging and setting up of cell-based experiments took place in a class II Microbiology Safety Cabinet under aseptic conditions. Detachment of adherent cells was performed by removing the media, washing the cells twice with sterile phosphate buffered saline (PBS)(recipe in appendix), followed by application of an appropriate volume of Trypsin-EDTA (Sigma). Cells were incubated at 37 °C for one to five min under observation until they detached from the flask. Cells grown in foetal bovine serum (FBS) containing media enabled trypsin to be inactivated by the addition of serum-containing media. Cells grown in serum-free media were removed from the flask, pelleted by spinning at 5000 x *g* at room temperature in a 50 mL tube and the trypsin containing supernatant removed, before resuspension in an appropriate volume of media. The required number of cells were then transferred to a new flask. Viable cell counts were obtained by diluting equal volumes of cell suspension with 0.4 % w/v Trypan blue stain in PBS and transferring 10 µl to fill the counting chamber of an improved Neubauer haemocytometer (Marienfeld Superior). Trypan blue negative, viable cells were then counted using an inverted microscope at 100 x magnification to calculate the concentration of viable cells in the suspension.

Human foetal foreskin fibroblast cells HFFF2 (ECACC 86031405) were cultured in fibroblast media (see appendix A). Cells were split 1:3, every three to four days when they reached approximately 80 % confluence, and were only used up to passage 20.

Neural progenitor (NP1) cells were isolated from tissue removed from an adult brain during epilepsy surgery performed at Stanford University Medical Centre (Wurdak *et al.*, 2010). NP1 have the capacity to proliferate (although for limited passages) and to differentiate into distinct cell types. NP1 were cultured in NP media (appendix A) and split 1:4 every 3-4 days. NP1 cells infected with HCMV were cultured in the same way.

2.2 Generation of Merlin-IE2-GFP stocks

Merlin-IE2-GFP HCMV was used for all experiments (obtained from Stanton lab, Cardiff) (Stanton *et al.*, 2010). Merlin is a low passage strain derived from a

clinical isolate. The GFP is a UL122 (IE2) GFP fusion, which allows facile identification of HCMV infected cells via GFP direct fluorescence. Merlin-IE2-GFP has 2 mutations from wild-type Merlin, one in UL128 and another in RL13, which are both necessary for efficient cell culture propagation. RL13 contains a single nucleotide insertion at position 11363, which causes a frameshift mutation. This mutation was acquired by the Merlin strain during early passage and is obligatory for cell culture work as expression of wild-type RL13 severely impairs *in vitro* replication in fibroblast and epithelial cell cultures (Stanton *et al.*, 2010). Merlin-IE2-GFP also contains a G to A (G → A) substitution at nucleotide 176311 of UL128, which introduces an in-frame stop codon that leads to premature termination of the UL128 protein. The ablation of UL128 is also advantageous for culture *in vitro* using fibroblasts. Stanton *et al.*, (2010) show that repair of the UL128 mutation results in growth defects of the virus in these cells.

Fibroblasts are highly permissive to HCMV replication and so are commonly used for growing HCMV stocks. To generate HCMV stocks, flasks of 90 % confluent HFFF2 cells were infected at a multiplicity of infection (MOI) of 0.1 plaque forming unit per cell (PFU/cell) using stocks obtained from the Stanton lab. Cells were monitored daily for GFP expression and cytopathic effect (CPE), including cytomegaly, rounding up and lifting off the flask, using an EVOS cell imaging system. Once ~80 % of cells displayed CPE, media was removed daily, spun at 5000 x g at room temperature in an Eppendorf 5810R centrifuge and the supernatant aliquoted and stored at -80 °C. Supernatants were then serially diluted onto naive HFFF2 cells to determine infectious titres by focus forming assay (see section 2.3.1). Merlin-IE2-GFP stock with defined titre generated as described here was then used for all future experiments.

2.3 Determination of virus titre

2.3.1 Supernatant titre by focus forming assay

HFFF2 or NP1 cells were seeded at a density of 8000 cells per well in a black walled 96 well plate (Greiner cellstar). 11 µl of HCMV containing supernatant was added to the first well containing 100 µl media and then 5 10-fold serial dilutions were performed in triplicate. At 72 hr post infection (h.p.i), infected cells were fixed in 4 % w/v paraformaldehyde (PFA) and immunofluorescent staining for HCMV IE (antibody - MAB8131) was performed (as described in section 2.4). Immunofluorescence staining was used to count IE+ve cells instead of counting GFP+ve cells as it is a more sensitive method. The number of IE +ve cells per well was counted using the EVOS cell imaging system, to calculate a titre in focus

forming units per millilitre (FFU/ml). An uninfected control well was used to determine any non-specific background fluorescence.

2.3.2 Intracellular titre by focus forming assay

HFFF2 or NP1 were infected with HCMV at an MOI of 1 pfu/cell in a 25 cm² cell culture flask and media replaced every third day for 10 days. Cell lysates were made by trypsinising the infected cells (see section 2.1) and pelleting them by centrifugation. Cells were resuspended in 200 µl of media (HFFF2 or NP media depending on the cell type to be inoculated) and subjected to 5 cycles of snap freezing in liquid nitrogen and thawing on a heat block set at 37 °C. HFFF2 cells were seeded at a density of 10⁴ cells per well in a black walled 96 well plate. 10 µl of lysate was added to the first well and 5 x 10-fold serial dilutions performed in triplicate. Cells were left for 72 hr before being fixed, stained and counted as described in section 2.3.1.

2.3.3 Infectious centre assay

HFFF2 or NP1 cells were infected at an MOI of 3 FFU/cell and left for 72 hr resulting in between 96 - 98 % GFP positivity, determined using an EVOS cell imaging system. Cells were detached and counted (as described in section 2.1), prior to serial dilution in HFFF2 media. A dilution corresponding to 100 HCMV infected NP1 or HFFF2 was introduced into each well of a black walled 96-well plate containing 8000 naïve HFFF2. Cells were allowed to settle overnight, before the number of GFP+ cells in each well were counted and recorded using the EVOS cell imaging system. After 72 hr the cells were fixed using 4 % w/v PFA and stained for HCMV IE (as per section 2.5). GFP+ and IE+ cells were counted to determine the increase in HCMV infected cells for each well recorded. Three technical repeats were performed and the average increase in infected cells per well calculated.

2.4 Western Blotting

Cells were lysed by removing media, washing cells and applying an appropriate volume of EBC or RIPA lysis buffer (for recipes see appendix A), for example 150µl per well of a six well plate (9 cm² area per well). Cells were then scraped off the plate into the lysis buffer and thoroughly resuspended by repeated pipetting using a p200 pipette tip. Lysates were clarified by pelleting the cell debris by spinning at 5000 x g at room temperature in an Eppendorf 5810R centrifuge and removing the cell lysate supernatant to a fresh 1.5 ml tube. Lysate protein concentration was determined by bicinchoninic acid (BCA) assay using the Pierce BCA Protein Assay kit (Thermo Fisher Scientific) as per kit

instructions, and protein concentration was normalised to the lowest concentration sample by addition of the appropriate volume of lysis buffer. Lysates were then mixed 1:1 with 2 x Laemmli buffer (for recipe see appendix A) and heated to 95 °C for 10 min. 5 µl of pre-stained Seeblue® Plus2 protein molecular weight markers (Invitrogen) were loaded into the first well followed by 5 µg (up to 15 µl) of protein lysate/Laemmli per sample into adjacent wells of a polyacrylamide gel. Hand cast 8 %, 10 % or 12 % polyacrylamide gel (see appendix A), or 4–15 % Mini-PROTEAN® TGX™ Precast Protein Gels (Biorad) were used and proteins were resolved by sodium dodecyl sulphate polyacrylamide gel electrophoresis (SDS-PAGE). SDS-PAGE was performed using Tris-glycine running buffer (for recipe see appendix A) and run at 120-160 V for 1-2 hr using the mini-PROTEAN system electrophoresis cells (Bio-Rad). The resolved proteins were transferred to methanol-activated polyvinylidene difluoride membrane PVDF (Immobilon-FL Merck Millipore) by semi-dry or wet transfer. Semi-dry transfer employed a TE77XP semi-dry transfer unit (Hoefer) as per manufacturer's instructions, with Towbin buffer (for recipe see appendix A) and transferred for 2 hr. Wet transfer was performed using the Mini Trans-Blot Cell (Biorad) with Towbin buffer (for recipe see appendix A). Wet transfer was run at 70 V for 90 min on ice. Following transfer, PVDF membranes were blocked in 5 % w/v skimmed milk powder or 5 % bovine serum albumin (BSA) in TBS-T (See appendix A) for 1 hr at room temperature with gentle shaking. Following three x 10 min washes with TBS-T, primary antibodies were diluted to working concentrations (see appendix A) in 5 % (w/v) skimmed milk powder or BSA in TBS-T, applied to membranes and incubated overnight with shaking at 4 °C. Following another 3 x 10 min washes with TBS-T, horseradish peroxidase conjugated secondary antibodies (SIGMA) were diluted in 5 % BSA w/v in TBS-T and membranes incubated for 1 hr at room temperature with shaking. Following a final series of 3 x 10 min washes with TBS-T, homemade enhanced chemiluminescence reagent (ECL) (for recipe see appendix A) or ECL prime western blotting detection reagent (Amersham, GE Healthcare Life Sciences) was applied to the membranes for 5 min. Chemiluminescence was imaged by exposure to x-ray film and development using medical film processor (SRX-101A, Konica Minolta Medical & Graphic, Inc.) in a darkroom. X-ray films were scanned and saved as TIF files. Alternatively, chemiluminescence was imaged using a ChemiDoc (Biorad).

2.5 Immunofluorescence (IF)

Cells were seeded onto either black walled, flat bottom fluorescence-optimised plastic 96 well plates (Greiner cellstar) or autoclaved 12 mm glass cover slips in

a 24 well plate. NP1 cells were cultured on plates or coverslips coated with 0.5 % poly-L-lysine/PBS (incubated at room temperature for 10 min before removal and washing with PBS) to improve adherence. Cells were washed 3 times in PBS prior to fixation using 4 % (w/v) PFA in PBS for 10 - 30 min (10 min for HFFF2, 30 min for NP1) at room temperature. Following fixation, cells were again washed 3 times with PBS before permeabilisation with 0.2 % (v/v) Trion X-100/PBS at room temperature for 5 min, followed by 3 more PBS washes. Primary antibodies were diluted to working concentrations in 10 % (v/v) FBS in PBS, applied to cells and incubated overnight at 4 °C. Primary antibody solution was removed and cells were washed 3 times with PBS before incubation for 1 hour at room temperature with fluorophore conjugated secondary antibody and Hoechst nuclear stain (1:20000) diluted in 5 % (v/v) FBS in PBS. Cells were washed 3 times in PBS before being left in PBS (96 well plates) or mounted on glass slides (coverslips) using ProLong Gold Antifade Mountant (Life Technologies). Images were taken using the EVOS and Nikon Ti-E microscopes. List of antibodies used in Appendix B.

2.6 Differentiation of neural progenitor cells

2.6.1 Serum titration

NP1 cells were seeded at 8000 cells per well in a 96 well plate and allowed to settle overnight in NP media. NP media, which contains 5 % FBS was removed and replaced with media containing 2.5 %, 0.5 % or 0 % FBS. Cells were imaged and viability assessed by Trypan blue staining (as described in section 2.1) at 24 hr post treatment.

2.6.2 Differentiation using DMSO

NP1 cells were seeded at 8000 cells per well in a 96 well plate and allowed to settle overnight in NP media. NP media was removed and replaced with 1.8 % DMSO in NP media (for recipe see appendix A). Cells were fixed at days 1, 3 and 5 post-treatment in 4 % w/v PFA (as described in section 2.4) and imaged, using the EVOS cell imaging system.

2.6.3 Differentiation using BMP4

NP1 cells were seeded at 8000 cells per well in a 96 well plate and allowed to settle overnight in NP media. NP media was removed and replaced with BMP4 differentiation media (for recipe see appendix A). Cells were fixed at days 1, 3, 5 and 7 of treatment in 4 % w/v PFA (as described in section 2.4) and imaged using the EVOS cell imaging system.

2.6.4 Differentiation using Walton *et al.*, (2006) protocol

Cells were treated according to the seven day neuronal differentiation protocol described by Walton *et al.*, (2006). NP1 were seeded at a 6×10^5 cells per well of a 6 well plate for protein lysate and RNA extraction or 1×10^5 on poly-L-lysine coated 8 mm glass coverslips in a 24 well plate for immunofluorescence. Cells were seeded in NP media and allowed to settle overnight. The NP media was removed and replaced with NP differentiation media (appendix A). Differentiation media was made fresh each time and replaced every other day for up to 7 days. Cells were lysed in EBC or RIPA buffer for protein samples, whilst RNA was extracted using the Qiagen RNeasy kit according to manufacturer's instructions (see 2.7). Coverslips were fixed at day 0, 1, 3, 5 and 7 in 4 % w/v PFA in PBS for 30 min for initial optimisation of differentiation. Later this was reduced to time points of day 0 and 5. To differentiate HCMV+ NP1, cells were grown to 90 % confluency and infected at an MOI of 3 FFU/cell. At 5 d.p.i, NP media was removed and differentiation media applied as described above.

2.7 RNA extraction

For RNA extraction, cells were plated at a density of 6×10^5 cells per well of a 6 well plate and allowed to settle overnight. Cells were washed twice with PBS before extraction using TRIzol (Thermo Fisher Scientific) or RNeasy (Qiagen) as detailed below.

2.7.1 RNeasy extraction

350 μ l of buffer RLT (lysis buffer) was added directly to the well and cells were scraped off using a cell scraper, mixed thoroughly by pipetting and transferred to a 1.5 ml tube. Lysates were vortexed briefly before being applied to a QIAshredder column (Qiagen) and centrifuged for 2 min at full speed in a microcentrifuge. The flow through of homogenised lysate was mixed with 350 μ l of 70 % ethanol/RNase free water by repeated pipetting. The full volume was transferred to a spin column from the RNeasy kit and centrifuged at $8000 \times g$ for 15 s using a microcentrifuge, discarding the flow through.

On-column DNA digest was performed using an RNase-Free DNase Set (Qiagen). First, 350 μ l of buffer RW1 was applied to the column and centrifuging at $8000 \times g$ for 15 s. The flow through was discarded and 80 μ l of DNase digest mix (10 μ l DNase I + 70 μ l buffer RDD) was applied directly to the column membrane and left to incubate at room temperature for 15 min. Next, 350 μ l Buffer RW1 was applied to the column and centrifuged again for 15 s at $8000 \times g$. The flow through was discarded and 500 μ l of buffer RPE added to the column

before being spun again at again for 15 s at 8000 x *g* and the flow through discarded. A second 500 µl of buffer RPE was added and the column spun for 2 minutes at 8000 x *g*. The column was then placed in a new 2 ml collection tube and centrifuged at full speed for 6 min to dry the membrane and remove any residual buffer contaminants. The RNeasy column was then placed in a new 1.5 ml collection tube and 30 µl of RNase free water applied directly to the column membrane. The column was then centrifuged at 8000 x *g* for 1 min to elute the RNA and the column was then discarded. Following elution, the RNA solution absorbance at 260/280 nm and 260/230 nm were determined using a NanoDrop spectrophotometer (Thermo Fisher Scientific), to determine concentration and purity. RNA was stored as aliquots at -80 °C.

2.7.2 TRizol extraction

1 mL of TRizol reagent was added directly to three times PBS-washed cells in one well of a 6 well plate. The lysate was pipetted repeatedly to ensure full lysis of the cells before transferring to a 1.5 ml tube. Samples were stored at – 20 °C at this point until all time points from the experiment had been collected. Extractions were then performed in parallel for each sample of the same experiment. Frozen TRizol lysates were thawed on ice and 200 µl of chloroform added before being vortex mixed and incubated at room temperature for 3 min. The lysate was centrifuged for 15 min at 12,000 x *g* at 4 °C for phase separation. The aqueous phase was transferred to a new 1.5 mL tube and 500 µl of isopropanol added and mixed by briefly vortexing before incubation for 10 min at room temperature. After incubation the samples were for centrifuged for 10 min at 12,000 x *g* at 4 °C. Supernatant was discarded taking care not to disturb the RNA pellet. The pellet was resuspended in 1 mL of 75 % EtOH, vortexed briefly and centrifuged for 5 min at 7500 x *g* at 4 °C. Supernatant was removed and the pellet air dried for 10 to 15 min. Once dried, the pellet was resuspended in 20 µl of nuclease free water and placed in a heat block set at 55–60 °C for 15 min. RNA concentration, 260/280 nm and 260/230 nm ratios were determined using the NanoDrop 1000 spectrophotometer (Thermo Fisher Scientific). RNA was stored at -80 °C.

2.8 Real-time quantitative polymerase chain reaction (RT-qPCR)

2.8.1 Generation of cDNA by reverse transcription

Reverse transcription was performed using the High-Capacity RNA-to-cDNA Kit (Applied Biosystems). The reaction was prepared by adding 10 µl of 2X RT Buffer Mix, 1 µl of 20X RT Enzyme Mix and 500 ng of RNA (up to 9 µl volume) were

added to a PCR tube and the volume made up to 20 μ l with nuclease free water. Negative controls were also set up as described above, one without the 20X RT Enzyme Mix and one without RNA. The reverse transcription was performed by placing the PCR tubes into a Virci 96 well thermocycler (Thermo Fisher Scientific) set to the following conditions; 37 $^{\circ}$ C for 60 min, 95 $^{\circ}$ C for 5 min and hold at 4 $^{\circ}$ C. cDNA was stored at -20 $^{\circ}$ C.

2.8.2 SYBR Green

SYBR Green PCR reactions were set up in a 384 well plate with the following components; 5 μ l SYBR green mix (Quanta ROX), 0.15 μ l of primer mix (each primer mixed together at 50 pmol / μ l), 4 μ l nuclease free water and 1 μ l cDNA (1:5 dilution). The reaction mix was well mixed by repeated pipetting before sealing the plate with optical adhesive film and briefly centrifuging to bring the contents to the bottom of the wells and eliminate any bubbles. The plate was run on the QuantStudio 7 Flex Real-Time PCR System (Thermo Fisher Scientific) using the following conditions: 3 min at 94 $^{\circ}$ C not repeated, followed by 40 cycles of 3 s at 94 $^{\circ}$ C then 30 s at 60 $^{\circ}$ C. A melt curve/dissociation was performed to check the specificity of the primers using the pre-programmed settings on the QuantStudio 7 Flex (Figure 2.1). Results were analysed using the $\Delta\Delta$ CT method (Rao *et al.*, 2013).

| Stage | Step | Ramp rate | Temperature | Time |
|------------------|--------------------------|---------------------|-----------------|------------|
| Melt Curve Stage | Step 1 | 1.6 $^{\circ}$ C/s | 95 $^{\circ}$ C | 15 seconds |
| | Step 2 | 1.6 $^{\circ}$ C/s | 60 $^{\circ}$ C | 1 minute |
| | Step 3 (Dissociation) | 0.05 $^{\circ}$ C/s | 95 $^{\circ}$ C | 15 seconds |

Figure 2.1 SYBR green melt curve protocol

SYBR green melt curve protocol for real-time PCR run on the QuantStudio 7 Real-Time PCR System.

2.8.3 TaqMan

TaqMan PCR was performed using the protocol supplied with the TaqMan[®] Advanced Master Mix (Applied Biosystems). Reactions were carried out in a 384 well plate with each well containing the following: TaqMan Fast Advanced MasterMix (2X) 5.00 μ l, nuclease free water 2.00 μ l, TaqMan Advanced miRNA Assay (20X) 0.5 μ l cDNA (1:5 dilution) 2.5 μ l. The reaction mix was well-mixed by repeated pipetting before sealing the plate with optical adhesive film and briefly centrifuging the plate to bring the contents to the bottom of the wells and eliminate any bubbles. The plate was run on a QuantStudio 7 Flex Real-Time PCR System (Thermo Fisher Scientific). The conditions were set as follows; hold

at 95 °C for 20 s for polymerase activation, followed by 40 cycles of denaturation at 95 °C for 1 s and anneal/extend at 60 °C for 20 s. The QuantStudio was run on fast mode. Results were analysed using the $\Delta\Delta\text{CT}$ method.

2.9 RNA sequencing

NP1 infected with HCMV at an MOI of 3 FFU/cell for 5 days and mock infected controls were seeded at a density of 6×10^5 cells per well of a 6 well plate and allowed to settle overnight. Cells were then treated using the Walton *et al.*, (2006) protocol (as described in section 2.6.4) and RNA was extracted on days 0 and 5 of the differentiation (using RNeasy as described in section 2.7.1). RNA samples were stored at -80 °C and shipped to Novogene on dry ice for sequencing.

2.9.1 Novogene RNA sequencing

RNAseq was performed by Novogene and the workflow is summarised in figure 2.2. To guarantee reliable data, quality control checks were performed at each step of the process. RNA samples were analysed using the LabChip GX Touch HT Bioanalyzer (Caliper Life Sciences) to ensure RNA quality and determine concentration. For cDNA library construction, purified messenger RNA was separated from the total RNA using poly-T oligo-attached magnetic beads. Messenger RNA was fragmented before synthesising the first strand cDNA using random hexamer primers. Second strand synthesis was executed using dTTP for non-directional library preparation. The non-directional library underwent end repair, A-tailing, adapter ligation, size selection, amplification, and purification. Libraries were checked utilising Qubit and real-time PCR for quantification. A bioanalyzer was used for detection of size distribution. Index-coded samples were pooled and the libraries were sequenced on an Illumina Novaseq 6000 platform at effective library concentrations. Paired-end 150bp reads were generated.

Raw reads in FASTQ format were processed through fastp. Clean reads were acquired by removing reads containing adapter and poly-N sequences and also reads of low quality. Downstream data analysis was based on the clean, high quality data.

The reference genomes used for read mapping were Homo sapiens (GRCh38/hg38) and Merlin HCMV AY446894. Paired-end clean reads were mapped to both reference genomes using HISAT2 software. To quantify the read numbers mapped to each gene, featureCounts software was employed. Reads per kilobase of exon model per million mapped read (RPKM) for each gene was calculated based on gene length and read count mapped to each gene. RPKM

is a commonly used method for estimating gene expression levels as it takes into account both sequencing depth and gene length.

Differential expression analysis was implemented between two sample groups (with three biological replicates per condition) with the DESeq2 R package, which determines differential expression in gene expression data through a model based on the negative binomial distribution. P values were adjusted using the Benjamini and Hochberg's procedure for controlling false discovery rate (FDR). Genes with an adjusted P value < 0.05 were designated as differentially expressed.

Two types of enrichment analysis were employed to summarise the large gene lists and identify biological pathways. Gene Ontology (GO) annotates genes to biological processes, molecular functions, and cellular components presented in a directed acyclic graph structure. Kyoto Encyclopedia of Genes and Genomes (KEGG) annotates genes to a biological pathway.

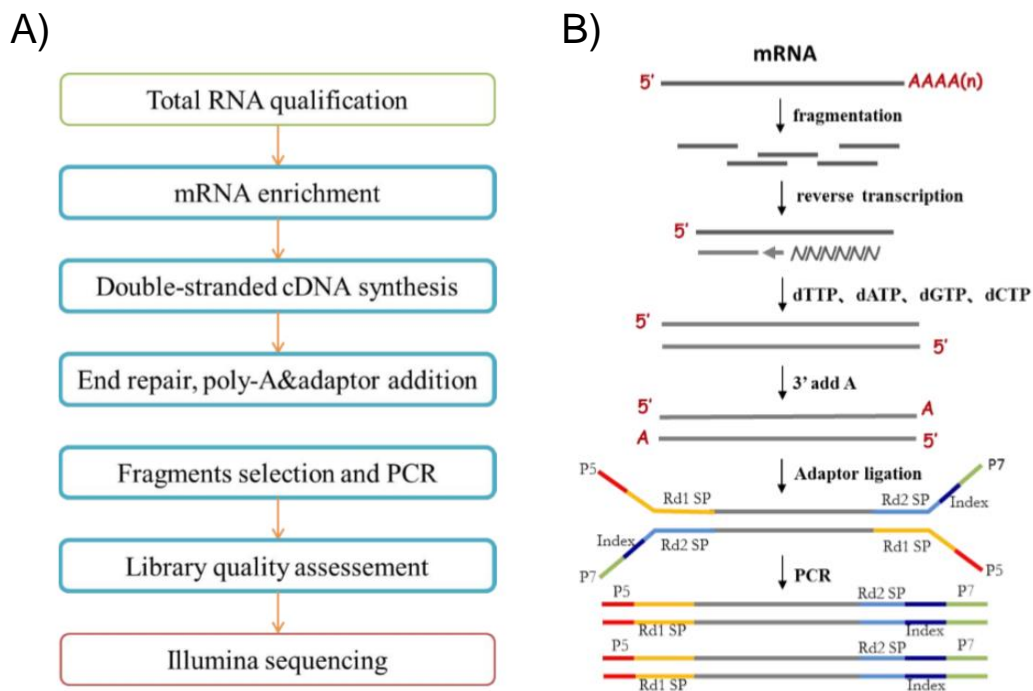


Figure 2.2 Novogene RNA sequencing method summary

A) Novogene RNA sequencing service workflow summary. B) cDNA library construction method summary.

Chapter 3 - Characterising HCMV infection of adult neural progenitor cells *in vitro*

3.1 Introduction

HCMV infection of the neonatal brain is the leading infectious cause of congenital disorders of the CNS. Intrauterine transmission of HCMV has an estimated worldwide incidence of 0.5 – 2.2%, with HCMV infected cells located primarily in the ventricular and subventricular zones of the neonatal brain (Becroft, 1981, Perlman and Argyle, 1992). Although several different cell types have been found to be infected, the highest degree of viral tropism is within neural progenitor cells (Teissier *et al.*, 2014). Work by Sun *et al.*, (2020) also suggests that HCMV predominantly targets neural progenitor cells of the SVZ during *in vitro* infection of human iPSC-derived brain organoids.

Following primary HCMV infection, lifelong latency is established, with estimates of worldwide seroprevalence in the adult population ranging from 70 to 100 % (Söderberg-Nauclér and Nelson, 1999, Zuhair *et al.*, 2019, Almaghrabi *et al.*, 2019). Hematopoietic progenitor cells and cells of the myeloid lineage are known to be reservoirs of latent HCMV infection *in vivo*. Latency is characterised by the presence HCMV genomes in the absence of virion production (Mendelson *et al.*, 1996, von Laer *et al.*, 1995). These cells have been the focus of studies on HCMV latency and reactivation, however there is a distinct lack of research exploring the possibility of other cellular reservoirs of latency. Interestingly, Tsutsui *et al.*, (2002) reported latent infection of MCMV in the brains of mice that were infected either as neonates or as young adults (Tsutsui *et al.*, 2002). Reactivation in mice latently infected for over 180 days post infection was observed in multiple regions of the brain, with the highest degree of reactivation in the SVZ. The authors suggest that the cells in which MCMV reactivation is occurring are most likely NSCs or NPs due to their expression of nestin and glial fibrillary acidic protein (GFAP), together with Bromodeoxyuridine (BrdU) labelling, indicating proliferating cells.

Several studies have reported the presence of HCMV antigen in GBM tumour samples, but not in the healthy surrounding brain tissue (Cobbs *et al.*, 2002, Mitchell *et al.*, 2008). Multiple groups have found a higher number of HCMV positive cells in GBM than in lower grade gliomas, linking HCMV with more aggressive tumours (Huang *et al.*, 2015, Bhattacharjee *et al.*, 2012). This notion is supported by research showing that HCMV seropositivity is linked with decreased survival in GBM patients (Foster *et al.*, 2019). Despite an array of studies reporting the detection of HCMV in GBM, several studies also report a

complete absence of HCMV in GBM samples using the same detection methods (Priel *et al.*, 2015, Garcia-Martinez *et al.*, 2017). Due to the discrepancies in detection rates, the association between HCMV and GBM remains controversial.

In recent years, the origins of GBM have begun to be elucidated, with similar findings from several papers, with most agreeing that GBM arises from stem or progenitor cells of the neural lineage. Lee *et al.*, (2018) present genetic evidence from deep sequencing that show GBM likely originates from NSC, which migrate from the SVZ and form high grade gliomas in distant areas of the brain. 56.3% of GBM patients in the study had low level driver mutations in the normal SVZ tissue that were observed at high levels in the corresponding tumour (Lee *et al.*, 2018). The literature suggests that cells of neural lineage (including neural stem cells and neural progenitor cells) in the adult brain are the most likely cells of origin for GBM, with Llaguno *et al.*, (2019) showing that cell of origin potential for GBM formation decreases with progression of neural lineage restriction.

Various studies have investigated HCMV infection of foetal forebrain derived, and embryonic stem cell (eSC) derived NP cells. However, research into HCMV in adult NP cells is lacking, despite the well documented presence of HCMV in GBM tumours within the adult brain (Cheeran *et al.*, 2005, Luo *et al.*, 2008, Belzile *et al.*, 2014).

Given that adult NP cells originating from the SVZ are a likely cell of origin for GBM and several studies have detected HCMV antigen in GBM tumours, we sought to characterise *in vitro* HCMV infection of primary adult neural progenitor cells. We hypothesised that adult neural progenitors could be a potential reservoir of latent infection in the adult brain, with the potential for reactivation of lytic infection, similar to that seen in the adult mouse brain with latent MCMV infection. Previous studies of HCMV infection in NP cells have used high passage laboratory strains, namely Towne and TB40, which are both known to have lost virulence and acquired multiple mutations during cell culture passaging. For this work Merlin-IE2-GFP obtained from the Stanton lab was utilised as it contains an IE2-GFP fusion which allows easy identification of HCMV infected cells due to GFP expression, plus this cell culture-viable strain is maintained at low passage. Thus, it has just two changes from the wild-type clinical isolate: one in RL13 and another in UL128, which are both necessary for the virus to replicate and grow to high titres *in vitro* (Stanton *et al.*, 2010). The predominant cells used for this work are NP1, a primary, non-transformed NP cell line derived from an adult brain during an epilepsy surgery as detailed in section 2.1.

3.2 Establishing HCMV culture and detection protocols

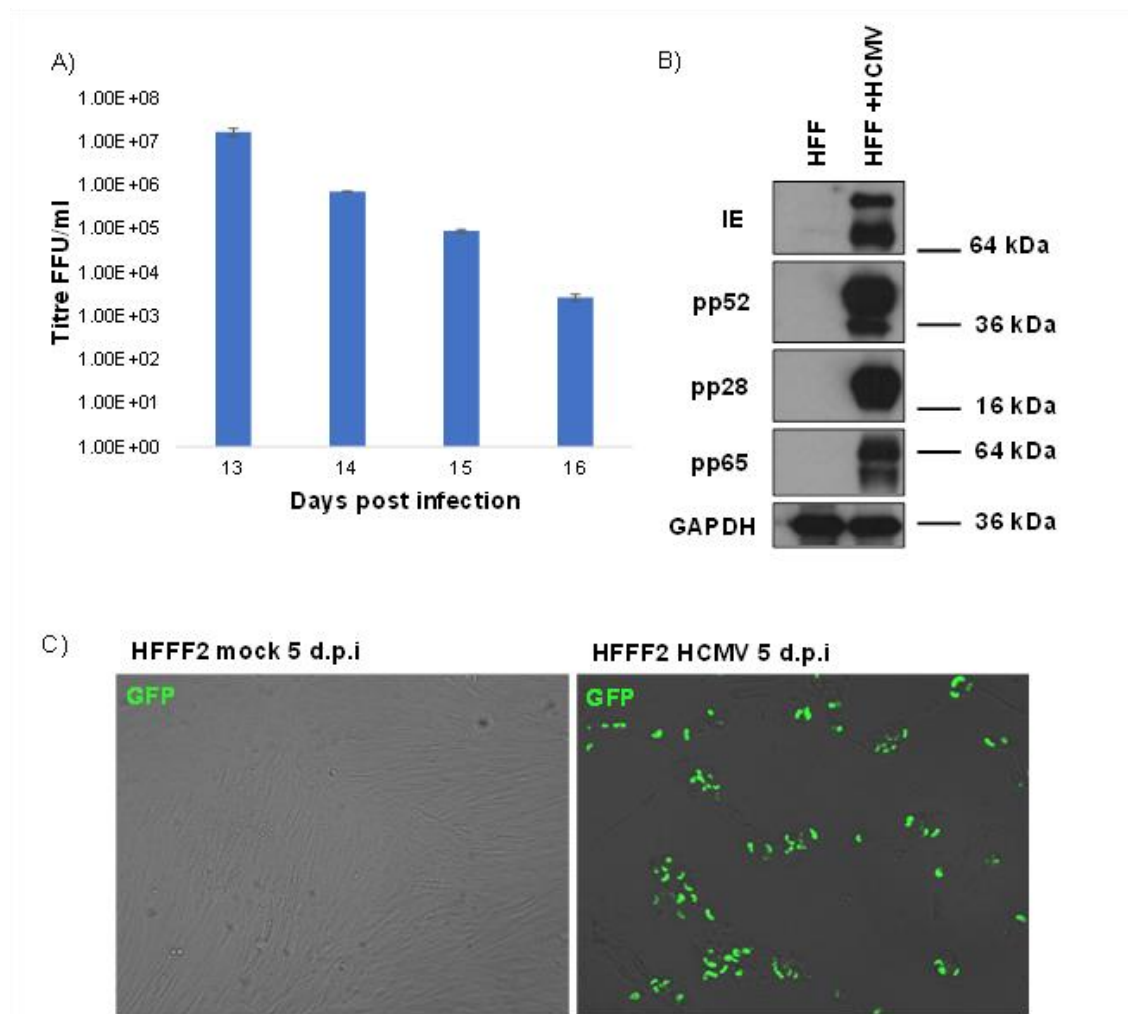


Figure 3.1 HCMV infection of human foetal foreskin fibroblast cells

A) Confluent HFFF2 were infected at an MOI of 0.1 FFU/cell and media replaced every third day until 100% CPE was visible. Supernatants were then collected daily, and cell debris removed by centrifugation. Collected supernatants were then titred by serial dilution onto naïve HFFF2 which were fixed in 4 % PFA at 72 h.p.i and stained for HCMV IE by immunofluorescence to count positive cells using the EVOS FL imaging system. N=3 technical repeats. B) Whole cell protein lysates of HCMV infected HFFF2 MOI=0.1 FFU/cell were collected at 14 d.p.i. Lysates were separated by SDS-PAGE and then immunoblotted using antibodies specific to HCMV IE, pp52, pp28, pp65 and GAPDH. C) HFFF2 cells +/- HCMV MOI 1 FFU/cell at 5 d.p.i imaged 260 x magnification using the EVOS FL imaging system showing viral GFP expression.

An initial priority was to establish Merlin HCMV culture in human foetal foreskin fibroblast cells, HFFF2, a cell line known to be permissive to HCMV and commonly used to grow high titre HCMV stocks. Merlin-IE2-GFP stocks were used to infect naïve HFFF2 at an MOI of 1 FFU/cell. HCMV associated GFP expression at 5 d.p.i is shown in Figure 3.1C with the majority of cells strongly

expressing GFP at this time point. The infected cells show a high level of CPE, manifesting as cytomegaly, rounding up and detachment from the flask.

To optimise detection of HCMV proteins, cell lysates were made at 14 d.p.i and western blotted (Section 2.4) using antibodies specific to HCMV IE, pp52, pp28, pp65 and GAPDH (see appendix B). The HCMV IE antibody detects both IE1 and IE2 proteins. Figure 3.1B shows detection of both IE1 and IE2, with IE1 (72 kDa) expression more abundant in HFFF2 at 14 d.p.i. HCMV early protein, pp52 (52 kDa) is also detected by western blot in HCMV+ HFFF2. Late proteins pp28 and pp65 are both also strongly expressed in HFFF2 at 14 d.p.i, indicating that HCMV is progressing through the IE, early and late phases of the lytic cycle. Taken together, the GFP expression seen at 5 d.p.i, the detection of HCMV IE proteins, early protein pp52 and late proteins pp28 and pp65 along with the supernatant titres in HCMV infected HFFF2 show that we have successfully generated infectious, replication competent Merlin-IE2-GFP stocks to be used to infect NP1 cells.

3.3 Characterising HCMV infection of adult neural progenitor cells

3.3.1 Infection of NP1 with HCMV

We have shown that adult neural progenitor cells, NP1 can be infected with HCMV infection in vitro. Figure 3.2.1A shows viral GFP expression in NP1 infected at an MOI of 1 at 5 d.p.i. Similarly to HFFF2, at 5 d.p.i over 70 % of NP1 cells were GFP positive. When infected at higher multiplicities of 5 and above (data not shown) a 99 % GFP+ population was observed repeatedly, suggesting that NP1 are universally susceptible to HCMV infection, despite being a highly heterogeneous cell type. When the same viral stocks were serially diluted onto NP1 and HFFF2 in a focus forming assay (detailed in section 2.5), a higher number of NP1 were infected (determined by GFP expression and immunofluorescence of HCMV IE) compared with HFFF2 (Figure 3.2.1C), supporting that NP1 are more permissive to HCMV infection.

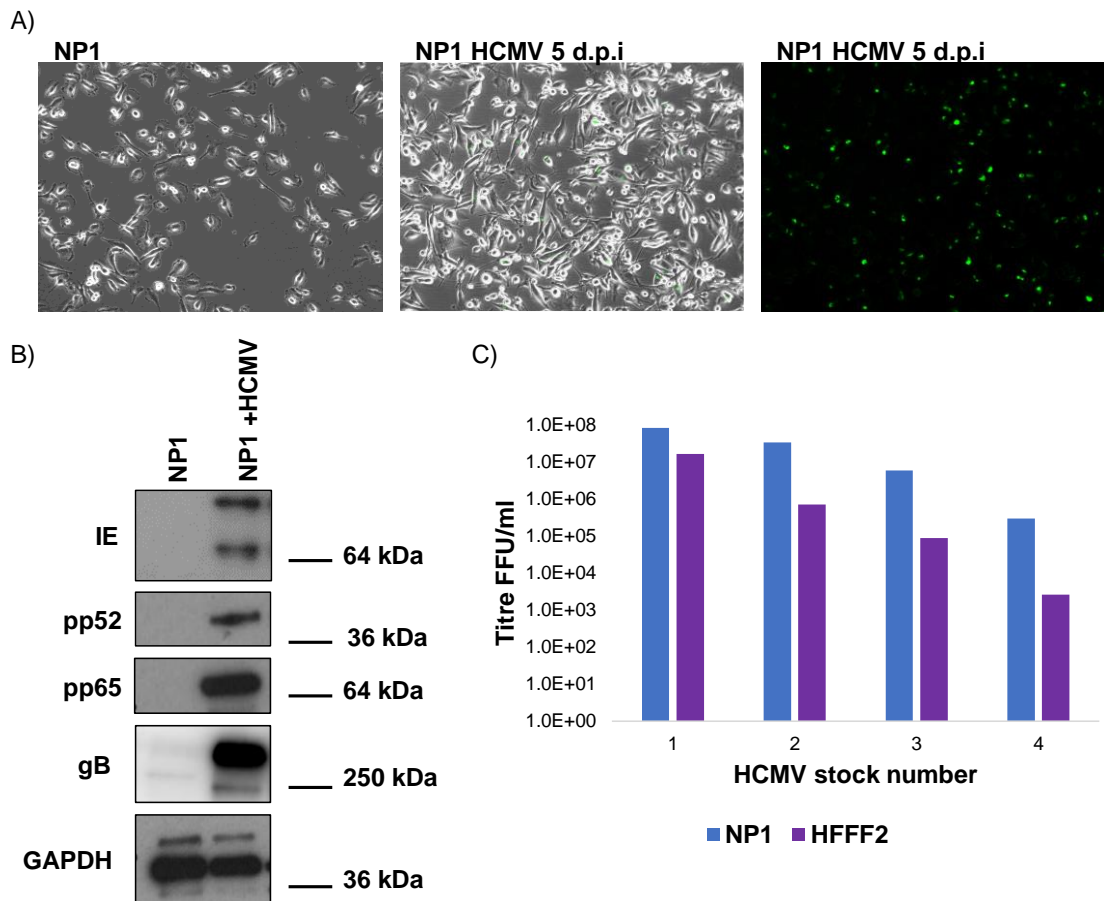


Figure 3.2.1 HCMV infection adult neural progenitor cells *in vitro*

A) Naïve NP1 cells and NP1 cells infected with HCMV at an MOI of 1 FFU/cell at 5 d.p.i. Viral GFP expression in green. Cells were imaged at 260 x magnification the EVOS cell imaging system. B) Western blots of protein lysates from mock NP1 and NP1 infected with HCMV at an MOI of 1 FFU/cell at 5 d.p.i. Membranes were probed for GAPDH (housekeeping), IE, pp52, pp65 and gB antibodies. C) HCMV viral stocks were generated from clarified supernatants of HFFF2 infected with HCMV at an MOI of 1 FFU/cell until 100 % CPE was observed. Stocks were titred by focus forming assay through serial dilution onto naïve NP1 and HFFF2 to compare relative permissibility.

It was important to determine if HCMV infection of NP1 was progressing through the temporal cascade of immediate early, early and late protein expression as is seen during natural *in vivo* infection of the neonatal brain, *ex vivo* infection of foetal NP cells, and *in vitro* infection of neural progenitor-like cells derived from iPSC's (Luo *et al.*, 2008, D'Aiuto *et al.*, 2012). Conversely, HCMV infection of embryonic stem cell (ESC) derived pre-rosette NSCs is non-progressive, with limited immediate early gene expression. However, when these cells were differentiated to neural progenitor cells transition to early gene expression occurred (Belzile *et al.*, 2014). This is reminiscent of CD34+ progenitor cells which harbour latent HCMV infection that can be reactivated upon differentiation, suggesting that cells of the neural lineage may be a reservoir of HCMV infection in the brain.

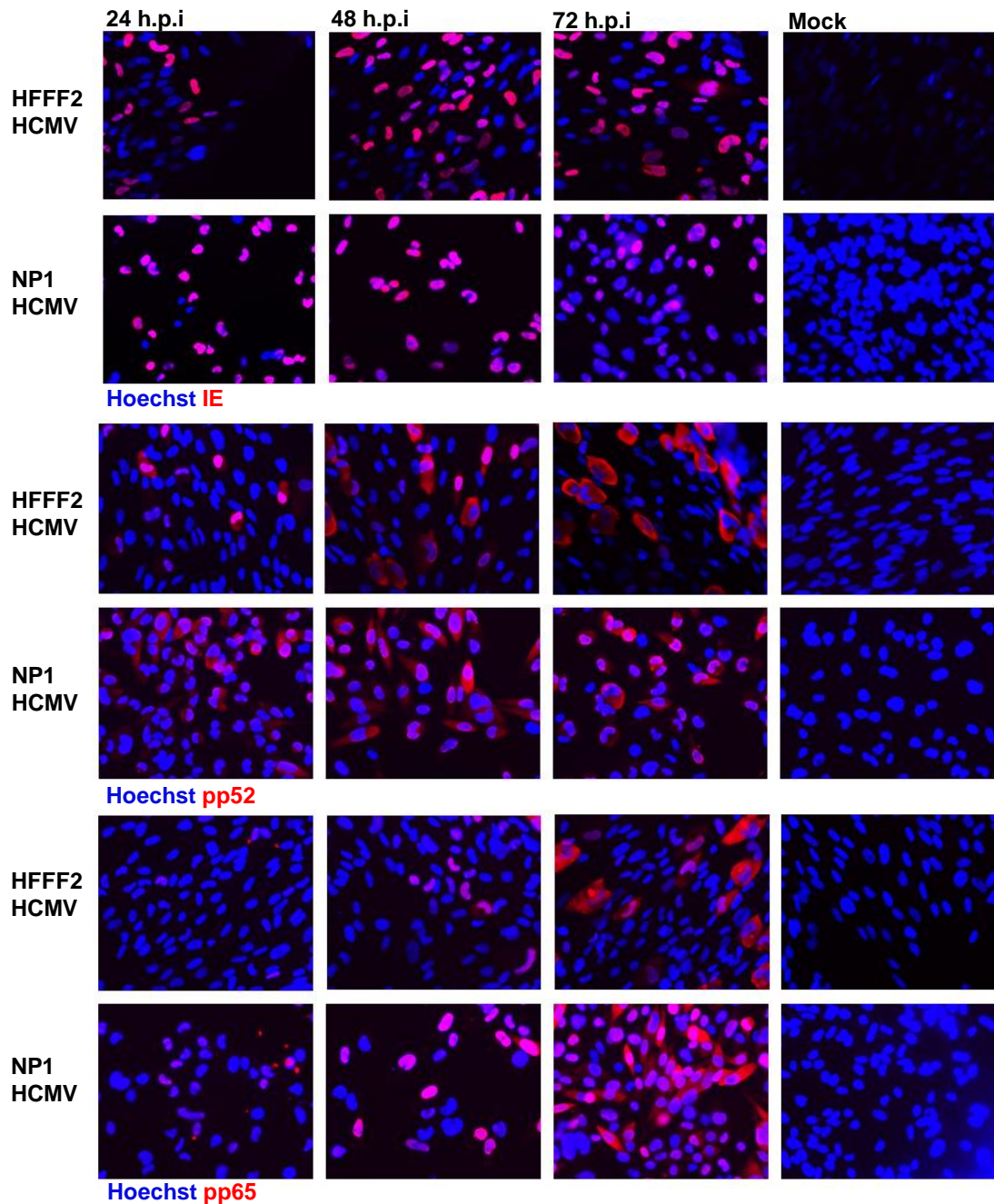


Figure 3.2.2 Immediate early, early and late protein expression in HCMV infection of adult neural progenitor cells *in vitro*

Immunofluorescence of HFFF2 and NP1 cells infected with HCMV at an MOI of 1 FFU/cell, fixed in 4 % PFA in PBS at 24, 48 and 72 h.p.i. Cells were permeabilised and stained with DNA stain Hoechst (blue) and antibodies against HCMV IE, pp52 and pp65 with Alexa Fluor 594 conjugated secondary antibodies (red) and GFP expression (green). Images were taken using the 10x objective of the Nikon Eclipse Ti-E Widefield Fluorescent Inverted Microscope.

We have shown that adult neural progenitor cells, NP1 can be infected with HCMV infection *in vitro*, but show very minimal CPE. Figure 3.2.1A shows viral

GFP expression in NP1 infected at an MOI of 1 FFU/cell at 5 d.p.i. Similarly, to IE1 and IE2 (immediate early), early and late proteins, including, pp52 (early), pp65, and gB (both late), were detected by western blot of NP1 at 5 d.p.i. This suggests that infection is progressing through the three phases of the HCMV gene expression temporal cascade (Figure 3.2.1B). This is supported by immunofluorescent staining for IE, pp52 and pp65 in figure 3.2.2. This shows nuclear IE expression at 24, 48 and 72 h.p.i in both HCMV infected NP1 and the control infected HFFF2. Early protein pp52 is visible in both the nucleus and cytoplasm of infected NP1 at 24, 48 and 72 h.p.i.

The distribution of pp52 is similar in both NP1 and HFFF2 at the first 2 time points, however by 72 h.p.i pp52 in HFFF2 has moved away from the nucleus and is concentrated at the cell periphery, whereas in NP1 pp52 staining is still present in the nucleus and shows a more uniform distribution throughout the cytoplasm.

The distribution of pp65 begins as bright cytoplasmic punctae in both infected HFFF2 and NP1, with some low-level nuclear staining in both cell types. By 48 h.p.i pp65 staining shifted to being predominantly nuclear in both infected NP1 and HFFF2. At 72 h.p.i the level of pp65 staining increased in both NP1 and HFFF2, with pp65 in both the nucleus and cytoplasm of both cell types. Notably HFFF2 display bright perinuclear foci of pp65, whilst NP1 do not.

3.4 Are adult neural progenitor cells fully permissive to the complete HCMV replication cycle?

Neural progenitor cells derived from neonatal autopsy tissue were shown to be fully permissive to *in vitro* HCMV infection with both Towne (laboratory adapted strain) and TR (a clinical isolate) (Luo *et al.*, 2008). The study showed that the full complement of immediate early, early and late proteins were expressed in these cells with relatively high numbers of virions produced and development of CPE. Neural progenitor-like cells from iPSC's were fully permissive to infection with HCMV laboratory-adapted strain Ad169, producing infectious virions in the supernatant that could be used to infect fibroblasts (D'Aiuto *et al.*, 2012). Conversely Belzile *et al.*, (2014) infected ESC derived neural progenitor-like cells with both Towne and TB40 and found that less than 1 % of cells could progress from IE to early gene expression, and very limited viral spread within an infected NP population could be detected by infectious centre assay. They also observed that the number of cells transitioning from IE to early expression increased when the cells were maintained in culture for more than 5 weeks.

3.4.1 Production of infectious HCMV particles from NP1 cells

Having determined that HCMV infection of NP1 was progressing through the immediate early, early and late gene expression, we wanted to find out if these cells were fully permissive to HCMV and producing infectious virus particles. Initially we titred supernatants taken from infected NP1 cells on to naïve HFFF2, alongside infectious HFFF2 supernatant as a positive control (as described in section 2.3.1). Figure 3.3.1A shows that no HFFF2 were infected when treated with supernatant from HCMV infected NP1. To determine if this was due to restricted tropism of particles produced by NP1, we also titred infected NP1 supernatant back on to naïve NP1 and again saw no infectivity (3.3.1B). We next determined whether virions produced in NP1 were capable of cell-to-cell spread. To do this we utilised the infectious centre assay protocol (section 2.3.3), where HCMV infected NP1 (or HCMV infected HFFF2 as a positive control) were seeded on to naïve HFFF2 and the number of subsequently infected cells determined by their expression of GFP and IE (immunofluorescence detailed in section 2.5). Although a small increase in the number of infected cells was detected when infected NP1 were seeded onto HFFF2, this is not significant as shown by the large error bars in figure 3.3.1C. A final attempt to detect infectivity was to search for intracellular or cell associated virus by testing for infectious HCMV within infected NP1 lysate. Lysate from infected NP1 cells was serially diluted onto naïve HFFF2 cells and titred by focus forming assay (method in section 2.3.2). Lysate from HCMV infected HFFF2 was used as a control. Figure 3.3D shows that a low titre of just 15 FFU/ml of HCMV was detected in the NP1 lysate. This is likely due to a limitation in this method due to transfer of intact NP1, rather than true detection of cell associated virus.

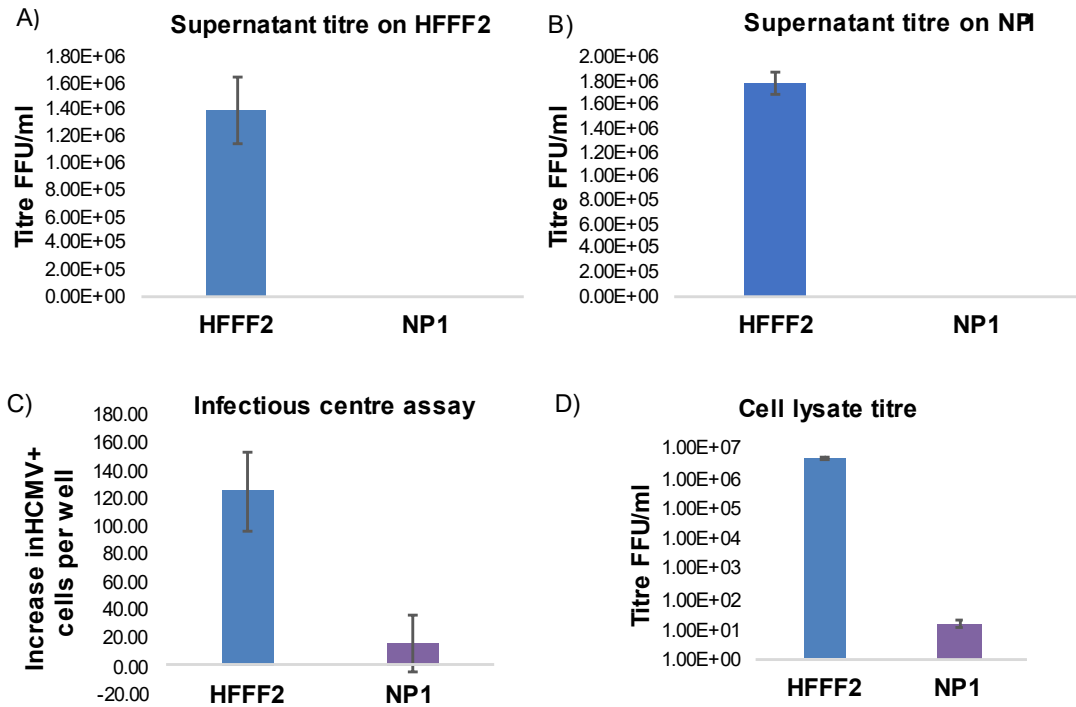


Figure 3.3.1 Detection of HCMV infectivity from HCMV infected NP1

A) HCMV infected HFFF2 and NP1 supernatant titre on naïve HFFF2, displayed as focus forming units per ml. B) HCMV infected HFFF2 and NP1 supernatant titre on naïve NP1. C) Infectious centre assay of infected NP1 seeded on to a monolayer of 10000 naïve HFFF2 or NP1, results displayed as increase in number of HCMV+ cells per well after 72 hrs. D) Cell lysates made from freeze thawing HFFF2 and NP1 infected with HCMV at an MOI of 1 FFU/cell for 10 days applied to naïve HFFF2 and number of GFP+ cells counted after 72 hrs to calculate titre in focus forming units per ml.

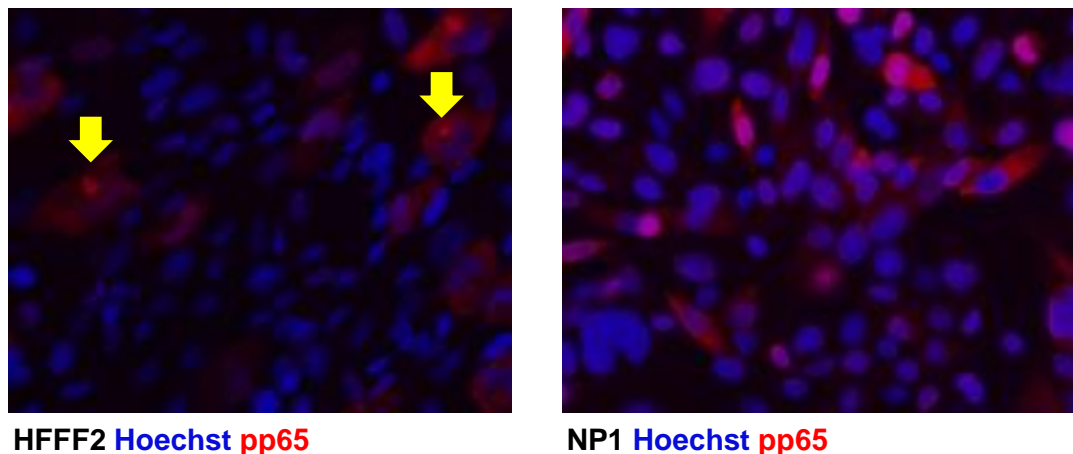


Figure 3.3.2 Localisation of pp65 in HCMV infected HFFF2 and NP1

HFFF2 and NP1 infected with HCMV at an MOI of 1 FFU/cell for 72 hrs. Cells were fixed in 4 % PFA in PBS and permeabilised. Cells were stained with DNA stain Hoechst (blue) and antibodies against HCMV pp65 and Alexa Fluor 594 conjugated secondary antibodies (red). Arrows indicating perinuclear concentration of pp65. Images were taken using the 10x objective of the Nikon Eclipse Ti-E Widefield Fluorescent Inverted Microscope.

3.4.2 Is the lack of virion production in HCMV infected NP1 due to lack of assembly compartment (AC) formation?

A characteristic feature of HCMV infected fibroblasts (including HFFF2) is a kidney-shaped nucleus which curves around the distinct perinuclear body of the AC. The accumulation of HCMV tegument proteins, including pp28 and pp65, along with envelope glycoproteins gB and gH to a structure co-localizing with the *trans*-Golgi network (TGN) was first described by Sanchez *et al.*, (2000). Nucleocapsids are formed in the nucleus before budding out through the nuclear membrane and releasing into the cytoplasm, where they must pass through the AC in order for efficient virion assembly to occur (Buser *et al.*, 2007, Gibson, 2008).

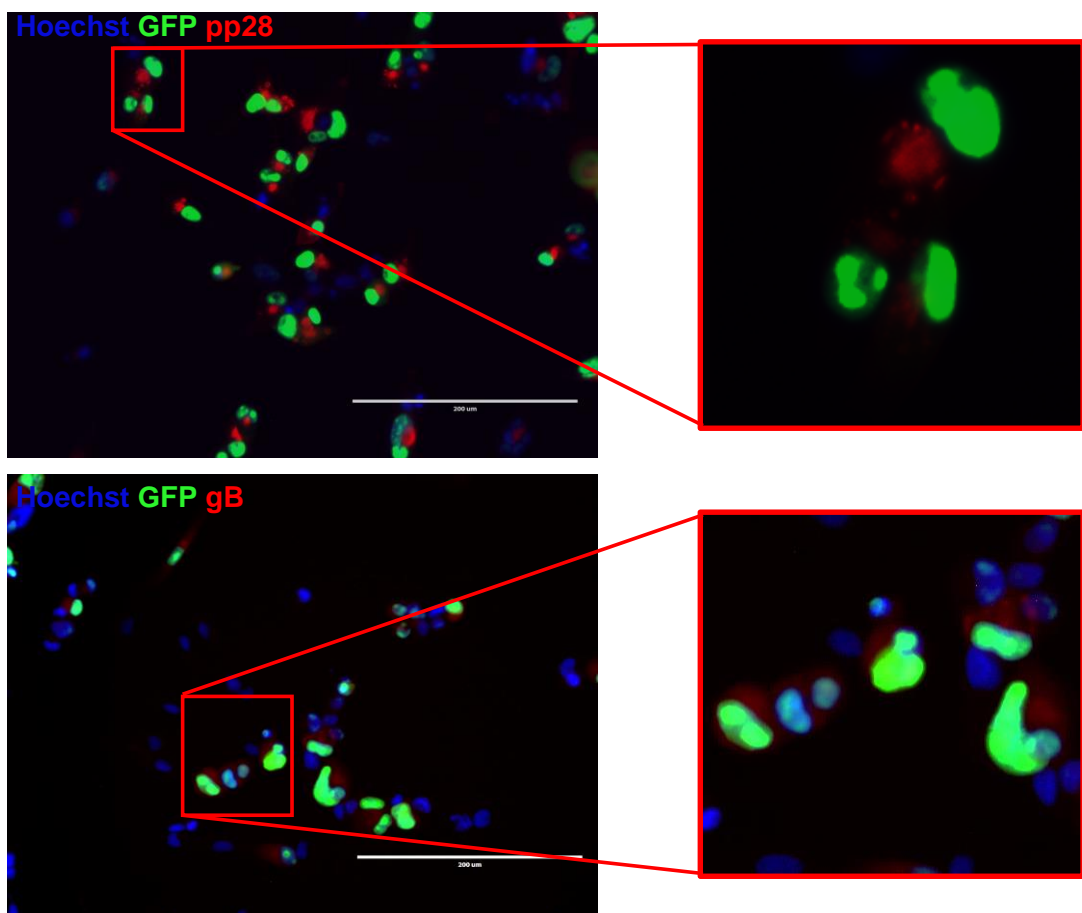


Figure 3.3.3 Immunofluorescent staining of HCMV pp28 and gB localisation to assess AC formation in HCMV infected NP1

NP1 infected with HCMV at an MOI of 1 FFU/cell fixed in 4 % PFA at 96 h.p.i. Cells were permeabilised and stained using primary antibodies against HCMV pp28 and gB with Alexa Fluor 594 (red) conjugated secondary antibodies, Hoechst DNA dye (blue) and viral GFP (green). Fluorescence was imaged at 260 x magnification using the EVOS cell imaging system.

Immunofluorescent staining for pp65, the most abundant HCMV tegument protein revealed a distinct pattern of localisation in NP1 compared to HFFF2 (Figure 3.3.2). Firstly, Hoechst staining showed that nuclei of HCMV infected NP1 fail to adopt the classic kidney-shape morphology as seen in infected HFFF2. Secondly, pp65 in HFFF2 was present both in the nucleus of infected cells and throughout the cytoplasm, with an intensely stained perinuclear accumulation detected from 72 h.p.i consistent with pp65 localising to the AC during virion assembly. By contrast, infected NP1 retained pp65 present in both the nucleus and throughout the cytoplasm, although the perinuclear accumulation was not observed in these cells. This raised the question: “do NP1 cells support the efficient formation of the HCMV AC”?

To determine whether the lack of perinuclear staining was specific to pp65, or instead represented the lack of a viable AC, immunofluorescent staining of HCMV infected NP1 was performed for pp28 and gB, as these are both known to localise to the AC during virion assembly (Sanchez *et al.*, 2000). Figure 3.3.3 shows that bright perinuclear spots of fluorescence were present in HCMV infected NP1 stained for both tegument protein pp28 and envelope glycoprotein gB. This suggests that a perinuclear AC-like compartment is forming in these cells, yet this lacks pp65. Thus, a lack of pp65 localisation to the AC in NP1 cells may explain the lack of infectious virus production.

3.5 Chronic infection of NP1 cells with HCMV

One of the defining characteristics of herpes viruses is their ability to establish lifelong infection of the host. Primary HCMV infection in most cell types (discussed in section 1.2.3) is initially lytic, during which time the majority of viral genes are expressed in a temporal cascade leading to production of new infectious particles (Wathen and Stinski, 1981). Following lytic infection, latency is established in some cell types (discussed in section 1.2.4), during which time viral gene expression decreases (Söderberg-Nauclér and Nelson, 1999). By limiting replication, HCMV avoids immune detection whilst maintaining viral episomes in host cells (Vossen *et al.*, 2002). Haematopoietic progenitor cells and cells of the myeloid lineage are known to harbour latent HCMV (Mendelson *et al.*, 1996 and Von Laer *et al.*, 1995). Despite neural cell types being highly permissive to HCMV infection *in vivo*, studies of HCMV latency in the human brain are limited. Belzile *et al.*, (2014) reported persistence of HCMV genomes in the absence of IE1 expression in primitive neural stem cells up to one month post infection *in vitro*. In contrast, Luo *et al.*, (2008) suggest that neurons are more likely to be a reservoir for HCMV latency in the brain due to their prolonged

survival post infection compared to neural progenitors or astroglia. Tsutsui *et al.*, (2002) studied *in vivo* infection of neonatal mice with MCMV and found neural stem cells or neural progenitor cells to be likely reservoirs of latency with reactivation in the SVZ of murine brains detected at over 180 days post infection. Having found NP1 can be infected with HCMV with the notable lack of detectable infectious particles and with less cell death than in HFFF2, we explored the possibility of NP1 supporting chronic or latent HCMV infection.

NP1 were infected with HCMV at an MOI of 1 FFU/cell resulting in a population with 92% of cells expressing virus-encoded GFP at 3 d.p.i. The cells were split 1:4 each time they reached around 80% confluency and GFP expression was monitored regularly (Figure 3.4A). GFP expression began to decrease from ~14 d.p.i, being lost completely by 63 d.p.i (Figure 3.4B). Following a period of no detectable GFP, the GFP returned in discrete pockets of infected cells around 85 d.p.i. GFP expression continued to appear and disappear sporadically for as long as the cells were maintained in culture (over 130 d.p.i), considerably longer than has been reported in similar cell types.

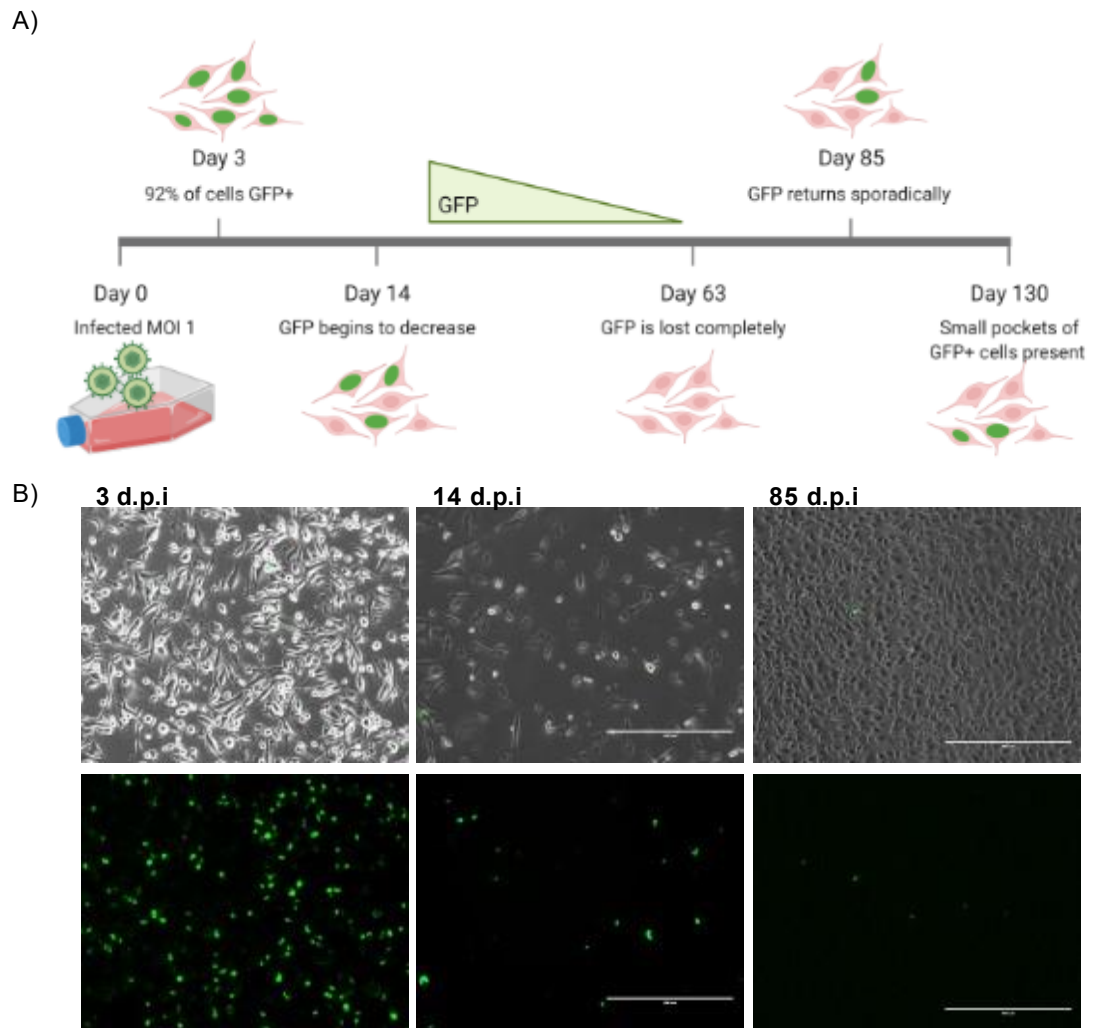


Figure 3.4 Long term HCMV infection of NP1

A) Schematic showing GFP expression over time in long term infection of NP1 infected with HCMV at an MOI of 1 FFU/cell (Made using Biorender). B) Viral GFP expression in NP1 infected with HCMV at an MOI of 1 FFU/cell, imaged at 260 x magnification using EVOS FL cell imaging system at day 3, 14 and 85 days post infection.

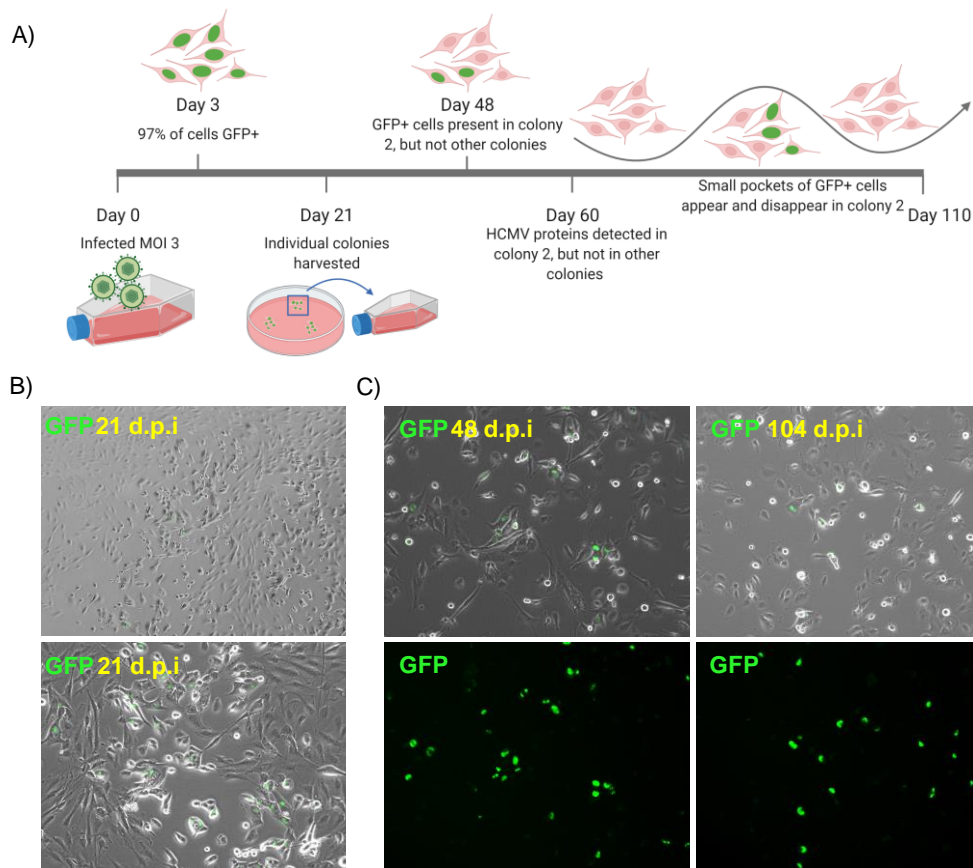


Figure 3.5.1 Isolation, expansion and longitudinal tracking of a chronically HCMV infected NP1 colony

A) Schematic of isolation of chronically infected HCMV NP1 colonies and GFP expression over 110 days post infection. B) NP1 infected with HCMV at an MOI of 3 FFU/cell at 21 days post infection, before colony isolation. Images taken using 4 x and 10 x objective of EVOS cell imaging system. C) GFP expression of colony 2 infected NP1 cells at 48 and 104 d.p.i at 260 x magnification using EVOS FL cell imaging system.

3.5.1 Isolation of individual HCMV infected cell clones

Following HCMV infection of 90 % confluent NP1 at an MOI of 3 FFU/cell, cells were seeded at a very low density, with just 2×10^5 cells in a 25 cm² flask, to generate colonies originating from single infected cells. At 21 d.p.i, 4 GFP+ colonies were identified and isolated using a sterile needle and pipette (figure 3.5.1A). Each colony was resuspended in NP media and transferred to a new flask to be expanded and then maintained as per NP1, described in section 2.1. Colonies were monitored regularly for GFP expression, with all but colony 2 losing GFP between isolation at 21 d.p.i and 46 d.p.i. Whilst GFP expression in colony 2 significantly decreased after 21 d.p.i, the proportion of GFP+ cells undulated over time, with GFP expression appearing and disappearing again, predominantly in secluded pockets of cells rather than distributed throughout the population, suggesting that NP1 can be chronically infected with HCMV (figure

3.5.1). Supernatant titre, cell lysate titre and infectious centre assays at 46 d.p.i showed no infectious virus production could be detected from colony 2 cells (data not shown).

Colony 2 cells were fixed in 4 % PFA at 60 d.p.i and immunofluorescence for HCMV IE, pp52 and pp65 performed as detailed in section 2.5. Figure 3.5.2 shows IE expression (red) is detected both in cells that are GFP+ and in some that are GFP-. The IRES-eGFP is located downstream of UL122 (IE2), so it is assumed that GFP expression indicates expression of IE2. The IE antibody used binds both IE1 and IE2, so the absence of GFP expression in these IE+ cells could indicate that only IE1 is being expressed. Also notable is the cytoplasmic IE expression present in all the cells. IE expression in HCMV infected HFFF2 and NP1 up to 72 h.p.i is strictly nuclear (shown in figure 3.2.2). Expression of early protein pp52 was also detected in colony 2 at 60 d.p.i, exclusively in cells also expressing GFP (Figure 3.5.2). Similarly, expression of late protein, pp65 was also observed, solely in GFP+ cells. Expression of early and late proteins suggests lytic infection of these cells.

Colony 2 cells that were frozen down in NP media containing 10 % DMSO were thawed at 37 °C and transferred to a 25 cm² cell culture flask and allowed to settle. Figure 3.5.3A shows GFP expression in colony 2 cells at 24, 48, 120 and 168 hrs post thaw. At the time of freezing ~3 % of cells were GFP+, but at 12 hrs post thaw 23 % of cells were expressing GFP (Figure 3.5.3B). We also observed an increase in cell death upon thawing Colony 2, compared to thawing non-infected NP1 cells of a similar passage.

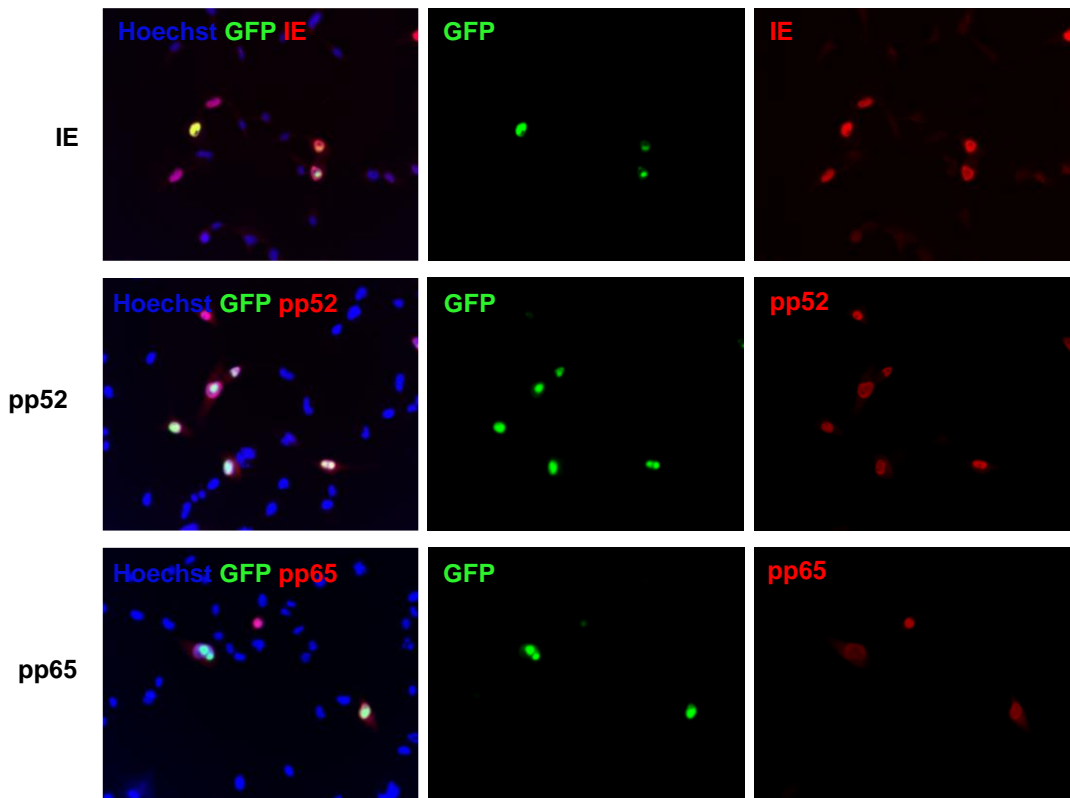


Figure 3.5.2 Immunofluorescence of colony 2 cells at 60 d.p.i stained for HCMV IE, pp52 and pp65

Immunofluorescence of colony 2 cells at 60 days post infection fixed with 4% PFA, permeabilised and stained with Hoechst DNA stain (blue) and antibodies against HCMV IE, pp52 and pp65 with Alexa Fluor 594 conjugated secondary antibodies (red) and GFP (green). Images were taken at 520 x magnification of the EVOS FL cell imaging system.

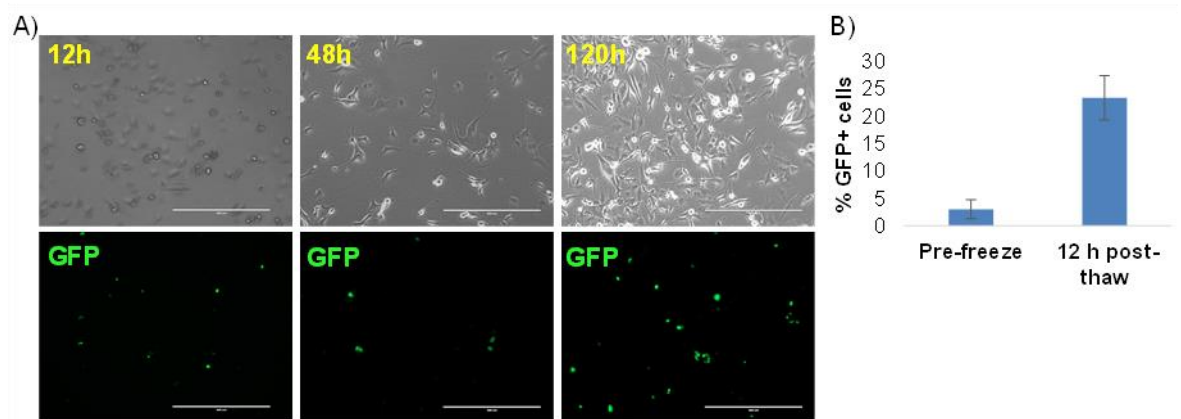


Figure 3.5.3 GFP expression in Colony 2 cells following freeze-thaw

A) Colony 2 chronically HCMV infected NP1 cells frozen at -80°C in 10 % DMSO in NP media at 68 d.p.i, thawed and grown in NP media. Cells and GFP expression imaged at 12, 48, 120 and 168 hrs post infection at 260 x magnification using the EVOS FL cell imaging system. B) Percentage of GFP positive colony 2 cells before freezing and post-thaw.

3.6 Discussion

To begin to investigate the potential link between HCMV and GBM, we needed to first explore HCMV infection of the likely cell of origin for these tumours, adult neural progenitor cells (Cobbs *et al.*, 2002, Mitchell *et al.*, 2008). The literature suggests that neural stem or progenitor cells originating in the SVZ of the brain are the most likely candidates for the cell of origin for GBM (Lee *et al.*, 2018, Llaguno *et al.*, 2019). Several studies have characterised HCMV infection of neural progenitor cells derived from foetal forebrain tissue and neural progenitor cells derived from embryonic stem cells (Cheeran *et al.*, 2005, Luo *et al.*, 2008, Belzile *et al.*, 2014). However, as HCMV antigen is present in GBM tumours arising in adult brains, this suggests that HCMV can be present in the adult brain. HCMV has previously been detected in the brains of adults with HIV infection AIDS and HCMV encephalitis can occur in the immunosuppressed (Bell, 1998). Although very rare, HCMV encephalitis has been described in immunocompetent, HIV negative patients (Micallef *et al.*, 2018). Our aim was therefore to establish if adult neural progenitor cells were permissive to HCMV infection and whether or not they could harbour long term, persistent infection. We determined that NP1, neural progenitor cells from an adult brain could be easily infected with HCMV *in vitro* with viral GFP expression detectable from 48 h.p.i (Figure 3.2A). Notably, when HFFF2 and NP1 are infected at the same MOI, a higher number of NP1 become infected and express GFP (Figure 3.2A). Immunofluorescence for immediate early, early and late HCMV proteins showed that the progression through the temporal cascade of HCMV lytic gene expression was occurring in NP1 cells (Figure 3.2.2). Despite this, we could not detect any secreted infectivity in the supernatant of infected NP1 cells when it was applied to naïve HFFF2 (Figure 3.3.1A). This absence of secreted infectivity led us to question whether virions were indeed being produced in NP1, but their tropism had become restricted to neural cells, which could explain the lack of infectivity in HFFF2, a fibroblast cell line. However, when we repeated the same experiment, but applied the supernatant onto naïve NP1 rather than HFFF2, we still didn't detect any infectivity, ruling out a restriction in tropism (Figure 3.3.1B). We also looked for cell to cell spread of virus from infected NP1, as Merlin HCMV has been shown to be capable of efficient cell to cell spread (Schultz *et al.*, 2020). We investigated this possibility using the infectious centre assay protocol, but again didn't see any robust detection of infectivity (Figure 3.3.1C). Although some wells did show a small increase in the number of infected cells, this can likely be attributed to variability in the counting the GFP+ and IE+ cells as is reflected by the large error bars. It is possible that some infected cells were missed during counting on day 1 of the experiment as GFP expression is not as

strong and less visible at day 1 as at the end point of the experiment. Our final attempt to detect virus production in NP1 was to investigate the possibility of cell associated virus being produced in these cells, by looking for infectious virus in HCMV infected NP1 whole cell lysates. Whilst a very low titre was detected by this method, which could indicate low level production of cell associated virus, this is more likely to be due to a limitation of the method (Figure 3.3.1D). The main limitation of the cell lysate method is that although a sample of the lysate was examined using the EVOS cell imaging system for remaining whole cells and none were visible, it is possible that not all the infected NP1 cells are being completely lysed and therefore a small number of GFP+ NP1 are being detected instead of GFP+ HFFF2. It is unlikely that HCMV produced by NP1 would be cell associated as the Merlin-IE2-GFP contains the mutation in UL128 which results in a stop codon and premature termination of the protein. Knockdown of UL128 is known to lead to release of virus that was previously strictly cell associated (Murrell *et al.*, 2017).

The lack of infectious particle production despite the production of immediate early, early and late HCMV proteins in NP1, suggests that the block in virion production is likely to be during the late phase of the virus life cycle. The migration of pp65 from the nuclei into the cytoplasm of NP1 implies that capsids assembled in the nucleus are egressing through the nuclear membrane to reach the cytoplasm (Figure 3.2.2). In fibroblasts and other permissive cell types, the assembly and subsequent transport of virions occurs by hijacking of host cell secretory machinery including endoplasmic reticulum (ER), Golgi apparatus, and endosomal network to form the viral AC (Moorman *et al.*, 2010). The concentrated spots of perinuclear pp65 staining that were present in HCMV infected HFFF2 at 72 h.p.i, but absent in NP1, together with the absence of the classical kidney-shaped nuclei associated with HCMV infection led us to hypothesise that there could be a defect in the formation of the AC in neural progenitor cells (Figure 3.3.2). In contrast to pp65, immunofluorescence of two other AC localising HCMV proteins, namely pp28 and gB, showed distinct perinuclear spots at 96 h.p.i (Figure 3.3.3) (Sanchez *et al.*, 2000). This suggests that the AC is forming in NP1 cells and that the lack of perinuclear localisation of pp65 is specific to that particular protein, not to all AC localising proteins. Further experiments would need to be done in order to elucidate why pp65 doesn't concentrate at the AC in these cells. Although pp65 is one of the most abundant tegument protein, it is not essential for virion production, so lack of localisation to the AC does not fully explain the lack of infectious particle production in NP1 (Malouli *et al.*, 2014). It is possible that the requirement for pp65 could be cell type specific. Also notable at the 96 hr time point, is that a small number of

infected NP1 cells do show the kidney-shaped nuclei, although the vast majority of cells do not (Figure 3.3.3). This continues to be the case at later time points (data not shown). This variation in nuclei morphology in infected NP1 could reflect the highly heterogeneous nature of the NP1 population.

The presence of HCMV antigen in tumours removed from adult GBM patients, denotes the presence of HCMV in the adult brain. Cobbs *et al.*, (2002) originally postulated that the HCMV antigen in glioma could be attributable to reactivation of a latent infection of astrocytic or endothelial cell types, or alternatively due to *de novo* infection of glial cells. There is little evidence in the literature to support the notion of HCMV persistence in the adult brain of immunocompetent individuals. This deficiency of literature can be largely attributed to ethical considerations and practical difficulties associated with identification and longitudinal study of individuals infected with HCMV at an early age. However, there is evidence of *in vivo* persistence of MCMV in murine brains of adult mice that were congenitally infected as neonates (Tsutsui *et al.*, 2002).

Due to the lack of information about HCMV persistence in the brain, it was important to determine if NP1 could support long term infection with HCMV. A flask of HFFF2 infected even at an MOI as low as 0.01 FFU/cell show 100 % cell death by between 14 and 21 d.p.i. In stark contrast to this, we detected both GFP and HCMV protein expression in NP1 populations infected at an MOI of 1 and 3 FFU/cell at over 130 and 110 d.p.i respectively (Figures 3.4 and 3.5.1). Although some initial cell death occurs in HCMV infected NP1, particularly at MOI of 3+ FFU/cell, the population as a whole continues to proliferate. We have not observed complete loss of detectable HCMV in these long-term infected cultures to date. Detection of HCMV was limited to 130 days due to time constraints on lab time, not due to loss of viral detection. This suggests that NP cells have the propensity to support long term infection. However, it is difficult to discern from the data whether this is a low level, chronic infection spreading slowly through the NP1 population or whether we are seeing latency with sporadic reactivation. The pattern of GFP+ cells appearing in close proximity to each other could be indicative of a very low-level chronic infection spreading to neighbouring cells (Figure 3.5.1C).

It is also possible that latent HCMV is being reactivated and subsequently spreading to neighbouring cells. Immunofluorescence of colony 2 at 60 d.p.i showed IE expression in cells that were GFP negative (Figure 3.5.2). As the IE antibody used in this experiment detects both IE1 and IE2 proteins, this could indicate the presence of IE1 in the absence of IE2 detection as the IRES-eGFP is inserted downstream of IE2. Whilst traditionally it was thought that IE

expression was completely absent during latency due to repression of the MIEP, consensus is now shifting due to transcriptomic data in latent infection of haematopoietic cells showing that viral genes are broadly expressed at extremely low levels (Cheng *et al.*, 2017, Shnayder *et al.*, 2018). Reeves and Sinclair (2013) reported dendritic cells carrying HCMV genomes with IE expression, but no virion production in contrast to circulating monocytes which carry HCMV genomes without IE expression. Another explanation for the detection of IE in the absence of GFP in infected NP1 could simply be that IE immunofluorescence is more sensitive detection method than simply looking for GFP expression. The presence of cytoplasmic IE in colony 2 is reminiscent of that seen in GBM by Soroceanu *et al.*, (2015). IE expression in fibroblasts is strictly nuclear and we found initial infection of NP1 also showed strictly expression. This cytoplasmic IE expression in the absence of detectable virion production demonstrates that long term infected HCMV infected NP1, share similarities to IE+ GBM tumour samples.

In summary we have shown that adult neural progenitor cells (NP1) can be infected with HCMV and progress through the temporal cascade of viral gene expression. Despite being highly infectable, NP1 show minimal cell death and produce very little or no infectious particles when maintained in culture. NP1 can harbour long term HCMV infection with GFP expression disappearing and reappearing sporadically. Cytoplasmic IE expression is present in long term HCMV infected NP1, supporting the possibility of adult neural progenitors being a potential cell of origin for GBM.

Chapter 4 - The effects of HCMV infection on neural progenitor cell differentiation

4.1 Introduction

NP cells are defined by their ability to give rise to both glial and neuronal cell types in the brain including neurons, astrocytes and oligodendrocytes (Merkle *et al.*, 2004, Kriegstein and Alvarez- Buylla, 2009). As well as being present in the embryonic brain where they play an important role in neural development, NPs also reside in the adult brain. Here they can be found in two distinct niches, the SGZ of the dentate gyrus, and the so-called “adult SVZ” which surrounds the lateral ventricles of the mature cerebral cortex (Martínez-Cerdeño and Noctor, 2018). It is thought that adult NP cells have less potency than those found in the embryonic brain (Kriegstein and Alvarez- Buylla, 2009). Whilst adult NPs have the ability to proliferate, they do not possess the capability to self-renew like NSCs. Accordingly, it has long been known that neurogenesis occurs in the adult brain of mammals, including humans, where newly generated neurons integrate into existing circuits (Smart, 1961, Eriksson *et al.*, 1998). Differentiation of NPs from both the SGZ and SVZ is the initial step of adult neurogenesis. Although the potential for neurogenesis decreases with age, human neurogenesis has been shown to occur far into old age (Boldrini *et al.*, 2018).

Several studies have investigated the effect of HCMV infection in foetal NP cells. Oderberg *et al.* (2006) reported that infection of foetal forebrain derived NPs using Towne and TB40 strains of HCMV led to a 55 % and 72 % inhibition of neuronal differentiation, respectively. Although the mechanism for this HCMV induced block in differentiation was unclear, it has been attributed to the expression of HCMV late genes. HCMV mediated induction of apoptosis was also observed in these cells. Luo *et al.* (2010) reported HCMV infection with Towne to induce premature and aberrant differentiation of neonatal NP cells. Liu *et al.*, (2017) also found HCMV infection disrupted differentiation of NP cells and dysregulated cell fate via downregulation of Hes1, a key component of the notch signalling pathway.

By contrast, research on the influence of HCMV infection on differentiation of the adult NP cells is distinctly lacking. As adult NP cells of the SVZ are a likely cell of origin for GBM and neutralisation of differentiation is thought to occur during the early stages of gliomagenesis, it was important to investigate the effects of HCMV infection on adult NP differentiation (Llaguno *et al.*, 2019, Hu *et al.*, 2013).

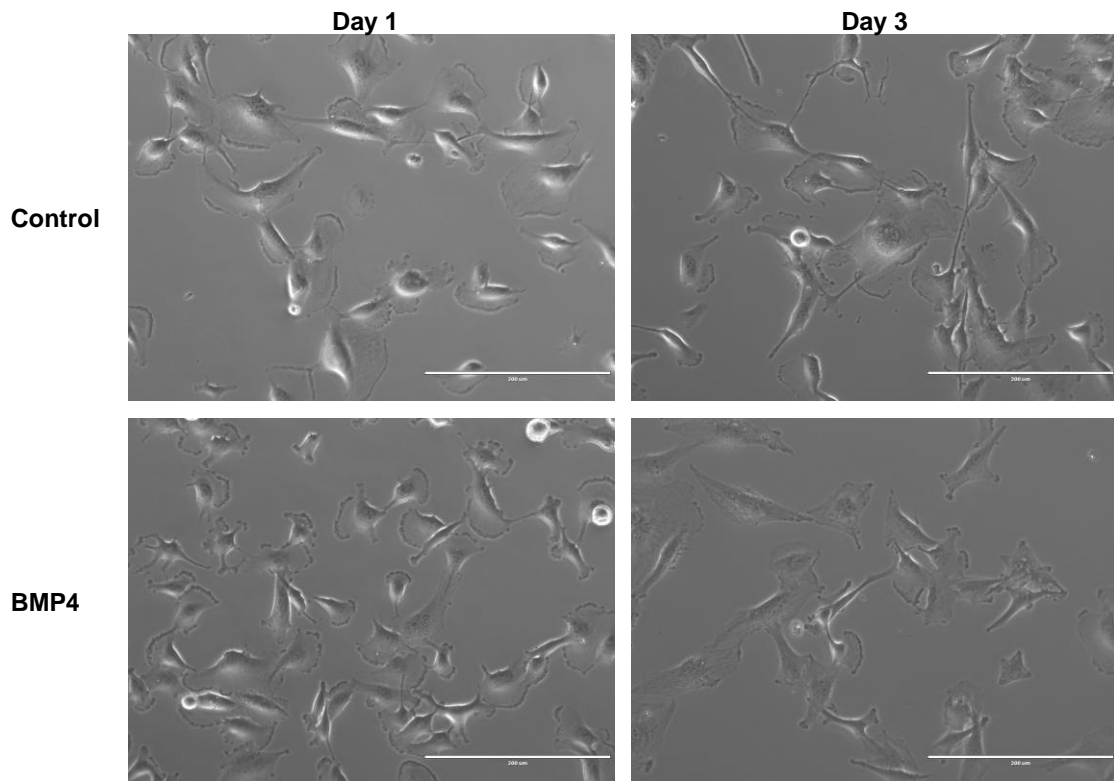


Figure 4.1 Phase images of NP1 treated with BMP4

NP1 cells treated with 100 ng/ml of BMP4 in NP media and control NP1 without treatment at day 1 and day 3 of treatment. Images taken using the 20 x objective of the EVOS cell imaging system. Scale bar = 200 µm

4.2 Establishing an *in vitro* model of neural progenitor cell differentiation

Several published differentiation protocols were compared to establish a viable method for *in vitro* differentiation of adult-derived NP1 cells and investigating the effect of HCMV infection. BMP4 treatment is known to promote neuronal and glial differentiation in neural stem cells (Gross *et al.*, 1996, Li, Cogswell and LoTurco 1998). Similarly, Cole, Murray and Xiao (2016), showed that BMP4 plays a role in differentiation of NP cells into all 3 major neural lineages; neurons, astrocytes and oligodendrocytes. Bonaguidi *et al.* (2005) found BMP4 treatment of neural stem cells increased the number of GFAP+ astrocytes.

Thus, NP1 cells were treated with 100 ng/ml BMP4 as described in section 2.6.3 for up to seven days and phase images (figure 4.1) showed limited change in morphology, suggesting the cells were not differentiating. For neuronal differentiation we would expect to see elongation of the cells and development of neuronal processes, whereas astrocytic differentiation results in stellate cells with multiple processes.

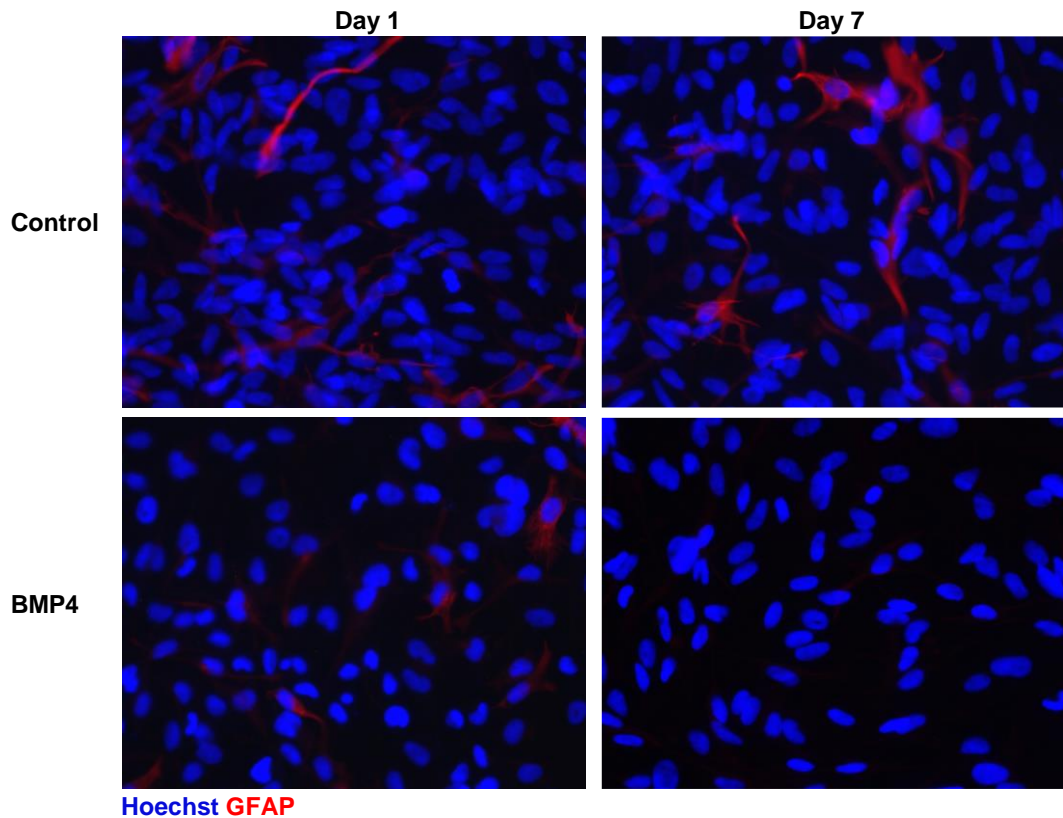


Figure 4.2 GFAP immunofluorescence of NP1 treated with BMP4

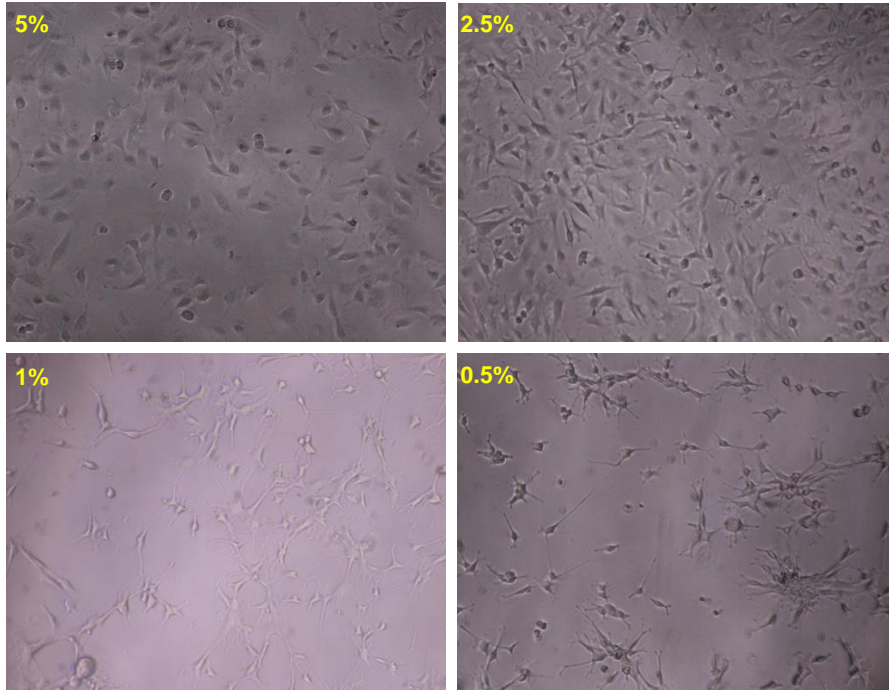
NP1 cells treated with 100ng/ml of BMP4 and untreated controls at day 1 and day 7 of treatment. Cells were fixed with 4% PFA and permeabilised before permeabilising and staining with a GFAP specific antibody (red) and Hoechst DNA stain (blue). Images were taken at 200 x magnification using the Nikon Ti-E Widefield Fluorescent Inverted Microscope.

To further investigate the possibility of astrocytic differentiation immunofluorescent staining using a specific antibody for GFAP was performed (figure 4.2). In the event of astrocytic differentiation, the number of GFAP+ cells would be expected to increase along with the overall level of GFAP expression. However, both the overall GFAP expression decreased, as did the number of GFAP+ cells in the population in the BMP4 treated cells compared to the control at day 7. This led us to discount BMP4 treatment as a viable differentiation method for NP1.

Howard *et al.* (1993) found that serum starvation of neuroblasts resulted in either apoptosis or differentiation. To determine whether this could differentiate NP1 we treated cells with serum free NP media. Removal of serum in our hands led to complete cell death in the cultures overnight. In an attempt to minimise cell death whilst inducing differentiation we performed a serum titration from 5 %, the concentration usually used for NP media, down to 0.5 %. Whilst NP1 treated with 2.5 % maintained a high percentage of viable cells, they did not show changes in morphology consistent with differentiation. NP1 treated with lower serum

concentrations of 1 % or 0.5 % did show distinct changes in morphology with the development of processes consistent with neuronal or astrocytic differentiation. Unfortunately, the number of viable cells at these concentrations were too low for this to be a workable differentiation protocol to combine with HCMV infection.

A)



B)

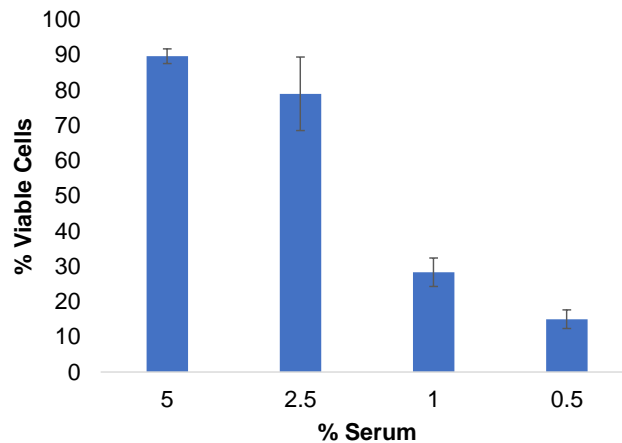


Figure 4.3 Serum starvation of NP1 cells

A) Phase images of NP1 treated with 5 %, 2.5 %, 1 % or 0.5 % serum for 24 hrs. Images taken at 260 x magnification using the EVOS cell imaging system. B) Percentage of viable NP1 cells after 24 hr of treatment with 5 %, 2.5 %, 1 % or 0.5 % serum. Viable cells counts were obtained by diluting equal volumes of cell suspension with 0.4 % Trypan blue in PBS and transferring to a haemocytometer for counting using an inverted microscope.

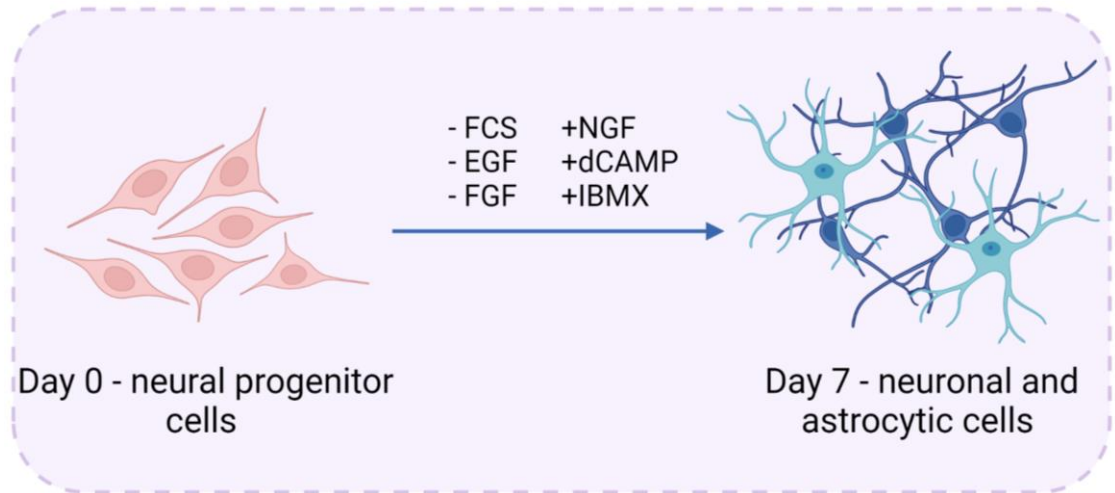


Figure 4.4 Summary of neural progenitor neuronal differentiation protocol

Schematic summary of Walton *et al.* (2006) seven day differentiation method for neural progenitor cells.

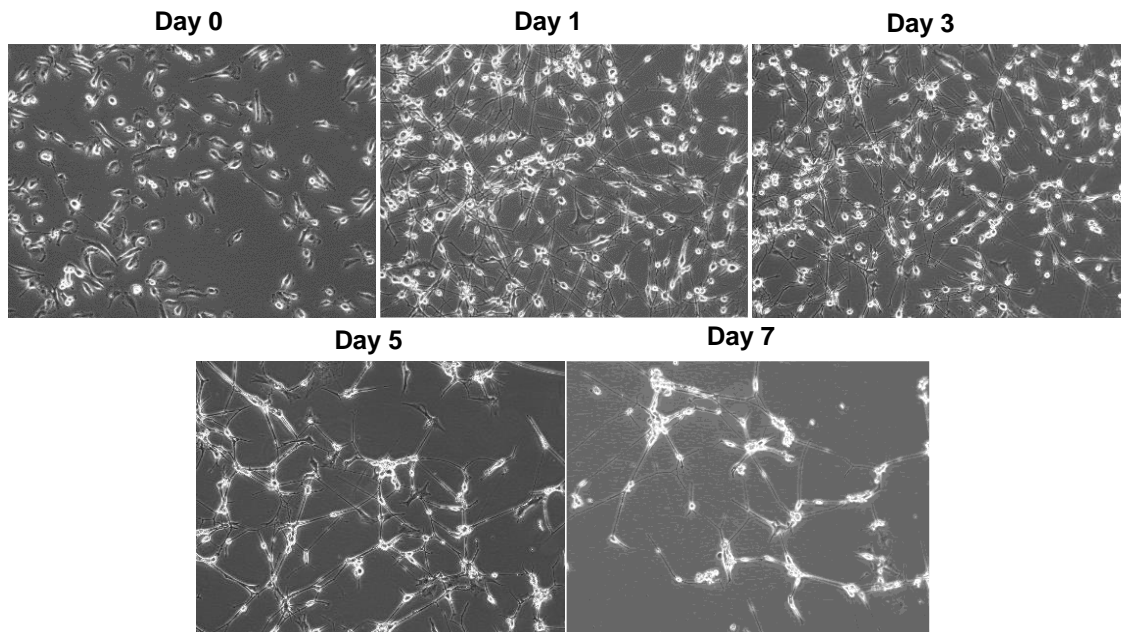


Figure 4.5 Neuronal differentiation of NP1

Differentiation of NP1 cells using the Walton *et al.* (2006) method for *in vitro* differentiation of adult neural progenitor cells. Phase images were taken at 260 x magnification using the EVOS FL cell imaging system at day 0,1,3,5 and 7 of differentiation treatment.

The Walton *et al.* (2006) paper describes a method for differentiation of adult NP cells derived from a 17 year old female undergoing surgery for intractable temporal lobe epilepsy that results in a predominantly neuronal population with a small proportion of astrocytic cells (detailed in section 2.6.4). When this protocol was applied to NP1 cells, they quickly developed a neuronal morphology with elongated processes and showed less cell death than previously tried methods (figure 4.5). After three days of differentiation, a transient subset of cells adopt a hybridised somato-dendritic morphology (cell body with dendrites) with astrocytic and neuronal markers. After five days of differentiation, maturing cells show a decrease in GFAP and continue to strongly express β -III-tubulin, displaying the morphology of immature neurons. In the original published study, this method of differentiating NP cells resulted in neuronal cells that had similar electrophysiological properties as immature neurons, including the ability to fire elicited action potentials.

To compare the differentiation of our NP1 cells, to that of the adult NP cells investigated in the original paper, immunofluorescent staining for the astrocytic marker GFAP was performed at day three of differentiation as this marker was used in the original paper to discriminate astrocytic cells from neuronal or oligodendrocytic cells (Walton *et al.*, 2006). Around 24 % of cells in the population were strongly expressing GFAP and display a multi-process morphology very similar to the “asteron” hybrid astrocytic/neuronal intermediate cell type shown in the Walton *et al.* 2006 paper. Similarly, immunofluorescent staining for the neuronal marker, β -III-tubulin, at day seven of differentiation (figure 4.6) is reminiscent of the β -III-tubulin immunofluorescence at day seven of differentiated NP cells in the Walton *et al.* paper. Taken together this data suggested we had successfully applied a differentiation protocol for hybrid neuronal/astrocytic differentiation of NP1 which could be taken forward to investigate the effects of HCMV upon NP differentiation.

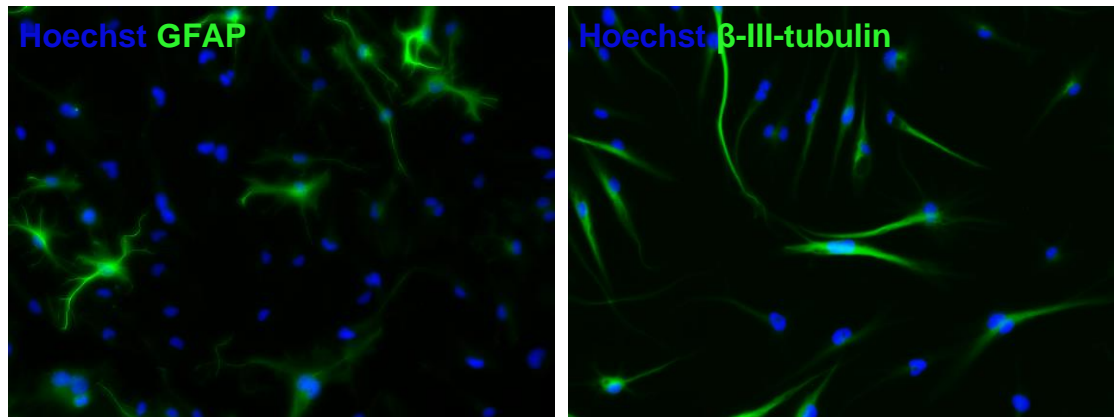


Figure 4.6 Comparison of GFAP and β -III-tubulin immunofluorescence in neuronal differentiation of NP1 cells

A) Immunofluorescence of NP1 cells stained for GFAP(green) and Hoechst DNA dye (blue) after 3 days of neuronal differentiation using the Walton *et al.* (2006) method. Image taken at 260 x magnification using the EVOS cell imaging system. B) Immunofluorescence of NP1 cells stained for β -III-tubulin (green) and Hoechst DNA dye (blue) at day 7 of neuronal differentiation using the Walton *et al.* (2006) method. Image taken at 260 x magnification using the EVOS cell imaging system.

4.3 HCMV infection perturbs *in vitro* differentiation of NP1

4.3.1 HCMV infection inhibits the development of neuronal morphology and disrupts neurite outgrowth during differentiation

We next applied the *in vitro* differentiation protocol above to infected NP1 cells to investigate the effects upon differentiation. NP1 were infected at an MOI of 3 FFU/cell which consistently led to ~95 % of cells expressing GFP at 72 h.p.i (data not shown). Differentiation media was applied to HCMV infected NP1 at 5 d.p.i with mock infected NP1 cultured for the same duration used as a control. From this point onwards, this will be referred to as differentiation protocol 1. Figure 4.7 shows that at day 0 (5 d.p.i with HCMV), the morphology of NP1 changed distinctly; naïve NP1 have a ruffled membrane at the leading edge of the cell which is often associated with motile cells, yet after five days of HCMV infection this ruffled edge is lost and many of the cells display a more elongated morphology (Mahankali *et al.*, 2011).

Due to the change in morphology cells were stained using phalloidin-Alexa Fluor 594 nm to visualise actin filaments and Hoechst DNA dye to stain nuclei (figure 4.8). This revealed a distinct change in the actin organisation of HCMV infected cells. F-actin is most concentrated at the ruffled edge of NP1, however at five

d.p.i the cells have lost the ruffled edges and the bright staining at the cell membrane is decreased. NP1 phalloidin staining also shows filopodia-like projections that are absent from HCMV-infected cells, which have a much smoother, more defined edge (figure 4.8). The HCMV infected NP1 have an elongated appearance and an area of concentrated speckled perinuclear phalloidin staining, consistent with the viral assembly compartment. At day one of differentiation, phase images of control NP1 (figure 4.7) show that the main body of the cells has shrunk and long neuronal processes have developed. In contrast, at day one of differentiation in HCMV infected cells, the main body of the cell remains much the same size and shape as at day 0, with far fewer neuronal projections. Where neurite outgrowth is present in the HCMV infected cells, the processes are generally shorter and have less branching. As differentiation progresses the difference in morphology between the mock and infected cells remains. Mock NP1 neurites become longer and thinner and establish contacts with those of neighbouring cells, whilst HCMV infected NP1 fail to develop neuronal morphology and maintain a much larger cell body. Whilst around 18 % of NP1 cells die off during neuronal differentiation, over 30 % of the HCMV infected cells die when differentiation media is applied (data not shown). This is evident from phase images as bright rounded up cells that are lifting off the plastic (also Trypan-blue permeable); this is particularly evident from day three onwards.

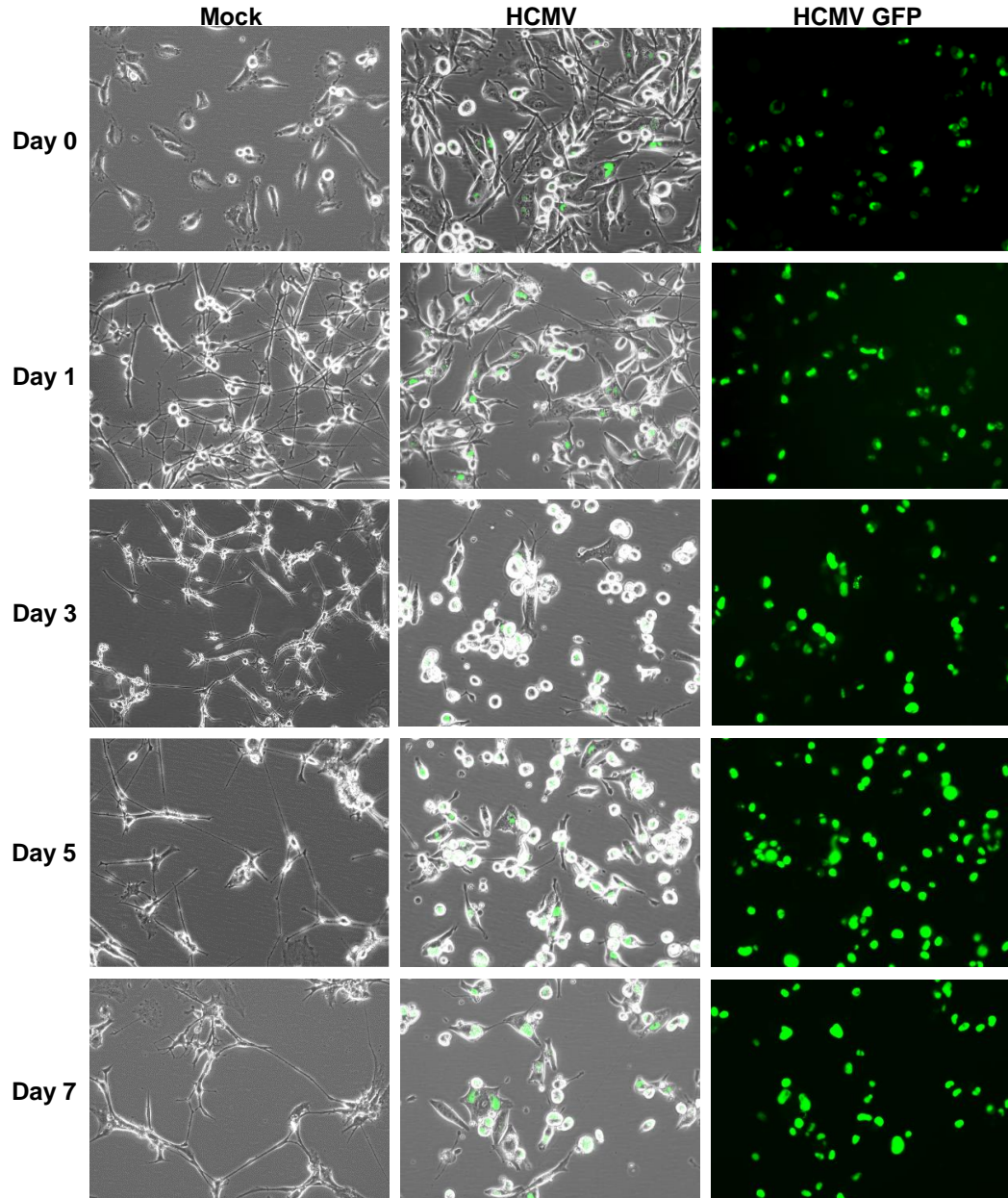


Figure 4.7 Differentiation of HCMV and mock infected NP1 showing virus-driven GFP expression

NP1 were infected at an MOI of 3 FFU/cell for 5 days, before being differentiated using a method for adult NP differentiation (Walton *et al.*, 2006). Phase images and GFP images were taken at day 0, 1, 3, 5 and 7 at 260 x magnification using the EVOS cell imaging system.

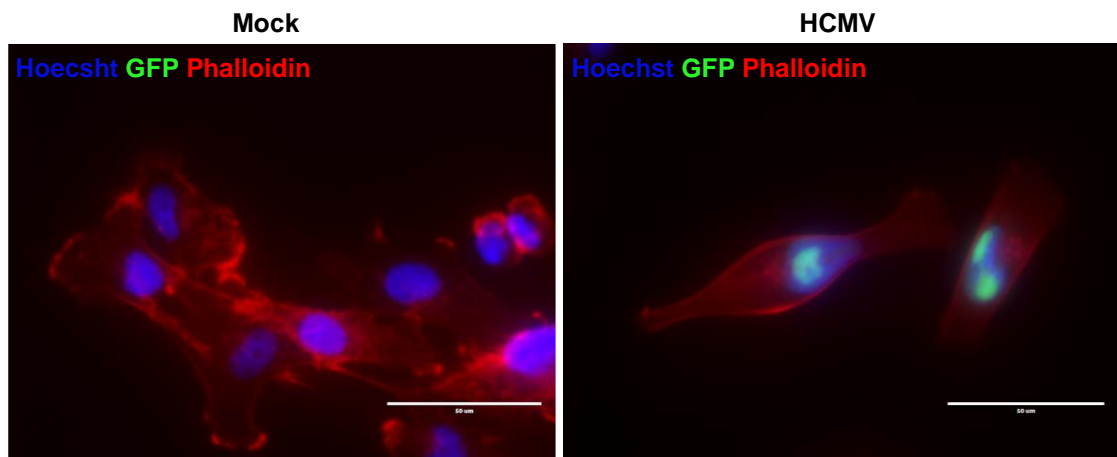


Figure 4.8 F-actin staining of Mock and HCMV infected NP1

Mock and HCMV infected cells at 5 d.p.i fixed in 4 % PFA, permeabilised and stained using phalloidin-Alexa Fluor 594 nm (red) to visualise F-actin, Hoechst DNA dye (blue) and viral GFP expression (green). Cells were imaged at 1560 x magnification using the EVOS cell imaging system.

Next, the neurite tracing function of the simple neurite tracer (SNT) plug-in for image J was used to quantify the differences in outgrowth between mock and HCMV infected NP1 cells. Neurite traces of mock vs HCMV infected NP1 at day 5 of differentiation are shown (traces in purple) in figure 4.9A. Neurite tracing was used to determine the average number of neurites with NP1 having on average 1.8 neurites per cell as opposed to HCMV infected NP1 which had only 0.4 neurites per cell (figure 4.9B). The average branch length of the neurites was also calculated, with mock NP1 having longer branch length than HCMV infected NP1 at 133 μm versus 81 μm respectively (Figure 4.9C). Finally, the average total neurite length per cell was calculated with mock NP1 having an average of 129 μm of neurite outgrowth per cell, compared to HCMV infected NP1 which had an average of just 31 μm per cell.

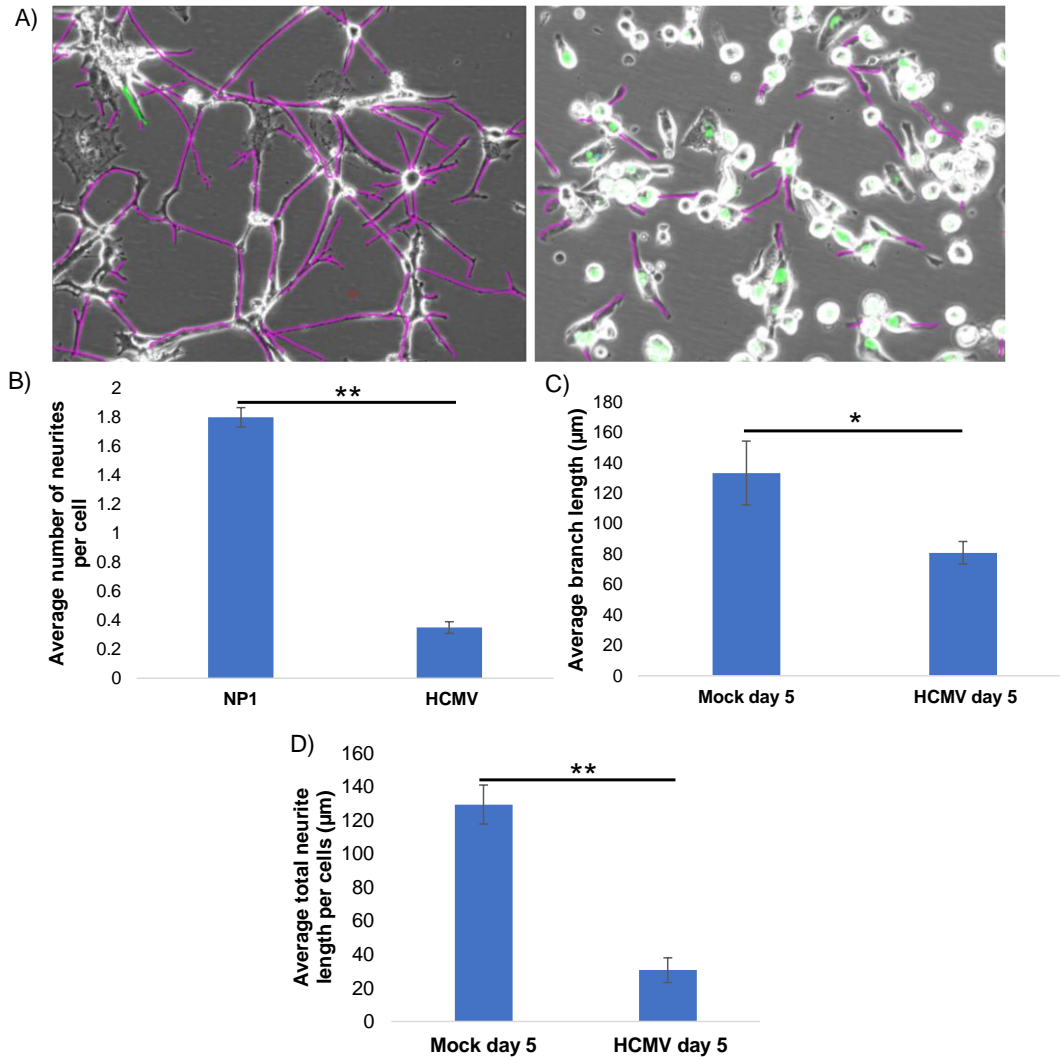


Figure 4.9 Neurite outgrowth at day 5 of differentiation in mock and HCMV infected NP1

A) Neurite tracing images using the SNT plug-in for Image J using phase images of mock and HCMV infected cells at day 5 of differentiation. Neurites traced in purple. B) Average number of neurites per cell in mock and HCMV infected NP1 at day 5 of differentiation quantified using ImageJ. C) Average branch length of neurites (μm) in mock and HCMV infected NP1 at day 5 of differentiation. D) Average total neurite length per cell (μm) in mock and HCMV infected NP1 at day 5 of differentiation (two-tailed student t-test, * $p \leq 0.05$, ** $p \leq 0.01$, *** $p \leq 0.001$, **** $p \leq 0.0001$, $n=3$)

4.3.2 The effect of HCMV infection on differentiation markers

The expression of a panel of NP differentiation markers was assessed by western blotting. Whilst this experiment was repeated five times, changes in western blotting equipment and reagents and reducing timepoints from day 0,1,3,5 and 7 to day 0 and 5 due to lab time restriction during the Covid-19 pandemic meant that the densitometry was not comparable, so one

representative set of western blots is shown in Figure 4.10. The stem cell marker nestin is replaced by cell type specific intermediate filament proteins such as neurofilament and GFAP during neurogenesis and gliogenesis (the formation of non-neuronal cells of the brain) respectively (Lin *et al.*, 1995). Nestin is expressed abundantly in NP1 cells, yet this decreased by 79% over the 7 day course of differentiation (figure 4.10A and B). At 5 d.p.i, (day 0 of differentiation), HCMV infection led to just a 21% decrease in nestin expression of mock-infected cells. However, unlike the incomplete decline in controls, nestin protein levels in HCMV infected NP decreased markedly throughout differentiation and were undetectable by day 7. Another stem cell marker, Sox2, a transcription factor essential for maintaining self-renewal in stem cells and many progenitor cells including NP, also decreased dramatically over the 7 day differentiation of NP1 (Figure 4.10A and D) (Fong *et al.*, 2008). However, after 5 days of HCMV infection Sox2 is undetectable and remains so throughout differentiation.

Proliferating cell nuclear antigen (PCNA) is a processivity factor for DNA polymerase δ ; PCNA expression is essential for cell cycle progression (Miyachi *et al.*, 1978). During differentiation of control NP1 cells, PCNA expression decreases by 88% between day 0 and day 7 (Figure 4.10A and C). This decrease is expected during neurogenesis as mature neurons exit the cell cycle and so do not proliferate (Purves *et al.*, 2001). Interestingly, whilst HCMV infected cells show a 51% decrease in PCNA compared to mock NP1 at day 0, they show an increase in PCNA expression over seven days of differentiation. By day 7, PCNA expression in HCMV infected cells has returned to virtually 100 % of that seen in mock NP1 at day 0.

Unlike previous studies that report a decrease in GFAP by day 5 of differentiation of adult neural progenitor cells we instead observed increased levels of GFAP protein in NP1 cells by the same method (Walton *et al.*, 2006). This could suggest that cells are differentiating towards a glial phenotype as opposed to a neuronal phenotype. It is also possible that NP1 cells are differentiated towards an "asterson" phenotype, where both astrocytic and neuronal markers are expressed. In HCMV infected NP1, GFAP expression more than doubled after five days of infection (HCMV 0). However, during five days of differentiation, GFAP decreases in HCMV infected cells, but increases in control NP1. This may indicate that whilst control cells are becoming more committed to an astrocytic phenotype, HCMV infected NP1 are becoming less astrocytic during differentiation.

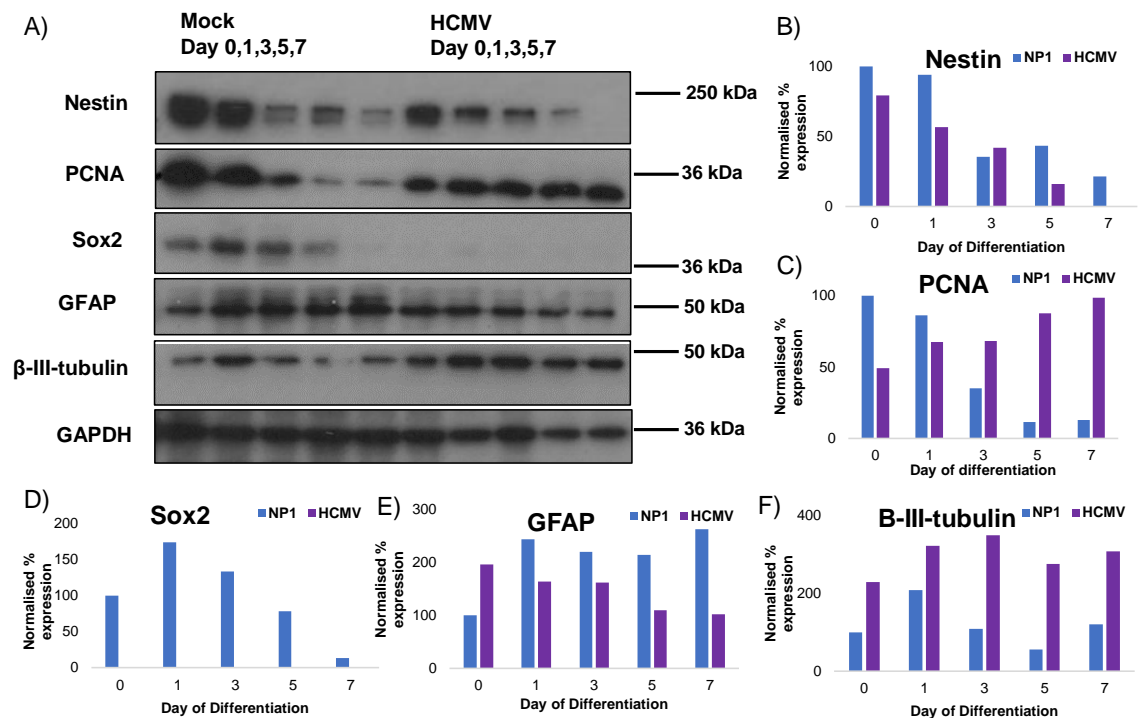


Figure 4.10 Protein expression during neural progenitor cell differentiation in HCMV infected NP1 cells

A) HCMV infected NP1 cells and mock infected controls were differentiated over 7 days using the Walton *et al.* (2006) method. Approximately 1×10^6 cells were lysed for Western blot analysis on day 0, 1, 3, 5 and 7. Membranes were probed for GAPDH, nestin, PCNA, Sox2, β -III-tubulin and GFAP. B) Nestin C) PCNA D) Sox2 E) GFAP F) β -III-tubulin. Quantification for B – F was performed using the ImageJ densitometry function to determine western blot band intensities in arbitrary densitometry units (ADU) which were subsequently normalised to GAPDH expression and presented as normalised percentage expression compared to NP1 day 0.

The neuronal marker, β -III-tubulin, fluctuates throughout NP1 differentiation. At day seven, β -III-tubulin levels are slightly higher than at day 0. This correlates with the expression seen in previous studies where newly generated neurons continued to express high levels of β -III-tubulin (Figure 4.10A and E) (Walton *et al.*, 2006). Following a 5 day HCMV infection (HCMV 0), β -III-tubulin levels more than doubled compared to mock NP1. Expression of β -III-tubulin remains consistently far higher in HCMV+ NP1 than that in mock NP1. By day 7 of differentiation, β -III-tubulin expression in HCMV infected NP1 increased to 134 % of that in HCMV 0.

Due to the maintenance of PCNA throughout the differentiation of HCMV infected NP1, we also looked at Ki67 expression by immunofluorescence. Ki67 expression is associated with specific stages of cellular DNA replication and cell division and is often used to identify highly proliferative (cancer) cells (Gerdes *et al.*, 1984). During differentiation of NP1 cells the percentage of Ki67+ cells

decreased from 94 % at day 0 to just 17 % at day 5. Similarly, 95 % of HCMV infected NP1 are Ki67+ at day 0. However, a much smaller decrease occurs during differentiation with 89 % of cells maintaining Ki67 expression at day 5 (Figure 4.11A and B). Notably, at day 5 of differentiation in the HCMV+ NP1 population, only cells which are GFP+ are expressing Ki67, suggesting that individual cells must be infected to retain Ki67 expression during differentiation, rather than Ki67 being maintained by the population as a whole.

4.4 CD133 expression is induced within HCMV infected NP1 during differentiation

CD133 (encoded by the *Prom1* locus) is one of the most commonly used markers for cancer initiating cells and is essential for GBM stem cell maintenance (Brescia *et al.*, 2013). Soroceanu *et al.* (2015) found that over 70 % of primary GBM cells from surgically resected tumours that expressed HCMV IE were also CD133+. *In vitro* HCMV infection of GBM cells has been shown to upregulate CD133 expression, resulting in a stem cell phenotype capable of forming neurospheres (Fornara *et al.*, 2016, Liu *et al.*, 2017). To investigate CD133 expression in HCMV infected NP1, protein lysates taken at day 0,1,3,5 and 7 were western blotted with a CD133 specific antibody. CD133 was not reliably detected in NP1 at any time point during differentiation, however in HCMV infected cells at day 0 (i.e. five days post-infection), CD133 expression was clearly present (Figure 4.12). Moreover, levels of CD133 significantly increased in the presence of HCMV, despite a constant differentiation stimulus, which usually drives NP1 away from a progenitor phenotype towards a neuronal phenotype. This suggests that not only are these cells resisting differentiation, they are also showing an increase in a marker of stemness.

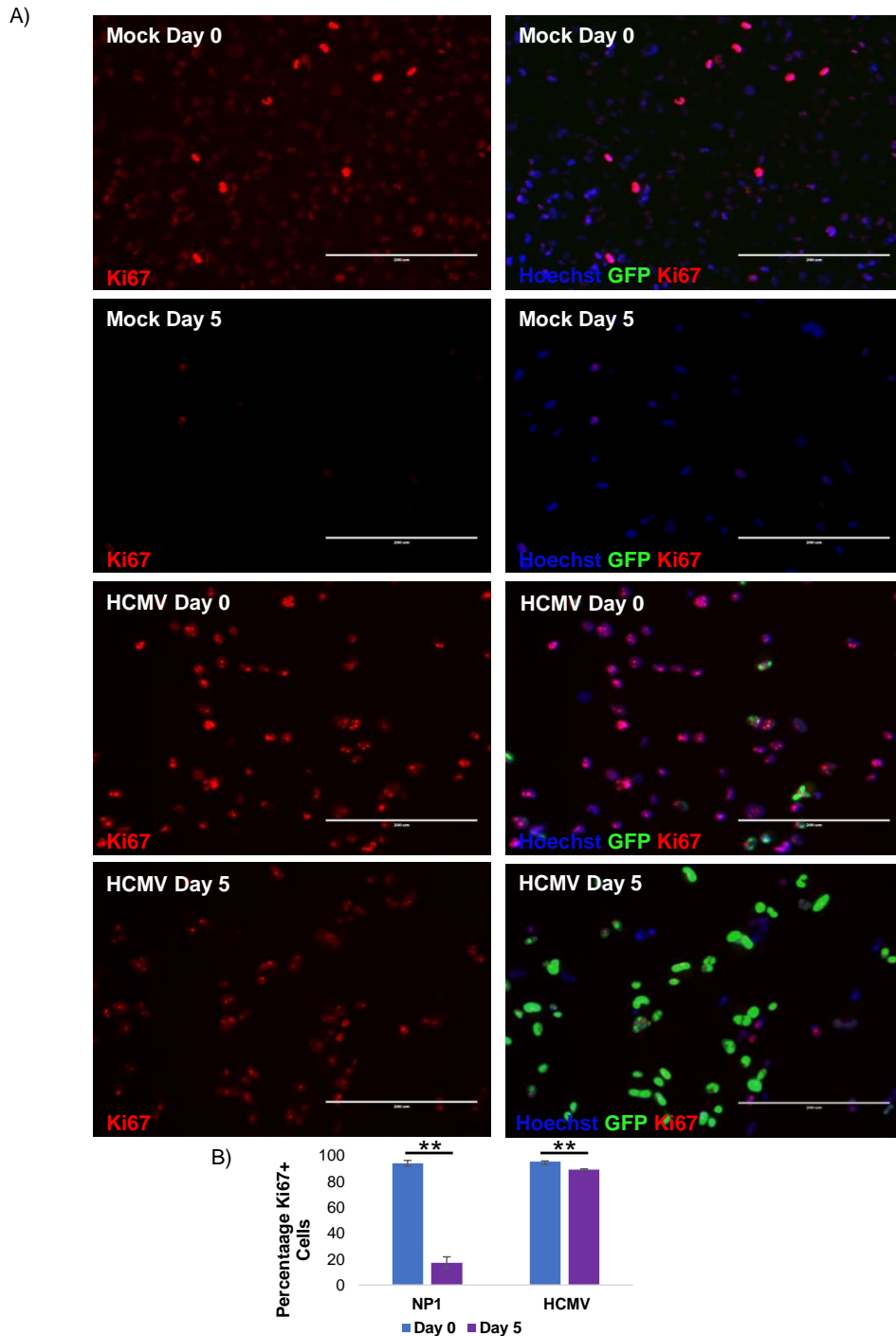


Figure 4.11 Ki67 expression in HCMV infected NP1 during differentiation

A) NP1 cells were infected with HCMV at an MOI of 3 FFU/cell and treated with differentiation media for 5 days. Mock infected NP1 were used as a control. Cells were fixed at day 0 and day 5 with 4 % PFA and permeabilised before immunofluorescence was performed with a Ki67 specific antibody (red) and Hoechst DNA stain (blue) and Viral GFP expression shown (green). Images were taken at 520 x magnification using the EVOS cell imaging system. B) Percentage of Ki67+ cells at day 0 and 5 of differentiation in mock NP1 and NP1 +HCMV. Cells were counted using the cell counting function on the EVOS cell imaging system with 3 fields of view per well quantified (two-tailed student t-test, * $p \leq 0.05$, ** $p \leq 0.01$, *** $p \leq 0.001$, **** $p \leq 0.0001$ n=3).

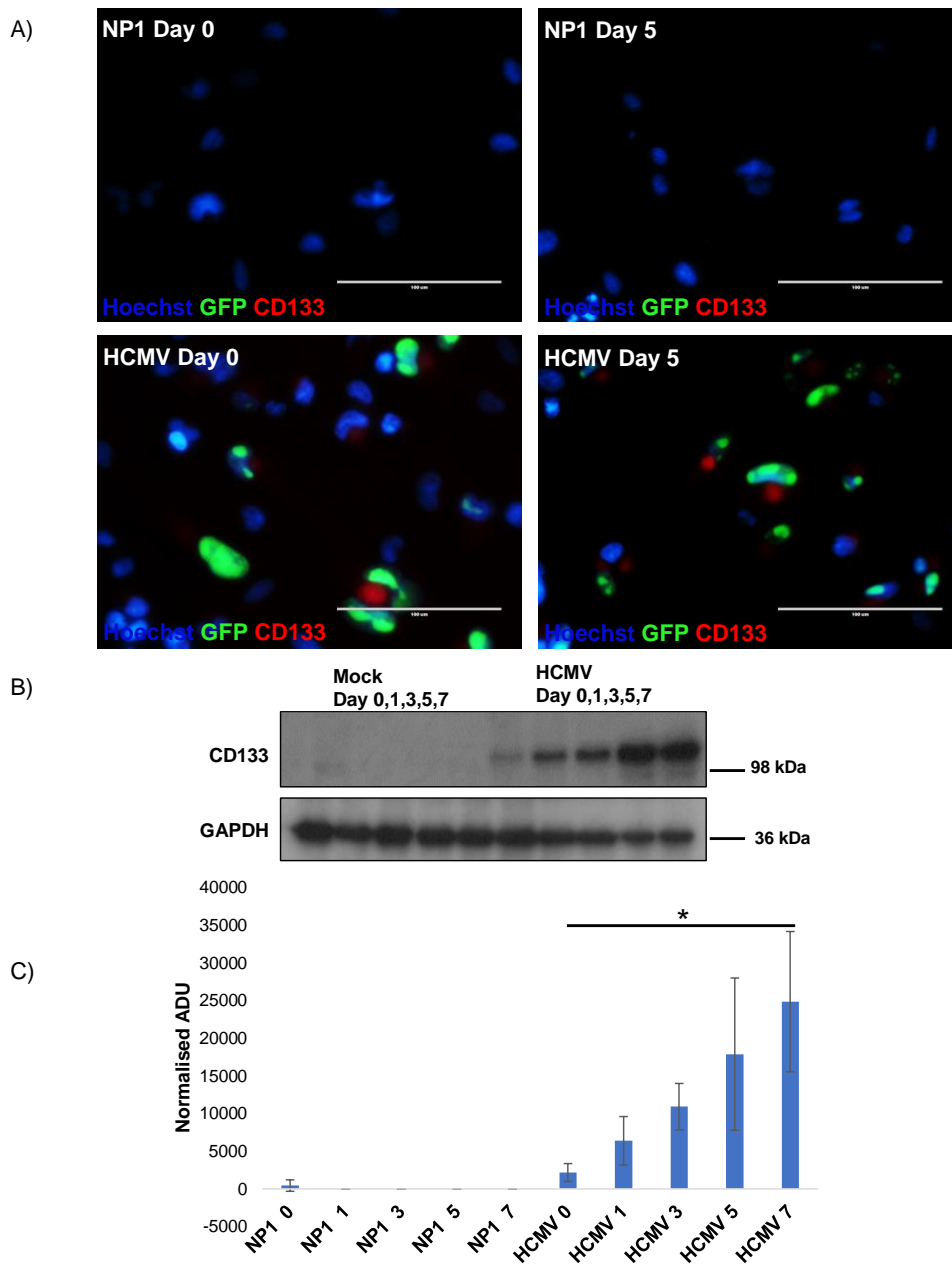


Figure 4.12 CD133 expression in HCMV infected NP1 cells during differentiation

A) NP1 infected with HCMV at an MOI of 3 FFU/cell and treated with differentiation media for 5 days. Mock infected NP1 were used as a control. Immunofluorescent staining was performed with a CD133 specific antibody (red) and Hoechst DNA stain (blue) and Viral GFP expression shown (green). Images taken using EVOS live cell imaging system B). NP1 cells were infected with HCMV at an MOI of 3 FFU/cell and treated with differentiation media for 5 days. Mock infected NP1 were used as a control. Approximately 1×10^6 cells were lysed for Western blot analysis on day 0, 1, 3, 5 and 7. Membranes were probed with a CD133 specific antibody and GAPDH antibody as a housekeeping control. C) Densitometry of CD133 western blots using ImageJ, expressed as normalised arbitrary densitometry units (ADU) (two-tailed student t-test, * $p \leq 0.05$, ** $p \leq 0.01$, *** $p \leq 0.001$, $n=3$).

4.5 Effects of differentiation on virus production

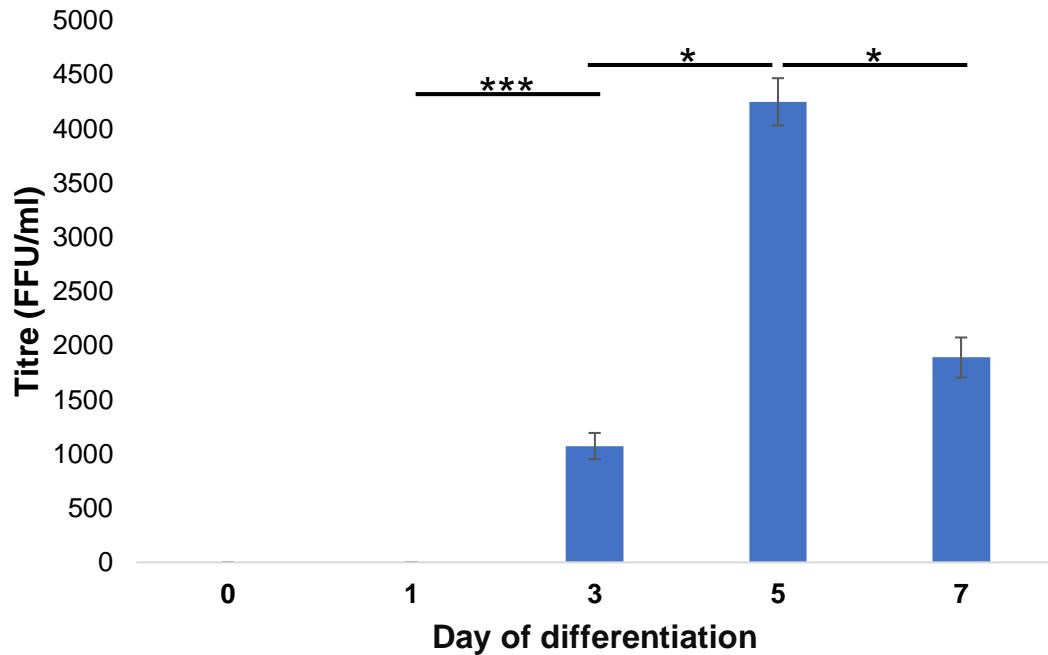


Figure 4.13 Supernatant titre from differentiation of HCMV infected NP1

NP1 were infected at an MOI of 3 FFU/cell for 5 days before being differentiated over 7 days. Supernatants were collected at day 0,1,3,5 and 7 and titres determined using focus forming assay by serial dilution of supernatants onto naïve NP1 cells. N=3. Two-tailed student t-test, * $p \leq 0.05$, ** $p \leq 0.01$, *** $p \leq 0.001$.

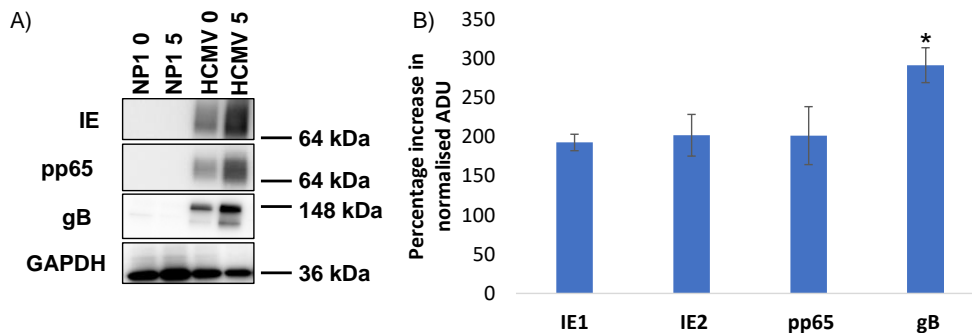


Figure 4.14 HCMV IE and pp65 expression during differentiation of HCMV infected NP1

A) HCMV infected NP1 cells and mock infected controls were differentiated over 5 days. Approximately 1×10^6 cells were lysed for Western blot analysis on day 0, and 5. Membranes were probed for GAPDH, HCMV gB, HCMV pp65 and HCMV IE (IE1 and IE2 specific). B) Quantification of IE1, IE2, pp65 and gB expression, normalised to GAPDH and expressed as percentage increase in normalised arbitrary densitometry units (ADU) (two-tailed student t-test, * $p \leq 0.05$, ** $p \leq 0.01$, *** $p \leq 0.001$, n=3).

As well as investigating the effects of HCMV infection upon NP1 differentiation, we investigated whether the virus life cycle was altered compared with infection

of cycling NP1 cells. As previously discussed in section 3.4.1, HCMV infected NP1 did not secrete infectious virus into the supernatant. Given that differentiation of CD34+ progenitors is essential for the production of virus particles and causes reactivation of latent infection, we determined whether differentiation of HCMV infected NP1 could also lead to production of virus particles (Söderberg-Nauclér *et al.*, 1997).

Supernatants were collected at day 0, 1, 3, 5 and 7 of differentiation of HCMV infected NP1. Supernatant titres were determined by focus forming assay as detailed in section 2.3.1. Figure 4.13 shows that no virus was detected at days 0 and 1 of differentiation, however by day 3 a measurable titre of $\sim 10^3$ FFU/mL was detected, which increased to $\sim 4 \times 10^3$ FFU/mL by day 5, then decreased again to $\sim 2 \times 10^3$ FFU/cell by day 5. In addition, expression of HCMV IE1, IE2, and the late proteins, pp65 and gB increased throughout differentiation relative to cycling cells (Figure 4.14).

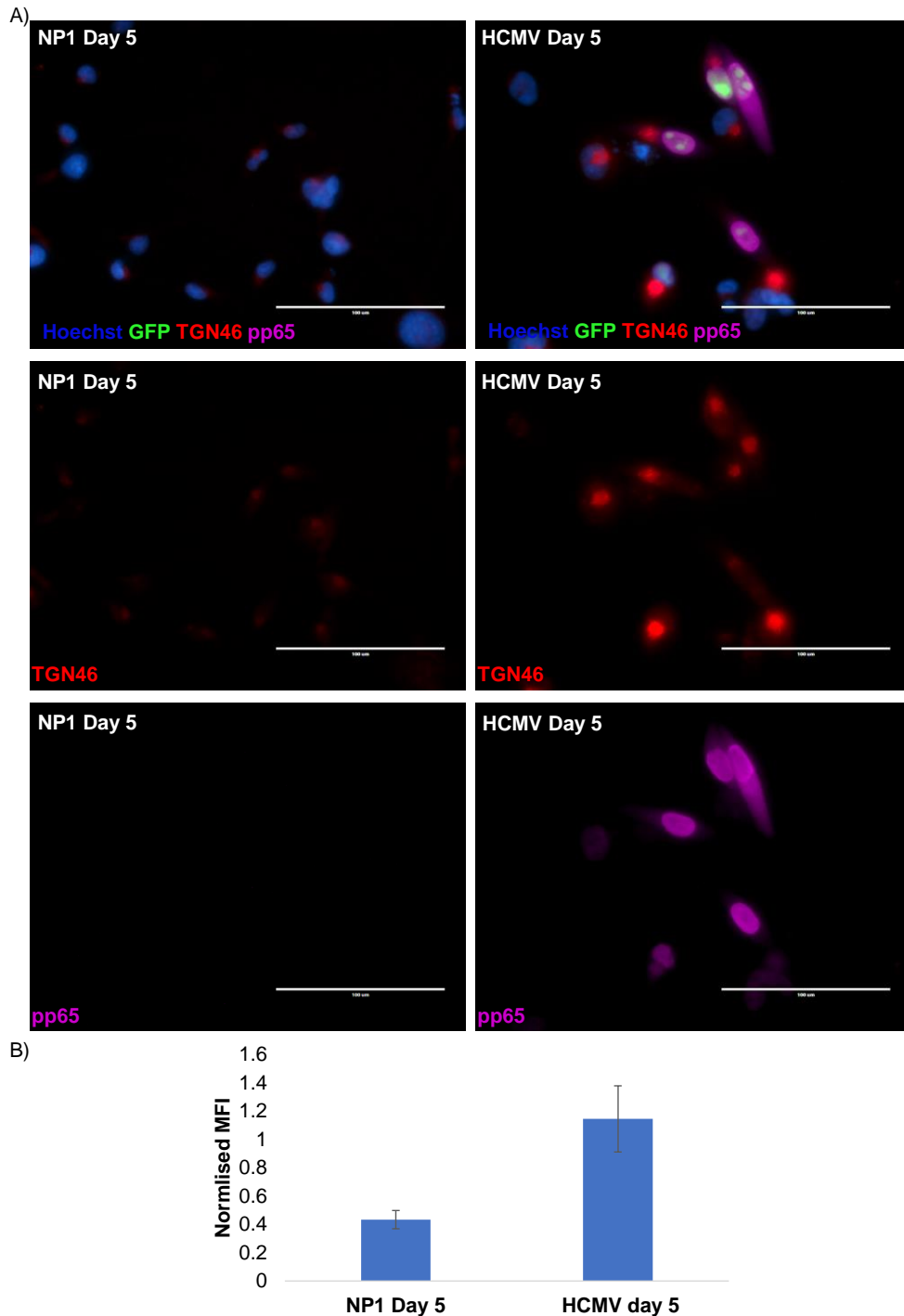


Figure 4.15 NP1 cells +/- HCMV at day 5 of differentiation stained for TGN46 and pp65

A) NP1 infected with HCMV at an MOI of 3 FFU/cell and treated with differentiation media for 5 days. Mock infected NP1 were used as a control. Cells were fixed at day 0 and day 5 with 4% PFA and permeabilised before immunofluorescence was performed with a TGN46 specific antibody (red) pp65 specific antibody (cyan) and Hoechst DNA stain (blue), Viral GFP expression shown (green). Images taken at 1040 x magnification using EVOS cell imaging system. B) Normalised mean fluorescence intensity (MFI) of TGN46 immunofluorescent staining, quantified using ImageJ (two-tailed student t-test, * $p \leq 0.05$, ** $p \leq 0.01$, *** $p \leq 0.001$, $n=3$)

During HCMV infection of NP1, immunofluorescence of the late protein, pp65 did not show concentration at the perinuclear AC, which is clearly visible in the lytic infection of HFFF2 (Figure 3.3.2). The increase in pp65 expression and the presence of infectious virus in the supernatant during differentiation, prompted investigation of pp65 localisation during differentiation. NP1+/- HCMV were fixed at day 0 and 5 of differentiation and immunofluorescence was performed, co-staining with antibodies specific to TGN46 and pp65. The TGN46 antibody recognises a host cell TGN integral membrane protein known to localise to the HCMV assembly compartment (Proctor *et al.*, 2018). Figure 4.15 shows an increase of TGN46 expression in HCMV+ NP1, which is present throughout the cytoplasm, but most concentrated in a bright perinuclear spot, a pattern consistent with the viral AC. HCMV pp65 is absent in the NP1 control, but is strongly expressed both in the nucleus and cytoplasm of HCMV infected cells at day 5 of differentiation. There is no bright perinuclear spot of pp65, suggesting that accumulation of pp65 at the AC does not occur in these cells, despite the release of infectious virions into the supernatant. As discussed previously (section 3.4.2) immunofluorescent staining for both pp28 and gB does localise in a bright perinuclear spot that is likely to be the viral AC.

4.5.1 HCMV gene expression during NP1 differentiation

To assess viral gene expression during differentiation, SYBR green RT-qPCR was performed on RNA extracted from HCMV infected cells at day 0 and day 5 of differentiation (section 2.8.2). The RT-qPCR analysis showed a global increase in viral gene expression at day 5 of differentiation. Consistent with the increase in IE protein by western blot, RT-qPCR shows a significant log₂fold increase in UL122 (IE2) gene expression. US28, a HCMV encoded chemokine receptor gene is also upregulated between day 0 and 5 of differentiation. UL111A, an orthologue of human IL-10, and UL44 (pp52) expression showed a marginal, non-significant increase in expression between day 0 and 5 of differentiation. Finally, gB, an abundant glycoprotein involved in viral entry, showed a significant increase in expression over 5 days of differentiation by RT-qPCR which was supported by an increase in protein expression shown by western blot (Figure 4.14).

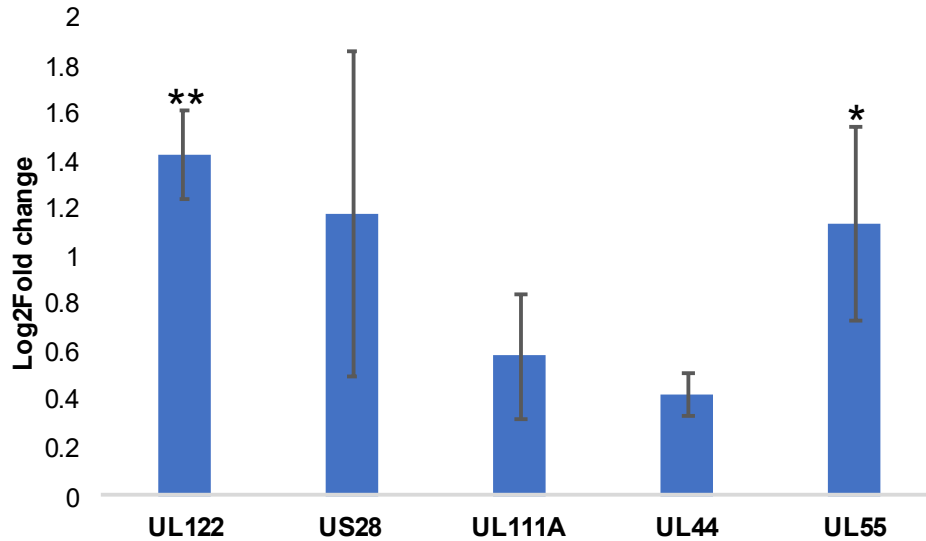


Figure 4.16 HCMV gene expression during differentiation of NP1

NP1 infected at an MOI of 1 FFU/cell for 5 days were differentiated for 5 days. RNA was extracted at day 0 and 5 of differentiation and cDNA was made. SYBR green qPCR was performed using primers specific to 18S and HCMV UL122, US28, UL111A, UL44 and UL55. Delta-delta CT analysis was performed to calculate Log2fold change in expression between day 0 and day 5 of differentiation (two-tailed student t-test $n=3$, $*p\leq 0.05$, $**p\leq 0.01$, $***p\leq 0.001$).

4.6 Infection of pre-differentiated NP1

Several studies have shown that neurons are permissive to HCMV infection, both *in vivo* and *in vitro*, and have therefore been suggested as reservoirs of HCMV infection within the brain (Poland *et al.*, 1994, Luo *et al.*, 2008). However, Cheeran *et al.* (2005) found that neuronal differentiation of foetus-derived neural precursor cells led to a decrease in viral expression due to MIEP repression. Astrocytes have also been shown to be fully permissive to HCMV *in vitro* (Lokensgard *et al.*, 1999). As the differentiation of NP1 results in a predominantly neuronal and astrocytic population, we wanted to determine if these cells could be infected post-differentiation and, if so, how the cells would be affected.

NP1 were differentiated for 5 days, before being infected with HCMV at an MOI of 3 FFU/cell. From here on, this will be referred to as differentiation protocol 2. Figure 4.17 shows viral GFP expression at 72 h.p.i, indicating that NP1 can be infected with HCMV post differentiation. Protocol 2 caused infected NP1 cells to lose their neuronal morphology and adopt a morphology very similar to NP1 HCMV+ (protocol 1) at day 5 and 7 of differentiation.

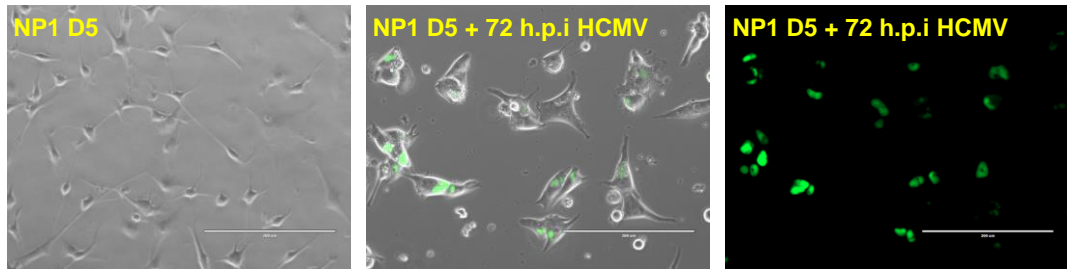


Figure 4.17 HCMV infection of differentiated NP1

NP1 were differentiated for 5 days before being infected with HCMV at an MOI of 3 FFU/cell for 72 hrs. Images show viral GFP expression (green) and were taken using the EVOS cell imaging system. Scale bar = 200 μ m

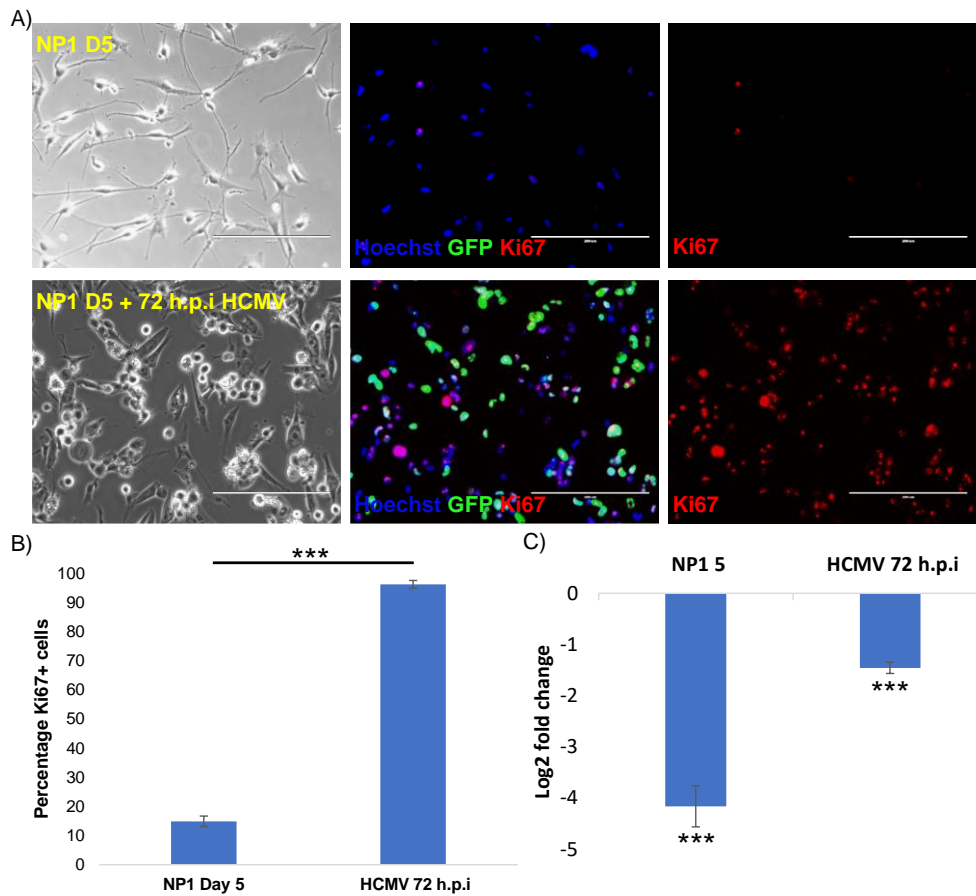


Figure 4.18 Ki67 expression in NP1 infected with HCMV at day 5 of differentiation

A) NP1 cells were differentiated for 5 days before being infected with HCMV at an MOI of 3 FFU/cell for 72 h.p.i. Cells were fixed at day 5 of differentiation and at 72 h.p.i. with 4 % PFA and permeabilised before immunofluorescence was performed with a Ki67 specific antibody (red) and Hoechst DNA stain (blue) and Viral GFP expression shown (green). Images were taken using the EVOS cell imaging system. Scale bar = 200 μ m B) The percentage of Ki67+ cells was calculated using the cell counter plug-in in ImageJ (two-tailed student t-test, * $p \leq 0.05$, ** $p \leq 0.01$, *** $p \leq 0.001$, $n=3$). C) Log2fold change in gene expression from taqman RT-qPCR for Ki67 in NP1 day 0, NP1 day 5 and HCMV 72 h.p.i (two-tailed student t-test, * $p \leq 0.05$, ** $p \leq 0.01$, *** $p \leq 0.001$, $n=2$).

4.6.1 Effects of HCMV infection post differentiation in NP1 cells

At day 5 of NP1 differentiation, just 17% of cells are Ki67 positive . When these cells are then infected at an MOI of 3 FFU/cell, Ki67 expression is restored with 96 % of cells Ki67 positive at 72 h.p.i (Figure 4.18). Accordingly, figure 4.19 shows that PCNA expression is decreased during NP1 5 day differentiation, but similarly to Ki67 is restored when the cells are subsequently infected with HCMV for 72 hr. The Glioblastoma stem cell marker, CD133 is also increased when differentiated NP1 are subsequently infected with HCMV for 72 hr (Figure 4.20).

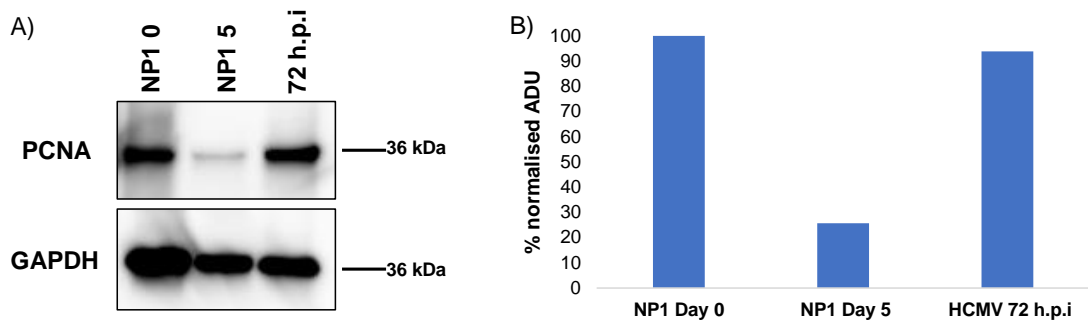


Figure 4.19 PCNA expression in NP1 infected with HCMV post differentiation

A) NP1 cells were differentiated over 5 days using the Walton *et al.* (2006) method before being infected with HCMV at an MOI of 3 FFU/cell for 72 hr. Approximately 1×10^6 cells were lysed for Western blot analysis on day 0 and 5. Membranes were probed for GAPDH and PCNA. B) Quantification of PCNA expression, normalised to GAPDH and expressed as arbitrary densitometry units (ADU).

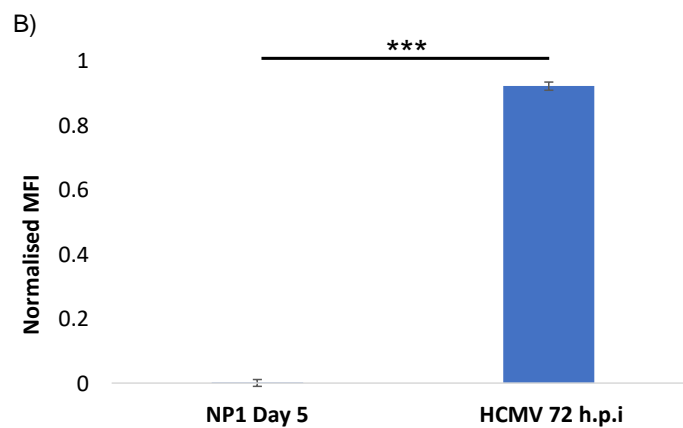
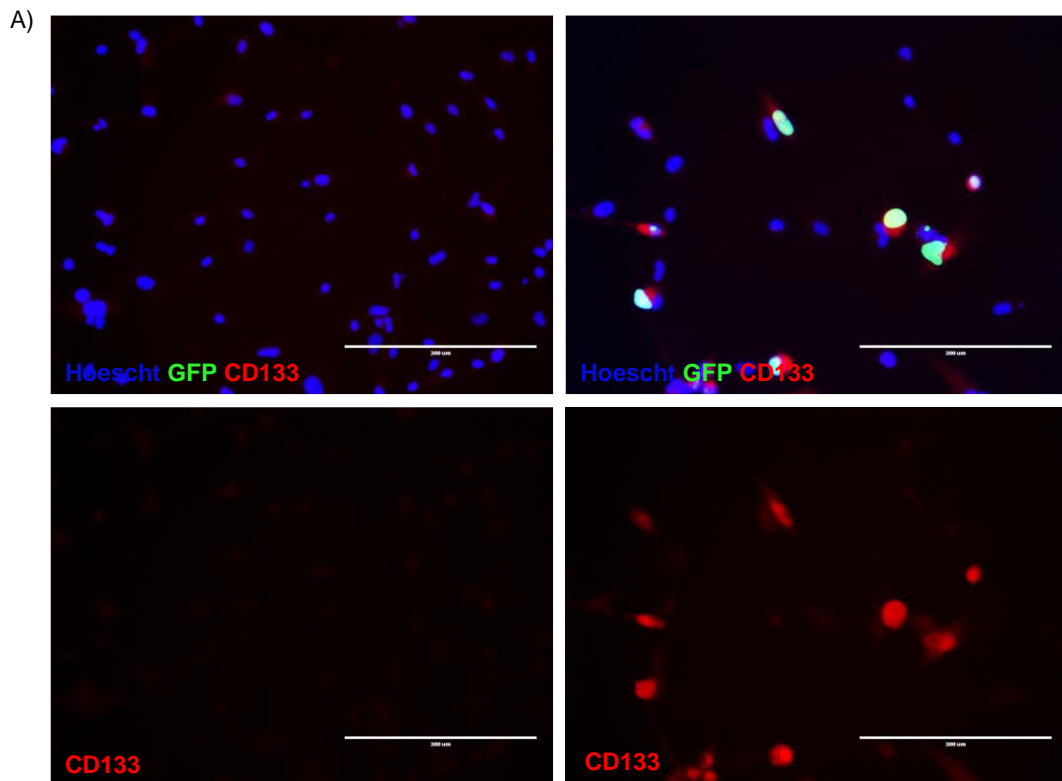


Figure 4.20 Immunofluorescence of CD133 in NP1 infected with HCMV post-differentiation

A) NP1 cells were differentiated for 5 days before being infected with HCMV at an MOI of 3 FFU/cell for 72 h.p.i. Cells were fixed at day 5 of differentiation and at 72 h.p.i with 4% PFA and permeabilised before immunofluorescence was performed with a CD133 specific antibody (red) and Hoechst DNA stain (blue) and viral GFP expression shown (green). Images were taken at 520 x magnification using of the EVOS cell imaging system. B) Mean fluorescence intensity (MFI) for CD133 was measured using ImageJ (two-tailed student t-test, * $p \leq 0.05$, ** $p \leq 0.01$, *** $p \leq 0.001$, $n=2$).

4.6.2 Does infection of differentiated NP1 with HCMV lead to productive infection?

To determine whether differentiated NP1 were fully permissive to productive HCMV infection, supernatants were taken at day 0 and 5 of differentiation and at 72 h.p.i and serially diluted onto naïve NP1 to determine titre (Section 2.3.1). At 72 h.p.i of differentiated NP1 cells, supernatants contained an average titre of 1.3×10^3 FFU/ml (Figure 4.2.1). This confirms that NP1 differentiated into a population of neurons and astrocytes are fully permissive and support production of HCMV particles, which are secreted into the supernatant. Immunofluorescence for pp65 (Figure 4.22), shows a brighter area of perinuclear pp65 which resembles the HCMV AC in HFFF2 (Figure 3.2.2). This localisation of pp65 is not seen for infected NP1 infected prior to differentiation or at day 5 of differentiation in NP1 differentiated from 5 d.p.i (Figure 4.15).

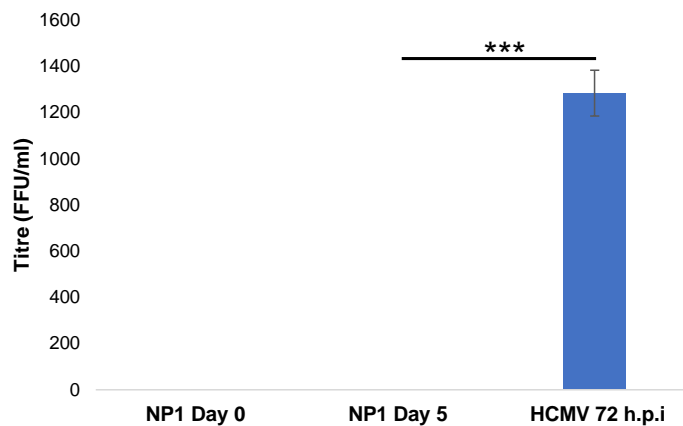


Figure 4.21 Supernatant titre of NP1 infected with HCMV post-differentiation

NP1 were differentiated over 5 days before being infected with HCMV at an MOI of 3 FFU/cell for 72 hr. Supernatants were collected at day 0 and 5 of differentiation and at 72 h.p.i. Supernatants were serially diluted onto naïve NP1 to determine titre using focus forming assay (two-tailed student t-test, * $p \leq 0.05$, ** $p \leq 0.01$, *** $p \leq 0.001$, $n=2$).

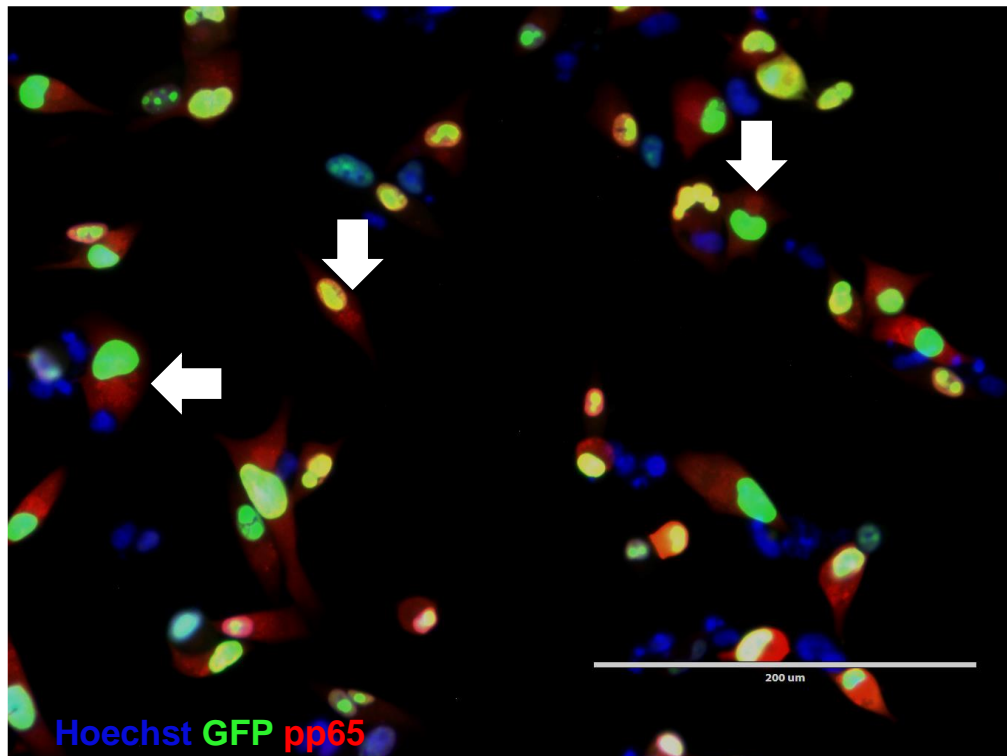


Figure 4.22 HCMV pp65 immunofluorescent staining in NP1 cells infected with HCMV post differentiation

A) NP1 cells were differentiated for 5 days before being infected with HCMV at an MOI of 3 FFU/cell for 72 h.p.i, before being fixed using 4 % PFA and permeabilised before immunofluorescence was performed with a HCMV pp65 specific antibody (red) and Hoechst DNA stain (blue) and viral GFP expression shown (green). White arrows indicate cells with clear bright perinuclear foci of pp65.

4.7 Differentiation of colony 2

As differentiation of latently infected myeloid cells leads to reactivation of HCMV and differentiation of HCMV infected NP1 leads to production of infectious virus particles being detected in the supernatant (Figure 4.13), we investigated the effects of differentiation of the chronically HCMV infected NP1 line, colony 2. As discussed in section 3.5.1, colony 2 maintained detectable GFP and IE expression up to 110 d.p.i. Colony 2 cells used for all differentiation experiments in this section were between 60 and 85 d.p.i and differentiated using the Walton *et al.* (2006) method.

Differentiation of colony 2 over 5 days lead to an increased percentage of GFP+ cells from 10% to 55% (figure 4.23). This suggests that differentiation of colony 2 is increasing viral IE expression. This is supported by the increase in IE expression detected by western blot (figure 4.24). Figure 4.24 also shows an increase in HCMV late proteins, pp65 and gB when colony 2 is differentiated.

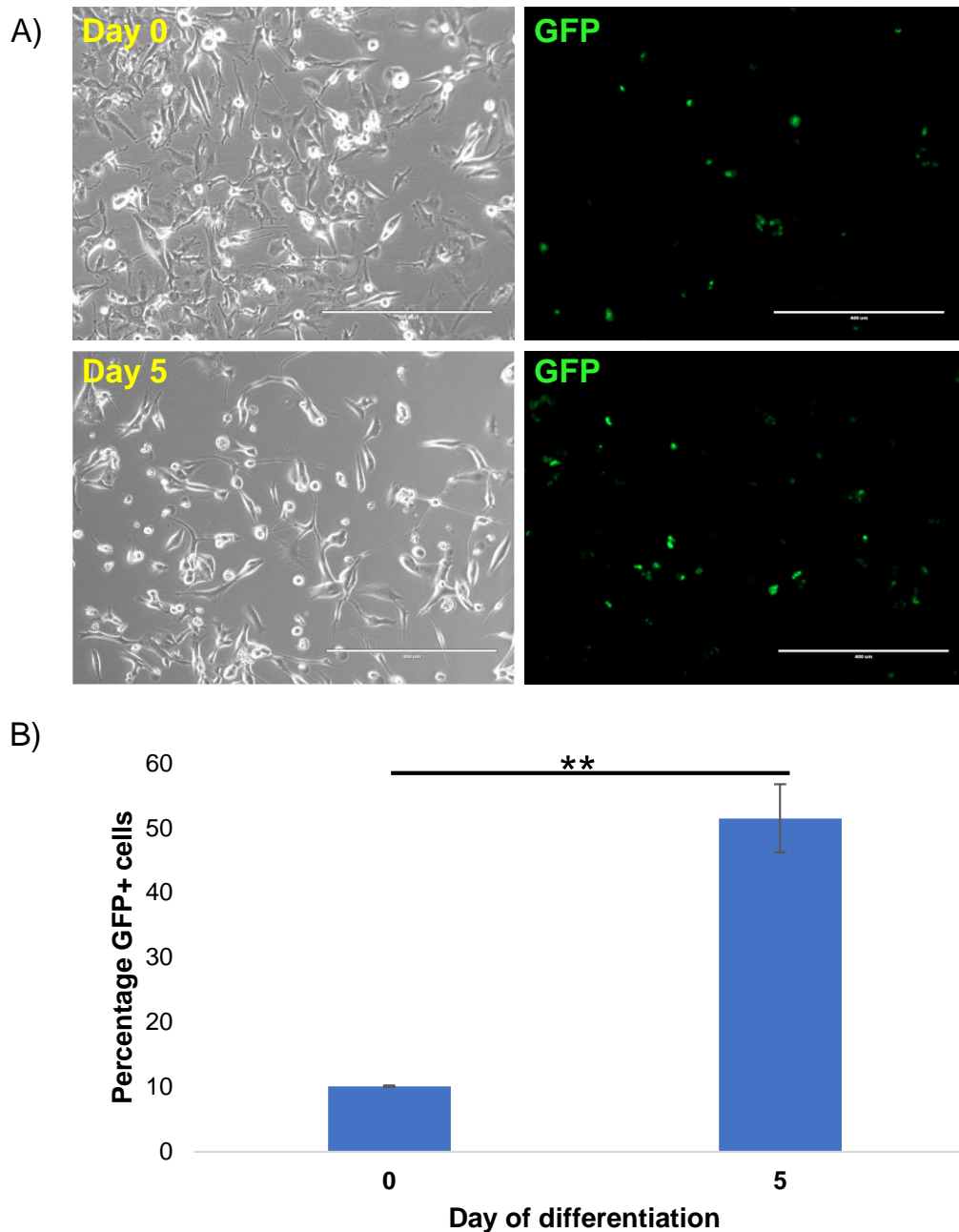


Figure 4.23 GFP expression during differentiation of colony 2

A) Colony 2 cells were differentiated over 5 days using the Walton *et al.* (2006) differentiation protocol. Phase and GFP images were taken at day 0 and 5 of differentiation using the EVOS cell imaging system. B) The percentage of cells expressing GFP was quantified using ImageJ cell counter plug-in (two-tailed student t-test, * $p \leq 0.05$, ** $p \leq 0.01$, *** $p \leq 0.001$, $n=3$)

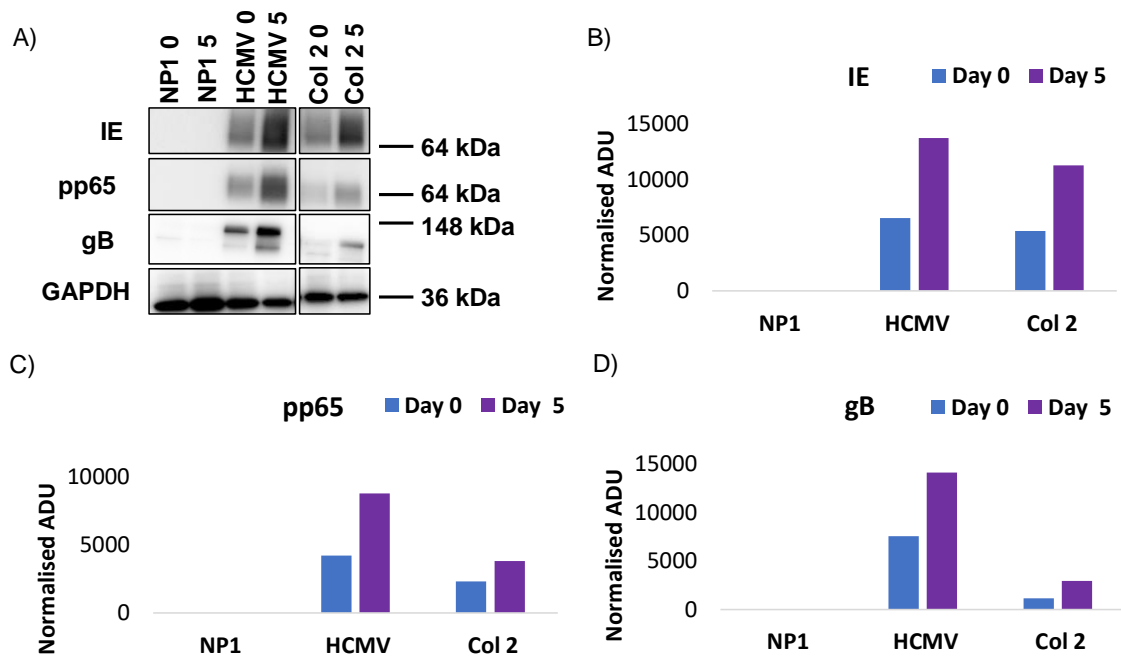


Figure 4.24 HCMV protein expression during differentiation of colony 2

A) Colony 2, HCMV+ NP1 at 5 d.p.i and mock infected NP1 controls were differentiated over 5 days using the Walton *et al.* (2006) method. Approximately 1×10^6 cells were lysed for Western blot analysis on day 0 and 5. Membranes were probed for GAPDH, HCMV IE, pp65 and gB. Densitometry quantification of B) IE C) pp65). D) gB protein expression, normalised to GAPDH and expressed as normalised arbitrary densitometry units (ADU).

SYBR green RT-qPCR showed significant increases in HCMV US28, UL44 and UL55 when colony 2 was differentiated (figure 5.25). Following 5 days of differentiation, US28 showed a significant increase in expression. UL55 (which encodes gB) showed a significant increase and UL44 (which encodes pp52) showed a dramatic significant increase. This dramatic increase in UL44 expression is important to note as it encodes pp52, which is a key component of the HCMV replication machinery, which may indicate an increase in viral DNA replication. The increase in HCMV viral chemokine receptor gene US28 is also particularly interesting as it has been highlighted as a potential viral oncogene with expression detected in around 60 % of GBM samples (Maussang *et al.*, 2006). UL122 showed a non-significant decrease in expression.

As well as increased HCMV gene expression, 5 day differentiation of colony 2 also led to detection of infectious HCMV in the supernatant, where none was detected prior to differentiation (figure 4.26). Although this increase in supernatant titre was not as dramatic as in the differentiation of 5 day infected NP1, it is particularly noteworthy as it could indicate a differentiation dependant reactivation of latent HCMV, particularly when considered together with the pan upregulation of HCMV genes.

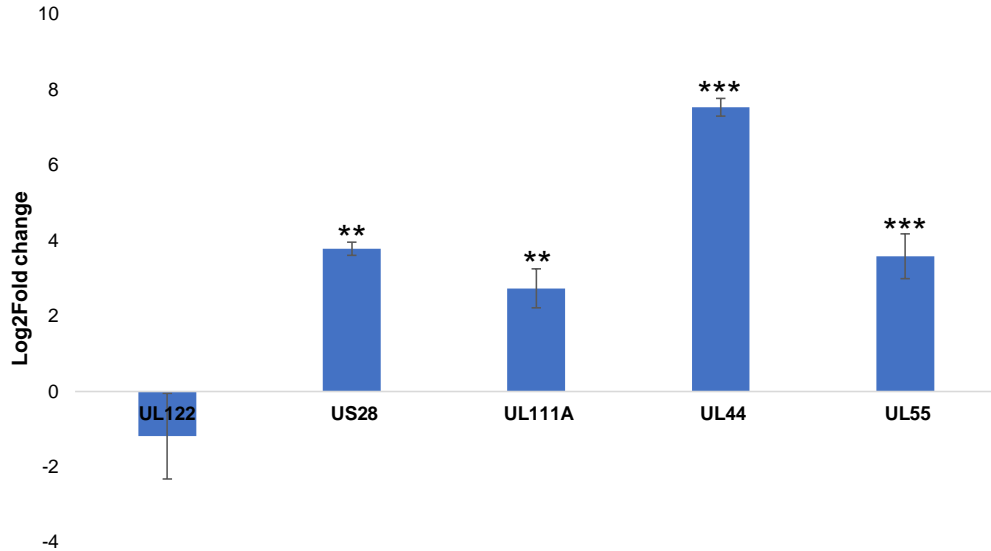


Figure 4.25 HCMV gene expression during differentiation of colony 2

Colony 2 cells between 60 and 80 d.p.i were differentiated for 5 days using the Walton *et al.* protocol. RNA was extracted at day 0 and 5 of differentiation and cDNA was made. SYBR green qPCR was performed using primers specific to 18S and HCMV UL122, US28, UL111A, UL44 and UL55. Delta-delta CT analysis was performed to calculate Log2fold change in expression between day 0 and day 5 of differentiation (two-tailed student t-test, * $p \leq 0.05$, ** $p \leq 0.01$, *** $p \leq 0.001$, $n=3$).

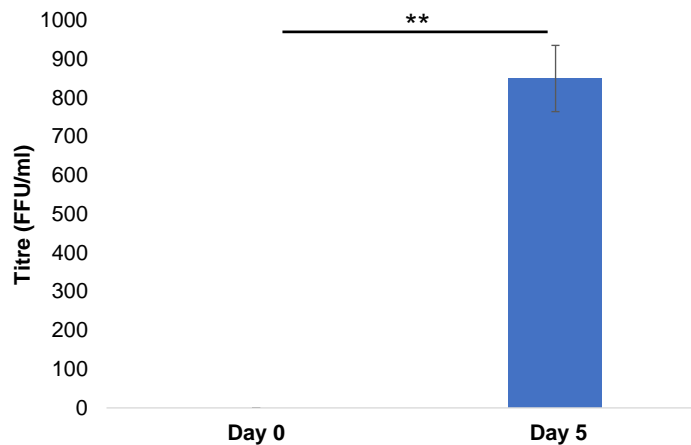


Figure 4.26 HCMV supernatant titres in differentiation of colony 2

Colony 2 cells were differentiated over 5 days using a published protocol (Walton *et al.*, 2006). Supernatants were collected at day 0 and day 5 and serially diluted onto naïve NP1 to determine titre through focus forming assay. Results displayed in focus forming units per ml (FFU/cell) (two-tailed student t-test, * $p \leq 0.05$, ** $p \leq 0.01$, *** $p \leq 0.001$, $n=3$).

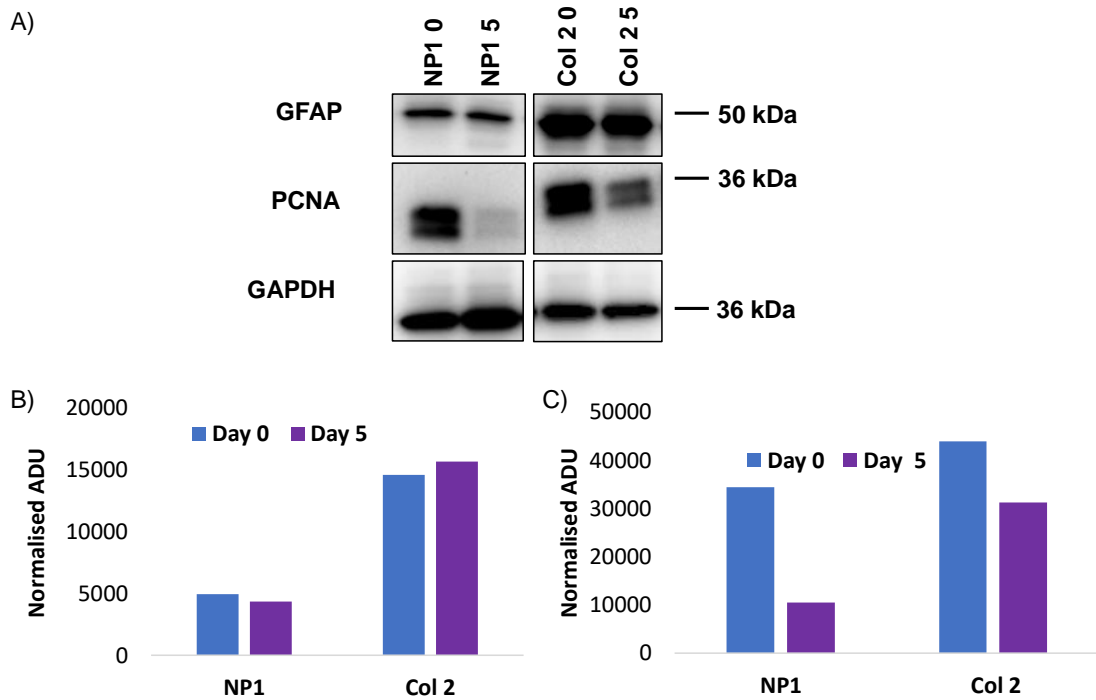


Figure 4.27 Expression of differentiation markers GFAP and PCNA in differentiation of colony 2

A) Colony 2 and NP1 at 5 d.p.i and mock infected NP1 controls were differentiated over 5 days using the Walton *et al.* (2006) method. Approximately 1×10^6 cells were lysed for Western blot analysis on day 0 and 5. Membranes were probed for GAPDH, GFAP and PCNA. B) Quantification of GFAP expression, normalised to GAPDH and expressed as normalised arbitrary densitometry units (ADU). C) Quantification of PCNA expression, normalised to GAPDH and expressed as normalised arbitrary densitometry units (ADU).

Expression of glial marker GFAP is increased in colony 2 cells compared to NP1 at day 0 and its expression is maintained through day 5 of differentiation in colony 2 (Figure 4.27). Proliferation marker PCNA is increased in colony 2 compared to NP1. By day 5 of differentiation, PCNA expression in the control NP1 has decreased by 70 % (Figure 4.27). However, PCNA expression in colony 2 decreases by just 29 % by day 5 of differentiation. Day 5 PCNA expression in colony 2 is 91% of that seen in NP1 at day 0.

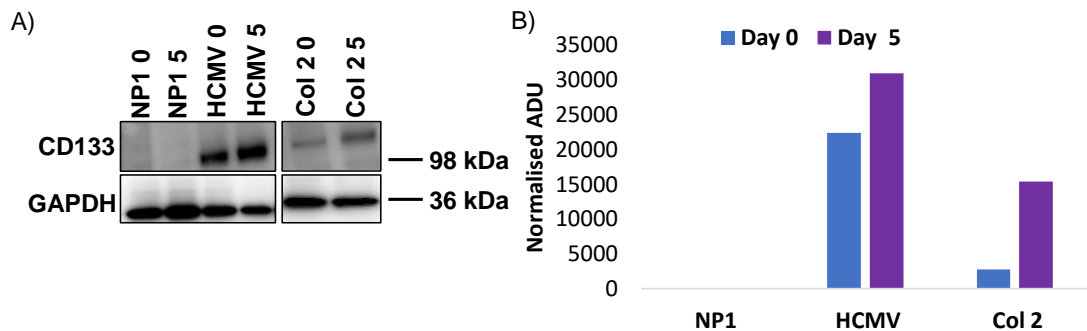


Figure 4.28 CD133 protein expression during differentiation of colony 2

A) Colony 2, NP1 + HCMV at 5 d.p.i and mock infected NP1 controls were differentiated over 5 days using the Walton *et al.* (2006) method. Approximately 1×10^6 cells were lysed for Western blot analysis on day 0 and 5. Membranes were probed for GAPDH and CD133. B) Quantification of CD133 expression, normalised to GAPDH and expressed as normalised ADU.

Glioblastoma stem cell marker CD133 is not expressed in NP1 at day 0 or 5 of differentiation, however infection with HCMV leads to CD133 expression at day 0 of differentiation and increases at day 5 (Figure 4.28). Colony 2 also retains CD133 expression at day 0, although it is lower than in recently HCMV infected cells. Similarly to the HCMV infected NP1 at 5 d.p.i, long term infected colony 2 also shows an increase in CD133 expression when differentiated for 5 days.

4.8 Discussion

The method used for differentiation was chosen as it has previously been used to differentiate adult NPs as opposed to other methods which have only been validated in foetal derived NPs (Walton *et al.*, 2006). Secondly, when optimising this protocol in our NP1 cells, we observed far less cell death with this method than in the serum starvation method, which drastically reduced cell viability with only 24 hr of treatment (Figure 4.3). It was important to choose a method that caused minimal cell death as it was to be combined with HCMV infection, which also causes some cell death in NP1. Thirdly, the distinct change in the morphology of NP1 seen using this method, along with consistently reproducible changes in markers of differentiation made it suitable to study the effects of HCMV on NP differentiation (Figure 4.5 and 4.10).

Immunofluorescence for GFAP at day 3 of differentiation and β -III-tubulin at day 7 strongly resembled the immunofluorescence for the same markers at the same time points shown previously, which indicated that differentiation of NP1 using this method was effective (Figure 4.6). We noted one discrepancy between our

NP1 differentiation and that documented in the paper the method was taken from. Where in the paper, there was a decrease in GFAP from day 5, differentiating NP1 show a slight increase in GFAP between day 5 and 7 (Figure 4.10E). This could be attributed to the inherently heterogeneous nature of primary adult NP cells. As this differentiation method is known to differentiate NP cells into both neurons and astrocytes, it is possible that differentiation of NP1 results in a population with a higher proportion of astrocytes compared to the predominantly neuronal population in the original paper. This is supported by the immunofluorescence for GFAP at day 3 of differentiation which shows that many of the cells are strongly expressing GFAP, a marker used for identifying astrocytes (Chiu *et al.*, 1981).

To ascertain the proportions of neuronal and astrocytic cells in the differentiated population, immunofluorescence co-staining for both GFAP and a mature neuronal marker such as NeuN, could be performed to discriminate between the two cell types. Another possibility is that NP1 are adopting the intermediate neuron/astrocyte “asterson” hybrid phenotype described by Walton *et al.*, in which case cells would co-express GFAP and neuronal marker, β -III-tubulin.

Despite HCMV infection perturbing neurite outgrowth compared to mock infected NP1, increased levels of pan neuronal marker β -III-tubulin were observed and were sustained throughout differentiation. This increase in expression of β -III-tubulin is the opposite of the decrease in β -III-tubulin seen when differentiating NSCs are infected with HCMV *in vitro* (Rolland *et al.*, 2016). Notably, overexpression of β -III-tubulin is a hallmark of GBM. The level of β -III-tubulin expression correlates with increasing malignancy in glioma and has been suggested to play a role in gliomagenesis (Katesetos *et al.*, 2009, Katesetos *et al.*, 2001,).

Ki67 is often used as a marker of proliferation as it is highly expressed in cycling cells, but significantly downregulated in G₀ resting cells (Gerdes *et al.*, 1984). Although it is regularly used as a marker of proliferation, Ki67 can also be expressed by cells that are arrested in G₁/S or G₂/M, so it is an indirect marker of proliferation. HCMV infection has long been known to disrupt the cell cycle at several points, a process mediated by multiple viral proteins (Jault *et al.* 1995, Bresnahan *et al.*, 1996). As HCMV mostly infects quiescent cells, it pushes them towards G₁ where it can hijack host cell replication mechanisms and bias them for viral DNA synthesis (Sarisky and Hayward, 1996). When cells are in the optimal G₁ phase, multiple signalling pathways are modulated by HCMV to allow for efficient viral gene expression, but stopping the cell entering S phase where

the host cell DNA is replicated. HCMV IE2 expression is known to block cell cycle progression at the G₁/S boundary (Wiebusch and Hagemeyer, 2001).

Although the cell cycle is usually arrested prior to host cell DNA synthesis in HCMV infection, an array of S/G₂/M phase associated proteins accumulate. In HCMV infection of cells in G₀/G₁, IE expression begins immediately, however if cells are in S or G₂, transcription of IE is repressed until the cells are in the favourable G₀/G₁ phase (Salvant, Fortunato and Spector, 1998). It is therefore possible that HCMV is maintaining Ki67 expression in NP1 throughout differentiation, through cell cycle arrest rather than by maintaining proliferation. All of the literature discussed above on the effects of HCMV on the cell cycle refers to HCMV infection of various types of fibroblast, with little known about the effects of HCMV on the cell cycle in the context of neural progenitor cell infection. Ki67 expression is also used when grading several types of cancer, due to its positive correlation with proliferation. (Gerdes *et al.*, 1987, Dowsett *et al.*, 2011). In glioma, Ki67 expression correlates with increasing WHO grade and overall patient survival (Dahlrot *et al.*, 2021). The maintenance of Ki67 in HCMV+ NP1 despite differentiation stimuli could be important in the context of GBM, where a higher number of HCMV+ tumour cells has been associated with higher grade gliomas and highly proliferative tumours which have elevated levels of Ki67 (Huang *et al.*, 2015).

PCNA expression decreases in protocol 1 NP1 differentiation, but is maintained throughout differentiation in HCMV+ NP1, with expression at day 7 equivalent to that in non-differentiated, non-infected NP1 (Figure 4.10). PCNA is an essential factor for DNA replication and regulator of cell cycle control which aids DNA replication by acting as a sliding clamp inducing processivity of DNA polymerase (Jónsson and Hübscher, 1997, Shibahara *et al.*, 1999). HCMV induction of both Ki67 and PCNA was first described by Mate *et al.* (1998), who noted increased PCNA and Ki67 in gastrointestinal, skin and kidney biopsy tissues that were HCMV+. However, HCMV induced PCNA expression in the presence of differentiation stimuli has not been described previously. PCNA is usually expressed in S phase, however HCMV induces synthesis of several S phase proteins, including PCNA, cyclins and thymidine kinases despite blocking G₁/S transition (Dittmer and Mockarski, 1997, Estes and Huang, 1997). Interestingly, not only can HCMV infection of NP1 maintain expression of Ki67 and PCNA during protocol 1, but in protocol 2, HCMV infection post-differentiation can restore PCNA and Ki67 in cells that had exited the cell cycle during differentiation. This suggests that HCMV could be pushing differentiated NP1 back into the cell cycle to a phase that is advantageous for virus production as previously documented in HCMV infected U373, a neuroblastoma cell line

(Murphy *et al.*, 2000). In order to determine whether the maintenance of Ki67 and PCNA during differentiation of HCMV+ NP1 is indicative of increased proliferation or simply a symptom of HCMV induced cell cycle arrest, further experiments such as proliferation assays would need to be conducted. In GBM and several other forms of malignant brain tumour, increasing PCNA labelling index values were found to significantly correlate with increasing grade as well as clinical outcome (Kayaselçuk *et al.*, 2002). In a mouse model of glioblastoma, PCNA was significantly elevated in the tumours of mice that had been perinatally infected with MCMV (Price *et al.*, 2018). Similarly, transduction of HCMV IE1 into glioma cell line U87 resulted in an increase of PCNA (Cobbs *et al.*, 2008).

Sox2 is a transcription factor associated with maintaining stemness and self-renewal in stem cells and is widely expressed in neuroectoderm and in neural progenitor cells during development (Bowles *et al.*, 2000, Masui *et al.*, 2007). Although Sox2 is expressed in some adult neural progenitor cells, it is not expressed across all neural progenitor populations (Hutton and Pevny, 2011). NP1 do express Sox2, which decreases over the 7 day course of differentiation to very low levels at day 7. However, when NP1 are infected with HCMV Sox2 expression is completely ablated by 5 d.p.i and is not expressed at all during the 7 day differentiation process. The loss of Sox2 due to HCMV infection of foetal derived neural progenitor cells is documented in the literature by Wu *et al.* (2019) who ascribe the loss to modulation via HCMV IE1. IE1 increases nuclear accumulation of STAT3 a transcriptional activator of Sox2 expression and prevents its activation by inhibiting STAT3 phosphorylation. Soroceanu *et al.* (2015), report the opposite in a mouse model of glioma, where IE1 expression increased the expression of Sox2 along with another stemness marker, Nestin. IE1 was found to co-localise with both Sox2 and Nestin in HCMV+ cells in tumour tissue samples. Nestin is also expressed in NP1 and decreases during differentiation. NP1 cells infected with HCMV show a decrease in Nestin expression which continues to decrease throughout differentiation and is undetectable by day 7. Luo *et al.* (2010) also found that HCMV infection of foetal neural progenitor cells led to a decrease in Nestin and Sox2. Investigation into the effects of HCMV infection of primary GBM cells *in vitro* by Fornara *et al.* (2015) found that infection induced a stem cell phenotype with upregulation of both Sox2 and Nestin along with other stem cell markers; Notch1, Oct4 and CD133, suggesting that HCMV has opposite effects on Sox2 and Nestin in GBM and healthy NP cells.

CD133 is a pentaspan transmembrane glycoprotein, which is often described as a cancer stem cell marker in the literature, although the accuracy of CD133 as a biomarker in this context has been controversial (Corbeil *et al.*, 2013). However,

there is consensus that CD133 can be used as a marker of GBM stem cells and can be used to identify GBM cells that are capable of forming neurospheres (Glumac and LeBeau, 2018). Fornara *et al.* (2016) found that a large proportion of CD133+ primary GBM cells also expressed HCMV IE. Additionally, higher co-expression of these 2 proteins correlated with poor patient survival. This is supported by Soroceanu *et al.* (2015) who found over 70 % of IE+ primary GBM cells were also CD133+. They also report that treatment with siRNA targeting HCMV IE in CD133+ GBM cells significantly reduced the ability to form neurospheres. CD133 was not detected in NP1 cells by immunofluorescence or western blot, however following 5 days of HCMV infection CD133 was detected by both methods. Despite CD133 usually being associated with stem cells and therefore decreasing with increasing differentiation, in HCMV+ NP1 CD133 expression actually increased in response to the differentiation stimulus. Additionally, HCMV infection of pre-differentiated NP1 cells also induced CD133 expression. This could suggest that rather than HCMV simply preferentially infecting CD133+ cells in GBM, it could actually be responsible for inducing CD133 expression, a potentially oncomodulatory effect. Taken together, the increase in neuronal marker β -III-tubulin, the maintenance of proliferation markers Ki67 and PCNA, the decrease of stem cell markers Nestin and Sox2 with the paradoxical induction of stem cell marker CD133 demonstrate that differentiation of NP1 is severely perturbed by HCMV infection. This disruption of differentiation in adult neural progenitor cells could be an important finding in terms of an oncomodulatory role for HCMV in GBM, particularly as neutralisation of differentiation is thought to be an early step in gliomagenesis and adult neural progenitors are a likely cell of origin for GBM (Hu *et al.*, 2015).

As differentiation of HCMV infected myeloid cells is known to be essential for lytic gene expression and virion production, it was important to determine whether NP1 differentiation would lead to production of virions (Chan *et al.*, 2012, Stevenson *et al.*, 2014). Infectious HCMV was detected in NP1 supernatants from day 3 of differentiation, peaking at day 5, supporting that differentiation induces virion production in HCMV+ NP1 (Figure 4.13). This peak in viral titre at day 5 is concurrent with an increase in HCMV gene expression as determined by qPCR (Figure 4.16). The pan-upregulation of HCMV genes is consistent with the ubiquitous increase in HCMV gene expression seen in differentiation induced reactivation from latency (Yee, Lin, Stinsky, 2007). Chromatinisation and epigenetic regulation of the HCMV genome is essential for restricting HCMV lytic gene expression, particularly IE genes and therefore maintaining latency (Reeves *et al.*, 2005). Reactivation from latency is initiated by restoration of expression of the IE genes including UL122 (IE2), which is upregulated during

differentiation by protocol 1 of HCMV+ NP1 (Taylor-Wiedeman *et al.*, 1994). It is well documented that differentiation in monocytes leads to changes in post-translational modifications of histones around the MIEP and reactivation of MIEP activity leading to lytic gene expression, so it is possible a similar effect could take place in neural progenitor cells (Reeves and Sinclair, 2013). Western blot shows the expression of IE1, IE2 and late proteins pp65 and gB increases throughout differentiation, which is unsurprising given the increase in infectious virion production. The production of virions in the absence of an apparent accumulation of pp65 at the AC, suggests that this is not necessary for viral production in NP1 cells.

Whilst it is likely that differentiation induced production of infectious virions from NP1 is due to changes induced by differentiation itself, it is also possible that components of the differentiation media could be having a direct effect on HCMV. The published differentiation protocol uses cAMP and 3-isobutyl-1-methylxanthine (IBMX), which is known to induce cAMP production (Parsons *et al.*, 1988). Multiple papers have found that treatment with cAMP or stimulation of the cAMP pathway induces reactivation of latent HCMV *in vitro* (Sadanari *et al.*, 1999, Keller *et al.*, 2007, Cheng *et al.*, 2017). However, none of these papers have satisfactorily determined whether this effect is differentiation independent. Keller *et al.* suggest that reactivation of IE expression in NT2 cells (a human pluripotent embryonal carcinoma cell line that can undergo neuronal differentiation *in vitro*) is due to effects on the MIEP and its enhancers and is therefore differentiation independent because the increase in IE transcription is rapid (from 2 hr post-treatment), though the only (de)differentiation marker they assessed in their study was Oct4, by western blot. It would be interesting to see if other differentiation markers were affected. It is also worth noting that despite an increase in HCMV gene expression, this particularly study did not detect a significant release of infectious progeny.

Differentiation of long-term infected NP1, colony 2 also led to production of infectious virions in the supernatant, albeit at a lower level than in differentiation of NP1 at 5 d.p.i (Figure 4.26). Interestingly, qPCR revealed that differentiation of colony 2 resulted in a different viral gene expression pattern than that seen in differentiation of HCMV+ NP1 at 5 d.p.i (Figure 4.25). Notably, UL44 which encodes a DNA polymerase processivity subunit, showed an increase in expression in differentiation between day 0 and 5 of protocol 1 differentiated HCMV+ NP1, whereas in colony 2 differentiation, a far greater log₂fold increase was observed. As this early gene is important for replication of viral DNA replication, it is likely that viral DNA replication is very limited in long term infection of colony 2, but is reinitiated by differentiation, similar to the

differentiation induced reactivation observed in latently infected monocytes (Sinigalia *et al.*, 2012). Overall, a far greater fold-change increase was seen in US28, UL111A, UL44 (pp52) and UL55 (gB) in colony 2 differentiation compared to protocol 1 differentiation. This is probably due to the fact that HCMV gene expression in colony 2 starts at a much lower level at day 0, rather than the recently infected NP1 that were differentiated at 5 d.p.i. This lower expression of viral genes is reflected in lower HCMV protein expression by western blots, where IE, pp65 and gB are expressed at lower levels in colony 2 at day 0, than in 5 d.p.i HCMV+ NP1 at day 0. Similar to differentiation of 5 d.p.i NP1, colony 2 also shows an increase in IE, pp65 and gB protein expression at day 5, which is reflected in the increase in virion production and release in the supernatant. Whether colony 2 is true latent HCMV infection reactivated by differentiation or simply a low-level chronic infection remains to be determined. To further investigate this, RNAseq analysis of HCMV genes may help to elucidate whether the gene expression pattern is similar to the latent expression profiles seen in other latency models or simply low level, IE driven lytic expression. Cheng *et al.* (2017) provide detailed HCMV transcriptome analysis of latency and reactivation associated viral gene expression, which could be utilised to analyse RNAseq of colony 2 differentiation. Investigation of the chromatin structure of the MIEP in these cells may also help distinguish latency from low level lytic infection in colony 2. Either way, this differentiation induced increase in viral gene expression production of infectious virions could have important implications if a similar scenario arises during differentiation of HCMV infected neural progenitor cells in the adult brain.

Colony 2 cells show an increase in GFAP expression compared to normal NP1 which is maintained throughout differentiation (Figure 4.27). Overexpression of GFAP has previously been reported in GBM, with Ahmadipour *et al.* (2020) finding a correlation between higher GFAP expression and shorter patient survival time (Reifenberger *et al.*, 1987). However, multiple studies have reported that in vitro HCMV infection of GBM cells leads to downregulation of GFAP in contrast to the upregulation seen in long term infected neural progenitor cells, colony 2 (Lee *et al.*, 2005, Koh *et al.*, 2009, Fornara *et al.*, 2016). Expression of PCNA is also higher in colony 2 than in NP1 and shows a smaller decrease in expression over the course of differentiation. In protocol 1 differentiation of HCMV+ NP1, PCNA is maintained throughout differentiation (Figure 4.10.A). As the decrease in PCNA is less than in NP1, but not maintained throughout differentiation of colony 2 as in protocol 1 HCMV+ NP1 this could indicate a mixed population where the HCMV+ cells are maintaining PCNA, but HCMV- cells are losing PCNA due to differentiation. To further explore this

Immunofluorescence for PCNA would help determine if PCNA expression is only in HCMV+ cells. A proliferation assay comparing colony 2 to NP1 could be used to determine if the increase in PCNA is accompanied by increased proliferation or if it is caused by HCMV mediated cell cycle dysregulation and induction of S phase associated proteins which support viral DNA replication.

Finally, GBM stem cell marker CD133 is also expressed in colony 2, albeit at a lower level than in 5 d.p.i HCMV infection of NP1 (Figure 4.28). Colony 2 shows an increase in CD133 expression during differentiation, like that seen in 5 d.p.i HCMV infected NP1. Again, this similar pattern of increased expression, but at a lower level could be reflective of a mixed population of HCMV+/- NP1 where HCMV+ cells are also CD133+ as seen in GBM, where CD133+ cells are often also expressing HCMV IE (Soroceanu *et al.*, 2015). Alternatively, this could indicate a population of latently infected NP1, with very low levels of viral gene expression and therefore decreased effect of CD133 expression when compared to the 5 d.p.i HCMV+ NP1 in protocol 1. In the context of HCMV in GBM, it is interesting that not only can adult neural progenitor cells harbour long term HCMV infection, but that this infection has long lasting effects on markers of stemness and proliferation as well as glial marker GFAP. It is also important that this long term infection continues to affect differentiation, with failure to adopt neuronal morphology and aberrant expression of GFAP, PCNA and CD133, long after the initial infection.

Taken together, HCMV's ability to perturb differentiation of adult neural progenitor cells both in recent and long-term infection and its ability to induce CD133 expression in both NP1 (including expression in long term infected colony 2) and in differentiated NP1 (protocol 2) despite the presence of differentiation stimuli could represent a HCMV mediated de-differentiation phenotype. A recent study found HCMV could induce de-differentiation of mature human mammary epithelial cells leading to transformation and a cancer cell phenotype (Nehme *et al.*, 2021). Induction of de-differentiation has also been demonstrated in other herpesviruses, namely the oncogenic EBV and KSHV (Xie *et al.*, 2021. Liu *et al.*, 2010). Additionally, KSHV has been shown to induce CD133 expression in infected lymphatic endothelial cells and expression of EBV Latent Membrane Protein 2A (LMP2A) protein upregulates CD133 expression in HONE-1, an epithelial carcinoma line (Port *et al.*, 2013). As CD133+ cells are also often HCMV IE+ in GBM samples, and oncogenic herpesviruses also induce CD133 expression, our finding of CD133 expression in HCMV infected NP1 suggests that HCMV drives cells towards a stem-like phenotype and could explain why HCMV seropositivity is associated with more aggressive tumours and poor prognosis in GBM (Soroceanu *et al.*, 2015, Foster *et al.*, 2019).

Chapter 5 – RNAseq analysis of the effects of HCMV on the differentiation of neural progenitor cells

5.1 RNAseq experimental design and quality control

RNAseq analysis was used to understand the effects of HCMV infection upon NP1 differentiation at the gene expression level. RNAseq involves sequencing the whole transcriptome of a sample and enables global analysis of changes in gene expression, which allowed us to get an overview of the pathways affected by HCMV infection, whilst also looking at expression changes of specific genes of interest, including viral genes. NP1 were infected and differentiated as detailed in section 2.6.4 and the sampling conditions are summarised in figure 5.1.

RNA was quantified and checked for purity in house using a NanoDrop and further sample QC performed by Novogene (Figure 5.2). All 12 samples passed quality control and RNAseq was performed by Novogene as detailed in section 2.9. Sample groups were named NP1_0 (NP1 day 0), NP1_5 (NP1 day 5), HCMV_0 (NP1 +HCMV day 0) and HCMV_5 (NP1 +HCMV day 5). Initial bioinformatics analysis was carried out by Novogene with subsequent analysis in house.

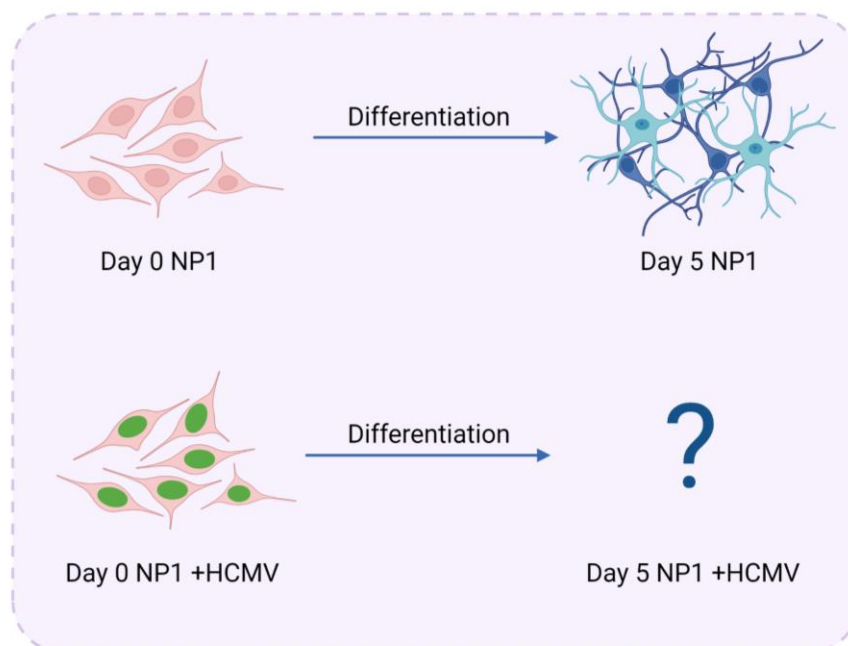


Figure 5.1 Experimental design for RNAseq analysis

Schematic summary of differentiation of NP1 +/-HCMV (MOI of 3 FFU/cell at 5 d.p.i) over 5 days using the Walton *et al.*, (2006) protocol. RNA samples were obtained at day 0 and 5 of differentiation of NP1 +/- HCMV.

A)

| Sample | Sample code | Conc (ng/ μ l) | Vol (μ l) | 260/280 | 260/230 |
|------------------|-------------|--------------------|----------------|---------|---------|
| NP1 Day 0 | NP1_0_1 | 178.2 | 20 | 2.11 | 2.30 |
| | NP1_0_2 | 129.4 | 20 | 2.12 | 2.19 |
| | NP1_0_3 | 120.0 | 20 | 2.11 | 2.32 |
| NP1 + HCMV Day 0 | HCMV_0_1 | 642.0 | 20 | 2.12 | 2.24 |
| | HCMV_0_2 | 584.9 | 20 | 2.13 | 2.24 |
| | HCMV_0_3 | 535.2 | 20 | 2.11 | 2.22 |
| NP1 Day 5 | NP1_5_1 | 178.5 | 20 | 2.04 | 2.33 |
| | NP1_5_2 | 204.3 | 20 | 2.05 | 2.31 |
| | NP1_5_3 | 173.7 | 20 | 2.06 | 2.40 |
| NP1 + HCMV Day 5 | HCMV_5_1 | 469.6 | 20 | 2.06 | 2.17 |
| | HCMV_5_2 | 686.5 | 20 | 2.12 | 2.08 |
| | HCMV_5_3 | 676.1 | 20 | 2.11 | 2.30 |

B)

| Sample | Sample code | Conc (ng/ μ l) | RIN |
|------------------|-------------|--------------------|-----|
| NP1 Day 0 | NP1_0_1 | 170 | 9.6 |
| | NP1_0_2 | 115 | 9.9 |
| | NP1_0_3 | 112 | 10 |
| NP1 + HCMV Day 0 | HCMV_0_1 | 469 | 9.5 |
| | HCMV_0_2 | 434 | 9.4 |
| | HCMV_0_3 | 396 | 9.3 |
| NP1 Day 5 | NP1_5_1 | 177 | 9.6 |
| | NP1_5_2 | 179 | 9.6 |
| | NP1_5_3 | 198 | 9.6 |
| NP1 + HCMV Day 5 | HCMV_5_1 | 512 | 8.9 |
| | HCMV_5_2 | 609 | 9.5 |
| | HCMV_5_3 | 552 | 9.5 |

Figure 5.2 RNA sample quality control

A) RNA sample quantification and quality control measured using NanoDrop 1000 spectrophotometer (Thermo Fisher Scientific). Novogene RNA sample specifications require minimum concentration of 20 ng/ μ L and 260/280 and 260/230 >2. B) RNA sample quantification and quality control carried out by Novogene using a LabChip GX Touch HT Bioanalyser (Caliper Life Sciences). Novogene RNA sample requirements state RIN should be >8. NP1_0 = untreated NP1. NP1_5 = NP1 differentiated over 5 days using Walton *et al.*, (2006) protocol. HCMV_0 = NP1 +HCMV infected at an MOI of 3 FFU/cell for 5 days, HCMV_5 = NP1 +HCMV infected at an MOI of 3 FFU/cell for 5 days and then differentiated over 5 days using Walton *et al.*, (2006) protocol.

5.2 RNAseq correlation

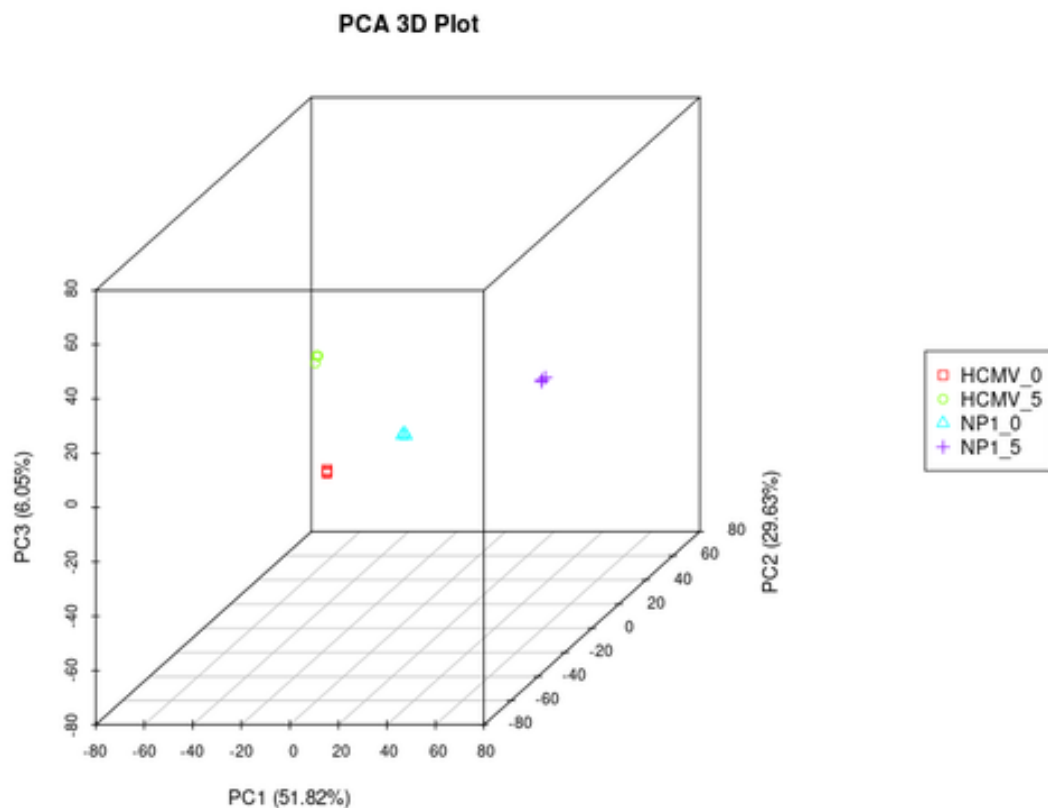


Figure 5.3 3D Principal component analysis (PCA)

3D Principal component analysis of RNA samples used for RNAseq. Each of the four groups NP1_0, NP1_5, HCMV_0 and HCMV_5 comprised three individual RNA samples from three experimental repeats.

Principal component analysis (PCA) reduces a gene expression dataset with multiple variables to 3 dimensions by constructing linear combinations of gene expression known as principal components (Jolliffe and Cadima, 2016). This analysis is used to increase interpretability of the data, whilst minimising loss of information. PCA is commonly used to identify patterns in large complex datasets and can therefore infer the quality of RNAseq data. PCA analysis of RNAseq data for sample groups NP1_0, NP1_5, HCMV_0 and HCMV_5 shows the gene expression profile for each group was distinct and that there was excellent overlap between the replicates of each group (Figure 5.3). Pearson correlation measures the strength of the linear relationship between two variables and is used to assess the similarity of pairs of RNA samples (Rovetta, 2020). For RNAseq it is recommended that all samples within a group display a correlation of >0.9 . Figure 5.4 shows that all replicates within groups had a correlation of >0.97 , indicating very high quality RNA sample replicates.

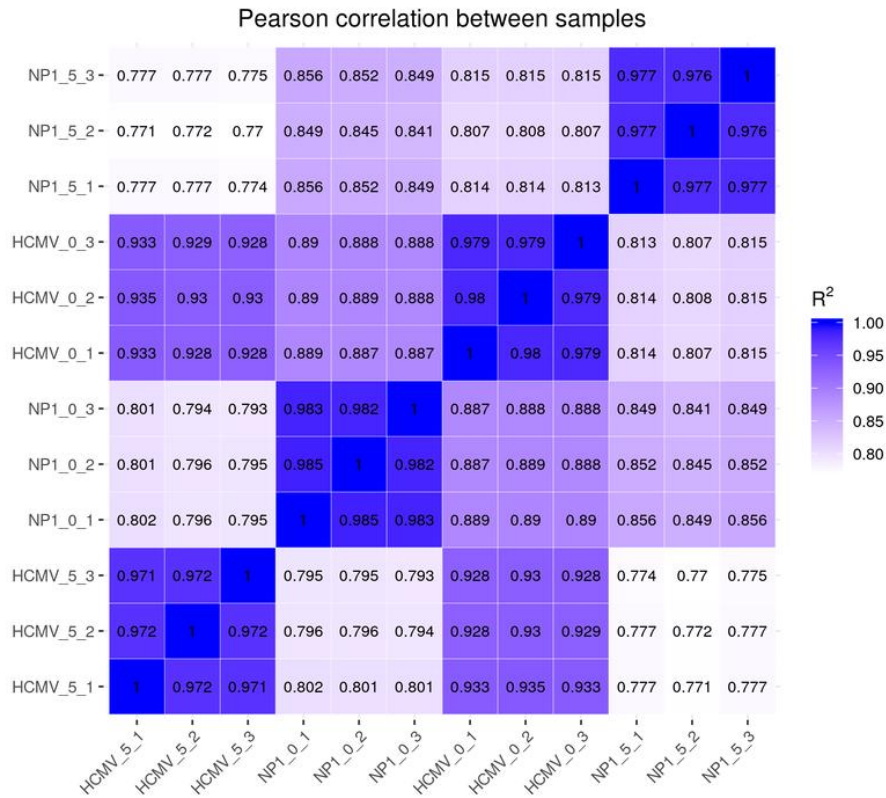


Figure 5.4 Pearson correlation between RNA samples

Pearson correlation of individual RNA samples with three replicates within each treatment group. Pearson correlation coefficient is a measurement of the strength of the relationship between two variables and their association with each other with R^2 of 1 indicating the strongest correlation. NP1_0 = untreated NP1. NP1_5 = NP1 differentiated over 5 days using Walton *et al.*, (2006) protocol. HCMV_0 = NP1 +HCMV infected at an MOI of 3 FFU/cell for 5 days, HCMV_5 = NP1 +HCMV infected at an MOI of 3 FFU/cell for 5 days and then differentiated over 5 days using Walton *et al.*, (2006) protocol.

5.3 RNAseq distribution

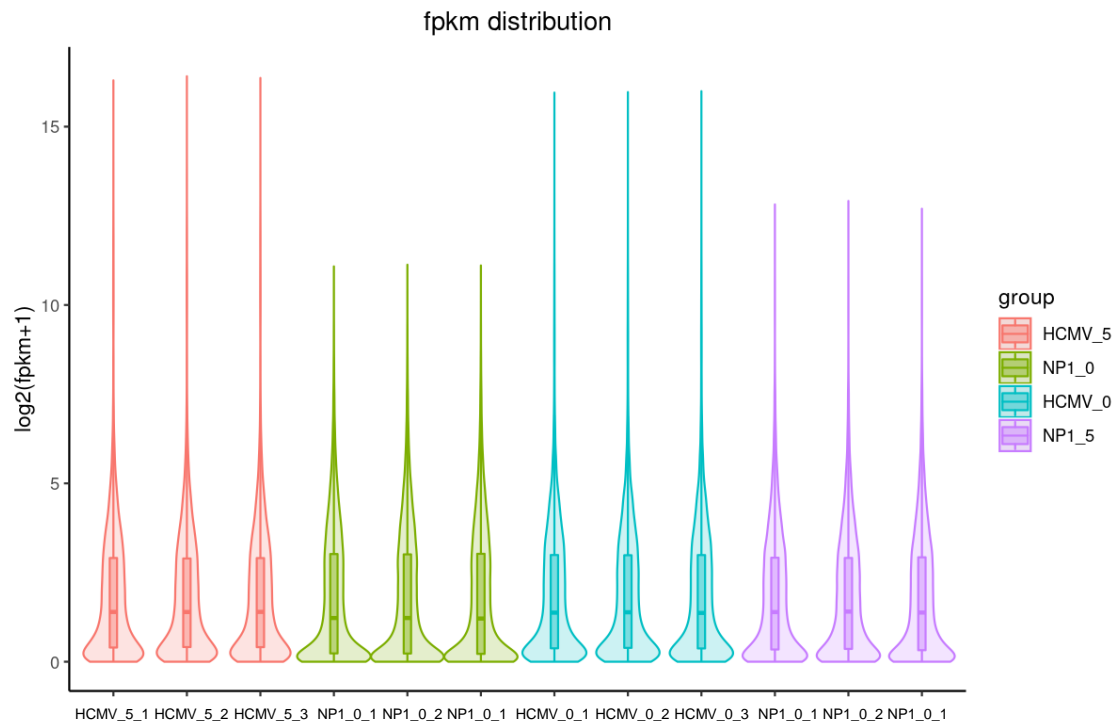


Figure 5.5 Violin plot of RNAseq sample FPKM distribution

Distribution of fragments per kilobase of transcript per million mapped reads (FPKM) for each RNA sample used for RNAseq. NP1_0 = untreated NP1. NP1_5 = NP1 differentiated over 5 days using Walton *et al.*, (2006) protocol. HCMV_0 = NP1 +HCMV infected at an MOI of 3 FFU/cell for 5 days, HCMV_5 = NP1 +HCMV infected at an MOI of 3 FFU/cell for 5 days and then differentiated over 5 days using Walton *et al.*, (2006) protocol.

Figure 5.5 shows the distribution of FPKM for all genes in a violin plot for each RNA sample used for RNAseq. The distribution pattern of FPKM is consistent between samples in the same groups and very similar between treatment groups, although groups with HCMV show higher maximum FPKM than the non-infected control groups, indicating that the highest expression of individual genes occurs in the infected groups. The median and interquartile range is highly consistent between all samples.

Figure 5.6 shows a heatmap of all statistically significant differentially expressed genes from all individual samples and groups. The cut offs applied to identify significantly differentially expressed genes were a Log₂Fold change of >1 or <-1 and padj of <0.01 (Koch *et al.*, 2018). Genes within the same cluster show the same trends in expression levels under different conditions. Notable features include a cluster of genes upregulated in HCMV_0 compared to controls, that are further upregulated in HCMV_5. There are also large clusters unique to NP1_0 and to NP1_5.

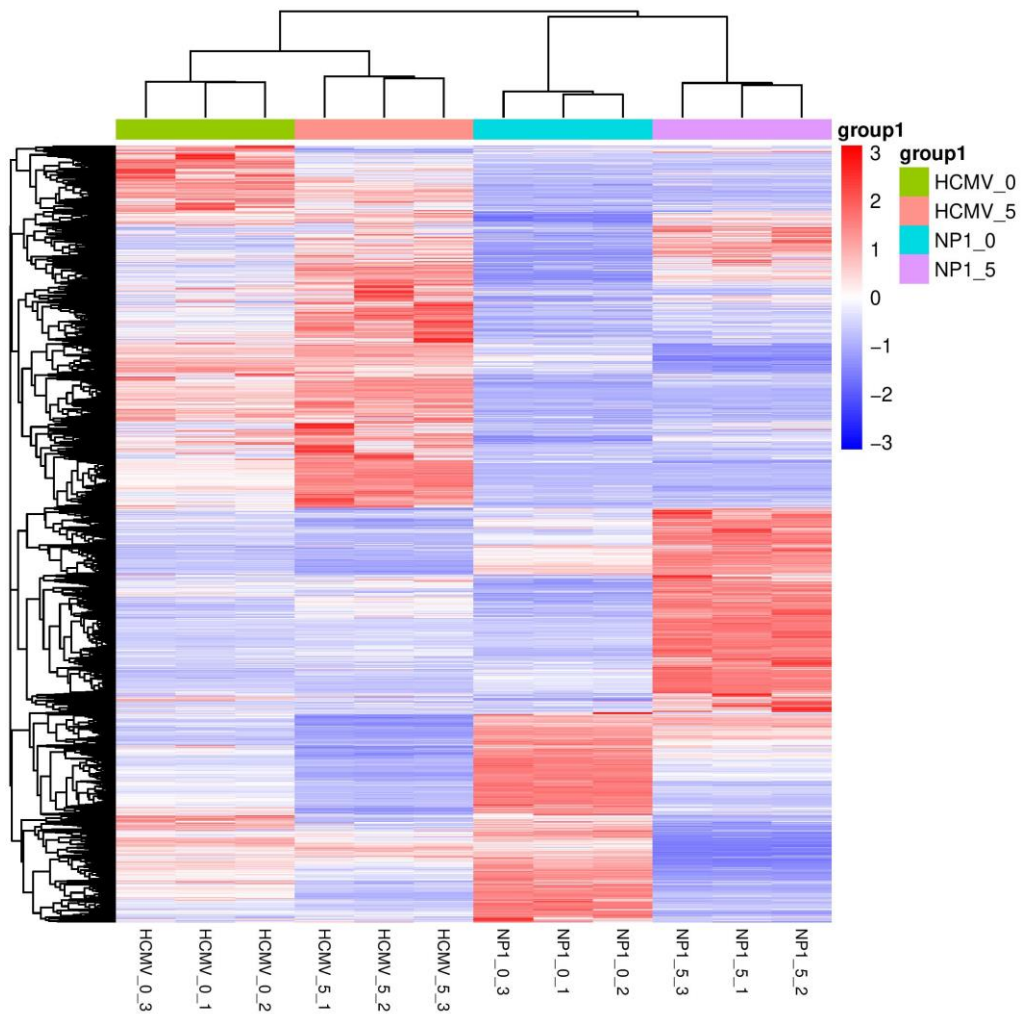


Figure 5.6 Hierarchical Clustering Heatmap of RNA-seq

Heatmap shows the overall results of FPKM cluster analysis, clustered using the $\log_2(\text{FPKM}+1)$ value. Red color indicates genes with high expression levels, and blue color indicates genes with low expression levels. The color ranging from red to blue indicates that $\log_2(\text{FPKM}+1)$ values were from large to small. NP1_0 = untreated NP1. NP1_5 = NP1 differentiated over 5 days using Walton *et al.*, (2006) protocol. HCMV_0 = NP1 +HCMV infected at an MOI of 3 FFU/cell for 5 days, HCMV_5 = NP1 +HCMV infected at an MOI of 3 FFU/cell for 5 days and then differentiated over 5 days using Walton *et al.*, (2006) protocol. Differentially expressed genes with a Log2Fold change of >1 or <-1 and padj of <0.01 were included in this analysis.

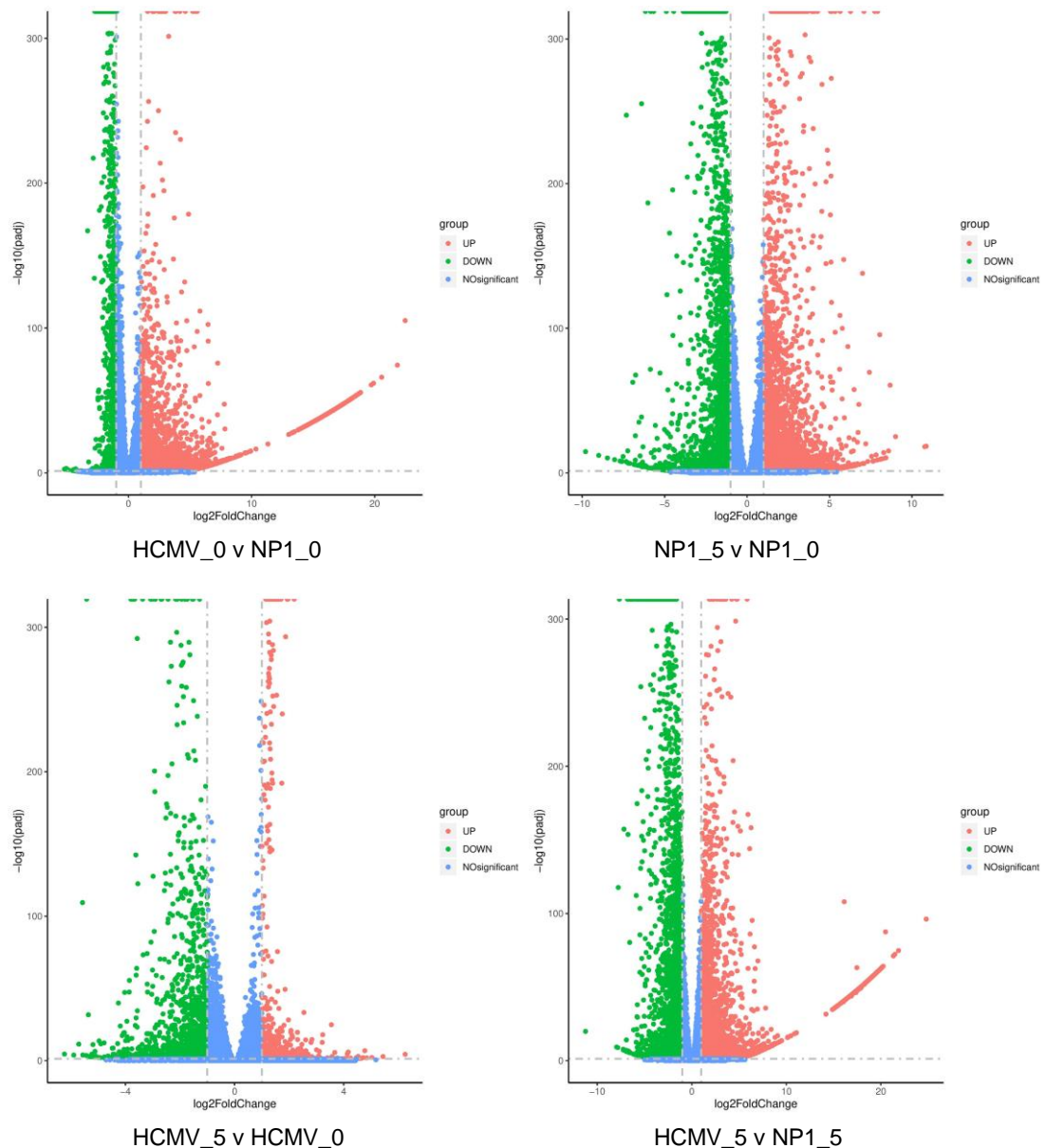


Figure 5.7 Volcano plots of RNAseq data

Volcano plots of differentially expressed genes identified by RNAseq of RNA isolated from the following samples: NP1_0 = untreated NP1. NP1_5 = NP1 differentiated over 5 days using Walton *et al.*, (2006) protocol. HCMV_0 = NP1 +HCMV infected at an MOI of 3 FFU/cell for 5 days, HCMV_5 = NP1 +HCMV infected at an MOI of 3 FFU/cell for 5 days and then differentiated over 5 days using Walton *et al.*, (2006) protocol. Differentially expressed genes with a Log2Fold change of >1 or <-1 and padj of <0.01 were deemed significantly differentially expressed.

Figure 5.7 shows volcano plots of all the differentially expressed genes identified through RNAseq analysis. Genes that did not satisfy the criteria of Log2Fold change of >1 or <-1 and padj of <0.01 are shown in blue, genes with significantly increased expression are shown in red and those with significantly decreased

expression are in green Figure 5.7. The spur of highly upregulated genes on the bottom right side of the plots for HCMV_0 v NP1_0 and HCMV_5 v NP1_5 represent the HCMV genes due to the human and viral genes being analysed together. Interestingly, far fewer genes were differentially expressed during differentiation of HCMV infected NP1 HCMV_5 v HCMV_0, than in the control group NP1_5 v NP1_0. Also notable is that at day 0, far more genes are upregulated by HCMV infection than are downregulated. However, by day 5 of differentiation the balance between genes that are upregulated and down regulated is much more even.

5.4 RNAseq analysis of neural progenitor differentiation markers

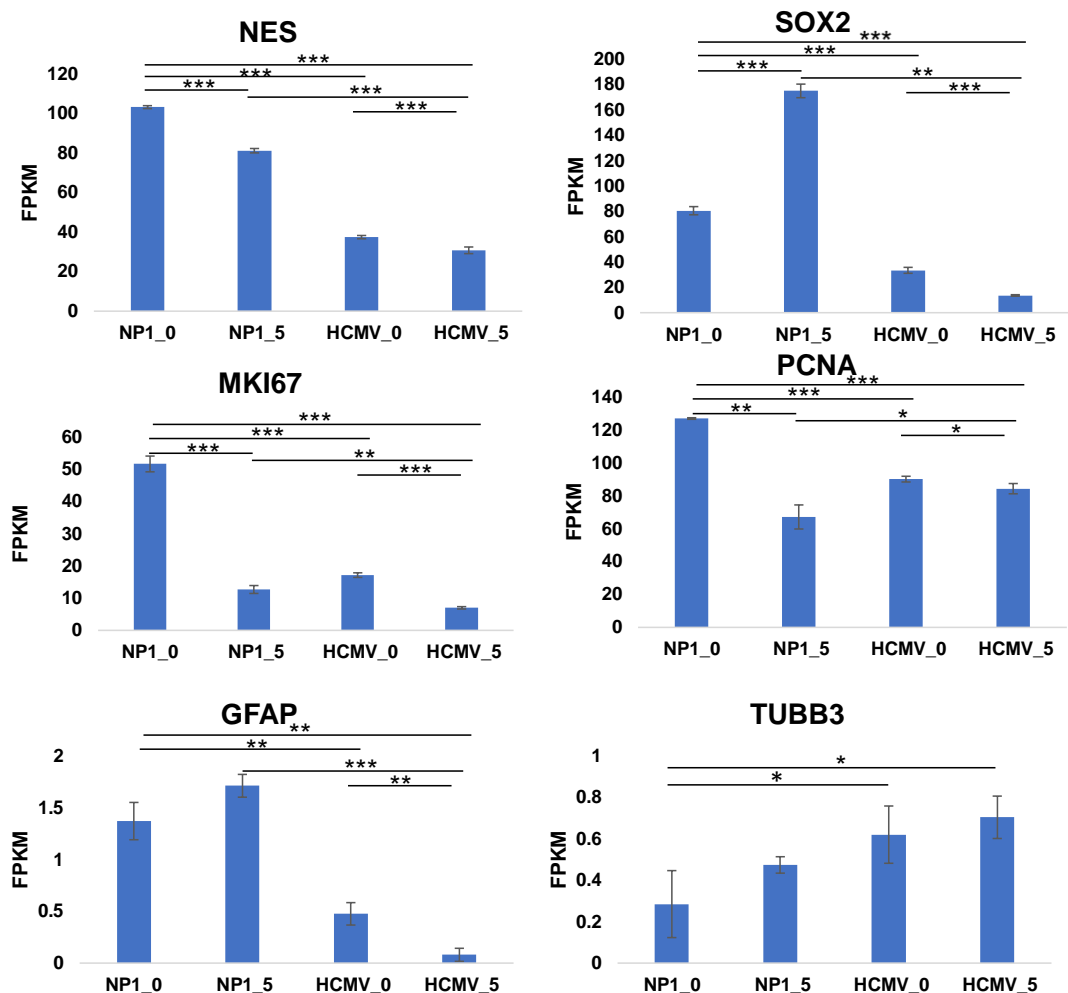


Figure 5.8 RNAseq FPKM of differentiation markers

RNAseq FPKM for NES, SOX2, MKI67, PCNA, GFAP and TUBB3. NP1_0 = untreated NP1. NP1_5 = NP1 differentiated over 5 days using Walton *et al.*, (2006) protocol. HCMV_0 = NP1 +HCMV infected at an MOI of 3 FFU/cell for 5 days, HCMV_5 = NP1 +HCMV infected at an MOI of 3 FFU/cell for 5 days and then differentiated over 5 days using Walton *et al.*, (2006) protocol.

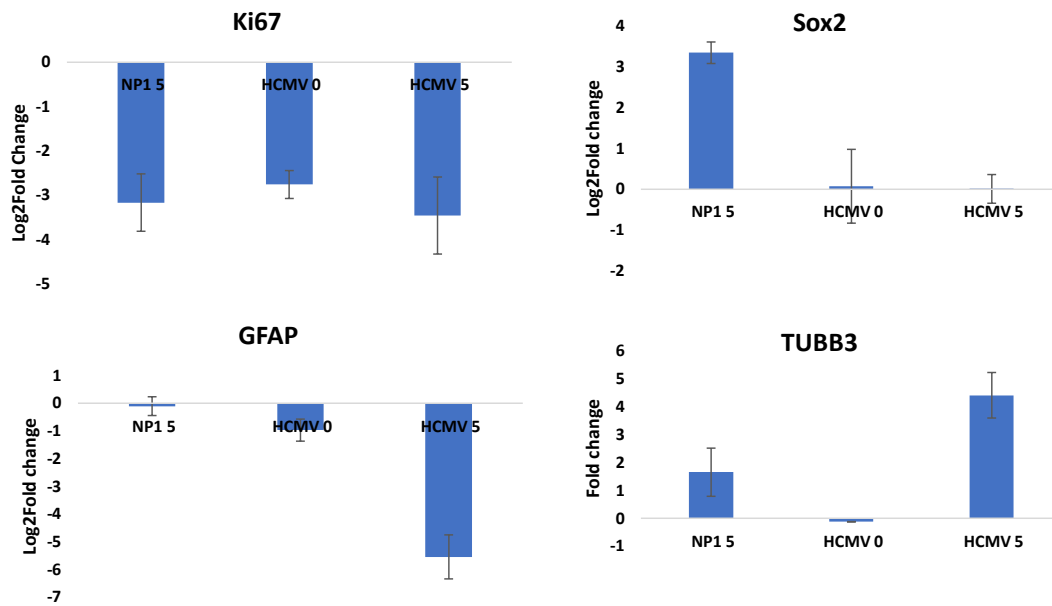


Figure 5.9 qPCR for differentiation markers

Log2fold change in gene expression by qPCR, calculated by $\Delta\Delta CT$ using GAPDH as a housekeeping gene. Fold change in gene expression shown for differentiation markers MKI67, SOX2, GFAP and TUBB3. NP1_0 = untreated NP1. NP1_5 = NP1 differentiated over 5 days using Walton et al., (2006) protocol. HCMV_0 = NP1 +HCMV infected at an MOI of 3 FFU/cell for 5 days, HCMV_5 = NP1 +HCMV infected at an MOI of 3 FFU/cell for 5 days and then differentiated over 5 days using Walton et al., (2006) protocol (two-tailed student t-test, * $p \leq 0.05$, ** $p \leq 0.01$, *** $p \leq 0.001$, $n=3$).

The effects of HCMV infection on the differentiation of NP1, specifically its effects on protein expression for differentiation markers including nestin, Sox2, Ki67, PCNA, GFAP and β -III-tubulin are described in section 4.3.2. To assess the changes in mRNA expression of these differentiation markers, FPKM from RNAseq was compared between groups (figure 5.8). The FPKM of stem and progenitor marker nestin (NES) showed a significant decrease between NP1_0 and NP1_5. HCMV infection also caused a significant decrease in NES expression between NP1_0 and HCMV_0 with expression decreasing even further when the HCMV+ NP1 were differentiated (HCMV_5). This correlates with the same pattern of protein expression seen by western blot in figure 4.10. Stem and progenitor marker Sox2 (SOX2) showed significantly increased gene expression by RNAseq analysis of FPKM between NP1_0 and NP1_5. HCMV_0 showed a marked decrease in SOX2 compared to NP1_0 and this decreased again between HCMV_0 and HCMV_5. Log2fold change from qPCR also shows NP1_5 as having the highest level of expression of SOX2 (figure 5.9), which is not reflected by western blot quantification of Sox2 protein. Western blot of Sox2 showed a decrease in protein between day 0 and day 5 in NP1 and a complete

loss of Sox2 in HCMV infected HCMV at both day 0 and 5 (figure 4.10). Sox 2 is regulated by CUL4A^{DET1-COP1} and OTUD7B which exert opposite effects on protein stability at a post-translational level during neural progenitor cell differentiation, which could account for the difference between gene and protein levels of this marker (Chun-ping *et al.*, 2018).

MKI67 (Ki67) FPKM is highest in NP1_0, decreasing dramatically with differentiation (figure 5.8). HCMV_0 shows a significant reduction compared to NP1_0 and is further reduced in HCMV_5. This pattern of MKI67 gene expression is mirrored in the qPCR data in figure 4.9. Whilst immunofluorescence for Ki67 in figure 4.11 showed that the percentage of NP1 cells expressing Ki67 falls from 94 % to 17 % between day 0 and 5, 89 % of HCMV+ NP1 were still Ki67+ at day 5. Ki67 expression is known to be underpinned by cell cycle regulation and Ki67 protein is known to be highly unstable throughout the cell cycle (Bruno and Darzynkiewicz, 1992). Whilst Ki67 accumulates during S, G2, and M phases, it is continuously degraded during G0 and G1 Miller *et al.*, 2018). The stability and cell cycle dependent degradation may account for the difference between Ki67 gene and protein expression. Additionally, as HCMV is known to modulate cell cycle, this could also affect the rate of Ki67 protein accumulation/degradation.

PCNA FPKM decreased between NP1_0 and NP1_5 which is reflected in a decrease in PCNA protein by western blot (Figure 5.8 and 4.10). HCMV_0 showed lower gene expression of PCNA by FPKM than NP1_0 and this decreased further during differentiation (HCMV_5). However, protein levels of PCNA in HCMV_5 by western blot had returned to that seen in NP1_0. This could be due to post-transcriptional, translational or post-translational regulation of PCNA. For example, PCNA degradation is known to be regulated through degradation promoting acetylation by CREB-binding protein (CBP), and p300 as well as it's binding to MutT homolog2 which prevents degradation (Yu *et al.*, 2009, Cazzalini *et al.*, 2014).

RNAseq and qPCR for astrocytic marker GFAP shows a very similar pattern of expression with higher expression in NP1_0 and NP1_5 than in HCMV_0 with lowest expression in HCMV_5 (figure 5.8 and 5.9). This pattern is reflected in protein expression by western blot, in which GFAP protein levels are higher throughout differentiation of NP1 and decrease through differentiation of HCMV+ NP1 (figure 4.10).

Both RNAseq and qPCR show a non-significant increase in neuronal marker, TUBB3 gene expression between NP1_0 and NP1_5. TUBB3 is significantly increased between NP1_0 and HCMV_0 and also between NP1_5 and HCMV_5

(Figure 5.8). Whilst qPCR shows a similar pattern of expression for TUBB3, the increase between the control and HCMV infected groups is not significant (figure 5.9). This general pattern of increased TUBB3 in HCMV+ NP1 is reflected in western blots for β -III-tubulin protein, which show higher levels in HCMV+ NP1 throughout differentiation, compared to NP1 controls (figure 4.10).

Notably, CD133 transcripts were not detected by RNAseq, despite a strong increase in CD133 protein expression during differentiation of HCMV+ NP1 detected by western blot and IF, using two different antibodies (Figure 4.12). This discrepancy could be due to sample preparation for RNAseq or secondary structure formation of the RNA (Rachinger *et al.*, 2021).

Given the discrepancies between RNA and protein levels for some of the canonical markers used in chapter 4, we undertook orthogonal validation of RNA-seq data based upon commonly used neuronal and astrocytic markers. Markers included in this analysis were all identified from a well-regarded commercially available list of neural lineage markers and differentially expressed in at least one of the five differentially expressed gene lists (Abcam, 2016). All five neuronal markers (GPM6A, RBFOX3, MAP2, SYP and DLG4) increased in NP1_5 v NP1_0, which is reassuring, given that the Walton *et al.* (2006) differentiation protocol results in predominately neuronal cells (figure 5.10). Glycoprotein M6A (GPM6A) encodes a neuronal membrane glycoprotein involved in neuron development, specifically synapse formation and plasticity (Leon *et al.*, 2021). Knockout of GPM6A in mice leads to impaired axon formation (Sato *et al.*, 2011). Whilst G6PMA is increased between NP1_5 v NP1_0, its expression is decreased in all other comparisons, with the largest decrease seen between HCMV_5 v NP1_5, with a log2fold change of -6.8. This large reduction in GPM6A expression could contribute to the reduced number and length of neurites in HCMV_5 compared to NP1_5 and is further evidence of impaired differentiation (figure 4.9).

However, whilst HCMV infection reduces expression of GPM6A, other neuronal markers were increased by HCMV infection. RNA Binding Fox-1 Homolog 3 (RBFOX3) is a commonly used marker for post-mitotic neurons and is important for neuronal development and maturation (Duan *et al.*, 2015). Expression of RBFOX3 is higher in HCMV infected NP1 than controls at both day 0 and day 5 of differentiation with a log2fold change of 2.06 between HCMV_0 v NP1_0 and 1.08 between HCMV_5 v NP1_5. RBFOX3 is known to be expressed in GSCs and has been shown to promote tumour growth in hepatocellular carcinoma due to its function as a TERT promoter-binding protein, promoting TERT expression (Marques *et al.*, 2021, Liu *et al.*, 2017).

Microtubule associated protein 2 (MAP2) is thought to be important for microtubule assembly, an integral process in neurogenesis (Dehmelt and Halpain, 2005). MAP2 expression is increased in NP1_5 v NP1_0, but also in HCMV_5 v NP1_5, though it is not differentially expressed in any of the other comparison groups.

SYP encodes synaptophysin, a membrane glycoprotein found in presynaptic vesicles (Wiedenman *et al.*, 1986). Synaptophysin (SYP) is increased in NP1_5 v NP1_0, HCMV_5 v HCMV_0 and HCMV_5 v NP1_0. This suggests that SYP expression increases during differentiation of HCMV+ NP1 in a similar pattern to that of the control NP1.

Finally, discs large MAGUK scaffold protein 4 (DLG4) forms part of the post-synaptic architecture and is only differentially expressed between NP1_5 v NP1_0, where it increases by a log₂fold change of 1.17 (Guang *et al.*, 2018). HCMV infected NP1 do not show an increase in DLG4 during differentiation, suggesting that this is affected by HCMV infection.

Overall, expression of several neuronal marker genes is dysregulated during differentiation of HCMV infected NP1. Whilst some genes such as RBFOX3 and MAP2 are increased in HCMV+ NP1, GPM6A expression is dramatically reduced. This disordered expression of neuronal markers is further evidence that HCMV infection profoundly disrupts differentiation of NP1.

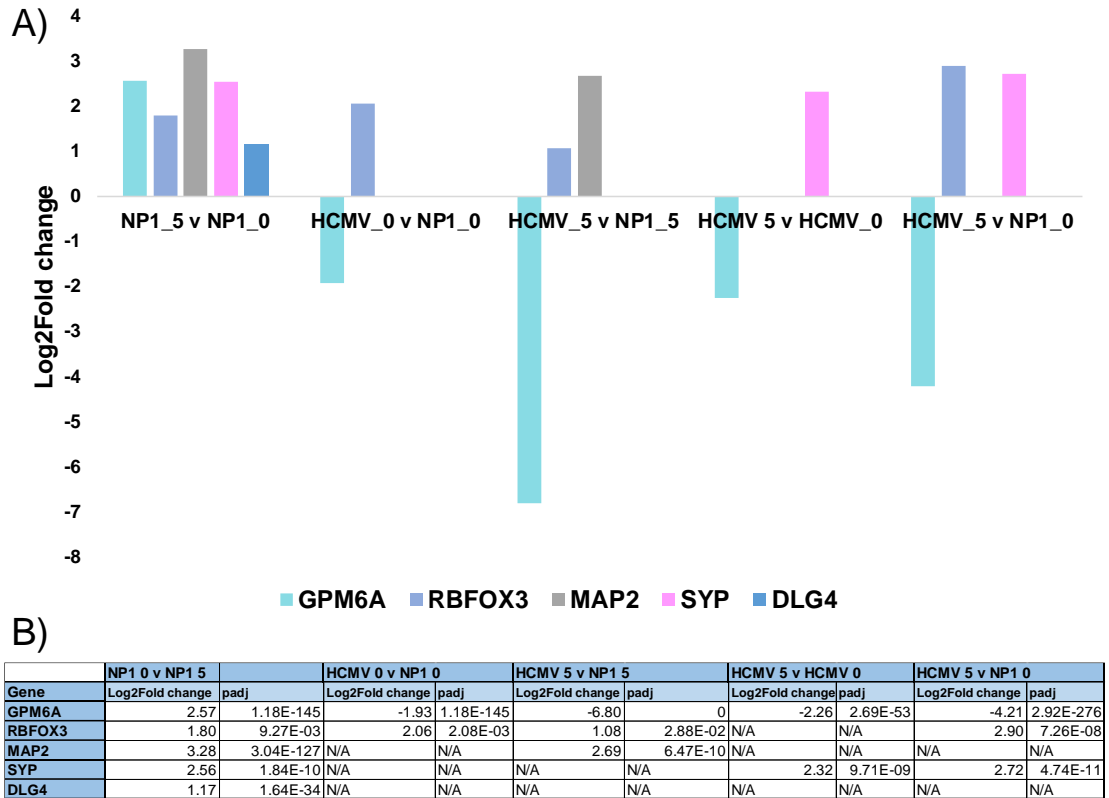


Figure 5.10 Neuronal marker differential gene expression

A) Differential gene expression of neuronal markers GPM6A, RBFOX3, MAP2, SYP and DLG4 from RNAseq analysis, expressed as Log2Fold change. NP1_0 = untreated NP1. NP1_5 = NP1 differentiated over 5 days using Walton *et al.*, (2006) protocol. HCMV_0 = NP1 +HCMV infected at an MOI of 3 FFU/cell for 5 days, HCMV_5 = NP1 +HCMV infected at an MOI of 3 FFU/cell for 5 days and then differentiated over 5 days using Walton *et al.*, (2006) protocol B) Table summarising differential expression of neuronal markers including Log2Fold change and padj.

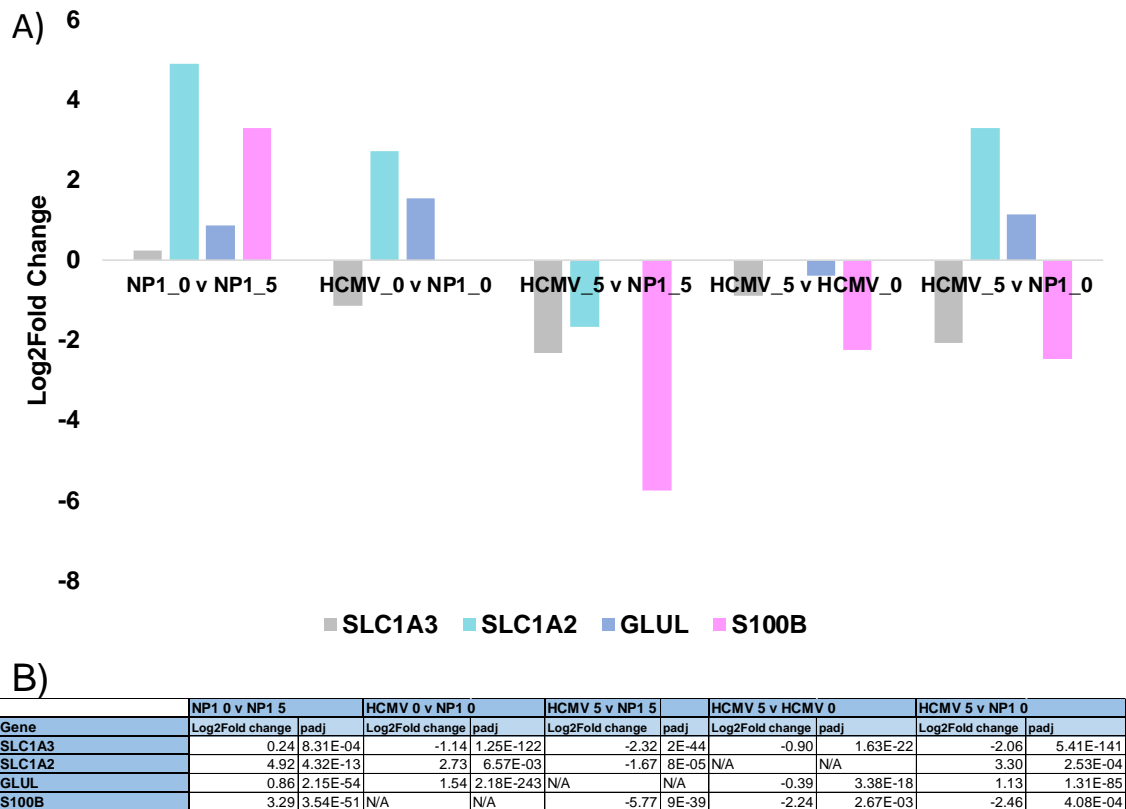


Figure 5.11 Astrocyte marker differential gene expression

A) Differential gene expression of astrocytic markers SLC1A3, SLC1A2, GLUL and S100B from RNAseq analysis, expressed as Log2Fold change. NP1_0 = untreated NP1. NP1_5 = NP1 differentiated over 5 days using Walton *et al.*, (2006) protocol. HCMV_0 = NP1 +HCMV infected at an MOI of 3 FFU/cell for 5 days, HCMV_5 = NP1 +HCMV infected at an MOI of 3 FFU/cell for 5 days and then differentiated over 5 days using Walton *et al.*, (2006) protocol B) Table summarising differential expression of astrocyte markers including Log2Fold change and padj.

Differential expression of astrocytic markers was also analysed as the differentiation protocol results in a mixed population of both neurons and astrocytes (Walton *et al.*, 2006). All four of the astrocyte markers, solute carrier family 1 member 3 (SLC1A3), solute carrier family 1 member 2 (SLC1A2), glutamate-ammonia ligase (GLUL) and S100 calcium binding protein B (S100B) were increased in NP1_5 v NP1_0, supporting that differentiation of NP1 by this method leads to astrocytic differentiation as well as neuronal (figure 5.11). SLC1A3 encodes a glutamate transporter which is involved in transportation of glutamate into astrocytes (Anderson and Swanson, 2000). SLC1A3 expression is decreased in HCMV_0 v NP1_0, HCMV_5 v NP1_5, HCMV_5 v HCMV_0 and HCMV_5 v NP1_0, indicating that HCMV infection decreases SLC1A3 expression in NP1 both with and without differentiation. SLC1A2 encodes the predominant glutamate transporter of the human brain, which clears glutamate from neuronal synapses to prevent excessive activation of glutamate receptors

(Stergachis *et al.*, 2019). SLC1A2 expression increased between HCMV_0 v NP1_0, is not differentially expressed between HCMV_5 and HCMV_0, but decreased expression in HCMV_5 v NP1_5. This suggests that whilst infection of NP1 with HCMV initially increases SLC1A2 expression, it does not increase during differentiation and fails to reach the same expression seen in differentiated NP1 at day 5.

Interestingly, decreased SLC1A3 and SLC1A2 expression has been associated with metastasis in GBM (Tong *et al.*, 2015). GLUL encodes glutamine synthetase, a marker expressed by all astrocytes (Montgomery, 1994). GLUL expression is increased in HCMV_0 v NP1_0, with a log₂fold change of 1.54, however unlike the increase observed during differentiation of NP1, GLUL decreases during differentiation of HCMV+ NP1 with a log₂fold change of -0.39 in HCMV_5 v HCMV_0. By day 5 of differentiation there is no difference in GLUL expression between HCMV_5 and NP1_5. The final astrocytic marker, S100B, encodes a calciprotein expressed in mature astrocytes (Raponi *et al.*, 2007). Whilst S100B expression increases during differentiation of NP1 and is not differentially expressed between HCMV_0 and NP1_0, its expression is decreased in HCMV_5 v NP1_5, HCMV_5 v HCMV_0 and HCMV_5 v NP1_0. At day 5 of differentiation, a log₂fold change of -5.77 is seen in HCMV_5 v NP1_5. Taken together, the dysregulation of astrocytic markers in the differentiation of HCMV+ NP1, further supports the hypothesis that HCMV infection perturbs the differentiation of NP1.

5.5 Enrichment analysis of differentially expressed genes

Enrichment analysis uses libraries of annotated and curated gene sets to ascribe functional biological terms to lists of genes. Enrichr is a gene set search engine that enables searching of hundreds of thousands of annotated gene sets automatically (Enrichr, 2022, Chen *et al.*, 2013). By inputting a list of genes, Enrichr identifies which annotated gene sets overlap with the input genes, using multiple databases including Kyoto Encyclopedia of Genes and Genomes (KEGG) (Chen *et al.*, 2013, Kuleshov *et al.*, 2016, Xie *et al.*, 2021). The KEGG pathway analysis available through Enrichr utilises the KEGG pathway database to identify molecular interactions, reactions and relation networks associated with the input gene list. The KEGG database includes an array of pathways including those associated with metabolism, genetic information processing, environmental information processing, cellular processes, organismal systems and human diseases (KEGG, 2021). To gain further insight into the changes in gene expression between the different sample groups, gene lists for all

differentially expressed genes, all genes with increased expression and all genes with decreased expression were put into Enrichr to generate KEGG pathway bar graphs. For this analysis cut offs of padj of ≤ 0.01 and Log2Fold change of ≥ 1 or ≤ -1 were applied.

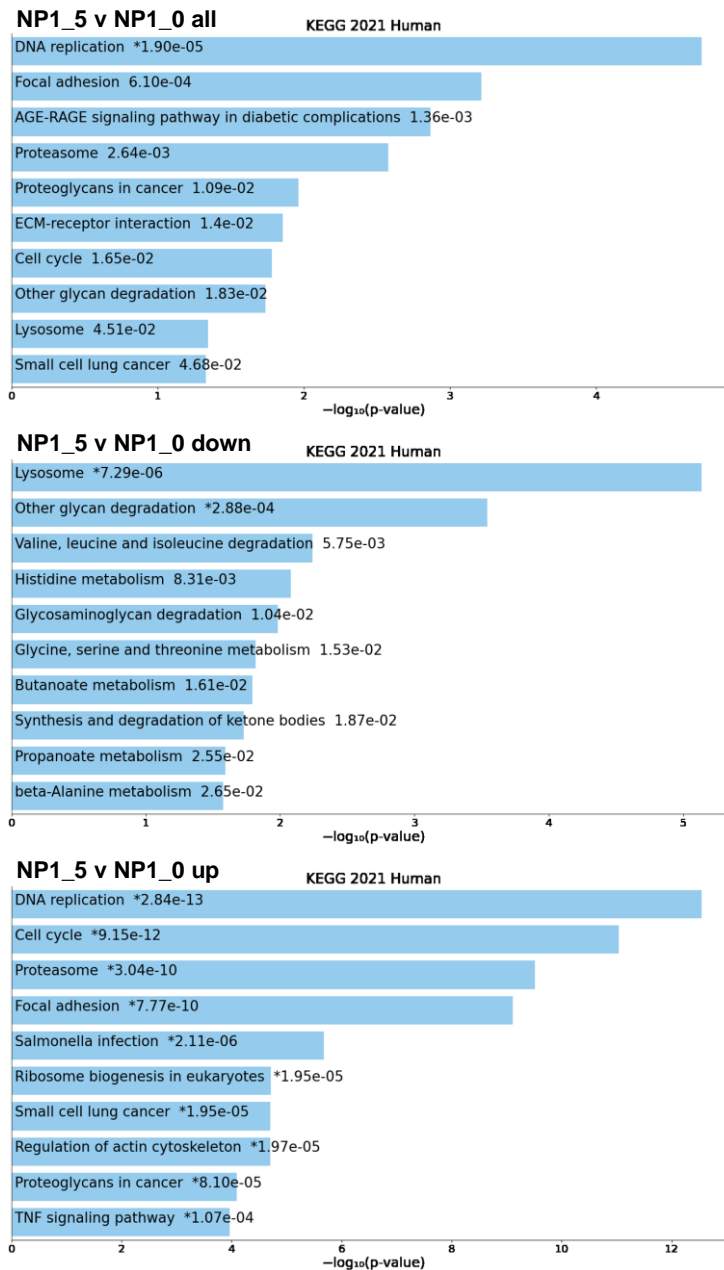


Figure 5.12 KEGG enrichment analysis of differentially expressed genes between NP1_5 and NP1_0

Enrichment analysis of differentially expressed genes between NP1_5 and NP1_0 using KEGG 2021 via Enrichr. Results displayed for all genes significantly differentially expressed (all), genes with increased expression (up) and genes with decreased expression (down) with cut offs for padj of ≤ 0.01 and Log2Fold change of ≥ 1 or ≤ -1 . The bar chart displays the top 10 enriched terms (ranked by p-value) within the KEGG 2021 library with corresponding p-value, calculated using Fisher's exact test. Blue bars indicate a p-value of < 0.05 and an asterisk indicates the term also has a significant adjusted p-value of < 0.05 .

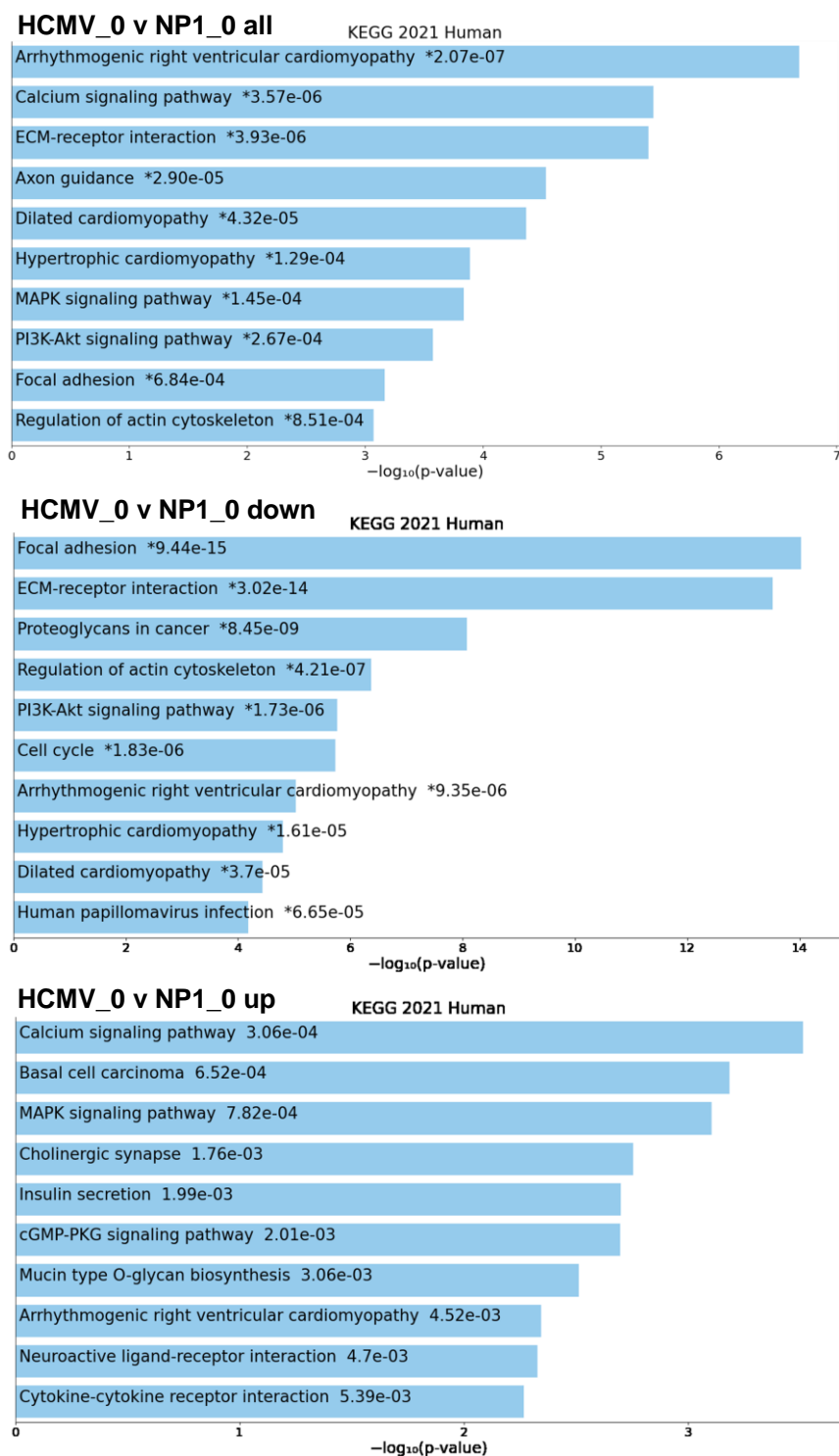


Figure 5.13 KEGG enrichment analysis of differentially expressed genes between HCMV_0 and NP1_0

Enrichment analysis of differentially expressed genes between HCMV_0 and NP1_0 using KEGG 2021 via Enrichr. Results displayed for all genes significantly differentially expressed (all), genes with increased expression (up) and genes with decreased expression (down) with cut offs for p_{adj} of ≤ 0.01 and $\text{Log}_2\text{Fold change}$ of ≥ 1 or ≤ -1 . The bar chart displays the top 10 enriched terms (ranked by p-value) within the KEGG 2021 library with corresponding p-value, calculated using Fisher's exact test. Blue bars indicate a p-value of < 0.05 and an asterisk indicates the term also has a significant adjusted p-value of < 0.05 .

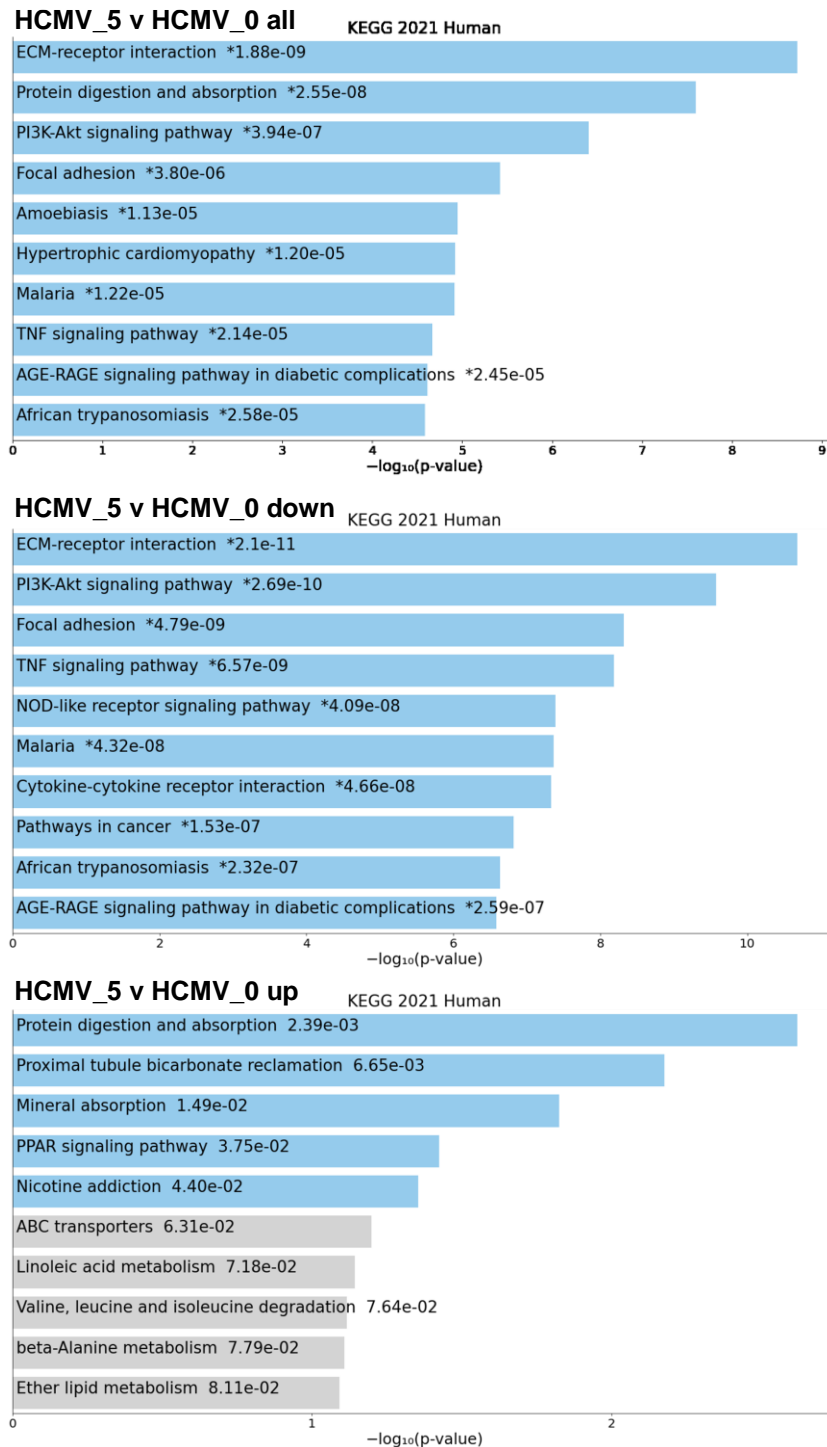


Figure 5.14 KEGG enrichment analysis of differentially expressed genes between HCMV_5 and HCMV_0

Enrichment analysis of differentially expressed genes between HCMV_5 and HCMV_0 using KEGG 2021 via Enrichr. Results displayed for all genes significantly differentially expressed (all), genes with increased expression (up) and genes with decreased expression (down) with cut offs for padj of ≤ 0.01 and Log2Fold change of ≥ 1 or ≤ -1 . The bar chart displays the top 10 enriched terms (ranked by p-value) within the KEGG 2021 library with corresponding p-value, calculated using Fisher's exact test. Blue bars indicate a p-value of < 0.05 and an asterisk indicates the term also has a significant adjusted p-value of < 0.05 .

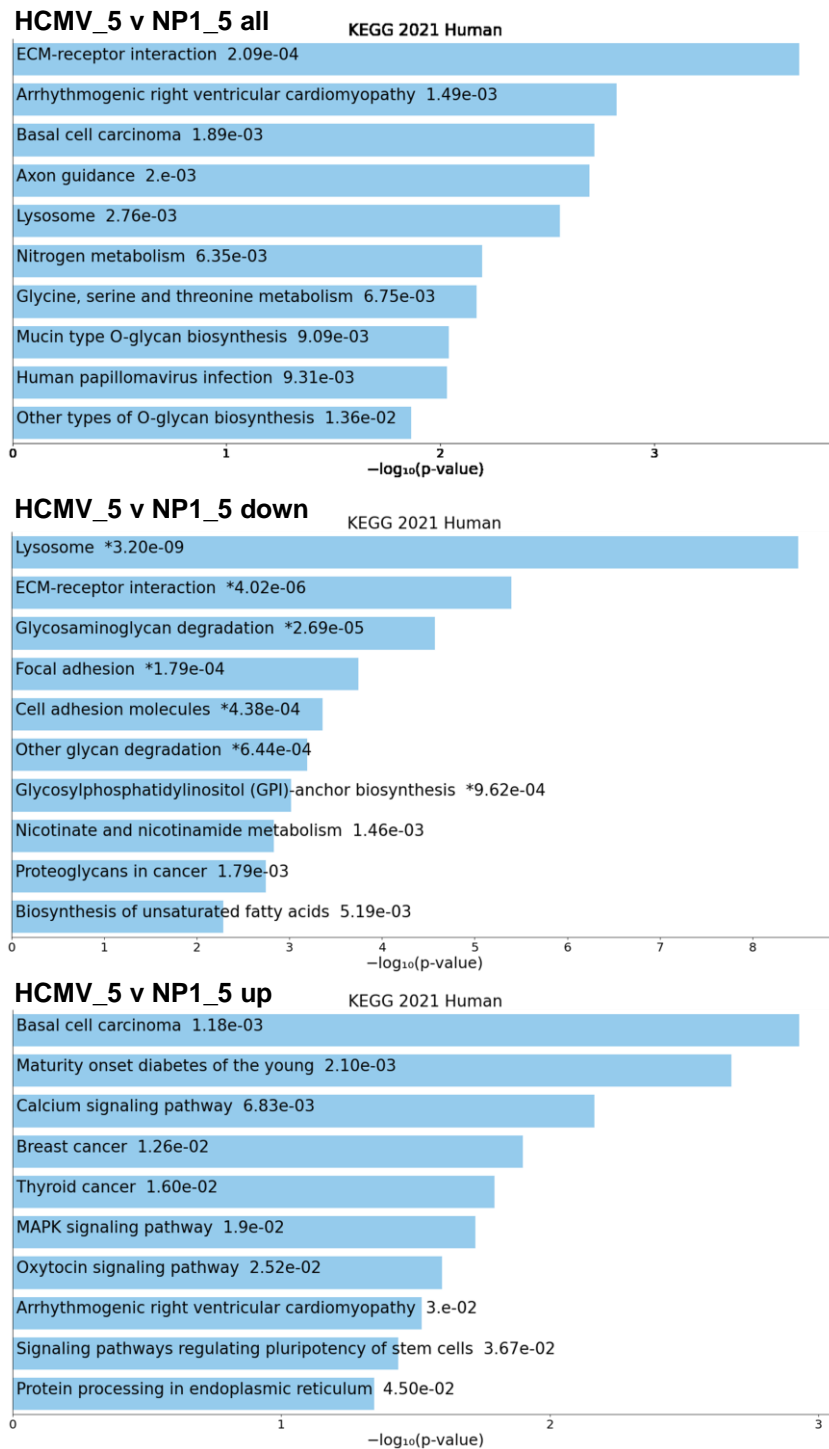


Figure 5.15 KEGG enrichment analysis of differentially expressed genes between HCMV_5 and NP1_5

Enrichment analysis of differentially expressed genes between HCMV_5 and NP1_5 using KEGG 2021 via Enrichr. Results displayed for all genes significantly differentially expressed (all), genes with increased expression (up) and genes with decreased expression (down) with cut offs for padj of ≤ 0.01 and Log2Fold change of ≥ 1 or ≤ -1 . The bar chart displays the top 10 enriched terms (ranked by p-value) within the KEGG 2021 library with corresponding p-value, calculated using Fisher's exact test. Blue bars indicate a p-value of < 0.05 and an asterisk indicates the term also has a significant adjusted p-value of < 0.05 .

| Differentially expressed Calcium signalling genes in HCMV_0 v NP1_0 | |
|---|---|
| Up | RET, RYR1, RYR2, CHRM3, CHRM1, FLT4, CHRM5, ATP2A3, ATP2A1, SLC8A2, EDNRB, FGF9, BDKRB2, CD38, CAMK1D, NGF, PLCB4, AGTR1, CASQ1, PLCB2, SLC25A4, CAMK2B, PDE1B, CHRNA7, PTAFR, CAMK2A, PDGFB, CACNA1B, ADRB1, MST1R, ADCY1, ADRB2, CACNA1C, ADCY8, CACNA1E, CACNA1H, CACNA1G, CACNA1I, ERBB3, HRH2, PTK2B, DRD1, NTSR1, DRD5, FGF21, NTRK1, NOS, GRIN2C, MCOLN1, GRIN2D, GRIN1, FGF17, P2RX7, GNAL, GDNF, FGF19, P2RX1, FGF18, FGFR4, FGFR2 |
| Down | PTGFR, MYLK2, PDE1C, EGF, NTRK3, VEGFC, ITPR2, PRKCA, TACR1, GRPR, FGF2, SLC8A1, MYLK, FGF5, HTR7, ASPH, ADORA2B, PDGFD, CAMK4, PDGFC, KDR, MET |

Figure 5.16 Differentially expressed calcium signalling genes in HCMV_0 v NP1_0

Differentially expressed genes between HCMV_0 and NP1_0 associated with calcium signalling, identified through KEGG enrichment using Enrichr. NP1_0 = untreated NP1. NP1_5 = NP1 differentiated over 5 days using Walton *et al.*, (2006) protocol. HCMV_0 = NP1 +HCMV infected at an MOI of 3 FFU/cell for 5 days, HCMV_5 = NP1 +HCMV infected at an MOI of 3 FFU/cell for 5 days and then differentiated over 5 days using Walton *et al.*, (2006) protocol. Differentially expressed genes with a Log2Fold change of >1 or <-1 and padj of <0.01 were included in this analysis.

| Differentially expressed PI3K-Akt genes in HCMV_0 v NP1_0 | |
|---|--|
| Up | CDKN1A, CSF3, CHRM1, LAMC3, FLT4, ITGA2B, PIK3CG, COMP, GHR, CCND2, CREB3L3, FGF9, CREB3L1, JAK3, IL6R, IL4R, VWF, PPP2R5B, NGF, EREG, CCNE1, COL4A4, EIF4E1B, DDIT4, IL3RA, SGK3, SGK1, SGK2, CREB5, TNXB, PRKAA2, LAMA1, LPAR1, PDGFB, LPAR2, PIK3R3, EFNA5, RELN, BCL2L11, ERBB3, GNG7, PCK2, FGF21, NTRK1, NGFR, BDNF, NOS3, EPOR, EFNA1, FGF17, NR4A1, EFNA3, EFNA2, LPAR5, PPP2R2C, FGF19, FGF18, ITGA11, IL2RB, COL9A3, FGFR4, PIK3AP1, FGFR2 |
| Down | ITGB1, CSF1, ITGB5, ITGB3, LAMA4, TNC, LAMC1, THBS2, FGF2, THBS1, IGF1R, FGF5, CCND1, PDGFD, PDGFC, KDR, SPP1, ITGB8, ITGAV, ITGA4, ANGPT1, LAMB3, ITGA3, EGF, ITGA2, FN1, VEGFC, PRKCA, LAMB1, RBL2, COL1A2, CDK6, COL4A2, PPP2R2B, COL6A2, COL6A1, GNB4, COL6A3, ITGA7, IL7R, MET |

Figure 5.17 Differentially expressed PI3K-Akt genes between HCMV_0 v NP1_0

Differentially expressed genes between HCMV_0 and NP1_0 associated with PI3K-Akt signalling, identified through KEGG enrichment using Enrichr. NP1_0 = untreated NP1. NP1_5 = NP1 differentiated over 5 days using Walton *et al.*, (2006) protocol. HCMV_0 = NP1 +HCMV infected at an MOI of 3 FFU/cell for 5 days, HCMV_5 = NP1 +HCMV infected at an MOI of 3 FFU/cell for 5 days and then differentiated over 5 days using Walton *et al.*, (2006) protocol. Differentially expressed genes with a Log2Fold change of >1 or <-1 and padj of <0.01 were included in this analysis.

| Differentially expressed axon guidance genes in HCMV_0 v NP1_0 |
|---|
| EPHB6, CAMK2B, SEMA3D, SRC, CAMK2A, SEMA3B, LRRC4, PIK3R3, SEMA3F, EFNA5, GNAI1, RND1, EFNB1, SHH, ABLIM1, ABLIM2, RRAS, PLXNA2, RAC2, EPHB1, NEO1, PLXNA4, WNT4, EPHA4, SEMA6C, SEMA4A, EPHA7, SEMA6A, UNC5A, EPHA8, UNC5B, SEMA6D, PTCH1, L1CAM, BMP7, GDF7, NFATC4, EFNA1, EFNA3, EFNA2, NGEF |
| SEMA5A, NTNG1, ITGB1, NRP1, WNT5B, RYK, WNT5A, LIMK1, PRKCA, UNC5C, PTPN11, ROBO1, EFNB2, CXCL12, RASA1, CFL1, PLXNA1, SLIT2, EPHB2, LRRC4C, MET, EPHA3 |
| Differentially expressed axon guidance genes in HCMV_5 v NP1_5 |
| EPHB6, CAMK2B, SEMA7A, SRC, PIK3CB, EFNA5, NTN1, MYL12A, RND1, SHH, PARD6B, RGS3, PPP3CC, RRAS, PLXNA2, RAC2, SLIT1, PAK6, EPHB1, HRAS, NEO1, WNT4, EPHA7, UNC5A, SEMA4D, UNC5B, SEMA6D, NFATC3, NFATC2, L1CAM, BMP7, EFNA1, ENAH, EFNA2, FES, NGEF, EPHA2 |
| SEMA5A, ITGB1, SEMA5B, NRP1, CAMK2D, SEMA3C, SEMA3A, LRRC4, NTN4, SEMA3G, PIK3CD, PIK3R1, ROBO1, GNAI2, EFNB2, EFNB3, DPYSL2, BOC, ABL1, SRGAP3, SLIT2, LRRC4C, PAK3, PLXNA4, EPHA5, SEMA6B, NTNG2, SEMA6A, LIMK1, SEMA4C, PRKCA, UNC5C, SEMA4F, RGMA, MYL5, CXCL12, SMO, PLXNB3, PLXNB1, BMPR1B, EPHA3 |

Figure 5.18 Differentially expressed axon guidance genes between HCMV_0 v NP1_0 and HCMV_5 v NP1_5

Differentially expressed genes between HCMV_0 and NP1_0 associated with axon guidance, identified through KEGG enrichment using Enrichr. NP1_0 = untreated NP1. NP1_5 = NP1 differentiated over 5 days using Walton et al., (2006) protocol. HCMV_0 = NP1 +HCMV infected at an MOI of 3 FFU/cell for 5 days, HCMV_5 = NP1 +HCMV infected at an MOI of 3 FFU/cell for 5 days and then differentiated over 5 days using Walton et al., (2006) protocol. Differentially expressed genes with a Log2Fold change of >1 or <-1 and padj of <0.01 were included in this analysis.

Enrichment analysis utilising KEGG 2021 highlighted a number of potentially important pathways that are dysregulated by HCMV infection of NP1. Axon guidance was identified in both HCMV_0 v NP1_0 and HCMV_5 v NP1_5 (figure 5.13 and 5.15). That this pathway is identified as being highly modulated by HCMV at both day 0 and day 5, makes it of particular interest. This change in the expression of 63/182 axon guidance genes at day 0 and 78/182 at day 5 suggests extensive dysregulation of this process and could potentially explain the reduction in the number and length of neurites between HCMV_5 and NP1_5 (figure 4.9). Figure 5.12 and 5.13 shows the differentially expressed genes HCMV_0 v NP1_0 and HCMV_5 v NP1_5 that are associated with axon guidance. Notably, SHH which encodes the morphogenetic sonic hedgehog protein (Shh), which is involved in both determining neuronal cell fate and also axon guidance was increased in HCMV_0 v NP1_0 and in HCMV_5 v NP1_5

(Charron *et al.*, 2003). Importantly, CD133+ GSCs have been shown to have increased Shh expression, and inhibition of Shh leads to decreased proliferation and reduction in spheroid formation (Hung *et al.*, 2020).

The MAPK pathway was in the top 10 terms returned for lists of genes with significantly increased expression for both HCMV_0 v NP1_0 (69/294 genes upregulated) and HCMV_5 v NP1_5 (64/294 genes upregulated) (Figures 5.13 and 5.15). Extracellular signal-regulated kinases (ERK)-MAPK is known to be activated by HCMV infection, mediated by HCMV gB, an interaction known to promote survival of latently HCMV infected cells (Boyle *et al.*, 1999, Reeves *et al.*, 2011). Hyperactivation of the MAPK signalling pathway is reported in GBM with over 80 % of GBM containing at least 1 mutation in the MAPK pathway (Krishna *et al.*, 2021). It would be interesting to determine if MAPK hyperactivation in GBM is associated with HCMV+ tumours.

The PI3K-Akt pathway is identified in the top 10 terms KEGG 21 from gene lists from HCMV_0 v NP1_0 (104/354 differentially expressed genes) and HCMV_5 v HCMV_0 (65/354 differentially expressed genes) suggesting that this pathway is dysregulated by HCMV (figure 5.14 and 5.15). The PI3K-Akt pathway is known to be modulated by HCMV, mediated through interaction with HCMV IE1 and IE2 (Yu and Alwine, 2002). Aberrant PI3K-Akt activation is reported in ~90 % of GBM's (Langhans *et al.*, 2017).

5.6 RNAseq co-expression analysis

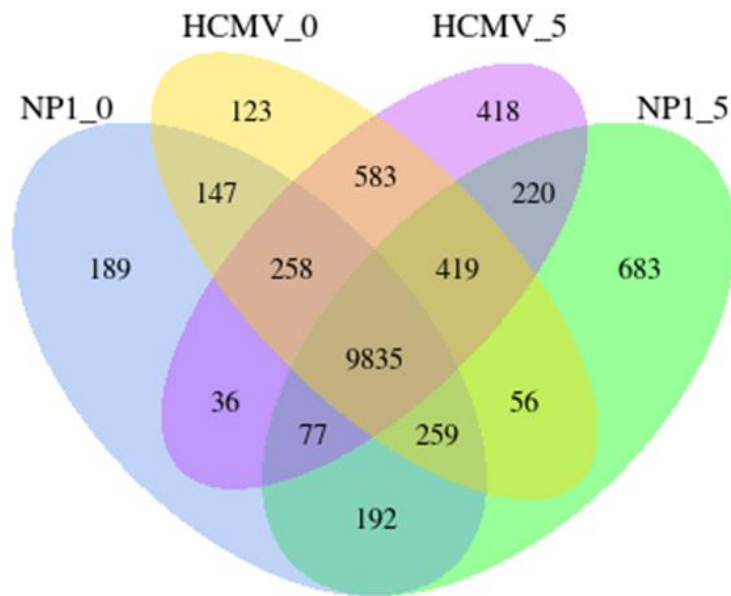


Figure 5.19 Venn diagram of RNAseq co-expression data

Venn diagram of co-expressed and specific genes for each sample group (NP1_0, NP1_5, HCMV_0 and HCMV_5), identified from RNAseq quantification of gene expression.

A Venn diagram of RNAseq co-expression was generated to identify genes that were uniquely expressed in each individual sample group (NP1_0, NP1_5, HCMV_0, HCMV_5) (Figure 5.19). To identify pathways associated with the gene lists generated from the Venn diagram, enrichment was performed using the Enrichr website to identify important pathways through the KEGG pathway database. Figure 5.19 shows 189 genes unique to NP1_0, 683 to NP1_5, 123 to HCMV_0 and 418 to HCMV_5. KEGG pathway bar charts associated with these gene sets are displayed in figure 5.20. Two particularly notable pathways identified in this analysis are the JAK-STAT signalling pathway and the MAPK pathway in HCMV_0. Four JAK-STAT genes were unique to HCMV_0, namely STAT5A and interleukins (IL) IL23A, IL24 and IL2RB, with 38/162 JAK-STAT genes differentially expressed between HCMV_0 and NP1_0. Five MAPK genes were unique to HCMV_0 calcium voltage-gated channel auxiliary subunit beta 1 (CACNB1), IL1A, IL1R1, FGF19 and MAP3K8, with 90/294 MAPK associated genes differentially expressed between HCMV_0 and NP1_0. Particularly notable is the increase in expression of FGF19, with a Log2Fold change of 8.4 between HCMV_0 and NP1_0. There is increasing evidence that FGF19 can increase proliferation and is known to play a role in tumorigenesis of cancers including hepatocellular carcinoma and colorectal cancer and is thus classified as an oncogene (Wu *et al.*, 2010, Wang *et al.*, 2019).

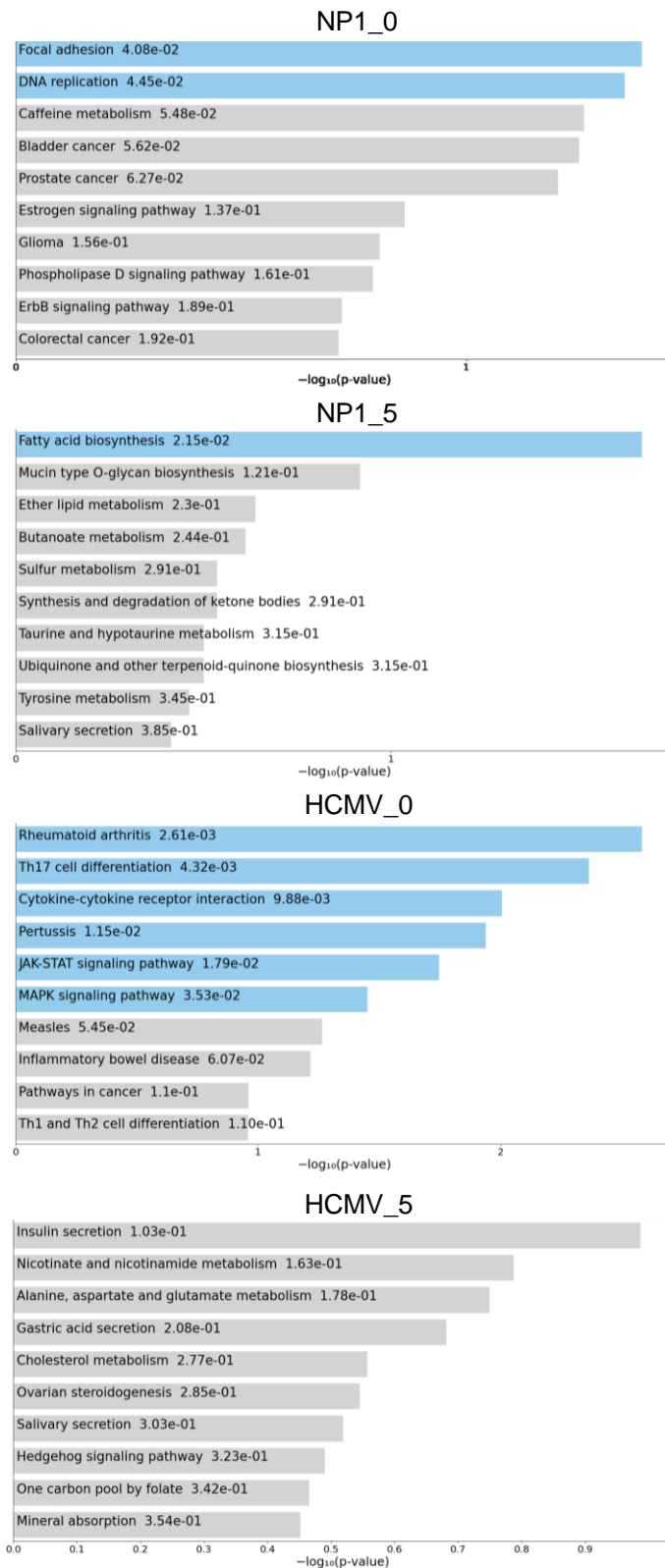


Figure 5.20 KEGG enrichment analysis of genes exclusive to NP1_0, NP1_5, HCMV_0 and HCMV_5

Lists of genes unique to NP1_0, NP1_5, HCMV_0 and HCMV_5 were enriched using Enrichr. The bar chart displays the top 10 enriched terms (ranked by p-value) within the KEGG 2021 library with corresponding p-value, calculated using Fisher's exact test. Blue bars indicate a p-value of <0.05 and an asterisk indicates the term also has a significant adjusted p-value of <0.05.

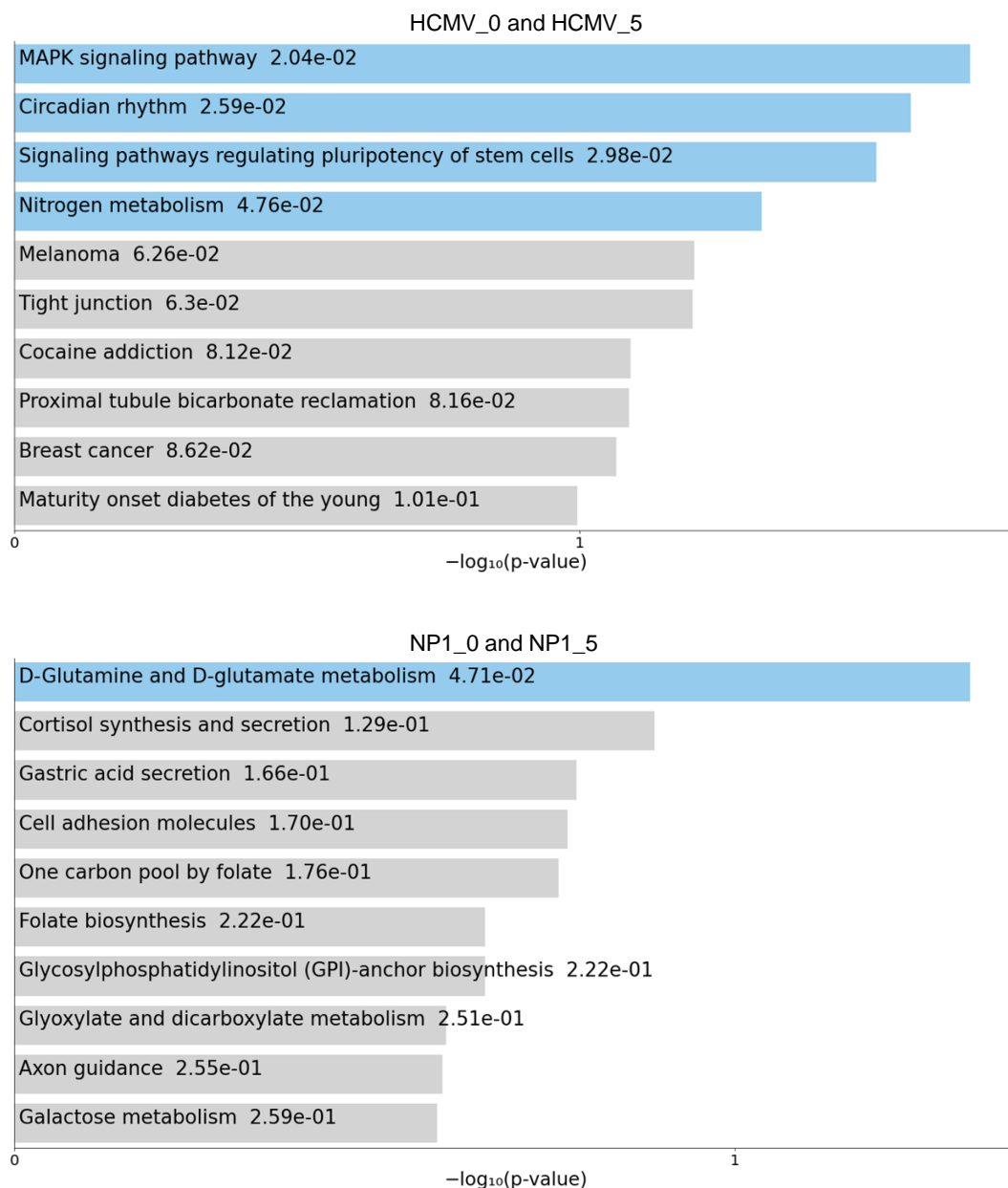


Figure 5.21 KEGG enrichment analysis of genes exclusively co-expressed in HCMV_0 and HCMV_5 and genes exclusively co-expressed in NP1_0 and NP1_5

Lists of genes exclusively co-expressed in HCMV_0 & HCMV_5 and NP1_0 & NP1_5 were enriched using Enrichr. The bar chart displays the top 10 enriched terms (ranked by p-value) within the KEGG 2021 library with corresponding p-value, calculated using Fisher's exact test. Blue bars indicate a p-value of <0.05 and an asterisk indicates the term also has a significant adjusted p-value of <0.05.

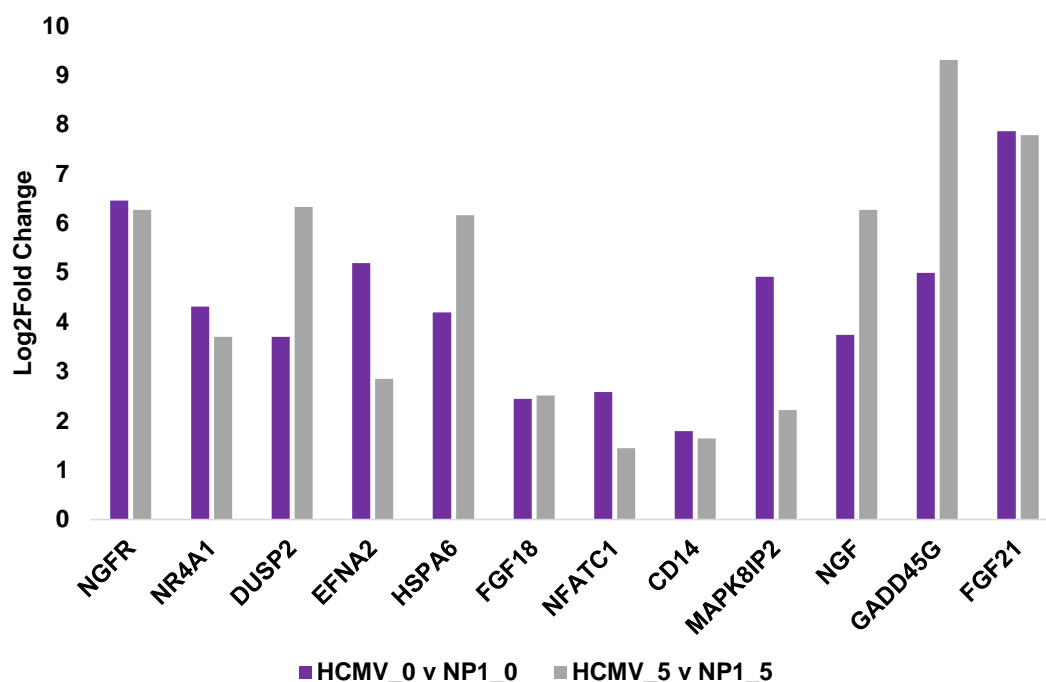


Figure 5.22 Expression of MAPK signalling pathway genes identified as expressed in HCMV_0 and HCMV_5, but not in NP1_0 or NP1_5

A list of genes identified as significantly expressed in HCMV_0 and HCMV_5, but not in NP1_0 or NP1_5 was enriched using Enrichr to identify associated KEGG terms. Genes associated with the MAPK signalling pathway as identified by KEGG enrichment plotted as Log2Fold change for HCMV_0 v NP1_0 and HCMV_5 and NP1_5.

The Venn diagram (figure 5.19) was also used to identify genes that were co-expressed in both control groups, NP1_0 and NP1_5, but not in infected HCMV_0 and HCMV_5 and vice versa. KEGG enrichment was again performed via Enrichr and the results displayed in figure 5.20. For genes co-expressed in NP1_0 and NP1_5, but not in HCMV_0 or HCMV_5, KEGG enrichment highlighted genes involved in D-glutamine and D-glutamate metabolism. This could indicate that HCMV+ NP1 are less astrocytic than non-infected controls as many of the markers for astrocytes are those involved in glutamine and glutamate metabolism (Anlauf and Enrouiche, 2013).

Interestingly, the most significant KEGG term in genes co-expressed in HCMV_0 and HCMV_5 was MAPK signalling pathway. 12 MAPK associated genes were identified as being expressed in HCMV_0 and HCMV_5, but not in NP1_0 and NP1_5 (Figure 5.22). Analysis of all differential expressed genes associated with the MAPK associated genes showed that between HCMV_0 and NP1_0 69/294 MAPK genes were upregulated and 21/294 were downregulated and between HCMV_5 and NP1_5 64/294 were upregulated and 37/294 were downregulated.

This is further evidence of MAPK dysregulation in NP1 due to HCMV infection. Notably, both nerve growth factor (NGF) and NGF receptor (NGFR) are significantly upregulated in HCMV_0 v NP1_0 and HCMV_5 v NP1_5. NGF is known to stimulate GBM proliferation through dysregulation of notch1 signalling (Park *et al.*, 2018). NGFR is highly expressed in GBM and has been shown to be oncogenic through inhibition of p53 (Zhou *et al.*, 2016). The simultaneous upregulation of NGF and its receptor could indicate an autocrine loop. NGF is also known to activate the PI3K-Akt pathway, which was identified as a significant pathway in HCMV_0 v NP1_0 by KEGG enrichment analysis (figure 5.13)(Chen *et al.*, 2008). Nuclear factor of activated T cells 1 (NFATC1) is exclusively expressed in HCMV+ NP1 and has been shown to promote invasion in GBM cells through induction of COX-2 (Wang *et al.*, 2015). Interestingly, PTSG2, which encodes COX-2 showed a log2fold change of 8.8 in HCMV_0 v NP1_0 and 5.7 in HCMV_5 v NP1_0. COX-2 expression is frequently elevated in GBM, correlates directly with tumour grade and is associated with shorter survival in GBM patients (Joki *et al.*, 2000). COX-2 has been implicated in tumorigenesis, proliferation, apoptosis, invasion, angiogenesis, and immunosuppression in GBM (Prayson *et al.*, 2002, Jiang and Dingledine, 2013, Hara and Okoyasu, 2004).

The third most significant KEGG term associated with co-expressed genes exclusive to HCMV_0 and HCMV_5 was signalling pathways regulating pluripotency of stem cells. The log2fold change in expression of the seven genes associated with pluripotency are shown in figure 5.23. Six out of the seven genes were not significantly differentially expressed during differentiation of HCMV infected NP1 (HCMV_5 v HCMV_0) (Miyamoto *et al.*, 2015). INHBE was the only gene of these seven to show a decrease in expression between HCMV_0 and HCMV_5 with a log2fold change of -1.1. Identification of these genes associated with the KEGG term “signalling pathways regulating pluripotency of stem cells” that were uniquely expressed by HCMV infected NP1 prompted analysis of the other differentially expressed genes associated with this term. HCMV infection of NP1 (HCMV_0 v NP1_0), resulted in differential expression of 33/143 genes, 27 of which had increased expression and only six with decreased expression in HCMV_0 v NP1_0, which indicates that pluripotency regulation is significantly disrupted by HCMV infection in NP1 (figure 5.24).

Krüppel-Like Factor 4 (KLF4) is a transcription factor that acts as an oncogene in GBM and is a key stemness marker in GSC's (Ray, 2016). KLF4 expression was dramatically increased during HCMV infection with a log2fold change of 4.8 in HCMV v NP1_0 and 5.1 in HCMV_5 v NP1_5. Two other pluripotency associated genes, OLIG2 and POU5F1, both known to be associated with GBM

and GSC's also showed increased expression in HCMV infected NP1 (Ashizawa *et al.*, 2013). OLIG2, a transcription factor ubiquitously expressed in GBM, which is thought to contribute to gliomagenesis and the phenotypic plasticity exhibited by GSC's showed a log2fold change of 7.2 in HCMV_0 v NP1_0 and 7.3 in HCMV_5 v NP1_5 (Lu *et al.*, 2001, Lu *et al.*, 2016). POU5F1, which encodes Oct4, a transcription factor that regulates self-renewal and survival and plays a key role in tumour initiation, had a log2fold change of 3.5 in HCMV_5 v NP1_5, despite not being differentially expressed in HCMV_0 v NP1_0 (Du *et al.*, 2009, Wang and Herlyn, 2015).

Jumonji And AT-Rich Interaction Domain Containing 2 (JARID2), a component of the polycomb repressive complex 2 (PRC2) expression is increased by a log2fold change of 1.1 in HCMV_0 v NP1_0. JARID2 expression has been shown to be implicated in GBM plasticity, particularly with resistance to treatment and recurrence, therefore this may be a key factor in HCMV reprogramming of NP1 (Rippaus *et al.*, 2019). Other pluripotency genes known to be expressed by GBM, namely, EGFR and NES, were expressed in all four sample groups, but did not show differential expression (Ashiwaza *et al.*, 2013). This extensive dysregulation of pluripotency associated genes by HCMV may be important in the context of GBM and particularly GSC's.

One of the key oncogenic effects of HCMV reported in HMECs is maintained by increased TERT expression (Kumar *et al.*, 2018). To examine whether TERT expression is increased in HCMV infection of NP1, the log2fold change of the TERT gene was analysed and is summarised in figure 5.25. In non-infected NP1 TERT expression decreases with differentiation, with a log2fold change of -1.47. Prior to differentiation, HCMV_0 v NP1_0 showed a log2fold increase of 0.78, by day five of differentiation, a log2fold increase of 2.65 was seen in HCMV_5 v NP1_5, with HCMV_5 v NP1_0 showing a log2fold increase of 1.21.

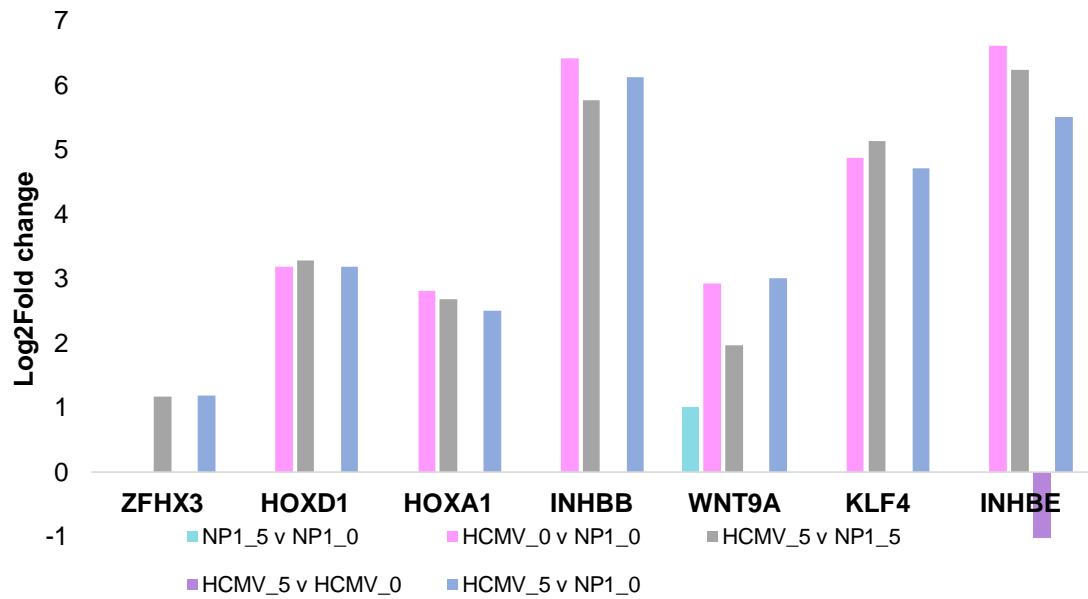


Figure 5.23 Expression of genes associated with signalling pathways regulating pluripotency of stem cells, co-expressed in HCMV_0 and HCMV_5, but not in NP1_0 or NP1_5

A list of genes identified as significantly expressed in HCMV_0 and HCMV_5, but not in NP1_0 or NP1_5 was enriched using Enrichr to identify associated KEGG terms. Genes associated with the MAPK signalling pathway as identified by KEGG enrichment plotted as Log2Fold change for HCMV_0 v NP1_0, HCMV_5 and NP1_5 and HCMV_5 v HCMV_0. NP1_0 = untreated NP1. NP1_5 = NP1 differentiated over 5 days using Walton *et al.*, (2006) protocol. HCMV_0 = NP1 +HCMV infected at an MOI of 3 FFU/cell for 5 days, HCMV_5 = NP1 +HCMV infected at an MOI of 3 FFU/cell for 5 days and then differentiated over 5 days using Walton *et al.*, (2006) protocol. Differentially expressed genes with a Log2Fold change of >1 or <-1 and padj of <0.01 were included in this analysis.

| HCMV_0 v NP1_0 | |
|------------------------|---|
| Up | WNT2B, HOXD1, ONECUT1, PIK3R3, WNT6, ACVR1C, WNT11, ZIC3, HOXA1, OTX1, JARID2, JAK3, WNT4, WNT10B, WNT10A, WNT7B, WNT7A, INHBB, AXIN2, WNT9A, KLF4, DUSP9, ACVR2A, INHBE, HAND1, FGFR4, FGFR2 |
| Down | SOX2, WNT5B, WNT5A, ID1, FGF2, IGF1R |
| HCMV_5 v NP1_5 | |
| Up | HOXD1, TCF7, ONECUT1, PIK3CB, WNT6, ACVR1C, WNT11, ZIC3, PCGF1, HOXA1, OTX1, HRAS, JAK3, WNT4, WNT10B, WNT10A, ZFH3, FZD5, WNT7B, AXIN1, WNT7A, LIFR, INHBB, WNT9A, WNT16, KLF4, ISL1, POU5F1, INHBE, MAPK11, HAND1, FGFR4, FGFR3 |
| Down | FZD1, SMAD2, FZD2, WNT2B, DLX5, FZD4, FZD6, FZD8, PIK3CD, PIK3R1, AXIN2, FGF2, ACVR2A, IGF1R, SOX2, MEIS1, AKT2, ID1, ID4, ID3, CTNNB1, BMPR1B, BMPR1A |
| HCMV_5 v HCMV_0 | |
| Up | FGFR3, FGFR2, WNT4 |
| Down | SOX2, FZD1, FZD2, WNT5B, DLX5, WNT5A, FZD6, ID1, LIF, ID3, FGF2, INHBE |
| NP1_5 v NP1_0 | |
| Up | FZD1, SMAD2, APC2, WNT2B, PIK3R3, WNT8B, PIK3R1, AXIN2, WNT9A, ACVR2A, MAPK13, SOX2, MEIS1, WNT11, ZIC3, CTNNB1, BMPR1B, FGFR4, FGFR2, FGFR1 |
| Down | ACVR1, PCGF6, SMAD3, WNT5B, FZD5, WNT7B, WNT5A, TCF7, LIF, WNT7A, LIFR, WNT16, POU5F1, TBX3, MYC, DVL1, ID1, IL6ST, SKIL, HRAS, WNT3 |

Figure 5.24 Expression of differentially expressed genes associated with signalling pathways regulating pluripotency of stem cells.

Table of differentially expressed genes associated with signalling pathways regulating pluripotency of stem cells in HCMV_0 v NP1_0, HCMV_5 v NP1_0, HCMV_5 v HCMV_0 and NP1_5 v NP1_0. NP1_0 = untreated NP1. NP1_5 = NP1 differentiated over 5 days using Walton *et al.*, (2006) protocol. HCMV_0 = NP1 +HCMV infected at an MOI of 3 FFU/cell for 5 days, HCMV_5 = NP1 +HCMV infected at an MOI of 3 FFU/cell for 5 days and then differentiated over 5 days using Walton *et al.*, (2006) protocol. Differentially expressed genes with a Log2Fold change of >1 or <-1 and padj of <0.01 were included in this analysis.

| | Log2fold change | padj |
|-----------------------|------------------------|-------------|
| NP1_5 v NP1_0 | -1.47 | 1.40E-03 |
| HCMV_0 v NP1_0 | 0.78 | 1.31E-02 |
| HCMV_5 v NP1_5 | 2.65 | 9.32E-14 |
| HCMV_5 v NP1_0 | 1.21 | 1.65E-04 |

Figure 5.25 Differential expression of TERT

Differential expression of TERT from RNAseq analysis expressed as log2fold change with corresponding padj values for all comparisons with differential expression.

5.7 Effects of differentiation on viral gene expression

RNAseq reads were also mapped to the merlin genome assembly AY446894 to analyse HCMV gene expression during NP1 infection and subsequent differentiation. No HCMV gene expression was detected in NP1_0 or NP1_5, confirming that NP1 do not harbour endogenous HCMV infection. RNAseq analysis detected expression of 168 HCMV genes during infection of NP1 (figure

5.26 and 5.27), with 121 viral genes significantly differentially expressed between HCMV_5 v HCMV_0, all of which showed increased expression (figure 5.28). Cut offs for significantly differentially expressed viral genes were padj of ≤ 0.01 and log2fold change of ≥ 1 or ≤ -1 . All genes with significant differential expression were increased between HCMV_5 v HCMV_0. This pan-increase in viral gene expression during differentiation is likely at least partly responsible for the dramatic increase in viral titre detected in HCMV+ NP1 supernatants throughout differentiation, though it is still unclear what is responsible for the switch from non-productive to productive infection when NP1 are differentiated (figure 4.13).

The most highly expressed HCMV transcript in HCMV_0 and second in HCMV_5 was RNA 2.7, which is known to be the most highly expressed HCMV transcript during lytic infection and is antiapoptotic (Gatherer *et al.*, 2011). Another of the most highly expressed HCMV genes in both HCMV_0 and HCMV_5 was RNA 4.9. HCMV RNA 4.9 is a long non-coding RNA that is involved in regulating viral DNA replication (Tai-Schmiedel *et al.*, 2020). Interestingly, HCMV RNA 4.9 has been detected in triple negative breast cancer (Banerjee *et al.*, 2015). Rosetto *et al.* (2013), showed that during latency RNA 4.9 interacts with the HCMV MIEP region, resulting in an increase of the repressive mark H3K27me3. Both RNA 2.7 and RNA 4.9 are detected during natural and experimental latency of CD14+ monocytes or CD34+ progenitor cells (Rosetto *et al.*, 2013).

UL22A was the most abundantly expressed HCMV gene in HCMV_5 and the second most abundant in HCMV_0. UL122A encodes miR-UI22A, which is known to interact with target genes for interferon 18 receptor precursor, histone 3 and BMP4 (Meshesha *et al.*, 2012, Lisboa *et al.*, 2015). MiR-122A has also been shown to downregulate SMAD3 which leads to the reactivation of latent HCMV in CD34+ haematopoietic progenitor cells (Hancock *et al.*, 2020).

The third and fourth most abundantly expressed transcripts in both HCMV_0 and HCMV_5 were UL4 and UL5, both members of the RL11 gene family of which little is known about their function. UL4 encodes three transcripts, two of which display early kinetics and one late. UL4 is known to encode a 48 kDa virion glycoprotein (Chang *et al.*, 1989). UL5 encoded protein pUL5 is expressed in the early phase of HCMV infection and despite localising to the viral AC is not incorporated into the virion. Additionally UL5 has been shown to interact with the cellular scaffold protein, IQ Motif Containing GTPase Activating Protein 1 (IQGAP1) (Anselmi *et al.*, 2020).

In differential expression analysis of viral genes between HCMV_5 and HCMV_0 the gene with the largest increase in expression was UL146, which encodes the protein vCXCL1, which has sequence similarity to CXC chemokines. VCXCL1

is known to increase expression of PD-L1 through the activation of STAT3 signalling and promote immune evasion (Hu *et al.*, 2020). Whilst CD274, the gene encoding programmed death-ligand 1 (PD-L1) showed a log2fold change of -0.67 in HCMV_0 v NP1_0, at day 5 of differentiation HCMV_5 v NP1_5 showed an increased expression with a log2fold change of 0.82. PD-L1 expression is known to be increased in GBM compared to lower grade gliomas and is associated with immunosuppression in the tumour microenvironment (Zhang *et al.*, 2017).

The second and third most upregulated viral genes between HCMV_5 v HCMV_0, were UL11 and UL10 respectively, which are also known to exert immunosuppressive activity. UL11 protein has been shown to interact with the receptor tyrosine phosphatase CD45, which results in disruption to T-cell function (Gabaev *et al.*, 2011). UL11 has also been linked with increased levels of the anti-inflammatory cytokine IL-10, which is known to be overexpressed in GBM and is associated with increased proliferation and motility, promoting invasion and tumour progression (Zhang *et al.*, 2019). UL10 encodes a protein that is known to be dispensable for viral replication, but is known to modulate the host immune response through interaction with receptors ubiquitously expressed on the cell surface of leukocytes (Bruno *et al.*, 2016).

| Gene | FPKM (average) | Gene | FPKM (average) | Gene | FPKM (average) |
|--------|----------------|--------|----------------|--------|----------------|
| RNA2.7 | 64299.12 | UL49 | 1044.09 | UL52 | 523.95 |
| UL22A | 37193.72 | RL11 | 1033.28 | UL87 | 521.52 |
| UL4 | 7047.17 | US13 | 1027.92 | UL45 | 519.33 |
| UL5 | 6537.51 | UL2 | 1027.10 | UL29 | 513.76 |
| UL40 | 5943.71 | UL32 | 1025.36 | UL14 | 508.52 |
| RNA4.9 | 5845.93 | UL135 | 1006.05 | UL77 | 503.34 |
| UL41A | 4723.07 | UL148C | 996.57 | UL20 | 493.29 |
| UL82 | 4438.53 | UL54 | 965.14 | UL70 | 490.95 |
| UL30A | 3940.11 | UL50 | 947.78 | US29 | 465.75 |
| UL83 | 3913.32 | US20 | 924.57 | UL86 | 445.31 |
| UL132 | 3531.33 | US32 | 921.75 | UL95 | 445.20 |
| UL145 | 3484.79 | UL13 | 888.57 | UL124 | 443.19 |
| UL148 | 3457.34 | UL53 | 873.89 | UL120 | 436.81 |
| UL141 | 3281.86 | UL55 | 862.78 | UL48 | 433.98 |
| UL42 | 2992.37 | UL75 | 816.26 | US27 | 429.11 |
| RL5A | 2759.14 | UL102 | 808.91 | US16 | 425.50 |
| UL144 | 2620.79 | US33A | 802.81 | UL130 | 418.24 |
| UL99 | 2436.16 | UL147 | 793.49 | UL6 | 407.81 |
| UL43 | 2387.65 | UL51 | 789.41 | UL27 | 407.64 |
| UL73 | 2257.97 | UL114 | 787.51 | UL74 | 404.63 |
| RL13 | 2221.43 | US31 | 785.52 | UL19 | 398.10 |
| UL44 | 2101.51 | UL38 | 779.87 | US24 | 388.15 |
| UL17 | 2101.11 | UL148A | 769.86 | UL103 | 383.30 |
| US18 | 2088.10 | UL24 | 750.94 | UL79 | 383.08 |
| UL138 | 2070.54 | UL148B | 738.40 | UL80 | 373.84 |
| UL111A | 2003.38 | UL133 | 738.16 | UL15A | 368.52 |
| UL139 | 2000.22 | US9 | 727.58 | UL76 | 367.24 |
| UL84 | 1959.54 | UL21A | 727.05 | US17 | 342.05 |
| UL30 | 1913.06 | UL89 | 707.94 | UL146 | 337.20 |
| UL140 | 1800.04 | UL16 | 677.94 | UL37 | 333.86 |
| UL115 | 1777.57 | RL10 | 658.01 | IRS1 | 321.19 |
| RL12 | 1767.64 | US15 | 656.79 | UL46 | 315.10 |
| UL147A | 1697.61 | UL97 | 650.35 | UL104 | 314.36 |
| UL100 | 1666.74 | UL93 | 649.54 | US23 | 311.22 |
| UL25 | 1634.16 | UL122 | 645.61 | UL123 | 310.59 |
| UL48A | 1584.05 | UL88 | 633.63 | TRS1 | 286.48 |
| UL78 | 1569.16 | US28 | 633.36 | RL1 | 277.81 |
| UL74A | 1553.82 | UL23 | 628.15 | UL10 | 259.78 |
| UL31 | 1531.43 | UL33 | 622.21 | US10 | 253.72 |
| UL136 | 1504.64 | UL96 | 601.26 | UL1 | 242.41 |
| UL112 | 1500.22 | US14 | 591.14 | US2 | 236.43 |
| US3 | 1462.93 | RNA5.0 | 586.28 | US11 | 228.72 |
| UL148D | 1398.01 | US34 | 576.25 | UL105 | 225.51 |
| UL116 | 1397.94 | UL35 | 564.46 | UL150 | 224.87 |
| UL34 | 1383.52 | UL91 | 563.36 | US26 | 224.52 |
| UL119 | 1350.16 | US30 | 556.15 | US21 | 223.48 |
| US12 | 1276.86 | US8 | 550.07 | UL131A | 221.48 |
| US1 | 1238.08 | UL71 | 547.01 | RL6 | 220.91 |
| UL94 | 1176.49 | US34A | 542.91 | UL121 | 217.79 |
| UL85 | 1173.63 | UL92 | 542.68 | UL47 | 202.19 |
| UL72 | 1169.04 | UL142 | 541.61 | UL57 | 201.46 |
| UL69 | 1164.08 | US6 | 541.36 | US7 | 182.01 |
| US19 | 1143.34 | UL56 | 539.20 | UL18 | 154.15 |
| UL117 | 1142.78 | UL11 | 531.53 | UL9 | 116.81 |
| UL98 | 1122.77 | US22 | 531.37 | RL9A | 100.18 |
| UL36 | 1062.75 | UL26 | 530.02 | UL8 | 64.70 |

Figure 5.26 Average FPKM of all HCMV genes in HCMV_0

Average RNA-seq FPKM values for HCMV genes in all three samples of group HCMV_0

| Gene | FPKM (average) | Gene | FPKM (average) | Gene | FPKM (average) |
|--------|----------------|--------|----------------|--------|----------------|
| UL22A | 84060.38 | RL11 | 2459.04 | UL95 | 1161.44 |
| RNA2.7 | 82535.59 | UL135 | 2361.91 | UL33 | 1138.27 |
| UL4 | 14188.03 | UL13 | 2359.43 | US27 | 1134.46 |
| UL5 | 12896.35 | US32 | 2261.09 | UL35 | 1117.24 |
| UL82 | 12267.72 | UL32 | 2259.37 | UL56 | 1093.35 |
| UL40 | 12239.31 | UL54 | 2186.20 | UL48 | 1074.52 |
| UL83 | 10890.30 | US19 | 2131.54 | UL21A | 1072.78 |
| UL30A | 10057.83 | US13 | 2128.06 | UL74 | 1067.05 |
| UL41A | 10053.43 | UL55 | 2120.27 | UL130 | 1037.52 |
| RNA4.9 | 7629.61 | US31 | 2082.59 | UL103 | 1032.72 |
| UL99 | 7308.17 | UL11 | 2080.22 | UL124 | 1016.34 |
| UL132 | 6722.91 | UL53 | 2064.64 | UL36 | 996.92 |
| UL42 | 6496.61 | UL49 | 2053.67 | UL10 | 993.88 |
| UL148 | 6391.47 | UL75 | 1993.18 | UL46 | 972.53 |
| UL145 | 5562.18 | UL89 | 1932.73 | US16 | 961.82 |
| UL138 | 5516.75 | UL148A | 1897.42 | US9 | 946.37 |
| UL73 | 5463.95 | UL114 | 1878.88 | UL76 | 898.76 |
| UL43 | 5408.18 | UL50 | 1871.90 | UL6 | 862.24 |
| RL13 | 5190.90 | UL133 | 1845.79 | US17 | 852.66 |
| UL111A | 5032.31 | UL88 | 1829.20 | UL104 | 840.59 |
| UL84 | 4924.04 | UL148B | 1823.37 | US6 | 839.95 |
| UL144 | 4882.83 | RL10 | 1762.15 | UL29 | 833.82 |
| UL44 | 4663.86 | UL51 | 1724.75 | UL19 | 822.77 |
| UL115 | 4600.88 | UL24 | 1714.70 | UL15A | 821.20 |
| UL30 | 4597.04 | UL122 | 1702.27 | UL1 | 819.37 |
| UL100 | 4456.01 | US20 | 1686.53 | RL1 | 813.43 |
| UL141 | 4354.08 | UL93 | 1665.07 | UL80 | 803.33 |
| UL147A | 4032.76 | US33A | 1664.40 | UL79 | 788.02 |
| UL78 | 3964.96 | UL97 | 1653.19 | UL20 | 774.03 |
| UL74A | 3961.46 | US28 | 1625.61 | US22 | 764.86 |
| UL136 | 3842.34 | UL102 | 1547.02 | TRS1 | 748.70 |
| RL5A | 3807.70 | US30 | 1544.09 | UL27 | 722.82 |
| UL148D | 3801.46 | UL146 | 1541.20 | IRS1 | 672.80 |
| UL25 | 3780.27 | UL96 | 1536.51 | UL37 | 669.22 |
| RL12 | 3775.21 | UL91 | 1528.23 | US24 | 646.11 |
| UL48A | 3581.97 | RNA5.0 | 1514.80 | US8 | 638.73 |
| UL17 | 3567.28 | UL87 | 1485.40 | UL150 | 604.77 |
| US18 | 3510.36 | UL45 | 1433.03 | UL105 | 584.39 |
| UL116 | 3480.60 | UL92 | 1426.35 | US21 | 583.15 |
| UL69 | 3471.42 | US15 | 1399.82 | UL121 | 566.59 |
| UL119 | 3409.18 | UL38 | 1386.57 | UL131A | 545.73 |
| UL139 | 3383.05 | UL71 | 1332.62 | UL47 | 522.51 |
| UL34 | 3332.55 | UL16 | 1310.53 | US26 | 517.68 |
| UL98 | 3209.06 | US29 | 1291.57 | US23 | 497.31 |
| UL31 | 3192.60 | UL70 | 1274.38 | US2 | 452.24 |
| UL140 | 3191.98 | US14 | 1267.15 | UL9 | 429.60 |
| UL94 | 3085.19 | UL26 | 1263.13 | UL123 | 407.14 |
| UL72 | 3075.67 | US34A | 1245.11 | US10 | 405.72 |
| UL2 | 3027.34 | UL23 | 1238.66 | UL142 | 400.15 |
| UL85 | 2975.61 | UL52 | 1238.55 | RL6 | 389.56 |
| UL112 | 2839.83 | UL77 | 1236.77 | US7 | 350.02 |
| UL117 | 2782.50 | UL14 | 1227.97 | US11 | 337.47 |
| US12 | 2597.69 | US34 | 1198.71 | UL57 | 316.96 |
| UL147 | 2594.21 | US3 | 1195.41 | UL18 | 287.20 |
| UL148C | 2499.41 | UL86 | 1192.45 | RL9A | 249.73 |
| US1 | 2483.78 | UL120 | 1185.79 | UL8 | 215.59 |

Figure 5.27 Average FPKM of all HCMV genes in HCMV_5

Average FPKM values for HCMV genes in all three samples of group HCMV_0

| Gene | Log2Fold | Gene | Log2Fold | Gene | Log2Fold | Gene | Log2Fold |
|--------|----------|--------|----------|--------|----------|-------|----------|
| UL146 | 2.18 | UL13 | 1.40 | US17 | 1.31 | UL24 | 1.18 |
| UL11 | 1.96 | US31 | 1.40 | RL9A | 1.31 | UL54 | 1.17 |
| UL10 | 1.93 | US27 | 1.40 | UL116 | 1.31 | UL43 | 1.17 |
| UL9 | 1.87 | UL74 | 1.39 | UL130 | 1.30 | UL48A | 1.17 |
| UL1 | 1.75 | UL122 | 1.39 | UL48 | 1.30 | UL22A | 1.17 |
| UL8 | 1.73 | UL72 | 1.39 | UL148B | 1.30 | US16 | 1.17 |
| UL147 | 1.70 | UL92 | 1.39 | UL148A | 1.29 | UL15A | 1.15 |
| UL46 | 1.62 | UL94 | 1.38 | UL131A | 1.29 | UL44 | 1.14 |
| UL99 | 1.58 | TRS1 | 1.38 | UL77 | 1.29 | UL32 | 1.13 |
| UL69 | 1.57 | UL95 | 1.38 | UL55 | 1.29 | UL51 | 1.12 |
| UL2 | 1.55 | US21 | 1.38 | US32 | 1.29 | UL42 | 1.11 |
| RL1 | 1.54 | UL121 | 1.37 | UL76 | 1.28 | UL80 | 1.10 |
| UL88 | 1.52 | UL70 | 1.37 | UL75 | 1.28 | US14 | 1.09 |
| UL98 | 1.51 | UL105 | 1.37 | UL71 | 1.28 | RL12 | 1.09 |
| UL87 | 1.50 | UL115 | 1.36 | UL117 | 1.28 | US15 | 1.08 |
| UL83 | 1.47 | RNA5.0 | 1.36 | UL73 | 1.27 | UL41A | 1.08 |
| US30 | 1.47 | UL47 | 1.36 | UL14 | 1.26 | UL6 | 1.07 |
| US29 | 1.46 | US28 | 1.35 | UL34 | 1.26 | IRS1 | 1.06 |
| UL82 | 1.46 | UL93 | 1.35 | UL30 | 1.26 | UL31 | 1.05 |
| UL45 | 1.46 | UL96 | 1.35 | UL114 | 1.25 | US34 | 1.05 |
| UL89 | 1.44 | UL136 | 1.35 | UL26 | 1.25 | US33A | 1.04 |
| UL148D | 1.44 | UL30A | 1.34 | RL11 | 1.24 | US13 | 1.04 |
| UL120 | 1.43 | UL74A | 1.34 | UL147A | 1.24 | UL19 | 1.04 |
| UL91 | 1.43 | UL97 | 1.34 | UL52 | 1.23 | UL40 | 1.03 |
| UL103 | 1.42 | UL85 | 1.33 | UL53 | 1.23 | UL79 | 1.03 |
| UL150 | 1.42 | UL78 | 1.33 | UL135 | 1.22 | US12 | 1.02 |
| UL86 | 1.41 | UL119 | 1.33 | RL13 | 1.22 | UL56 | 1.01 |
| RL10 | 1.41 | UL84 | 1.32 | UL25 | 1.20 | UL4 | 1.00 |
| UL104 | 1.41 | UL111A | 1.32 | US26 | 1.20 | | |
| UL100 | 1.41 | UL148C | 1.32 | US34A | 1.19 | | |
| UL138 | 1.41 | UL133 | 1.31 | UL124 | 1.19 | | |

Figure 5.28 Differentially expressed HCMV genes during differentiation of HCMV infected NP1

Differential expression of HCMV genes in RNAseq analysis of HCMV_5 v HCMV_0 with cut-offs applied for padj of ≤ 0.01 and log2fold change of ≥ 1 or ≤ -1 .

5.8 Discussion

RNAseq analysis of NP1 +/- HCMV and +/- differentiation revealed the extent of the transcriptional changes associated with HCMV infection in NP1, both before and after differentiation treatment. Enrichment analysis revealed a multitude of pathways that could be involved in the perturbation of differentiation in HCMV+ NP1 and also may contribute to gliomagenesis. The significant disruption to gene expression related to axon guidance may explain how HCMV perturbs neurite

outgrowth (Figure 4.9 and 5.18). Han *et al.*, (2017) showed that HCMV IE2 transduced embryonic NP's developed short neurites compared to control cells and also possessed nonradially oriented processes. They also noted that when IE2 transduced NP's implanted into embryonic mouse brains, IE2+ callosal axons were unable cross the midline in leading to defects in the corpus callosum, indicating that HCMV perturbed neurite development has functional consequences within the brain.

To determine whether IE2 is also responsible for the dysregulation of axon guidance and neurite formation in adult NP1's, NP1 could be transfected with IE2 and differentiated using the Walton *et al.*, (2006) protocol and neurite outgrowth measured. It would also be interesting to time-lapse the differentiation of IE2 transduced NP1, HCMV infected NP1 and control NP1 using the Incucyte Zoom to watch the differences in neurite development over time. Further work could determine if the disruption to neurite outgrowth has functional effects, such as the electrophysiology protocol used in the Walton *et al.* (2006) paper. Axon guidance molecules including semaphorins and slits have been shown to be present in many cancers, including cancers outside of the CNS and are thought to play a role in both migration and apoptosis (Chedotal *et al.*, 2005). As RNAseq highlighted dysregulation of the expression of slit and semaphorin genes, this may be another area that requires further investigation.

The calcium signalling pathway was the second most significantly influenced KEGG pathway in Enrichr analysis of all differentially expressed genes in HCMV_5 v HCMV_0 and the most significant pathway identified from the list of genes with increased expression in this group. Calcium signalling was also significantly dysregulated in KEGG analysis of HCMV_5 v NP1_5. HCMV has previously been shown to disrupt calcium signalling in NPs derived from iPSCs and this causes functional and developmental defects in organoid formation (Sison *et al.*, 2019). HCMV genes that have been shown to play a role in the disruption of calcium signalling include US21, UL37, and US28 (Dunn and Munger, 2020). Interestingly, UL146 encodes a viral chemokine vCXCL1 and was the most upregulated viral gene in HCMV_5 v HCMV_0. The UL146 encoded protein is known to act as an agonist to the human chemokines CXCR1 and CXCR2 which are integral in intracellular calcium release (Penfold *et al.*, 1999). HCMV proteins including gB are also known to bind the human epidermal growth factor receptor (EGFR), initiating release of intracellular calcium in the same way the native ligand of this receptor, EGF does (Wang *et al.*, 2003). EGF mediated calcium release has previously been reported to play a role in modulation of growth and migration in glioma cells as well as gliomagenesis (Bryant *et al.*, 2004, Maklad *et al.*, 2019). The effects of HCMV on calcium

signalling in NP1 warrants further *in vitro* investigation of protein expression and viral-host protein interactions due to the importance of this pathway in gliomagenesis and GBM progression.

Significant dysregulation of genes involved in the PI3K-Akt pathway was associated with HCMV infection of NP1. Viral mediated activation of the PI3K-Akt pathway is essential for HCMV entry and has previously been ascribed to HCMV gB binding PDGFR α , (Johnson *et al.*, 2001, Cobbs *et al.*, 2014). As gB was expressed in HCMV_0 and HCMV_5, with increased protein levels at day 5, this could therefore be involved in the dysregulation of the PI3K-Akt pathway. Interestingly, rapid PI3K-Akt activation via the interaction of UL135 and UL138 with host (EGFR) is also seen in the early phase of establishment of latency by HCMV in CD34+ stem cells (Kim *et al.*, 2017). Inhibition of PI3K has been shown to reactivate latent HCMV in the same cells (Buehler *et al.*, 2016). With this in mind, it would be interesting to look at expression of genes within the PI3K-Akt pathway and specifically PI3K-Akt activation in the chronically HCMV infected colony 2. With PI3K-Akt activation reported in >90 % of glioblastomas and endogenous gB detected in GBM samples, this could be an important area for further research, particularly looking at interactions between HCMV proteins and elements of the PI3K-Akt pathway (Cobbs *et al.*, 2014). Previous studies have failed to find viable GBM treatments using PI3K-Akt inhibitors due to the difficulties associated with getting such compounds across the blood brain barrier (Colardo *et al.*, 2021).

HCMV mediated disruption of MAPK signalling may also be key in understanding the role HCMV could play in GBM. The MAPK signalling cascade responds to an array of extracellular signals to regulate several fundamental cellular processes, including control of growth, proliferation, differentiation, migration and apoptosis (Sun *et al.*, 2015). MAPK signalling pathway was identified as significantly affected in KEGG analysis of both HCMV_0 v NP1_0 and HCMV_5 v NP1_5 (Figure 5.134 and 5.15) as well as being the most significant pathway in KEGG analysis of co-expressed genes unique to groups HCMV_0 and HCMV_5 (Figure 5.18). Similarly to calcium signalling and PI3K-Akt, MAPK signalling can also be activated through binding of EGF to EGFR (Walker *et al.*, 1998). MAPK has been shown to be activated by HCMV gB, leading to a pro-survival response and also playing a key role in the establishment of latency (Reeves *et al.*, 2012). HCMV has been shown to increase the migration and invasion of GBM cells through the c-Jun N-terminal kinases pathway (JNK), which is one of the signalling pathways of the MAPK family (Zhu *et al.*, 2020). Importantly, JNK is required for both gliomagenesis and maintenance of stemness in GSC's (Kitanaka *et al.*, 2019). Further to this, the inhibition of JNK leads to loss of tumour initiating capacity in

GCS's. One particularly notable gene in both the classical and JNK pathways of MAPK signalling is FOS, a proto-oncogene that encodes c-Fos. Overexpression of c-Fos is associated with GBM and has been implicated in proliferation, differentiation, angiogenesis, invasion, and metastasis, with expression of this gene correlating with prognosis (Liu *et al.*, 2016). FOS expression showed a log2fold change of 2.37 in HCMV_0 v NP1_0. Further analysis of MAPK signalling in HCM+ NP1 compared to NP1 and also GBM cells may elucidate if HCMV causes similar dysregulation to that seen in GBM.

The cancer stem cell model suggests a population of stem-like cells with a number of driver mutations that have the propensity to both self-renew and give rise to differentiated progeny, thus explaining heterogeneity within tumours (Bonnet and Dick, 1997). This model of tumourigenesis was first described in acute myeloid leukaemia which originates from a haematopoietic progenitor and is now a widely accepted model of tumourigenesis. GSC's are thought to arise from the SVZ and play a key role in the pathogenesis of GBM due to their capability for self-renewal and differentiation and are thought to drive both recurrence and resistance to treatment (Ignatova *et al.*, 2002, Piper *et al.*, 2021). The presence of GSC's is also thought to contribute to the high levels of intratumour heterogeneity associated with GBM (Johnson *et al.*, 2014). KEGG analysis of genes uniquely co-expressed in HCMV_0 and HCMV highlighted "signalling pathways regulating pluripotency of stem cells". Of the seven genes identified as expressed in HCMV+ NP1, but not in controls, six did not have differential expression during differentiation. As pluripotency associated genes often show a decrease in expression as cells become more differentiated, this may signify that HCMV infection not only switches on expression of pluripotency genes, but also renders NP cells refractory to differentiation. A key gene identified as highly upregulated by HCMV infection of NP1 was KLF4. KLF4 is well-known as one of the four Yamanaka factors, which, together with the other factors, can reprogram terminally differentiated cells to induce pluripotency (Takahashi and Yamanaka, 2006). Expression of POU5F1, which encodes Oct4, and MYC (increased by a log2fold of 0.74, so not included in further analysis due to the cut offs applied) which encodes c-myc are also Yamanaka factors and were also increased in HCMV_5 v NP1_5. This increase in three of the four Yamanaka factors may indicate that HCMV is transcriptionally reprogramming NP1 through increasing expression of factors known to induce pluripotency. Crucially, aberrant expression of all three of these genes outside of their normal roles in development has been shown to be tumourigenic, thus all three being classified as oncogenes (Schmidt., 1999, Qi *et al.*, 2018, Wang *et al.*, 2013). However, SOX2, the fourth Yamanaka factor and arguably the one that is most

commonly associated with GBM and specifically HCMV infection in GBM showed significantly decreased gene and protein expression in HCMV infected NP1 compared to controls (Soroceanu *et al.*, 2015). It would be interesting to compare SOX2 expression in chronically infected colony2 to that in NP1 and HCMV+ NP1 (5 d.p.i) to see if this changes with long term infection. HCMV has been shown to confer stem-like properties to GBM cells upon *in vitro* infection leading to enhanced growth as tumourspheres (Soroceanu *et al.*, 2015). This increase in stem-like properties was attributed to HCMV IE proteins, with an IE1-deficient strain failing to lead to enhanced tumoursphere formation. Interestingly, the same study showed that RNAi mediated inhibition of IE expression in endogenously HCMV infected patient derived GSC's was sufficient to prevent tumoursphere formation. Further investigation is needed to determine whether IE expression in NP1 has a similar effect on neurosphere formation.

The increased expression of telomerase gene TERT in HCMV infected NP1 both prior to and post differentiation may be an important pro-oncogenic change in NP cells. Upregulation of telomerase is known to enable replicative immortality, a hallmark of cancer (Hanahan and Weinberg, 2011). The majority of GBM samples show telomerase activation (Hakin-Smith *et al.*, 2003, Tchirkov *et al.*, 2003). In GBM samples HCMV IE1 has been shown to colocalise with TERT, with correlation in levels of expression (Straat *et al.*, 2009). Expression of IE1 alone was enough to increase TERT expression in GBM cells. This increased TERT activation may be a key finding in determining the role of HCMV in gliomagenesis.

Early studies of HCMV latency proposed that latency was characterised by the majority of the viral genome being silenced through chromatin remodelling and repression of the MIEP leading to a limited subset of latency-associated genes being expressed in the absence of so-called lytic gene expression (Reeves *et al.*, 2005). However, in recent years studies have refuted this model due to evidence of a much broader pool of viral transcripts expressed in both natural and experimental latency (Cheng *et al.*, 2017, Schnayder *et al.*, 2018). Recent evidence from meta-analysis of transcriptomic studies of naturally latently HCMV infected cells, suggests that HCMV does not have a defined latency specific transcriptional program as previously thought (Schwartz and Stern-Ginossar, 2019). Instead, it was determined that such cells exhibit a transcriptional program very similar to that of lytic infection, albeit at a much lower level. Therefore, it would be interesting to further investigate the levels of HCMV transcripts in NP1 infection. Whilst HCMV_5 v HCMV_0 shows a pan increase in viral gene expression, without a non-differentiated day 5 HCMV+ NP1 control, it is not possible to determine whether this increase is induced by differentiation or if viral

transcript accumulation would have occurred simply through five further days of infection. If indeed this increase is specific to differentiation, this together with the switch from non-productive to productive infection seen during HCMV+ NP1 differentiation may imply that adult NP are a potential reservoir of HCMV latency and that differentiation dependant reactivation occurs in NP1. It would be useful to monitor levels of viral gene expression over a longer time course of infection, to get a better idea of how HCMV infection progresses in these cells. Comparison of viral gene expression levels between HCMV_0, HCMV_5 and colony 2 (+/- differentiation) may also be valuable in elucidating whether NP1 are indeed capable of supporting latency and reactivation of HCMV.

One of the main limitations of the RNAseq experiment discussed in this chapter in terms of identifying potential oncogenic or oncomodulatory changes, is the relatively short time frame of infection. In patients, glioma development likely happens over weeks, months and even years, with Stensjøen *et al.* (2018) estimating that on average GBM development begins around 330 days prior to diagnosis. Additionally, if natural HCMV infection is driving gliomagenesis, the initial infection was likely acquired many years, even decades prior to gliomagenesis. Therefore, for future work, RNAseq of colony 2 would be a logical next step. Going forward, it will be important to determine whether the changes in transcription discussed in this chapter are reflected in both protein expression and phenotypic changes.

Chapter 6 – Final discussion

This study has shown that HCMV can infect adult NP cells *in vitro*, leading to expression of IE, early and late protein expression, but lacking detectable infectious virion production. It remains unclear what causes this block in viral production in NP1, but could be important in explaining the fact that NP1 can support chronic infection with HCMV *in vitro* over a period of several months as seen in colony 2. Further work needs to be conducted to fully elucidate the nature of this long-term infection to determine if it is true viral latency, or simply a low-level grumbling infection with minimal virion production. Single cell transcriptomics of colony 2 could be key in establishing the nature of this chronic HCMV infection of NP1. Firstly, it could reveal the proportion of cells that are expressing HCMV genes in the absence of detectable GFP expression and secondly, it may help to determine whether sporadic GFP expression is due to low level, chronic infection spreading slowly from cell to cell or due to latency and subsequent reactivation. Another possibility for further analysing the nature of HCMV infection in colony 2, would be to sort the GFP+ cells from the GFP- cells and RNAseq the two groups to see if the viral transcriptional profiles showed distinct patterns of viral gene expression and whether this is consistent with latent and reactivated gene expression. The ability of adult NP to support HCMV infection for several months post infection suggests that these cells are a potential reservoir for latent infection in the adult brain. This may be important in explaining how HCMV genomes, RNA and a limited subset of viral proteins are present in GBM tumours in the absence of infectious virions.

Differentiation stimuli lifts the block in HCMV virion production in NP1 and leads to infectious virus in NP1 supernatants from day three of differentiation onwards. A similar effect is seen upon differentiation of long-term infected colony 2, which leads to increased GFP expression and production of virus in the supernatant. This phenomenon of differentiation dependent virus production is reminiscent of the differentiation dependant reactivation from latency that is seen in HCMV+ monocytes (Chan *et al.*, 2012, Stevenson *et al.*, 2014). Further work needs to be conducted to determine if this is a strictly differentiation dependant effect, or a direct effect of one of the reagents used in the differentiation protocol. Cheng *et al.* (2017), used dibutyryl cAMP and IBMX (both of which are used in the differentiation protocol), to reactivate latent HCMV infection of an *in vitro* infected GBM line. The study attributes the effects of dibutyryl cAMP/IBMX treatment to its effects on the PKA-CREB signalling pathway, however as this pathway is known to play a key role in regulation of neuronal differentiation, it remains unclear as to if Cheng *et al.* were also inducing differentiation of their GBM cells.

In light of this, it may be prudent to try other NP differentiation methods that do not include dibutyryl cAMP and IBMX to determine if this phenomenon is differentiation dependant. It would be interesting to differentiate GBM cells from GBM that have been shown to harbour HCMV antigens, to see if HCMV can be reactivated from these cells in a similar way to HCMV+ NP1.

HCMV infection perturbs the differentiation of NP1 cells, resulting in failure to adopt neuronal or astrocytic morphology, dysregulation in the expression of several key differentiation markers including GFAP and β -III-tubulin. Increased β -III-tubulin is associated with GBM and is thought to contribute to tumour development and progression (Katsetos *et al.*, 2011). Maintenance of PCNA and Ki67 throughout differentiation suggests dysregulation of the cell cycle by HCMV, which may potentially promote proliferation. HCMV has long been known to modulate the cell cycle to optimise conditions for viral gene expression (Salvant *et al.*, 1998). HCMV drives cells into G1, but prevents G1/S transition, despite the expression of several S-phase proteins including PCNA (Dittmer and Mockarski, 1997). The early stages of oncogenesis involve dysregulation of the cell cycle and this is seen in other oncogenic viruses including EBV, which promotes G1/S transition through a variety of latency associated viral genes and KSHV, which also promotes cell cycle progression, particularly through its oncogenic LANA (Paladino *et al.*, 2014, Wei *et al.*, 2016). To determine whether the HCMV dependant maintenance of Ki67 and PCNA does confer increased proliferation to NP1 cells, a proliferation assay could be performed. It would be interesting to compare the proliferation of NP1 at various stages of HCMV infection, including in colony 2. Differentiating HCMV+ NP1 show induction of expression of CD133 protein, the expression of which is usually limited to stem cells. This is particularly notable as in GBM, HCMV IE expression is associated with a CD133+ subpopulation and *in vitro* infection of GBM led to increased CD133 expression (Fornara *et al.*, 2016). Interestingly, oncogenic herpesviruses KSHV and EBV are also known to induce CD133 expression, through effects on the notch and hedgehog signalling pathways respectively (Liu *et al.*, 2010, Lun *et al.*, 2014). Induction of CD133 expression may indicate a HCMV mediated de-differentiation of NP1. However, the lack of detection of CD133 transcripts in HCMV+ NP1 by RNAseq is concerning and thus requires further investigation.

Enrichment analysis of RNAseq data highlighted HCMV mediated modulation of axon guidance and several key signalling pathways that may indicate an oncogenic or oncomodulatory effect in HCMV infection of adult NP cells. These include dysregulation of calcium signalling, PI3K-Akt signalling, MAPK signalling and signalling pathways regulating pluripotency of stem cells. The effects of HCMV infection on axon guidance may explain the deficiency in developing

neuronal processes during differentiation of HCMV+ NP1. Calcium signalling, PI3K-Akt signalling and MAPK signalling have been shown to be interconnected, including in astrocytic cells, so the simultaneous dysregulation of these three pathways by HCMV is unsurprising (Jiang *et al.*, 2015). Calcium signalling disruption has been attributed to several HCMV proteins, including pUS28 and pUL146, the HCMV with moths upregulated expression during differentiation of HCMV+ NP1 (Dunn and Munger, 2020(Penfold *et al.*, 1999). Calcium signalling is known to regulate neurogenesis and is extensively dysregulated in GBM, where it can promote growth and tumourigenesis (Toth *et al.*, 2016, Maklad *et al.*, 2019). Further experiments are required to determine if the changes in gene expression within the calcium signalling pathway associated with HCMV infection of NP1 lead to functional effects on calcium signalling and if so, how these changes affect differentiation of these cells. PI3K-Akt is known to be an important regulator of neuronal differentiation and so the dysregulation of this pathway by HCMV in NP1 may contribute to the perturbation of differentiation observed (Sánchez-Alegría *et al.*, 2018). HCMV infection of GBM cells in vitro was found to induce PI3K activation which led to increased migration and invasion (Cobbs *et al.*, 2007). Further investigation of the effects of HCMV infection on the PI3K-Akt signalling pathway in NP1 are needed to determine whether HCMV does indeed activate this pathway in adult neural progenitor cells and what the effects of this activation are in terms of contributing to oncogenesis. MAPK signalling has been associated with GBM initiation and tumourigenesis (Krishna *et al.*, 2012). The effects of HCMV infection on MAPK signalling gene expression in NP1 highlighted by RNAseq analysis need to be further evaluated to determine if this is responsible for HCMV induced effects on differentiation and if this could possibly contribute to tumourigenesis in HCMV+ NP1.

Whilst bulk RNAseq gives a good whole population overview of transcriptional changes associated with HCMV infection of NP1, single cell RNAseq may be useful to gain a deeper understanding of the changes occurring and to assess the heterogeneity across populations. Firstly, as NP1 are a primary derived cell type, there is likely to be significant heterogeneity within the population. It would be interesting to see if prior to differentiation, some individual cells are already exhibiting more stem cell, neuronal or astrocytic like transcriptional programs than the population as a whole. As the differentiation protocol used is known to result in neuronal, astrocytic and hybrid so-called “asterons” it would be useful to look post differentiation for distinct gene expression patterns associated with each of these sub-populations. Single cell RNAseq gene set enrichment may be utilised to determine if the pathways highlighted by bulk RNAseq in this study are unique to sub-populations or common across the whole population. For example,

as GSC's only represent a small number of cells within GBM, it could be important to understand if HCMV induced pluripotency gene expression is limited to a subset of NP1 cells or a population wide effect (Ahmed *et al.*, 2015). Looking at single cell RNAseq analysis of HCMV infected NP1 may also reveal sub-population of cells with different transcriptomic profiles that could perhaps be useful in determining why HCMV infection leads to cell death in some NP1, but not in all.

KEGG enrichment analysis showed that HCMV infection of NP1 modulated gene expression linked with pluripotency signalling in stem cells. Several of the genes identified as having increased expression in this analysis are associated with GSCs, including OLIG2, POU5F1 (Oct4) and KLF4, all of which have been shown to be oncogenic (Du *et al.*, 2009, Trépant *et al.*, 2014, Ray *et al.*, 2017). However, SOX2 gene and protein expression in NP1 actually decreased in response to HCMV infection. Sox2 expression is usually increased in GSCs and its expression has been shown to increase upon HCMV infection of GBM cells (Fornara *et al.*, 2016). Despite this, the increased expression of JARID2, MYC, OLIG2, POU5F1 and KLF4 seen by RNAseq, combined with the increase in CD133 expression seen by IF and western blot may indicate that transcriptional reprogramming towards a more stem like phenotype is occurring in HCMV infection of NP1. This transcriptional reprogramming and potential de-differentiation is reminiscent of the "unlocking phenotypic plasticity" hallmark of cancer recently described by Hanahan (2022). In order to determine whether the effects of HCMV modulated expression of pluripotency signalling genes identified in NP1 confers a similar effect that seen in HCMV+ GSC's, a neurosphere formation assay with non-infected NP1 control would be an important experiment to conduct. Further to this, if HCMV does indeed increase neurosphere formation, HCMV+ NP1 could be used for an orthotopic transfer *in vivo* to establish whether or not such cells are tumourigenic, as one of the key features of GSC's is their ability to form tumours upon *in vivo* transplantation (Lathia *et al.*, 2015). It may also be interesting to compare the tumourigenic potential of newly infected NP1 against the chronically infected colony 2. It would also be useful to perform IF on HCMV+ NP1 to look at the distribution of the proteins of the genes identified in the KEGG "signalling pathways regulating pluripotency of stem cells" to see if their expression is consistently increased throughout the population or if the expression is limited to a subset of cells. Single cell RNAseq may also be useful in identifying if the increased transcription of pluripotency associated genes occurs throughout the population or in a discrete subpopulation of NP1. If future work indicates that increased pluripotency associated gene/protein expression is limited to a specific subpopulation of

HCMV+ NP1, it may also be necessary to isolate these cells using specific markers to determine if the subpopulation has greater tumourigenic potential than the population as a whole.

Whilst this study has shown that HCMV can infect differentiated NP1 that have undergone differentiation via the Walton et al. (2006) protocol, very little has been done to characterise the consequence of HCMV infection in these cells. Evidence of Ki67 and PCNA restoration and induction of CD133 expression may indicate de-differentiation of these cells in response to HCMV infection, however thorough analysis of other differentiation markers is required to confirm this. If this is indeed the case, it is further evidence that HCMV can transcriptionally reprogram and unlock phenotypic plasticity of cells at several different stages of the neural cell lineage.

In conclusion, this study has shown that HCMV can infect primary adult NP cells *in vitro* and that these cells can continue to proliferate whilst supporting a long-term infection. HCMV infection of NP1 does not lead to robust production of infectious virions, but differentiation leads to virus being released into the supernatant. HCMV perturbs the differentiation of NP1 and induces expression of several stem cell markers that may indicate dedifferentiation and are also expressed in GSCs. Several signalling pathways are dysregulated by HCMV infection of NP1 that may play a key role in oncogenesis. Importantly, HCMV infection of NP1 increases TERT expression, which does not diminish with differentiation, which may confer replicative immortality. Together, this may represent an oncogenic or oncomodulatory effect of HCMV in adult NP cells.

Appendix A - Recipes

BMP4 differentiation media – DMEM/F12, 5 % FBS, 1 % B-27 supplement, 0.5 % N-2 supplement, 1 % GlutaMax-1 Supplement, 100 ng/ml BMP4

EBC lysis buffer - 50 mM Tris HCl pH 8.0, 140 mM NaCl, 100 mM NaF, 200 μ M Na₃VO₄, 0.1 % (w/v) SDS, 1 % (v/v) Triton X100, 1 tablet protease inhibitor per 50 ml (complete ULTRA tablets, Roche)

ECL Reagent - Solution 1: 0.4 mM p-Coumaric acid, 2.5 mM Luminol, 0.1 Tris pH 8.5; Solution 2: 0.02 % (v/v) H₂O₂ 0.1 mM Tris pH 8.5

Fibroblast media – DMEM, 10 % FBS, 50 000 units Penicillin, and 50 mg Streptomycin (Sigma)

Laemmli buffer - 100 mM Tris HCl pH 6.8, 4 % SDS, 20 % (v/v) Glycerol, 10 mM DTT, 0.025 % (w/v) Bromophenol Blue

NP media - DMEM/F12, 5 % FBS, 20ng/ml FGF, 20ng/ml EGF, 1 % B-27 supplement, 0.5 % N-2 supplement, 1 % GlutaMax-1 Supplement.

Tris-buffered Saline (TBS) -50 mM Tris HCl pH 7.5, 150 mM NaCl

TBS-T - TBS with 0.1 % v/v Tween 20

Running buffer - 25 mM Tris base pH 8.0, 250 mM Glycine, 0.1 % (w/v) SDS

Towbin transfer buffer - 25 mM Tris base, 250 mM Glycine, 20 % (v/v) Methanol

Walton differentiation media - DMEM/F12, 1 % B-27 supplement, 0.5 % N-2 supplement, 1 % GlutaMax-1 Supplement, 0.5 mM 3-isobutyl-1-methylxanthine (IBMX), 0.5 mM 1-dibutyl cAMP, and 25 ng/ml neuronal growth factor (NGF)

Hand poured acrylamide gel recipe

Resolving gel - 8, 10, 12 or 15 % (v/v) Acrylamide 390 mM Tris (pH 8.8) 0.1 % (v/v) SDS 0.1 % (v/v) ammonium persulphate 0.04 % (v/v) Tetramethylethylenediamine

Stacking gel - 5% (v/v) Acrylamide 130 mM Tris (pH 6.8) 0.1 % (v/v) SDS 0.1 % (v/v) ammonium persulphate 0.1 % (v/v) Tetramethylethylenediamine

Appendix B – List of antibodies

Primary antibodies

| Antibody | Supplier and Code | Species | Clonality | WB dilution | IF dilution |
|----------------------|----------------------|---------|-----------|-------------|-------------|
| β -III-tubulin | Biologend 801202 | Mouse | Mono | 1:1000 | 1:200 |
| CD133 | Biorbyt orb99113 | Rabbit | Poly | 1:500 | 1:200 |
| CD133 | Cell Signalling 5860 | Rabbit | Mono | 1:1000 | 1:250 |
| GAPDH | Ambion AM4300 | Mouse | Mono | 1:20000 | N/A |
| GFAP | Agilent Z0334 | Rabbit | Poly | 1:1000 | 1:200 |
| HCMV pp28 | Santa Cruz sc-56975 | Mouse | Mono | 1:1000 | 1:200 |
| HCMV pp52 | Santa Cruz sc-69744 | Mouse | Mono | 1:1000 | 1:200 |
| HCMV pp65 | Santa Cruz sc-56976 | Mouse | Mono | 1:1000 | 1:200 |
| HCMV pp72 | Santa Cruz sc-69834 | Mouse | Mono | 1:1000 | 1:200 |
| HCMV gB | Santa Cruz sc-69742 | Mouse | Mono | 1:1000 | 1:200 |
| HCMV IE | MAB8131 | Mouse | Mono | 1:1000 | 1:200 |
| Ki67 | Abcam Ab16667 | Rabbit | Mono | 1:200 | 1:50 |
| Nestin | Millipore MAB5326 | Mouse | Mono | 1:1000 | 1:200 |
| PCNA | Abcam Ab29 | Rabbit | Mono | 1:1000 | N/A |
| Sox2 | Cell signalling 3579 | Rabbit | Mono | 1:1000 | 1:400 |
| TGN46 | Abcam Ab50595 | Rabbit | Poly | 1:200 | 1:100 |

Western blot secondary antibodies

| Antibody | Supplier and Code | Species | Clonality | WB dilution |
|-----------------|-------------------|---------|-----------|-------------|
| anti Mouse HRP | Sigma A4416 | Goat | Poly | 1/5000 |
| anti Rabbit HRP | Sigma A6154 | Goat | Poly | 1/5000 |

Immunofluorescence secondary antibodies

| Antibody | Supplier | Species | Dilution |
|-----------------|------------|---------|----------|
| Anti-mouse 594 | Invitrogen | Goat | 1:500 |
| Anti-rabbit 594 | Invitrogen | Goat | 1:500 |
| Anti-mouse 594 | Invitrogen | Donkey | 1:500 |
| Anti-rabbit 594 | Invitrogen | Donkey | 1:500 |

References

- Aaku-Saraste, E., Hellwig, A. and Huttner, W.B. 1996. Loss of occludin and functional tight junctions, but not ZO-1, during neural tube closure--remodeling of the neuroepithelium prior to neurogenesis. *Dev Biol.* **180**(2), pp.664-679.
- Abaitua, F., Hollinshead, M., Bolstad, M., Crump, C.M. and O'Hare, P. 2012. A Nuclear localization signal in herpesvirus protein VP1-2 is essential for infection via capsid routing to the nuclear pore. *J Virol.* **86**(17), pp.8998-9014.
- Ackerman, S. 1992. *Discovering the Brain.*
- Acosta, C., Anderson, H.D. and Anderson, C.M. 2017. Astrocyte dysfunction in Alzheimer disease. *J Neurosci Res.* **95**(12), pp.2430-2447.
- Adler, B. and Sinzger, C. 2009. Endothelial cells in human cytomegalovirus infection: one host cell out of many or a crucial target for virus spread? *Thromb Haemost.* **102**(6), pp.1057-1063.
- Adler, S.P., Manganello, A.M., Lee, R., McVoy, M.A., Nixon, D.E., Plotkin, S., Mocarski, E., Cox, J.H., Fast, P.E., Nesterenko, P.A., Murray, S.E., Hill, A.B. and Kemble, G. 2016. A Phase 1 Study of 4 Live, Recombinant Human Cytomegalovirus Towne/Toledo Chimera Vaccines in Cytomegalovirus-Seronegative Men. *J Infect Dis.* **214**(9), pp.1341-1348.
- Ahmadipour, Y., Gembruch, O., Pierscianek, D., Sure, U. and Jabbarli, R. 2020. Does the expression of glial fibrillary acid protein (GFAP) stain in glioblastoma tissue have a prognostic impact on survival? *Neurochirurgie.* **66**(3), pp.150-154.
- Ahmed, A.U., Auffinger, B. and Lesniak, M.S. 2013. Understanding glioma stem cells: rationale, clinical relevance and therapeutic strategies. *Expert Rev Neurother.* **13**(5), pp.545-555.
- Ahmed, M., Lock, M., Miller, C.G. and Fraser, N.W. 2002. Regions of the herpes simplex virus type 1 latency-associated transcript that protect cells from apoptosis in vitro and protect neuronal cells in vivo. *J Virol.* **76**(2), pp.717-729.
- Akhavan, D., Cloughesy, T.F. and Mischel, P.S. 2010. mTOR signaling in glioblastoma: lessons learned from bench to bedside. *Neuro Oncol.* **12**(8), pp.882-889.
- Akrigg, A., Wilkinson, G.W. and Oram, J.D. 1985. The structure of the major immediate early gene of human cytomegalovirus strain AD169. *Virus Res.* **2**(2), pp.107-121.
- Alcantara Llaguno, S., Chen, J., Kwon, C.H., Jackson, E.L., Li, Y., Burns, D.K., Alvarez-Buylla, A. and Parada, L.F. 2009. Malignant astrocytomas originate from neural stem/progenitor cells in a somatic tumor suppressor mouse model. *Cancer Cell.* **15**(1), pp.45-56.
- Alcantara Llaguno, S., Sun, D., Pedraza, A.M., Vera, E., Wang, Z., Burns, D.K. and Parada, L.F. 2019. Cell-of-origin susceptibility to glioblastoma formation declines with neural lineage restriction. *Nat Neurosci.* **22**(4), pp.545-555.
- Al-Hajj, M., Wicha, M.S., Benito-Hernandez, A., Morrison, S.J. and Clarke, M.F. 2003. Prospective identification of tumorigenic breast cancer cells. *Proc Natl Acad Sci U S A.* **100**(7), pp.3983-3988.
- Alibek, K., Baiken, Y., Kakpenova, A., Mussabekova, A., Zhussupbekova, S., Akan, M. and Sultankulov, B. 2014. Implication of human herpesviruses in oncogenesis through immune evasion and suppression. *Infect Agent Cancer.* **9**(1), p3.
- Almaghrabi, M.K., Alwadei, A.D., Alyahya, N.M., Alotaibi, F.M., Alqahtani, A.H., Alahmari, K.A., Alqahtani, M.S., Alayed, A.S., Moosa, R. and Ali, A.S. 2019.

- Seroprevalence of Human Cytomegalovirus in Pregnant Women in the Asir Region, Kingdom of Saudi Arabia. *Intervirology*. **62**(5-6), pp.205-209.
- Alvarez-Buylla, A., García-Verdugo, J.M. and Tramontin, A.D. 2001. A unified hypothesis on the lineage of neural stem cells. *Nat Rev Neurosci*. **2**(4), pp.287-293.
- Alwine, J.C. 2012. The human cytomegalovirus assembly compartment: a masterpiece of viral manipulation of cellular processes that facilitates assembly and egress. *PLoS Pathog*. **8**(9), pe1002878.
- Anderholm, K.M., Bierle, C.J. and Schleiss, M.R. 2016. Cytomegalovirus Vaccines: Current Status and Future Prospects. *Drugs*. **76**(17), pp.1625-1645.
- Anderson, C.M. and Swanson, R.A. 2000. Astrocyte glutamate transport: review of properties, regulation, and physiological functions. *Glia*. **32**(1), pp.1-14.
- Anlauf, E. and Derouiche, A. 2013. Glutamine synthetase as an astrocytic marker: its cell type and vesicle localization. *Front Endocrinol (Lausanne)*. **4**, p144.
- Anselmi, G., Giuliani, M., Vezzani, G., Ferranti, R., Gentile, M., Cortese, M., Amendola, D., Pacchiani, N., D'Aurizio, R., Bruno, L., Uematsu, Y., Merola, M. and Maione, D. 2020. Characterization of pUL5, an HCMV protein interacting with the cellular protein IQGAP1. *Virology*. **540**, pp.57-65.
- Aoki, Y., Yarchoan, R., Wyvill, K., Okamoto, S., Little, R.F. and Tosato, G. 2001. Detection of viral interleukin-6 in Kaposi sarcoma-associated herpesvirus-linked disorders. *Blood*. **97**(7), pp.2173-2176.
- Arbuckle, J.H., Medveczky, M.M., Luka, J., Hadley, S.H., Luegmayer, A., Ablashi, D., Lund, T.C., Tolar, J., De Meirleir, K., Montoya, J.G., Komaroff, A.L., Ambros, P.F. and Medveczky, P.G. 2010. The latent human herpesvirus-6A genome specifically integrates in telomeres of human chromosomes in vivo and in vitro. *Proc Natl Acad Sci U S A*. **107**(12), pp.5563-5568.
- Arend, K.C., Ziehr, B., Vincent, H.A. and Moorman, N.J. 2016. Multiple Transcripts Encode Full-Length Human Cytomegalovirus IE1 and IE2 Proteins during Lytic Infection. *J Virol*. **90**(19), pp.8855-8865.
- Arnoult, D., Bartle, L.M., Skaletskaya, A., Poncet, D., Zamzami, N., Park, P.U., Sharpe, J., Youle, R.J. and Goldmacher, V.S. 2004. Cytomegalovirus cell death suppressor vMIA blocks Bax- but not Bak-mediated apoptosis by binding and sequestering Bax at mitochondria. *Proc Natl Acad Sci U S A*. **101**(21), pp.7988-7993.
- Ashizawa, T., Miyata, H., Iizuka, A., Komiyama, M., Oshita, C., Kume, A., Nogami, M., Yagoto, M., Ito, I., Oishi, T., Watanabe, R., Mitsuya, K., Matsuno, K., Furuya, T., Okawara, T., Otsuka, M., Ogo, N., Asai, A., Nakasu, Y., Yamaguchi, K. and Akiyama, Y. 2013. Effect of the STAT3 inhibitor STX-0119 on the proliferation of cancer stem-like cells derived from recurrent glioblastoma. *Int J Oncol*. **43**(1), pp.219-227.
- Atabani, S.F., Smith, C., Atkinson, C., Aldridge, R.W., Rodriguez-Perálvarez, M., Rolando, N., Harber, M., Jones, G., O'Riordan, A., Burroughs, A.K., Thorburn, D., O'Beirne, J., Milne, R.S., Emery, V.C. and Griffiths, P.D. 2012. Cytomegalovirus replication kinetics in solid organ transplant recipients managed by preemptive therapy. *Am J Transplant*. **12**(9), pp.2457-2464.
- Atanasiu, D., Whitbeck, J.C., Cairns, T.M., Reilly, B., Cohen, G.H. and Eisenberg, R.J. 2007. Bimolecular complementation reveals that glycoproteins gB and gH/gL of herpes simplex virus interact with each other during cell fusion. *Proceedings of the National Academy of Sciences*. **104**(47), p18718.

- Awasthi, S., Isler, J.A. and Alwine, J.C. 2004. Analysis of splice variants of the immediate-early 1 region of human cytomegalovirus. *J Virol.* **78**(15), pp.8191-8200.
- Azevedo, F.A., Carvalho, L.R., Grinberg, L.T., Farfel, J.M., Ferretti, R.E., Leite, R.E., Jacob Filho, W., Lent, R. and Herculano-Houzel, S. 2009. Equal numbers of neuronal and nonneuronal cells make the human brain an isometrically scaled-up primate brain. *J Comp Neurol.* **513**(5), pp.532-541.
- Babić, M., Krmpotić, A. and Jonjić, S. 2011. All is fair in virus-host interactions: NK cells and cytomegalovirus. *Trends Mol Med.* **17**(11), pp.677-685.
- Backovic, M. and Jardetzky, T.S. 2009. Class III viral membrane fusion proteins. *Current opinion in structural biology.* **19**(2), pp.189-196.
- Baker, S.J., Fearon, E.R., Nigro, J.M., Hamilton, S.R., Preisinger, A.C., Jessup, J.M., vanTuinen, P., Ledbetter, D.H., Barker, D.F., Nakamura, Y., White, R. and Vogelstein, B. 1989. Chromosome 17 deletions and p53 gene mutations in colorectal carcinomas. *Science.* **244**(4901), pp.217-221.
- Ball, C.B., Li, M., Parida, M., Hu, Q., Ince, D., Collins, G.S., Meier, J.L. and Price, D.H. 2022. Human Cytomegalovirus IE2 Both Activates and Represses Initiation and Modulates Elongation in a Context-Dependent Manner. *mBio.* **13**(3), pe0033722.
- Ballon, G., Chen, K., Perez, R., Tam, W. and Cesarman, E. 2011. Kaposi sarcoma herpesvirus (KSHV) vFLIP oncoprotein induces B cell transdifferentiation and tumorigenesis in mice. *J Clin Invest.* **121**(3), pp.1141-1153.
- Banerjee, S., Wei, Z., Tan, F., Peck, K.N., Shih, N., Feldman, M., Rebbeck, T.R., Alwine, J.C. and Robertson, E.S. 2015. Distinct microbiological signatures associated with triple negative breast cancer. *Sci Rep.* **5**, p15162.
- Bao, B., Ahmad, A., Azmi, A.S., Ali, S. and Sarkar, F.H. 2013. Overview of cancer stem cells (CSCs) and mechanisms of their regulation: implications for cancer therapy. *Curr Protoc Pharmacol.* **Chapter 14**, pUnit 14.25.
- Barami, K. 2010. Oncomodulatory mechanisms of human cytomegalovirus in gliomas. *J Clin Neurosci.* **17**(7), pp.819-823.
- Barkovich, A.J. and Girard, N. 2003. Fetal brain infections. *Childs Nerv Syst.* **19**(7-8), pp.501-507.
- Baron, S. 1996. Medical Microbiology.
- Baryawno, N., Rahbar, A., Wolmer-Solberg, N., Taher, C., Odeberg, J., Darabi, A., Khan, Z., Sveinbjörnsson, B., Fuskevåg, O.M., Segerström, L., Nordenskjöld, M., Siesjö, P., Kogner, P., Johnsen, J.I. and Söderberg-Nauclér, C. 2011. Detection of human cytomegalovirus in medulloblastomas reveals a potential therapeutic target. *J Clin Invest.* **121**(10), pp.4043-4055.
- Bechtel, J.T. and Shenk, T. 2002. Human cytomegalovirus UL47 tegument protein functions after entry and before immediate-early gene expression. *J Virol.* **76**(3), pp.1043-1050.
- Becroft, D.M. 1981. Prenatal cytomegalovirus infection: epidemiology, pathology and pathogenesis. *Perspect Pediatr Pathol.* **6**, pp.203-241.
- Bego, M., Maciejewski, J., Khaiboullina, S., Pari, G. and St Jeor, S. 2005. Characterization of an antisense transcript spanning the UL81-82 locus of human cytomegalovirus. *J Virol.* **79**(17), pp.11022-11034.
- Beisser, P.S., Laurent, L., Virelizier, J.L. and Michelson, S. 2001. Human cytomegalovirus chemokine receptor gene US28 is transcribed in latently infected THP-1 monocytes. *J Virol.* **75**(13), pp.5949-5957.
- Bell, J.E. 1998. The neuropathology of adult HIV infection. *Rev Neurol (Paris).*

154(12), pp.816-829.

Belzile, J.P., Stark, T.J., Yeo, G.W. and Spector, D.H. 2014. Human cytomegalovirus infection of human embryonic stem cell-derived primitive neural stem cells is restricted at several steps but leads to the persistence of viral DNA. *J Virol.* **88**(8), pp.4021-4039.

Bhat, K.P., Salazar, K.L., Balasubramaniyan, V., Wani, K., Heathcock, L., Hollingsworth, F., James, J.D., Gumin, J., Diefes, K.L., Kim, S.H., Turski, A., Azodi, Y., Yang, Y., Doucette, T., Colman, H., Sulman, E.P., Lang, F.F., Rao, G., Copray, S., Vaillant, B.D. and Aldape, K.D. 2011. The transcriptional coactivator TAZ regulates mesenchymal differentiation in malignant glioma. *Genes Dev.* **25**(24), pp.2594-2609.

Bhattacharjee, B., Renzette, N. and Kowalik, T.F. 2012. Genetic analysis of cytomegalovirus in malignant gliomas. *J Virol.* **86**(12), pp.6815-6824.

Biron, K.K., Stanat, S.C., Sorrell, J.B., Fyfe, J.A., Keller, P.M., Lambe, C.U. and Nelson, D.J. 1985. Metabolic activation of the nucleoside analog 9-[(2-hydroxy-1-(hydroxymethyl)ethoxy)methyl]guanine in human diploid fibroblasts infected with human cytomegalovirus. *Proc Natl Acad Sci U S A.* **82**(8), pp.2473-2477.

Bleeker, F.E., Atai, N.A., Lamba, S., Jonker, A., Rijkeboer, D., Bosch, K.S., Tigchelaar, W., Troost, D., Vandertop, W.P., Bardelli, A. and Van Noorden, C.J. 2010. The prognostic IDH1(R132) mutation is associated with reduced NADP+-dependent IDH activity in glioblastoma. *Acta Neuropathol.* **119**(4), pp.487-494.

Bodaghi, B., Jones, T.R., Zipeto, D., Vita, C., Sun, L., Laurent, L., Arenzana-Seisdedos, F., Virelizier, J.L. and Michelson, S. 1998. Chemokine sequestration by viral chemoreceptors as a novel viral escape strategy: withdrawal of chemokines from the environment of cytomegalovirus-infected cells. *J Exp Med.* **188**(5), pp.855-866.

Boeckh, M., Leisenring, W., Riddell, S.R., Bowden, R.A., Huang, M.L., Myerson, D., Stevens-Ayers, T., Flowers, M.E., Cunningham, T. and Corey, L. 2003. Late cytomegalovirus disease and mortality in recipients of allogeneic hematopoietic stem cell transplants: importance of viral load and T-cell immunity. *Blood.* **101**(2), pp.407-414.

Boehme, K.W., Guerrero, M. and Compton, T. 2006. Human cytomegalovirus envelope glycoproteins B and H are necessary for TLR2 activation in permissive cells. *J Immunol.* **177**(10), pp.7094-7102.

Bonnet, D. and Dick, J.E. 1997. Human acute myeloid leukemia is organized as a hierarchy that originates from a primitive hematopoietic cell. *Nat Med.* **3**(7), pp.730-737.

Boppana, S.B., Fowler, K.B., Britt, W.J., Stagno, S. and Pass, R.F. 1999. Symptomatic congenital cytomegalovirus infection in infants born to mothers with preexisting immunity to cytomegalovirus. *Pediatrics.* **104**(1 Pt 1), pp.55-60.

Boppana, S.B., Pass, R.F., Britt, W.J., Stagno, S. and Alford, C.A. 1992. Symptomatic congenital cytomegalovirus infection: neonatal morbidity and mortality. *Pediatr Infect Dis J.* **11**(2), pp.93-99.

Boppana, S.B., Rivera, L.B., Fowler, K.B., Mach, M. and Britt, W.J. 2001. Intrauterine transmission of cytomegalovirus to infants of women with preconceptional immunity. *N Engl J Med.* **344**(18), pp.1366-1371.

Borst, E.M. and Messerle, M. 2005. Analysis of human cytomegalovirus oriLyt sequence requirements in the context of the viral genome. *J Virol.* **79**(6), pp.3615-3626.

Bowles, J., Schepers, G. and Koopman, P. 2000. Phylogeny of the SOX family

- of developmental transcription factors based on sequence and structural indicators. *Dev Biol.* **227**(2), pp.239-255.
- Boyle, K.A., Pietropaolo, R.L. and Compton, T. 1999. Engagement of the cellular receptor for glycoprotein B of human cytomegalovirus activates the interferon-responsive pathway. *Mol Cell Biol.* **19**(5), pp.3607-3613.
- Bravo Cruz, A.G. and Damania, B. 2019. Models of Oncoproteins Encoded by Kaposi's Sarcoma-Associated Herpesvirus. *J Virol.* **93**(11).
- Brescia, P., Ortensi, B., Fornasari, L., Levi, D., Broggi, G. and Pelicci, G. 2013. CD133 is essential for glioblastoma stem cell maintenance. *Stem Cells.* **31**(5), pp.857-869.
- Bresnahan, W.A., Boldogh, I., Thompson, E.A. and Albrecht, T. 1996. Human cytomegalovirus inhibits cellular DNA synthesis and arrests productively infected cells in late G1. *Virology.* **224**(1), pp.150-160.
- Britt, W.J. and Mach, M. 1996. Human cytomegalovirus glycoproteins. *Intervirology.* **39**(5-6), pp.401-412.
- Brock, I., Krüger, M., Mertens, T. and von Einem, J. 2013. Nuclear targeting of human cytomegalovirus large tegument protein pUL48 is essential for viral growth. *J Virol.* **87**(10), pp.6005-6019.
- Broussard, G. and Damania, B. 2020. Regulation of KSHV Latency and Lytic Reactivation. *Viruses.* **12**(9).
- Bruno, L., Cortese, M., Monda, G., Gentile, M., Calò, S., Schiavetti, F., Zedda, L., Cattaneo, E., Piccioli, D., Schaefer, M., Notomista, E., Maione, D., Carfi, A., Merola, M. and Uematsu, Y. 2016. Human cytomegalovirus pUL10 interacts with leukocytes and impairs TCR-mediated T-cell activation. *Immunol Cell Biol.* **94**(9), pp.849-860.
- Bruno, S. and Darzynkiewicz, Z. 1992. Cell cycle dependent expression and stability of the nuclear protein detected by Ki-67 antibody in HL-60 cells. *Cell Prolif.* **25**(1), pp.31-40.
- Bryant, J.A., Finn, R.S., Slamon, D.J., Cloughesy, T.F. and Charles, A.C. 2004. EGF activates intracellular and intercellular calcium signaling by distinct pathways in tumor cells. *Cancer Biol Ther.* **3**(12), pp.1243-1249.
- Buehler, J., Zeltzer, S., Reitsma, J., Petrucelli, A., Umashankar, M., Rak, M., Zagallo, P., Schroeder, J., Terhune, S. and Goodrum, F. 2016. Opposing Regulation of the EGF Receptor: A Molecular Switch Controlling Cytomegalovirus Latency and Replication. *PLoS Pathog.* **12**(5), pe1005655.
- Buser, C., Walther, P., Mertens, T. and Michel, D. 2007. Cytomegalovirus primary envelopment occurs at large infoldings of the inner nuclear membrane. *J Virol.* **81**(6), pp.3042-3048.
- Buxmann, H., Hamprecht, K., Meyer-Wittkopf, M. and Friese, K. 2017. Primary Human Cytomegalovirus (HCMV) Infection in Pregnancy. *Dtsch Arztebl Int.* **114**(4), pp.45-52.
- Camarena, V., Kobayashi, M., Kim, J.Y., Roehm, P., Perez, R., Gardner, J., Wilson, A.C., Mohr, I. and Chao, M.V. 2010. Nature and duration of growth factor signaling through receptor tyrosine kinases regulates HSV-1 latency in neurons. *Cell Host Microbe.* **8**(4), pp.320-330.
- Cannon, M.J., Hyde, T.B. and Schmid, D.S. 2011. Review of cytomegalovirus shedding in bodily fluids and relevance to congenital cytomegalovirus infection. *Rev Med Virol.* **21**(4), pp.240-255.
- Cao, S., Wang, C., Zheng, Q., Qiao, Y., Xu, K., Jiang, T. and Wu, A. 2011. STAT5 regulates glioma cell invasion by pathways dependent and independent of STAT5 DNA binding. *Neurosci Lett.* **487**(2), pp.228-233.

- Cargnello, M. and Roux, P.P. 2011. Activation and function of the MAPKs and their substrates, the MAPK-activated protein kinases. *Microbiol Mol Biol Rev.* **75**(1), pp.50-83.
- Cavallin, L.E., Ma, Q., Naipauer, J., Gupta, S., Kurian, M., Locatelli, P., Romanelli, P., Nadji, M., Goldschmidt-Clermont, P.J. and Mesri, E.A. 2018. KSHV-induced ligand mediated activation of PDGF receptor- α drives Kaposi's sarcomagenesis. *PLoS Pathog.* **14**(7), pe1007175.
- Caviness, K., Bughio, F., Crawford, L.B., Streblow, D.N., Nelson, J.A., Caposio, P. and Goodrum, F. 2016. Complex Interplay of the UL136 Isoforms Balances Cytomegalovirus Replication and Latency. *mBio.* **7**(2), pe01986.
- Cazzalini, O., Sommati, S., Tillhon, M., Dutto, I., Bachi, A., Rapp, A., Nardo, T., Scovassi, A.I., Necchi, D., Cardoso, M.C., Stivala, L.A. and Prosperi, E. 2014. CBP and p300 acetylate PCNA to link its degradation with nucleotide excision repair synthesis. *Nucleic Acids Res.* **42**(13), pp.8433-8448.
- Cepeda, V., Esteban, M. and Fraile-Ramos, A. 2010. Human cytomegalovirus final envelopment on membranes containing both trans-Golgi network and endosomal markers. *Cell Microbiol.* **12**(3), pp.386-404.
- Cesarman, E., Damania, B., Krown, S.E., Martin, J., Bower, M. and Whitby, D. 2019. Kaposi sarcoma. *Nat Rev Dis Primers.* **5**(1), p9.
- Cesarman, E., Damania, B., Krown, S.E., Martin, J., Bower, M. and Whitby, D. 2019. Kaposi sarcoma. *Nat Rev Dis Primers.* **5**(1), p9.
- Cesarman, E., Mesri, E.A. and Gershengorn, M.C. 2000. Viral G protein-coupled receptor and Kaposi's sarcoma: a model of paracrine neoplasia? *J Exp Med.* **191**(3), pp.417-422.
- Chakraborty, S., Veettil, M.V. and Chandran, B. 2012. Kaposi's Sarcoma Associated Herpesvirus Entry into Target Cells. *Front Microbiol.* **3**, p6.
- Chakravarti, A., Zhai, G., Suzuki, Y., Sarkesh, S., Black, P.M., Muzikansky, A. and Loeffler, J.S. 2004. The prognostic significance of phosphatidylinositol 3-kinase pathway activation in human gliomas. *J Clin Oncol.* **22**(10), pp.1926-1933.
- Chan, G., Nogalski, M.T., Stevenson, E.V. and Yurochko, A.D. 2012. Human cytomegalovirus induction of a unique signalsome during viral entry into monocytes mediates distinct functional changes: a strategy for viral dissemination. *J Leukoc Biol.* **92**(4), pp.743-752.
- Chang, C.P., Vesole, D.H., Nelson, J., Oldstone, M.B. and Stinski, M.F. 1989. Identification and expression of a human cytomegalovirus early glycoprotein. *J Virol.* **63**(8), pp.3330-3337.
- Chang, J., Renne, R., Dittmer, D. and Ganem, D. 2000. Inflammatory cytokines and the reactivation of Kaposi's sarcoma-associated herpesvirus lytic replication. *Virology.* **266**(1), pp.17-25.
- Chang, W.L., Baumgarth, N., Yu, D. and Barry, P.A. 2004. Human cytomegalovirus-encoded interleukin-10 homolog inhibits maturation of dendritic cells and alters their functionality. *J Virol.* **78**(16), pp.8720-8731.
- Chang, Y., Moore, P.S., Talbot, S.J., Boshoff, C.H., Zarkowska, T., Godden-Kent, Paterson, H., Weiss, R.A. and Mitnacht, S. 1996. Cyclin encoded by KS herpesvirus. *Nature.* **382**(6590), p410.
- Charron, F., Stein, E., Jeong, J., McMahon, A.P. and Tessier-Lavigne, M. 2003. The morphogen sonic hedgehog is an axonal chemoattractant that collaborates with netrin-1 in midline axon guidance. *Cell.* **113**(1), pp.11-23.
- Chédotal, A., Kerjan, G. and Moreau-Fauvarque, C. 2005. The brain within the tumor: new roles for axon guidance molecules in cancers. *Cell Death Differ.*

12(8), pp.1044-1056.

Cheeran, M.C., Hu, S., Ni, H.T., Sheng, W., Palmquist, J.M., Peterson, P.K. and Lokensgard, J.R. 2005. Neural precursor cell susceptibility to human cytomegalovirus diverges along glial or neuronal differentiation pathways. *J Neurosci Res.* **82**(6), pp.839-850.

Cheeran, M.C., Lokensgard, J.R. and Schleiss, M.R. 2009. Neuropathogenesis of congenital cytomegalovirus infection: disease mechanisms and prospects for intervention. *Clin Microbiol Rev.* **22**(1), pp.99-126, Table of Contents.

Chen, D.H., Jiang, H., Lee, M., Liu, F. and Zhou, Z.H. 1999. Three-dimensional visualization of tegument/capsid interactions in the intact human cytomegalovirus. *Virology.* **260**(1), pp.10-16.

Chen, E.Y., Tan, C.M., Kou, Y., Duan, Q., Wang, Z., Meirelles, G.V., Clark, N.R. and Ma'ayan, A. 2013. Enrichr: interactive and collaborative HTML5 gene list enrichment analysis tool. *BMC Bioinformatics.* **14**, p128.

Chen, H.P. and Chan, Y.J. 2014. The oncomodulatory role of human cytomegalovirus in colorectal cancer: implications for clinical trials. *Front Oncol.* **4**, p314.

Chen, J. 2012. Roles of the PI3K/Akt pathway in Epstein-Barr virus-induced cancers and therapeutic implications. *World J Virol.* **1**(6), pp.154-161.

Chen, J.Y., Zheng, T.L., Zhou, T., Hu, P.W., Huang, M.J., Xu, X. and Pei, X.F. 2016. Human cytomegalovirus prevalence and distribution of glycoprotein B, O genotypes among hospitalized children with respiratory infections in West China, 2009–2014. *Tropical Medicine & International Health.* **21**(11), pp.1428-1434.

Chen, X.Z., Chen, H., Castro, F.A., Hu, J.K. and Brenner, H. 2015. Epstein-Barr virus infection and gastric cancer: a systematic review. *Medicine (Baltimore).* **94**(20), pe792.

Chen, Y.L., Law, P.Y. and Loh, H.H. 2008. NGF/PI3K signaling-mediated epigenetic regulation of delta opioid receptor gene expression. *Biochem Biophys Res Commun.* **368**(3), pp.755-760.

Cheng, S., Caviness, K., Buehler, J., Smithey, M., Nikolich-Žugich, J. and Goodrum, F. 2017. Transcriptome-wide characterization of human cytomegalovirus in natural infection and experimental latency. *Proc Natl Acad Sci U S A.* **114**(49), pp.E10586-E10595.

Cheng, S., Jiang, X., Yang, B., Wen, L., Zhao, F., Zeng, W.B., Liu, X.J., Dong, X., Sun, J.Y., Ming, Y.Z., Zhu, H., Rayner, S., Tang, Q., Fortunato, E. and Luo, M.H. 2017. Infected T98G glioblastoma cells support human cytomegalovirus reactivation from latency. *Virology.* **510**, pp.205-215.

Chiu, F.C., Norton, W.T. and Fields, K.L. 1981. The cytoskeleton of primary astrocytes in culture contains actin, glial fibrillary acidic protein, and the fibroblast-type filament protein, vimentin. *J Neurochem.* **37**(1), pp.147-155.

Chiu, Y.F. and Sugden, B. 2018. Plasmid Partitioning by Human Tumor Viruses. *J Virol.* **92**(9).

Chuang, J.H., Tung, L.C. and Lin, Y. 2015. Neural differentiation from embryonic stem cells in vitro: An overview of the signaling pathways. *World J Stem Cells.* **7**(2), pp.437-447.

Chugh, P., Matta, H., Schamus, S., Zachariah, S., Kumar, A., Richardson, J.A., Smith, A.L. and Chaudhary, P.M. 2005. Constitutive NF-kappaB activation, normal Fas-induced apoptosis, and increased incidence of lymphoma in human herpes virus 8 K13 transgenic mice. *Proc Natl Acad Sci U S A.* **102**(36), pp.12885-12890.

- Clarke, M.F., Dick, J.E., Dirks, P.B., Eaves, C.J., Jamieson, C.H., Jones, D.L., Visvader, J., Weissman, I.L. and Wahl, G.M. 2006. Cancer stem cells-- perspectives on current status and future directions: AACR Workshop on cancer stem cells. *Cancer Res.* **66**(19), pp.9339-9344.
- Close, W.L., Glassbrook, J.E., Gurczynski, S.J. and Pellett, P.E. 2018. Infection-Induced Changes Within the Endocytic Recycling Compartment Suggest a Roadmap of Human Cytomegalovirus Egress. *Front Microbiol.* **9**, p1888.
- Cobbs, C., Khan, S., Matlaf, L., McAllister, S., Zider, A., Yount, G., Rahlin, K., Harkins, L., Bezrookove, V., Singer, E. and Soroceanu, L. 2014. HCMV glycoprotein B is expressed in primary glioblastomas and enhances growth and invasiveness via PDGFR-alpha activation. *Oncotarget.* **5**(4), pp.1091-1100.
- Cobbs, C.S., Harkins, L., Samanta, M., Gillespie, G.Y., Bharara, S., King, P.H., Nabors, L.B., Cobbs, C.G. and Britt, W.J. 2002. Human cytomegalovirus infection and expression in human malignant glioma. *Cancer Res.* **62**(12), pp.3347-3350.
- Cobbs, C.S., Soroceanu, L., Denham, S., Zhang, W., Britt, W.J., Pieper, R. and Kraus, M.H. 2007. Human cytomegalovirus induces cellular tyrosine kinase signaling and promotes glioma cell invasiveness. *J Neurooncol.* **85**(3), pp.271-280.
- Cobbs, C.S., Soroceanu, L., Denham, S., Zhang, W. and Kraus, M.H. 2008. Modulation of oncogenic phenotype in human glioma cells by cytomegalovirus IE1-mediated mitogenicity. *Cancer Res.* **68**(3), pp.724-730.
- Cohen, J.I. 2020. Herpesvirus latency. *J Clin Invest.* **130**(7), pp.3361-3369.
- Cohrs, R.J. and Gilden, D.H. 2003. Varicella zoster virus transcription in latently-infected human ganglia. *Anticancer Res.* **23**(3A), pp.2063-2069.
- Cojohari, O., Peppenelli, M.A. and Chan, G.C. 2016. Human Cytomegalovirus Induces an Atypical Activation of Akt To Stimulate the Survival of Short-Lived Monocytes. *J Virol.* **90**(14), pp.6443-6452.
- Colardo, M., Segatto, M. and Di Bartolomeo, S. 2021. Targeting RTK-PI3K-mTOR Axis in Gliomas: An Update. *Int J Mol Sci.* **22**(9).
- Collins-McMillen, D., Buehler, J., Peppenelli, M. and Goodrum, F. 2018. Molecular Determinants and the Regulation of Human Cytomegalovirus Latency and Reactivation. *Viruses.* **10**(8).
- Collins-McMillen, D., Rak, M., Buehler, J.C., Igarashi-Hayes, S., Kamil, J.P., Moorman, N.J. and Goodrum, F. 2019. Alternative promoters drive human cytomegalovirus reactivation from latency. *Proc Natl Acad Sci U S A.* **116**(35), pp.17492-17497.
- Conboy, T.J., Pass, R.F., Stagno, S., Alford, C.A., Myers, G.J., Britt, W.J., McCollister, F.P., Summers, M.N., McFarland, C.E. and Boll, T.J. 1987. Early clinical manifestations and intellectual outcome in children with symptomatic congenital cytomegalovirus infection. *J Pediatr.* **111**(3), pp.343-348.
- Corbeil, D., Karbanová, J., Fargeas, C.A. and Jászai, J. 2013. Prominin-1 (CD133): Molecular and Cellular Features Across Species. *Adv Exp Med Biol.* **777**, pp.3-24.
- Crough, T., Beagley, L., Smith, C., Jones, L., Walker, D.G. and Khanna, R. 2012. Ex vivo functional analysis, expansion and adoptive transfer of cytomegalovirus-specific T-cells in patients with glioblastoma multiforme. *Immunol Cell Biol.* **90**(9), pp.872-880.
- Crough, T. and Khanna, R. 2009. Immunobiology of human cytomegalovirus: from bench to bedside. *Clin Microbiol Rev.* **22**(1), pp.76-98, Table of Contents.

- Cui, C.P., Zhang, Y., Wang, C., Yuan, F., Li, H., Yao, Y., Chen, Y., Li, C., Wei, W., Liu, C.H., He, F., Liu, Y. and Zhang, L. 2018. Dynamic ubiquitylation of Sox2 regulates proteostasis and governs neural progenitor cell differentiation. *Nat Commun.* **9**(1), p4648.
- Dai, Y., Tang, Y., He, F., Zhang, Y., Cheng, A., Gan, R. and Wu, Y. 2012. Screening and functional analysis of differentially expressed genes in EBV-transformed lymphoblasts. *Virology* **9**, p77.
- Daida, K., Ishiguro, Y., Eguchi, H., Machida, Y., Hattori, N. and Miwa, H. 2016. Cytomegalovirus-associated encephalomyelitis in an immunocompetent adult: a two-stage attack of direct viral and delayed immune-mediated invasions. case report. *BMC Neurol.* **16**(1), p223.
- D'Aiuto, L., Di Maio, R., Heath, B., Raimondi, G., Milosevic, J., Watson, A.M., Bamne, M., Parks, W.T., Yang, L., Lin, B., Miki, T., Mich-Basso, J.D., Arav-Boger, R., Sibille, E., Sabunciyar, S., Yolken, R. and Nimgaonkar, V. 2012. Human induced pluripotent stem cell-derived models to investigate human cytomegalovirus infection in neural cells. *PLoS One.* **7**(11), pe49700.
- Dang, L., White, D.W., Gross, S., Bennett, B.D., Bittinger, M.A., Driggers, E.M., Fantin, V.R., Jang, H.G., Jin, S., Keenan, M.C., Marks, K.M., Prins, R.M., Ward, P.S., Yen, K.E., Liao, L.M., Rabinowitz, J.D., Cantley, L.C., Thompson, C.B., Vander Heiden, M.G. and Su, S.M. 2009. Cancer-associated IDH1 mutations produce 2-hydroxyglutarate. *Nature.* **462**(7274), pp.739-744.
- Das, S., Ortiz, D.A., Gurczynski, S.J., Khan, F. and Pellett, P.E. 2014. Identification of human cytomegalovirus genes important for biogenesis of the cytoplasmic virion assembly complex. *J Virol.* **88**(16), pp.9086-9099.
- Davis, D.A., Rinderknecht, A.S., Zoetewij, J.P., Aoki, Y., Read-Connoles, E.L., Tosato, G., Blauvelt, A. and Yarchoan, R. 2001. Hypoxia induces lytic replication of Kaposi sarcoma-associated herpesvirus. *Blood.* **97**(10), pp.3244-3250.
- De Leo, A., Calderon, A. and Lieberman, P.M. 2020. Control of Viral Latency by Episome Maintenance Proteins. *Trends Microbiol.* **28**(2), pp.150-162.
- de Wit, R.H., Mujčić-Delić, A., van Senten, J.R., Fraile-Ramos, A., Siderius, M. and Smit, M.J. 2016. Human cytomegalovirus encoded chemokine receptor US28 activates the HIF-1 α /PKM2 axis in glioblastoma cells. *Oncotarget.* **7**(42), pp.67966-67985.
- Debanne, D., Campanac, E., Bialowas, A., Carlier, E. and Alcaraz, G. 2011. Axon physiology. *Physiol Rev.* **91**(2), pp.555-602.
- Decker, T. and Kovarik, P. 2000. Serine phosphorylation of STATs. *Oncogene.* **19**(21), pp.2628-2637.
- Deczkowska, A., Keren-Shaul, H., Weiner, A., Colonna, M., Schwartz, M. and Amit, I. 2018. Disease-Associated Microglia: A Universal Immune Sensor of Neurodegeneration. *Cell.* **173**(5), pp.1073-1081.
- Dehmelt, L. and Halpain, S. 2005. The MAP2/Tau family of microtubule-associated proteins. *Genome Biol.* **6**(1), p204.
- Depledge, D.P., Sadaoka, T. and Ouwendijk, W.J.D. 2018. Molecular Aspects of Varicella-Zoster Virus Latency. *Viruses.* **10**(7).
- Desai, P.J. 2000. A null mutation in the UL36 gene of herpes simplex virus type 1 results in accumulation of unenveloped DNA-filled capsids in the cytoplasm of infected cells. *J Virol.* **74**(24), pp.11608-11618.
- DeYoung, A., Pennelly, R.R., Tan-Wilson, A.L. and Noble, R.W. 1976. Kinetic studies on the binding affinity of human hemoglobin for the 4th carbon monoxide molecule, L4. *J Biol Chem.* **251**(21), pp.6692-6698.

- Dittmer, D. and Mocarski, E.S. 1997. Human cytomegalovirus infection inhibits G1/S transition. *J Virol.* **71**(2), pp.1629-1634.
- Doetsch, F., Caillé, I., Lim, D.A., García-Verdugo, J.M. and Alvarez-Buylla, A. 1999. Subventricular zone astrocytes are neural stem cells in the adult mammalian brain. *Cell.* **97**(6), pp.703-716.
- Dolan, A., Cunningham, C., Hector, R.D., Hassan-Walker, A.F., Lee, L., Addison, C., Dargan, D.J., McGeoch, D.J., Gatherer, D., Emery, V.C., Griffiths, P.D., Sinzger, C., McSharry, B.P., Wilkinson, G.W. and Davison, A.J. 2004. Genetic content of wild-type human cytomegalovirus. *J Gen Virol.* **85**(Pt 5), pp.1301-1312.
- Dollard, S.C., Grosse, S.D. and Ross, D.S. 2007. New estimates of the prevalence of neurological and sensory sequelae and mortality associated with congenital cytomegalovirus infection. *Rev Med Virol.* **17**(5), pp.355-363.
- Dowsett, M., Nielsen, T.O., A'Hern, R., Bartlett, J., Coombes, R.C., Cuzick, J., Ellis, M., Henry, N.L., Hugh, J.C., Lively, T., McShane, L., Paik, S., Penault-Llorca, F., Prudkin, L., Regan, M., Salter, J., Sotiriou, C., Smith, I.E., Viale, G., Zujewski, J.A., Hayes, D.F. and Group, I.K.-i.B.C.W. 2011. Assessment of Ki67 in breast cancer: recommendations from the International Ki67 in Breast Cancer working group. *J Natl Cancer Inst.* **103**(22), pp.1656-1664.
- Drew, W.L., Miner, R.C., Marousek, G.I. and Chou, S. 2006. Maribavir sensitivity of cytomegalovirus isolates resistant to ganciclovir, cidofovir or foscarnet. *J Clin Virol.* **37**(2), pp.124-127.
- Du, Z., Jia, D., Liu, S., Wang, F., Li, G., Zhang, Y., Cao, X., Ling, E.A. and Hao, A. 2009. Oct4 is expressed in human gliomas and promotes colony formation in glioma cells. *Glia.* **57**(7), pp.724-733.
- Duan, W., Zhang, Y.P., Hou, Z., Huang, C., Zhu, H., Zhang, C.Q. and Yin, Q. 2016. Novel Insights into NeuN: from Neuronal Marker to Splicing Regulator. *Mol Neurobiol.* **53**(3), pp.1637-1647.
- Duarte, C.W., Willey, C.D., Zhi, D., Cui, X., Harris, J.J., Vaughan, L.K., Mehta, T., McCubrey, R.O., Khodarev, N.N., Weichselbaum, R.R. and Gillespie, G.Y. 2012. Expression signature of IFN/STAT1 signaling genes predicts poor survival outcome in glioblastoma multiforme in a subtype-specific manner. *PLoS One.* **7**(1), pe29653.
- Dunn, D.M. and Munger, J. 2020. Interplay Between Calcium and AMPK Signaling in Human Cytomegalovirus Infection. *Front Cell Infect Microbiol.* **10**, p384.
- Dupont, L., Du, L., Poulter, M., Choi, S., McIntosh, M. and Reeves, M.B. 2019. Src family kinase activity drives cytomegalovirus reactivation by recruiting MOZ histone acetyltransferase activity to the viral promoter. *J Biol Chem.* **294**(35), pp.12901-12910.
- Dziurzynski, K., Wei, J., Qiao, W., Hatiboglu, M.A., Kong, L.Y., Wu, A., Wang, Y., Cahill, D., Levine, N., Prabhu, S., Rao, G., Sawaya, R. and Heimberger, A.B. 2011. Glioma-associated cytomegalovirus mediates subversion of the monocyte lineage to a tumor propagating phenotype. *Clin Cancer Res.* **17**(14), pp.4642-4649.
- E, X., Meraner, P., Lu, P., Perreira, J.M., Aker, A.M., McDougall, W.M., Zhuge, R., Chan, G.C., Gerstein, R.M., Caposio, P., Yurochko, A.D., Brass, A.L. and Kowalik, T.F. 2019. OR14I1 is a receptor for the human cytomegalovirus pentameric complex and defines viral epithelial cell tropism. *Proceedings of the National Academy of Sciences.* **116**(14), p7043.
- Edwards, A.M., Bochkarev, A. and Frappier, L. 1998. Origin DNA-binding

- proteins. *Curr Opin Struct Biol.* **8**(1), pp.49-53.
- El Chaer, F., Shah, D.P. and Chemaly, R.F. 2016. How I treat resistant cytomegalovirus infection in hematopoietic cell transplantation recipients. *Blood.* **128**(23), pp.2624-2636.
- Eliassen, E., Lum, E., Pritchett, J., Ongradi, J., Krueger, G., Crawford, J.R., Phan, T.L., Ablashi, D. and Hudnall, S.D. 2018. Human Herpesvirus 6 and Malignancy: A Review. *Front Oncol.* **8**, p512.
- Emery, V.C. 2001. Investigation of CMV disease in immunocompromised patients. *J Clin Pathol.* **54**(2), pp.84-88.
- Enders, G., Daiminger, A., Bäder, U., Exler, S. and Enders, M. 2011. Intrauterine transmission and clinical outcome of 248 pregnancies with primary cytomegalovirus infection in relation to gestational age. *J Clin Virol.* **52**(3), pp.244-246.
- Engelman, J.A., Luo, J. and Cantley, L.C. 2006. The evolution of phosphatidylinositol 3-kinases as regulators of growth and metabolism. *Nat Rev Genet.* **7**(8), pp.606-619.
- Englund, C., Fink, A., Lau, C., Pham, D., Daza, R.A., Bulfone, A., Kowalczyk, T. and Hevner, R.F. 2005. Pax6, Tbr2, and Tbr1 are expressed sequentially by radial glia, intermediate progenitor cells, and postmitotic neurons in developing neocortex. *J Neurosci.* **25**(1), pp.247-251.
- EPSTEIN, M.A., ACHONG, B.G. and BARR, Y.M. 1964. VIRUS PARTICLES IN CULTURED LYMPHOBLASTS FROM BURKITT'S LYMPHOMA. *Lancet.* **1**(7335), pp.702-703.
- Eriksson, P.S., Perfilieva, E., Björk-Eriksson, T., Alborn, A.M., Nordborg, C., Peterson, D.A. and Gage, F.H. 1998. Neurogenesis in the adult human hippocampus. *Nat Med.* **4**(11), pp.1313-1317.
- Estes, J.E. and Huang, E.S. 1977. Stimulation of cellular thymidine kinases by human cytomegalovirus. *J Virol.* **24**(1), pp.13-21.
- Fan, Q.W. and Weiss, W.A. 2010. Targeting the RTK-PI3K-mTOR axis in malignant glioma: overcoming resistance. *Curr Top Microbiol Immunol.* **347**, pp.279-296.
- Feingold, K.R., Anawalt, B., Boyce, A., Chrousos, G., de Herder, W.W., Dhatariya, K., Dungan, K., Hershman, J.M., Hofland, J., Kalra, S., Kaltsas, G., Koch, C., Kopp, P., Korbonits, M., Kovacs, C.S., Kuohung, W., Laferrère, B., Levy, M., McGee, E.A., McLachlan, R., Morley, J.E., New, M., Purnell, J., Sahay, R., Singer, F., Sperling, M.A., Stratakis, C.A., Trencé, D.L. and Wilson, D.P. 2000. Endotext.
- Fiacco, T.A., Agulhon, C. and McCarthy, K.D. 2009. Sorting out astrocyte physiology from pharmacology. *Annu Rev Pharmacol Toxicol.* **49**, pp.151-174.
- Fish, K.N., Soderberg-Naucler, C., Mills, L.K., Stenglein, S. and Nelson, J.A. 1998. Human cytomegalovirus persistently infects aortic endothelial cells. *J Virol.* **72**(7), pp.5661-5668.
- Fong, H., Hohenstein, K.A. and Donovan, P.J. 2008. Regulation of self-renewal and pluripotency by Sox2 in human embryonic stem cells. *Stem Cells.* **26**(8), pp.1931-1938.
- Fornara, O., Bartek, J., Rahbar, A., Odeberg, J., Khan, Z., Peredo, I., Hamerlik, P., Stragliotto, G., Landázuri, N. and Söderberg-Nauclér, C. 2016. Cytomegalovirus infection induces a stem cell phenotype in human primary glioblastoma cells: prognostic significance and biological impact. *Cell Death Differ.* **23**(2), pp.261-269.
- Forte, E., Zhang, Z., Thorp, E.B. and Hummel, M. 2020. Cytomegalovirus

- Latency and Reactivation: An Intricate Interplay With the Host Immune Response. *Front Cell Infect Microbiol.* **10**, p130.
- Fortunato, E.A., Sommer, M.H., Yoder, K. and Spector, D.H. 1997. Identification of domains within the human cytomegalovirus major immediate-early 86-kilodalton protein and the retinoblastoma protein required for physical and functional interaction with each other. *J Virol.* **71**(11), pp.8176-8185.
- Foster, H., Piper, K., DePledge, L., Li, H.F., Scanlan, J., Jae-Guen, Y., Boeckh, M. and Cobbs, C. 2019. Human cytomegalovirus seropositivity is associated with decreased survival in glioblastoma patients. *Neurooncol Adv.* **1**(1), pvdz020.
- Foulon, I., Naessens, A., Foulon, W., Casteels, A. and Gordts, F. 2008. Hearing loss in children with congenital cytomegalovirus infection in relation to the maternal trimester in which the maternal primary infection occurred. *Pediatrics.* **122**(6), pp.e1123-1127.
- Fowler, K.B., Stagno, S., Pass, R.F., Britt, W.J., Boll, T.J. and Alford, C.A. 1992. The outcome of congenital cytomegalovirus infection in relation to maternal antibody status. *N Engl J Med.* **326**(10), pp.663-667.
- Frappier, L. 2012. The Epstein-Barr Virus EBNA1 Protein. *Scientifica (Cairo).* **2012**, p438204.
- Frascaroli, G., Lecher, C., Varani, S., Setz, C., van der Merwe, J., Brune, W. and Mertens, T. 2018. Human Macrophages Escape Inhibition of Major Histocompatibility Complex-Dependent Antigen Presentation by Cytomegalovirus and Drive Proliferation and Activation of Memory CD4. *Front Immunol.* **9**, p1129.
- Frascaroli, G., Varani, S., Moepps, B., Sinzger, C., Landini, M.P. and Mertens, T. 2006. Human cytomegalovirus subverts the functions of monocytes, impairing chemokine-mediated migration and leukocyte recruitment. *J Virol.* **80**(15), pp.7578-7589.
- Friborg, J., Kong, W., Hottiger, M.O. and Nabel, G.J. 1999. p53 inhibition by the LANA protein of KSHV protects against cell death. *Nature.* **402**(6764), pp.889-894.
- Friedmann-Morvinski, D., Bushong, E.A., Ke, E., Soda, Y., Marumoto, T., Singer, O., Ellisman, M.H. and Verma, I.M. 2012. Dedifferentiation of neurons and astrocytes by oncogenes can induce gliomas in mice. *Science.* **338**(6110), pp.1080-1084.
- Fritsch, B. and Northcutt, R.G. 1993. Origin and migration of trochlear, oculomotor and abducent motor neurons in *Petromyzon marinus* L. *Brain Res Dev Brain Res.* **74**(1), pp.122-126.
- Gabaev, I., Steinbrück, L., Pokoyski, C., Pich, A., Stanton, R.J., Schwinzer, R., Schulz, T.F., Jacobs, R., Messerle, M. and Kay-Fedorov, P.C. 2011. The human cytomegalovirus UL11 protein interacts with the receptor tyrosine phosphatase CD45, resulting in functional paralysis of T cells. *PLoS Pathog.* **7**(12), pe1002432.
- Gabor, F., Jahn, G., Sedmak, D.D. and Sinzger, C. 2020. Downregulation of MHC Class I Molecules by HCMV Occurs During All Phases of Viral Replication but Is Not Always Complete. *Front Cell Infect Microbiol.* **10**, p283.
- Gabrielli, L., Bonasoni, M.P., Lazzarotto, T., Lega, S., Santini, D., Foschini, M.P., Guerra, B., Baccolini, F., Piccirilli, G., Chierighin, A., Petrisli, E., Gardini, G., Lanari, M. and Landini, M.P. 2009. Histological findings in fetuses congenitally infected by cytomegalovirus. *J Clin Virol.* **46 Suppl 4**, pp.S16-21.
- Gabrielli, L., Bonasoni, M.P., Santini, D., Piccirilli, G., Chierighin, A., Petrisli,

- E., Dolcetti, R., Guerra, B., Piccioli, M., Lanari, M., Landini, M.P. and Lazzarotto, T. 2012. Congenital cytomegalovirus infection: patterns of fetal brain damage. *Clin Microbiol Infect.* **18**(10), pp.E419-427.
- Gao, C.F., Xie, Q., Su, Y.L., Koeman, J., Khoo, S.K., Gustafson, M., Knudsen, B.S., Hay, R., Shinomiya, N. and Vande Woude, G.F. 2005. Proliferation and invasion: plasticity in tumor cells. *Proc Natl Acad Sci U S A.* **102**(30), pp.10528-10533.
- Gao, X., Ikuta, K., Tajima, M. and Sairenji, T. 2001. 12-O-tetradecanoylphorbol-13-acetate induces Epstein-Barr virus reactivation via NF-kappaB and AP-1 as regulated by protein kinase C and mitogen-activated protein kinase. *Virology.* **286**(1), pp.91-99.
- Garcia-Martinez, A., Alenda, C., Irlles, E., Ochoa, E., Quintanar, T., Rodriguez-Lescure, A., Soto, J.L. and Barbera, V.M. 2017. Lack of cytomegalovirus detection in human glioma. *Virology.* **14**(1), p216.
- Gatherer, D., Seirafian, S., Cunningham, C., Holton, M., Dargan, D.J., Baluchova, K., Hector, R.D., Galbraith, J., Herzyk, P., Wilkinson, G.W. and Davison, A.J. 2011. High-resolution human cytomegalovirus transcriptome. *Proc Natl Acad Sci U S A.* **108**(49), pp.19755-19760.
- Gerdes, J., Lemke, H., Baisch, H., Wacker, H.H., Schwab, U. and Stein, H. 1984. Cell cycle analysis of a cell proliferation-associated human nuclear antigen defined by the monoclonal antibody Ki-67. *J Immunol.* **133**(4), pp.1710-1715.
- Gerdes, J., Stein, H., Pileri, S., Rivano, M.T., Gobbi, M., Ralfkiaer, E., Nielsen, K.M., Pallesen, G., Bartels, H. and Palestro, G. 1987. Prognostic relevance of tumour-cell growth fraction in malignant non-Hodgkin's lymphomas. *Lancet.* **2**(8556), pp.448-449.
- Gerna, G., Sarasini, A., Patrone, M., Percivalle, E., Fiorina, L., Campanini, G., Gallina, A., Baldanti, F. and Revello, M.G. 2008. Human cytomegalovirus serum neutralizing antibodies block virus infection of endothelial/epithelial cells, but not fibroblasts, early during primary infection. *J Gen Virol.* **89**(Pt 4), pp.853-865.
- Gibson, W. 2008. Structure and formation of the cytomegalovirus virion. *Curr Top Microbiol Immunol.* **325**, pp.187-204.
- Glumac, P.M. and LeBeau, A.M. 2018. The role of CD133 in cancer: a concise review. *Clin Transl Med.* **7**(1), p18.
- Godden-Kent, D., Talbot, S.J., Boshoff, C., Chang, Y., Moore, P., Weiss, R.A. and Mitnacht, S. 1997. The cyclin encoded by Kaposi's sarcoma-associated herpesvirus stimulates cdk6 to phosphorylate the retinoblastoma protein and histone H1. *J Virol.* **71**(6), pp.4193-4198.
- Goldner, T., Hewlett, G., Ettischer, N., Ruebsamen-Schaeff, H., Zimmermann, H. and Lischka, P. 2011. The novel anticytomegalovirus compound AIC246 (Letermovir) inhibits human cytomegalovirus replication through a specific antiviral mechanism that involves the viral terminase. *J Virol.* **85**(20), pp.10884-10893.
- Goncalves, P.H., Ziegelbauer, J., Uldrick, T.S. and Yarchoan, R. 2017. Kaposi sarcoma herpesvirus-associated cancers and related diseases. *Curr Opin HIV AIDS.* **12**(1), pp.47-56.
- Goodrum, F., Caviness, K. and Zagallo, P. 2012. Human cytomegalovirus persistence. *Cell Microbiol.* **14**(5), pp.644-655.
- Grassian, A.R., Parker, S.J., Davidson, S.M., Divakaruni, A.S., Green, C.R., Zhang, X., Slocum, K.L., Pu, M., Lin, F., Vickers, C., Joud-Caldwell, C., Chung,

- F., Yin, H., Handly, E.D., Straub, C., Growney, J.D., Vander Heiden, M.G., Murphy, A.N., Pagliarini, R. and Metallo, C.M. 2014. IDH1 mutations alter citric acid cycle metabolism and increase dependence on oxidative mitochondrial metabolism. *Cancer Res.* **74**(12), pp.3317-3331.
- Greijer, A.E., Dekkers, C.A. and Middeldorp, J.M. 2000. Human cytomegalovirus virions differentially incorporate viral and host cell RNA during the assembly process. *J Virol.* **74**(19), pp.9078-9082.
- Grinde, B. 2013. Herpesviruses: latency and reactivation - viral strategies and host response. *J Oral Microbiol.* **5**.
- Gross, R.E., Mehler, M.F., Mabie, P.C., Zang, Z., Santschi, L. and Kessler, J.A. 1996. Bone morphogenetic proteins promote astroglial lineage commitment by mammalian subventricular zone progenitor cells. *Neuron.* **17**(4), pp.595-606.
- Groves, I.J., Sinclair, J.H. and Wills, M.R. 2020. Bromodomain Inhibitors as Therapeutics for Herpesvirus-Related Disease: All BETs Are Off? *Front Cell Infect Microbiol.* **10**, p329.
- Guang, S., Pang, N., Deng, X., Yang, L., He, F., Wu, L., Chen, C., Yin, F. and Peng, J. 2018. Synaptopathology Involved in Autism Spectrum Disorder. *Front Cell Neurosci.* **12**, p470.
- Guito, J. and Lukac, D.M. 2015. KSHV reactivation and novel implications of protein isomerization on lytic switch control. *Viruses.* **7**(1), pp.72-109.
- Hahn, G., Revello, M.G., Patrone, M., Percivalle, E., Campanini, G., Sarasini, A., Wagner, M., Gallina, A., Milanese, G., Koszinowski, U., Baldanti, F. and Gerna, G. 2004. Human Cytomegalovirus UL131-128 Genes Are Indispensable for Virus Growth in Endothelial Cells and Virus Transfer to Leukocytes. *Journal of Virology.* **78**(18), p10023.
- Haidar Ahmad, S., Pasquereau, S., El Baba, R., Nehme, Z., Lewandowski, C. and Herbein, G. 2021. Distinct Oncogenic Transcriptomes in Human Mammary Epithelial Cells Infected With Cytomegalovirus. *Front Immunol.* **12**, p772160.
- Hakin-Smith, V., Jellinek, D.A., Levy, D., Carroll, T., Teo, M., Timperley, W.R., McKay, M.J., Reddel, R.R. and Royds, J.A. 2003. Alternative lengthening of telomeres and survival in patients with glioblastoma multiforme. *Lancet.* **361**(9360), pp.836-838.
- Halassa, M.M. and Haydon, P.G. 2010. Integrated brain circuits: astrocytic networks modulate neuronal activity and behavior. *Annu Rev Physiol.* **72**, pp.335-355.
- Halliday, J., Helmy, K., Pattwell, S.S., Pitter, K.L., LaPlant, Q., Ozawa, T. and Holland, E.C. 2014. In vivo radiation response of proneural glioma characterized by protective p53 transcriptional program and proneural-mesenchymal shift. *Proc Natl Acad Sci U S A.* **111**(14), pp.5248-5253.
- Han, D., Byun, S.H., Kim, J., Kwon, M., Pleasure, S.J., Ahn, J.H. and Yoon, K. 2017. Human Cytomegalovirus IE2 Protein Disturbs Brain Development by the Dysregulation of Neural Stem Cell Maintenance and the Polarization of Migrating Neurons. *J Virol.* **91**(17).
- Hanahan, D. 2022. Hallmarks of Cancer: New Dimensions. *Cancer Discov.* **12**(1), pp.31-46.
- Hanahan, D. and Weinberg, R.A. 2011. Hallmarks of cancer: the next generation. *Cell.* **144**(5), pp.646-674.
- Hancock, M.H., Crawford, L.B., Pham, A.H., Mitchell, J., Struthers, H.M., Yurochko, A.D., Caposio, P. and Nelson, J.A. 2020. Human Cytomegalovirus miRNAs Regulate TGF- β to Mediate Myelosuppression while Maintaining Viral Latency in CD34. *Cell Host Microbe.* **27**(1), pp.104-114.e104.

- Hansen, S.G., Powers, C.J., Richards, R., Ventura, A.B., Ford, J.C., Siess, D., Axthelm, M.K., Nelson, J.A., Jarvis, M.A., Picker, L.J. and Fröh, K. 2010. Evasion of CD8+ T cells is critical for superinfection by cytomegalovirus. *Science*. **328**(5974), pp.102-106.
- Hara, A. and Okayasu, I. 2004. Cyclooxygenase-2 and inducible nitric oxide synthase expression in human astrocytic gliomas: correlation with angiogenesis and prognostic significance. *Acta Neuropathol.* **108**(1), pp.43-48.
- Harkins, L., Volk, A.L., Samanta, M., Mikolaenko, I., Britt, W.J., Bland, K.I. and Cobbs, C.S. 2002. Specific localisation of human cytomegalovirus nucleic acids and proteins in human colorectal cancer. *Lancet*. **360**(9345), pp.1557-1563.
- Harkins, L.E., Matlaf, L.A., Soroceanu, L., Klemm, K., Britt, W.J., Wang, W., Bland, K.I. and Cobbs, C.S. 2010. Detection of human cytomegalovirus in normal and neoplastic breast epithelium. *Herpesviridae*. **1**(1), p8.
- Hartmann, P., Ramseier, A., Gudat, F., Mihatsch, M.J. and Polasek, W. 1994. [Normal weight of the brain in adults in relation to age, sex, body height and weight]. *Pathologe*. **15**(3), pp.165-170.
- Harvala, H., Stewart, C., Muller, K., Burns, S., Marson, L., MacGilchrist, A. and Johannessen, I. 2013. High risk of cytomegalovirus infection following solid organ transplantation despite prophylactic therapy. *J Med Virol*. **85**(5), pp.893-898.
- Hatton, O.L., Harris-Arnold, A., Schaffert, S., Krams, S.M. and Martinez, O.M. 2014. The interplay between Epstein-Barr virus and B lymphocytes: implications for infection, immunity, and disease. *Immunol Res*. **58**(2-3), pp.268-276.
- Heimberger, A.B., Sun, W., Hussain, S.F., Dey, M., Crutcher, L., Aldape, K., Gilbert, M., Hassenbusch, S.J., Sawaya, R., Schmittling, B., Archer, G.E., Mitchell, D.A., Bigner, D.D. and Sampson, J.H. 2008. Immunological responses in a patient with glioblastoma multiforme treated with sequential courses of temozolomide and immunotherapy: case study. *Neuro Oncol*. **10**(1), pp.98-103.
- Herbein, G. 2018. The Human Cytomegalovirus, from Oncomodulation to Oncogenesis. *Viruses*. **10**(8).
- Herculano-Houzel, S. 2009. The human brain in numbers: a linearly scaled-up primate brain. *Front Hum Neurosci*. **3**, p31.
- Hetzenecker, S., Helenius, A. and Krzyzaniak, M.A. 2016. HCMV Induces Macropinocytosis for Host Cell Entry in Fibroblasts. *Traffic*. **17**(4), pp.351-368.
- Hewitt, E.W. 2003. The MHC class I antigen presentation pathway: strategies for viral immune evasion. *Immunology*. **110**(2), pp.163-169.
- Homman-Loudiyi, M., Hultenby, K., Britt, W. and Söderberg-Nauclér, C. 2003. Envelopment of human cytomegalovirus occurs by budding into Golgi-derived vacuole compartments positive for gB, Rab 3, trans-golgi network 46, and mannosidase II. *J Virol*. **77**(5), pp.3191-3203.
- Honda, H. and Miyake, A. 1975. Taxic to a conjugation-inducing substance in the ciliate *Blepharisma*. *Nature*. **257**(5528), pp.678-680.
- Hong, Y., Jeong, H., Park, K., Lee, S., Shim, J.Y., Kim, H., Song, Y., Park, S., Park, H.Y., Kim, V.N. and Ahn, K. 2021. STING facilitates nuclear import of herpesvirus genome during infection. *Proc Natl Acad Sci U S A*. **118**(33).
- Howard, M.K., Burke, L.C., Mailhos, C., Pizzey, A., Gilbert, C.S., Lawson, W.D., Collins, M.K., Thomas, N.S. and Latchman, D.S. 1993. Cell cycle arrest of proliferating neuronal cells by serum deprivation can result in either apoptosis or differentiation. *J Neurochem*. **60**(5), pp.1783-1791.
- Hu, J., Ho, A.L., Yuan, L., Hu, B., Hua, S., Hwang, S.S., Zhang, J., Hu, T.,

- Zheng, H., Gan, B., Wu, G., Wang, Y.A., Chin, L. and DePinho, R.A. 2013. From the Cover: Neutralization of terminal differentiation in gliomagenesis. *Proc Natl Acad Sci U S A*. **110**(36), pp.14520-14527.
- Hu, L., Wen, Z., Chen, J., Chen, Y., Jin, L. and Shi, H. 2020. The cytomegalovirus UL146 gene product vCXCL1 promotes the resistance of hepatic cells to CD8. *Biochem Biophys Res Commun*. **532**(3), pp.393-399.
- Huang, R., Qian, D., Hu, M., Zhang, X., Song, J., Li, L., Chen, H. and Wang, B. 2015. Association between human cytomegalovirus infection and histone acetylation level in various histological types of glioma. *Oncol Lett*. **10**(5), pp.2812-2820.
- Huber, M.T. and Compton, T. 1998. The Human Cytomegalovirus UL74 Gene Encodes the Third Component of the Glycoprotein H-Glycoprotein L-Containing Envelope Complex. *Journal of Virology*. **72**(10), p8191.
- Hung, H.C., Liu, C.C., Chuang, J.Y., Su, C.L. and Gean, P.W. 2020. Inhibition of Sonic Hedgehog Signaling Suppresses Glioma Stem-Like Cells Likely Through Inducing Autophagic Cell Death. *Front Oncol*. **10**, p1233.
- Hurley, J.B., Simon, M.I., Teplow, D.B., Robishaw, J.D. and Gilman, A.G. 1984. Homologies between signal transducing G proteins and ras gene products. *Science*. **226**(4676), pp.860-862.
- Hutton, S.R. and Pevny, L.H. 2011. SOX2 expression levels distinguish between neural progenitor populations of the developing dorsal telencephalon. *Dev Biol*. **352**(1), pp.40-47.
- Ignatova, T.N., Kukekov, V.G., Laywell, E.D., Suslov, O.N., Vrionis, F.D. and Steindler, D.A. 2002. Human cortical glial tumors contain neural stem-like cells expressing astroglial and neuronal markers in vitro. *Glia*. **39**(3), pp.193-206.
- Isaacson, M.K., Juckem, L.K. and Compton, T. 2008. Virus entry and innate immune activation. *Curr Top Microbiol Immunol*. **325**, pp.85-100.
- Isomura, H., Stinski, M.F., Murata, T., Yamashita, Y., Kanda, T., Toyokuni, S. and Tsurumi, T. 2011. The human cytomegalovirus gene products essential for late viral gene expression assemble into prereplication complexes before viral DNA replication. *J Virol*. **85**(13), pp.6629-6644.
- Jackson, J.W., Hancock, T.J., LaPrade, E., Dogra, P., Gann, E.R., Masi, T.J., Panchanathan, R., Miller, W.E., Wilhelm, S.W. and Sparer, T.E. 2019. The Human Cytomegalovirus Chemokine vCXCL-1 Modulates Normal Dissemination Kinetics of Murine Cytomegalovirus. *mBio*. **10**(3).
- Jarvis, M.A. and Nelson, J.A. 2007. Human cytomegalovirus tropism for endothelial cells: not all endothelial cells are created equal. *J Virol*. **81**(5), pp.2095-2101.
- Jault, F.M., Jault, J.M., Ruchti, F., Fortunato, E.A., Clark, C., Corbeil, J., Richman, D.D. and Spector, D.H. 1995. Cytomegalovirus infection induces high levels of cyclins, phosphorylated Rb, and p53, leading to cell cycle arrest. *J Virol*. **69**(11), pp.6697-6704.
- Jean Beltran, P.M. and Cristea, I.M. 2014. The life cycle and pathogenesis of human cytomegalovirus infection: lessons from proteomics. *Expert Rev Proteomics*. **11**(6), pp.697-711.
- Jean-Pierre, V., Lupo, J., Buisson, M., Morand, P. and Germi, R. 2021. Main Targets of Interest for the Development of a Prophylactic or Therapeutic Epstein-Barr Virus Vaccine. *Front Microbiol*. **12**, p701611.
- Jenkins, C., Abendroth, A. and Slobedman, B. 2004. A novel viral transcript with homology to human interleukin-10 is expressed during latent human cytomegalovirus infection. *J Virol*. **78**(3), pp.1440-1447.

- Jiang, J. and Dingledine, R. 2013. Role of prostaglandin receptor EP2 in the regulations of cancer cell proliferation, invasion, and inflammation. *J Pharmacol Exp Ther.* **344**(2), pp.360-367.
- Jiang, J.H., Ge, G., Gao, K., Pang, Y., Chai, R.C., Jia, X.H., Kong, J.G. and Yu, A.C. 2015. Calcium Signaling Involvement in Cadmium-Induced Astrocyte Cytotoxicity and Cell Death Through Activation of MAPK and PI3K/Akt Signaling Pathways. *Neurochem Res.* **40**(9), pp.1929-1944.
- Jiang, J.H., Wang, N., Li, A., Liao, W.T., Pan, Z.G., Mai, S.J., Li, D.J., Zeng, M.S., Wen, J.M. and Zeng, Y.X. 2006. Hypoxia can contribute to the induction of the Epstein-Barr virus (EBV) lytic cycle. *J Clin Virol.* **37**(2), pp.98-103.
- Johnson, B.E., Mazor, T., Hong, C., Barnes, M., Aihara, K., McLean, C.Y., Fouse, S.D., Yamamoto, S., Ueda, H., Tatsuno, K., Asthana, S., Jalbert, L.E., Nelson, S.J., Bollen, A.W., Gustafson, W.C., Charron, E., Weiss, W.A., Smirnov, I.V., Song, J.S., Olshen, A.B., Cha, S., Zhao, Y., Moore, R.A., Mungall, A.J., Jones, S.J.M., Hirst, M., Marra, M.A., Saito, N., Aburatani, H., Mukasa, A., Berger, M.S., Chang, S.M., Taylor, B.S. and Costello, J.F. 2014. Mutational analysis reveals the origin and therapy-driven evolution of recurrent glioma. *Science.* **343**(6167), pp.189-193.
- Johnson, R.A., Wang, X., Ma, X.L., Huong, S.M. and Huang, E.S. 2001. Human cytomegalovirus up-regulates the phosphatidylinositol 3-kinase (PI3-K) pathway: inhibition of PI3-K activity inhibits viral replication and virus-induced signaling. *J Virol.* **75**(13), pp.6022-6032.
- Joki, T., Heese, O., Nikas, D.C., Bello, L., Zhang, J., Kraeft, S.K., Seyfried, N.T., Abe, T., Chen, L.B., Carroll, R.S. and Black, P.M. 2000. Expression of cyclooxygenase 2 (COX-2) in human glioma and in vitro inhibition by a specific COX-2 inhibitor, NS-398. *Cancer Res.* **60**(17), pp.4926-4931.
- Jolliffe, I.T. and Cadima, J. 2016. Principal component analysis: a review and recent developments. *Philos Trans A Math Phys Eng Sci.* **374**(2065), p20150202.
- Jones, T., Ramos da Silva, S., Bedolla, R., Ye, F., Zhou, F. and Gao, S.J. 2014. Viral cyclin promotes KSHV-induced cellular transformation and tumorigenesis by overriding contact inhibition. *Cell Cycle.* **13**(5), pp.845-858.
- Jónsson, Z.O. and Hübscher, U. 1997. Proliferating cell nuclear antigen: more than a clamp for DNA polymerases. *Bioessays.* **19**(11), pp.967-975.
- Ju, H., Li, X., Li, H., Wang, X., Wang, H., Li, Y., Dou, C. and Zhao, G. 2013. Mediation of multiple pathways regulating cell proliferation, migration, and apoptosis in the human malignant glioma cell line U87MG via unphosphorylated STAT1: laboratory investigation. *J Neurosurg.* **118**(6), pp.1239-1247.
- Kabanova, A., Marcandalli, J., Zhou, T., Bianchi, S., Baxa, U., Tsybovsky, Y., Lilleri, D., Silacci-Fregni, C., Foglierini, M., Fernandez-Rodriguez, B.M., Druz, A., Zhang, B., Geiger, R., Pagani, M., Sallusto, F., Kwong, P.D., Corti, D., Lanzavecchia, A. and Perez, L. 2016. Platelet-derived growth factor- α receptor is the cellular receptor for human cytomegalovirus gHgLgO trimer. *Nat Microbiol.* **1**(8), p16082.
- Kagele, D., Rossetto, C.C., Tarrant, M.T. and Pari, G.S. 2012. Analysis of the interactions of viral and cellular factors with human cytomegalovirus lytic origin of replication, oriLyt. *Virology.* **424**(2), pp.106-114.
- Kalejta, R.F. 2008. Functions of human cytomegalovirus tegument proteins prior to immediate early gene expression. *Curr Top Microbiol Immunol.* **325**, pp.101-115.

- Kalejta, R.F. 2008. Tegument proteins of human cytomegalovirus. *Microbiol Mol Biol Rev.* **72**(2), pp.249-265, table of contents.
- Katsetos, C.D., Del Valle, L., Geddes, J.F., Assimakopoulou, M., Legido, A., Boyd, J.C., Balin, B., Parikh, N.A., Maraziotis, T., de Chadarevian, J.P., Varakis, J.N., Matsas, R., Spano, A., Frankfurter, A., Herman, M.M. and Khalili, K. 2001. Aberrant localization of the neuronal class III beta-tubulin in astrocytomas. *Arch Pathol Lab Med.* **125**(5), pp.613-624.
- Katsetos, C.D., Draber, P. and Kavallaris, M. 2011. Targeting β III-tubulin in glioblastoma multiforme: from cell biology and histopathology to cancer therapeutics. *Anticancer Agents Med Chem.* **11**(8), pp.719-728.
- Katsetos, C.D., Dráberová, E., Legido, A., Dumontet, C. and Dráber, P. 2009. Tubulin targets in the pathobiology and therapy of glioblastoma multiforme. I. Class III beta-tubulin. *J Cell Physiol.* **221**(3), pp.505-513.
- Kayaselçuk, F., Zorludemir, S., Gümürdühü, D., Zeren, H. and Erman, T. 2002. PCNA and Ki-67 in central nervous system tumors: correlation with the histological type and grade. *J Neurooncol.* **57**(2), pp.115-121.
- Keller, M.J., Wu, A.W., Andrews, J.I., McGonagill, P.W., Tibesar, E.E. and Meier, J.L. 2007. Reversal of human cytomegalovirus major immediate-early enhancer/promoter silencing in quiescently infected cells via the cyclic AMP signaling pathway. *J Virol.* **81**(12), pp.6669-6681.
- Kempermann, G., Gage, F.H., Aigner, L., Song, H., Curtis, M.A., Thuret, S., Kuhn, H.G., Jessberger, S., Frankland, P.W., Cameron, H.A., Gould, E., Hen, R., Abrous, D.N., Toni, N., Schinder, A.F., Zhao, X., Lucassen, P.J. and Frisén, J. 2018. Human Adult Neurogenesis: Evidence and Remaining Questions. *Cell Stem Cell.* **23**(1), pp.25-30.
- Kempermann, G., Song, H. and Gage, F.H. 2015. Neurogenesis in the Adult Hippocampus. *Cold Spring Harb Perspect Biol.* **7**(9), pa018812.
- Kettenmann, H., Hanisch, U.K., Noda, M. and Verkhratsky, A. 2011. Physiology of microglia. *Physiol Rev.* **91**(2), pp.461-553.
- Kew, V.G., Yuan, J., Meier, J. and Reeves, M.B. 2014. Mitogen and stress activated kinases act co-operatively with CREB during the induction of human cytomegalovirus immediate-early gene expression from latency. *PLoS Pathog.* **10**(6), pe1004195.
- Kim, E.S. 2018. Letermovir: First Global Approval. *Drugs.* **78**(1), pp.147-152.
- Kim, J.H., Collins-McMillen, D., Buehler, J.C., Goodrum, F.D. and Yurochko, A.D. 2017. Human Cytomegalovirus Requires Epidermal Growth Factor Receptor Signaling To Enter and Initiate the Early Steps in the Establishment of Latency in CD34. *J Virol.* **91**(5).
- Kinney, G.A. and Spain, W.J. 2002. Synaptically evoked GABA transporter currents in neocortical glia. *J Neurophysiol.* **88**(6), pp.2899-2908.
- Kitanaka, C., Sato, A. and Okada, M. 2013. JNK Signaling in the Control of the Tumor-Initiating Capacity Associated with Cancer Stem Cells. *Genes Cancer.* **4**(9-10), pp.388-396.
- Koch, C.M., Chiu, S.F., Akbarpour, M., Bharat, A., Ridge, K.M., Bartom, E.T. and Winter, D.R. 2018. A Beginner's Guide to Analysis of RNA Sequencing Data. *Am J Respir Cell Mol Biol.* **59**(2), pp.145-157.
- Koh, K., Lee, K., Ahn, J.H. and Kim, S. 2009. Human cytomegalovirus infection downregulates the expression of glial fibrillary acidic protein in human glioblastoma U373MG cells: identification of viral genes and protein domains involved. *J Gen Virol.* **90**(Pt 4), pp.954-962.
- Kole, M.H. and Stuart, G.J. 2012. Signal processing in the axon initial segment.

Neuron. **73**(2), pp.235-247.

Kondo, K., Xu, J. and Mocarski, E.S. 1996. Human cytomegalovirus latent gene expression in granulocyte-macrophage progenitors in culture and in seropositive individuals. *Proc Natl Acad Sci U S A*. **93**(20), pp.11137-11142.

Koontz, T., Bralic, M., Tomac, J., Pernjak-Pugel, E., Bantug, G., Jonjic, S. and Britt, W.J. 2008. Altered development of the brain after focal herpesvirus infection of the central nervous system. *J Exp Med*. **205**(2), pp.423-435.

Kreisl, T.N., Kim, L., Moore, K., Duic, P., Royce, C., Stroud, I., Garren, N., Mackey, M., Butman, J.A., Camphausen, K., Park, J., Albert, P.S. and Fine, H.A. 2009. Phase II trial of single-agent bevacizumab followed by bevacizumab plus irinotecan at tumor progression in recurrent glioblastoma. *J Clin Oncol*. **27**(5), pp.740-745.

Kreso, A. and Dick, J.E. 2014. Evolution of the cancer stem cell model. *Cell Stem Cell*. **14**(3), pp.275-291.

Kriegstein, A. and Alvarez-Buylla, A. 2009. The glial nature of embryonic and adult neural stem cells. *Annu Rev Neurosci*. **32**, pp.149-184.

Krishna, B.A., Humby, M.S., Miller, W.E. and O'Connor, C.M. 2019. Human cytomegalovirus G protein-coupled receptor US28 promotes latency by attenuating c-fos. *Proc Natl Acad Sci U S A*. **116**(5), pp.1755-1764.

Krishna, B.A., Lau, B., Jackson, S.E., Wills, M.R., Sinclair, J.H. and Poole, E. 2016. Transient activation of human cytomegalovirus lytic gene expression during latency allows cytotoxic T cell killing of latently infected cells. *Sci Rep*. **6**, p24674.

Krishna, K.V., Dubey, S.K., Singhvi, G., Gupta, G. and Kesharwani, P. 2021. MAPK pathway: Potential role in glioblastoma multiforme. *Interdisciplinary Neurosurgery*. **23**, p100901.

Kuhn, S., Gritti, L., Crooks, D. and Dombrowski, Y. 2019. Oligodendrocytes in Development, Myelin Generation and Beyond. *Cells*. **8**(11).

Kuleshov, M.V., Jones, M.R., Rouillard, A.D., Fernandez, N.F., Duan, Q., Wang, Z., Koplev, S., Jenkins, S.L., Jagodnik, K.M., Lachmann, A., McDermott, M.G., Monteiro, C.D., Gundersen, G.W. and Ma'ayan, A. 2016. Enrichr: a comprehensive gene set enrichment analysis web server 2016 update. *Nucleic Acids Res*. **44**(W1), pp.W90-97.

Kumar, A., Coquard, L., Pasquereau, S., Russo, L., Valmary-Degano, S., Borg, C., Pothier, P. and Herbein, G. 2016. Tumor control by human cytomegalovirus in a murine model of hepatocellular carcinoma. *Mol Ther Oncolytics*. **3**, p16012.

Kumar, A., Pareek, V., Faiq, M.A., Ghosh, S.K. and Kumari, C. 2019. ADULT NEUROGENESIS IN HUMANS: A Review of Basic Concepts, History, Current Research, and Clinical Implications. *Innov Clin Neurosci*. **16**(5-6), pp.30-37.

Kumar, A., Tripathy, M.K., Pasquereau, S., Al Moussawi, F., Abbas, W., Coquard, L., Khan, K.A., Russo, L., Algros, M.P., Valmary-Degano, S., Adotevi, O., Morot-Bizot, S. and Herbein, G. 2018. The Human Cytomegalovirus Strain DB Activates Oncogenic Pathways in Mammary Epithelial Cells. *EBioMedicine*. **30**, pp.167-183.

Kwiatkowski, D.L., Thompson, H.W. and Bloom, D.C. 2009. The polycomb group protein Bmi1 binds to the herpes simplex virus 1 latent genome and maintains repressive histone marks during latency. *J Virol*. **83**(16), pp.8173-8181.

La Rosa, C. and Diamond, D.J. 2012. The immune response to human CMV. *Future Virol*. **7**(3), pp.279-293.

Labuhn, M., Jones, G., Speel, E.J., Maier, D., Zweifel, C., Gratzl, O., Van Meir,

- E.G., Hegi, M.E. and Merlo, A. 2001. Quantitative real-time PCR does not show selective targeting of p14(ARF) but concomitant inactivation of both p16(INK4A) and p14(ARF) in 105 human primary gliomas. *Oncogene*. **20**(9), pp.1103-1109.
- Langhans, J., Schneelee, L., Trenkler, N., von Bandemer, H., Nonnenmacher, L., Karpel-Massler, G., Siegelin, M.D., Zhou, S., Halatsch, M.E., Debatin, K.M. and Westhoff, M.A. 2017. The effects of PI3K-mediated signalling on glioblastoma cell behaviour. *Oncogenesis*. **6**(11), p398.
- Lasserre, A., Blaizeau, F., Gorwood, P., Bloch, K., Chauvin, P., Liard, F., Blanchon, T. and Hanslik, T. 2012. Herpes zoster: family history and psychological stress-case-control study. *J Clin Virol*. **55**(2), pp.153-157.
- Lathia, J.D., Mack, S.C., Mulkearns-Hubert, E.E., Valentim, C.L. and Rich, J.N. 2015. Cancer stem cells in glioblastoma. *Genes Dev*. **29**(12), pp.1203-1217.
- Lawrence, M.S., Stojanov, P., Mermel, C.H., Robinson, J.T., Garraway, L.A., Golub, T.R., Meyerson, M., Gabriel, S.B., Lander, E.S. and Getz, G. 2014. Discovery and saturation analysis of cancer genes across 21 tumour types. *Nature*. **505**(7484), pp.495-501.
- Lecoite, D., Héry, C., Janabi, N., Dussaix, E. and Tardieu, M. 1999. Differences in kinetics of human cytomegalovirus cell-free viral release after in vitro infection of human microglial cells, astrocytes and monocyte-derived macrophages. *J Neurovirol*. **5**(3), pp.308-313.
- Lee, G., Auffinger, B., Guo, D., Hasan, T., Deheeger, M., Tobias, A.L., Kim, J.Y., Atashi, F., Zhang, L., Lesniak, M.S., James, C.D. and Ahmed, A.U. 2016. Dedifferentiation of Glioma Cells to Glioma Stem-like Cells By Therapeutic Stress-induced HIF Signaling in the Recurrent GBM Model. *Mol Cancer Ther*. **15**(12), pp.3064-3076.
- Lee, J.H., Lee, J.E., Kahng, J.Y., Kim, S.H., Park, J.S., Yoon, S.J., Um, J.Y., Kim, W.K., Lee, J.K., Park, J., Kim, E.H., Chung, W.S., Ju, Y.S., Park, S.H., Chang, J.H. and Kang, S.G. 2018. Human glioblastoma arises from subventricular zone cells with low-level driver mutations. *Nature*. **560**(7717), pp.243-247.
- Lee, K., Jeon, K., Kim, J.M., Kim, V.N., Choi, D.H., Kim, S.U. and Kim, S. 2005. Downregulation of GFAP, TSP-1, and p53 in human glioblastoma cell line, U373MG, by IE1 protein from human cytomegalovirus. *Glia*. **51**(1), pp.1-12.
- Lee, K.M., Choi, K.H. and Ouellette, M.M. 2004. Use of exogenous hTERT to immortalize primary human cells. *Cytotechnology*. **45**(1-2), pp.33-38.
- Lee, S.H., Albright, E.R., Lee, J.H., Jacobs, D. and Kalejta, R.F. 2015. Cellular defense against latent colonization foiled by human cytomegalovirus UL138 protein. *Sci Adv*. **1**(10), pe1501164.
- León, A., Aparicio, G.I. and Scorticati, C. 2021. Neuronal Glycoprotein M6a: An Emerging Molecule in Chemical Synapse Formation and Dysfunction. *Front Synaptic Neurosci*. **13**, p661681.
- Li, B., Severson, E., Pignon, J.C., Zhao, H., Li, T., Novak, J., Jiang, P., Shen, H., Aster, J.C., Rodig, S., Signoretti, S., Liu, J.S. and Liu, X.S. 2016. Comprehensive analyses of tumor immunity: implications for cancer immunotherapy. *Genome Biol*. **17**(1), p174.
- Li, H., Liu, S., Hu, J., Luo, X., Li, N., M Bode, A. and Cao, Y. 2016. Epstein-Barr virus lytic reactivation regulation and its pathogenic role in carcinogenesis. *Int J Biol Sci*. **12**(11), pp.1309-1318.
- Li, S. and Wen, X. 2017. Seropositivity to herpes simplex virus type 2, but not type 1 is associated with cervical cancer: NHANES (1999-2014). *BMC Cancer*.

17(1), p726.

Li, W., Cogswell, C.A. and LoTurco, J.J. 1998. Neuronal differentiation of precursors in the neocortical ventricular zone is triggered by BMP. *J Neurosci.* **18**(21), pp.8853-8862.

Li, Z., Pang, J., Dong, L. and Yu, X. 2021. Structural basis for genome packaging, retention, and ejection in human cytomegalovirus. *Nat Commun.* **12**(1), p4538.

Liang, Q.C., Xiong, H., Zhao, Z.W., Jia, D., Li, W.X., Qin, H.Z., Deng, J.P., Gao, L., Zhang, H. and Gao, G.D. 2009. Inhibition of transcription factor STAT5b suppresses proliferation, induces G1 cell cycle arrest and reduces tumor cell invasion in human glioblastoma multiforme cells. *Cancer Lett.* **273**(1), pp.164-171.

Limaye, A.P. 2002. Ganciclovir-resistant cytomegalovirus in organ transplant recipients. *Clin Infect Dis.* **35**(7), pp.866-872.

Lin, R.C., Matesic, D.F., Marvin, M., McKay, R.D. and Brüstle, O. 1995. Re-expression of the intermediate filament nestin in reactive astrocytes. *Neurobiol Dis.* **2**(2), pp.79-85.

Lisboa, L.F., Egli, A., O'Shea, D., Åsberg, A., Hartmann, A., Rollag, H., Pang, X.L., Tyrrell, D.L., Kumar, D. and Humar, A. 2015. Hcmv-miR-UL22A-5p: A Biomarker in Transplantation With Broad Impact on Host Gene Expression and Potential Immunological Implications. *Am J Transplant.* **15**(7), pp.1893-1902.

Lischka, P. and Zimmermann, H. 2008. Antiviral strategies to combat cytomegalovirus infections in transplant recipients. *Curr Opin Pharmacol.* **8**(5), pp.541-548.

Liu, C., Clark, P.A., Kuo, J.S. and Kalejta, R.F. 2017. Human Cytomegalovirus-Infected Glioblastoma Cells Display Stem Cell-Like Phenotypes. *mSphere.* **2**(3).

Liu, C., Sage, J.C., Miller, M.R., Verhaak, R.G., Hippenmeyer, S., Vogel, H., Foreman, O., Bronson, R.T., Nishiyama, A., Luo, L. and Zong, H. 2011. Mosaic analysis with double markers reveals tumor cell of origin in glioma. *Cell.* **146**(2), pp.209-221.

Liu, R., Li, X., Tulpule, A., Zhou, Y., Scehnet, J.S., Zhang, S., Lee, J.S., Chaudhary, P.M., Jung, J. and Gill, P.S. 2010. KSHV-induced notch components render endothelial and mural cell characteristics and cell survival. *Blood.* **115**(4), pp.887-895.

Liu, T., Li, W., Lu, W., Chen, M., Luo, M., Zhang, C., Li, Y., Qin, G., Shi, D., Xiao, B., Qiu, H., Yu, W., Kang, L., Kang, T., Huang, W., Yu, X., Wu, X. and Deng, W. 2017. RBFOX3 Promotes Tumor Growth and Progression via hTERT Signaling and Predicts a Poor Prognosis in Hepatocellular Carcinoma. *Theranostics.* **7**(12), pp.3138-3154.

Liu, X.J., Jiang, X., Huang, S.N., Sun, J.Y., Zhao, F., Zeng, W.B. and Luo, M.H. 2017. Human cytomegalovirus infection dysregulates neural progenitor cell fate by disrupting Hes1 rhythm and down-regulating its expression. *Virology.* **32**(3), pp.188-198.

Liu, Z.G., Jiang, G., Tang, J., Wang, H., Feng, G., Chen, F., Tu, Z., Liu, G., Zhao, Y., Peng, M.J., He, Z.W., Chen, X.Y., Lindsay, H., Xia, Y.F. and Li, X.N. 2016. c-Fos over-expression promotes radioresistance and predicts poor prognosis in malignant glioma. *Oncotarget.* **7**(40), pp.65946-65956.

Lo, H.W., Cao, X., Zhu, H. and Ali-Osman, F. 2008. Constitutively activated STAT3 frequently coexpresses with epidermal growth factor receptor in high-grade gliomas and targeting STAT3 sensitizes them to Iressa and alkylators.

Clin Cancer Res. **14**(19), pp.6042-6054.

Lokensgard, J.R., Cheeran, M.C., Gekker, G., Hu, S., Chao, C.C. and Peterson, P.K. 1999. Human cytomegalovirus replication and modulation of apoptosis in astrocytes. *J Hum Virol.* **2**(2), pp.91-101.

Louis, D.N., Perry, A., Reifenberger, G., von Deimling, A., Figarella-Branger, D., Cavenee, W.K., Ohgaki, H., Wiestler, O.D., Kleihues, P. and Ellison, D.W. 2016. The 2016 World Health Organization Classification of Tumors of the Central Nervous System: a summary. *Acta Neuropathol.* **131**(6), pp.803-820.

Lu, F., Chen, Y., Zhao, C., Wang, H., He, D., Xu, L., Wang, J., He, X., Deng, Y., Lu, E.E., Liu, X., Verma, R., Bu, H., Drissi, R., Fouladi, M., Stemmer-Rachamimov, A.O., Burns, D., Xin, M., Rubin, J.B., Bahassi, E.M., Canoll, P., Holland, E.C. and Lu, Q.R. 2016. Olig2-Dependent Reciprocal Shift in PDGF and EGF Receptor Signaling Regulates Tumor Phenotype and Mitotic Growth in Malignant Glioma. *Cancer Cell.* **29**(5), pp.669-683.

Lu, Q.R., Park, J.K., Noll, E., Chan, J.A., Alberta, J., Yuk, D., Alzamora, M.G., Louis, D.N., Stiles, C.D., Rowitch, D.H. and Black, P.M. 2001. Oligodendrocyte lineage genes (OLIG) as molecular markers for human glial brain tumors. *Proc Natl Acad Sci U S A.* **98**(19), pp.10851-10856.

Lučin, P., Jug Vučko, N., Karleuša, L., Mahmutefendić Lučin, H., Blagojević Zagorac, G., Lisnić, B., Pavišić, V., Marčelić, M., Grabušić, K., Brizić, I. and Lukanović Jurić, S. 2020. Cytomegalovirus Generates Assembly Compartment in the Early Phase of Infection by Perturbation of Host-Cell Factors Recruitment at the Early Endosome/Endosomal Recycling Compartment/Trans-Golgi Interface. *Front Cell Dev Biol.* **8**, p563607.

Ludwig, A. and Hengel, H. 2009. Epidemiological impact and disease burden of congenital cytomegalovirus infection in Europe. *Euro Surveill.* **14**(9), pp.26-32.

Lukac, D.M. and Alwine, J.C. 1999. Effects of human cytomegalovirus major immediate-early proteins in controlling the cell cycle and inhibiting apoptosis: studies with ts13 cells. *J Virol.* **73**(4), pp.2825-2831.

Lun, S.W., Cheung, S.T. and Lo, K.W. 2014. Cancer stem-like cells in Epstein-Barr virus-associated nasopharyngeal carcinoma. *Chin J Cancer.* **33**(11), pp.529-538.

Luo, M.H., Hannemann, H., Kulkarni, A.S., Schwartz, P.H., O'Dowd, J.M. and Fortunato, E.A. 2010. Human cytomegalovirus infection causes premature and abnormal differentiation of human neural progenitor cells. *J Virol.* **84**(7), pp.3528-3541.

Luo, M.H., Schwartz, P.H. and Fortunato, E.A. 2008. Neonatal neural progenitor cells and their neuronal and glial cell derivatives are fully permissive for human cytomegalovirus infection. *J Virol.* **82**(20), pp.9994-10007.

Macias, M.P. and Stinski, M.F. 1993. An in vitro system for human cytomegalovirus immediate early 2 protein (IE2)-mediated site-dependent repression of transcription and direct binding of IE2 to the major immediate early promoter. *Proc Natl Acad Sci U S A.* **90**(2), pp.707-711.

Maertens, J., Cordonnier, C., Jaksch, P., Poiré, X., Uknis, M., Wu, J., Wijatyk, A., Saliba, F., Witzke, O. and Villano, S. 2019. Maribavir for Preemptive Treatment of Cytomegalovirus Reactivation. *N Engl J Med.* **381**(12), pp.1136-1147.

Mahankali, M., Peng, H.J., Cox, D. and Gomez-Cambronero, J. 2011. The mechanism of cell membrane ruffling relies on a phospholipase D2 (PLD2), Grb2 and Rac2 association. *Cell Signal.* **23**(8), pp.1291-1298.

Maklad, A., Sharma, A. and Azimi, I. 2019. Calcium Signaling in Brain Cancers:

- Roles and Therapeutic Targeting. *Cancers (Basel)*. **11**(2).
- Malatesta, P., Hartfuss, E. and Götz, M. 2000. Isolation of radial glial cells by fluorescent-activated cell sorting reveals a neuronal lineage. *Development*. **127**(24), pp.5253-5263.
- Malinger, G., Lev, D., Zahalka, N., Ben Aroia, Z., Watemberg, N., Kidron, D., Sira, L.B. and Lerman-Sagie, T. 2003. Fetal cytomegalovirus infection of the brain: the spectrum of sonographic findings. *AJNR Am J Neuroradiol*. **24**(1), pp.28-32.
- Malouli, D., Hansen, S.G., Nakayasu, E.S., Marshall, E.E., Hughes, C.M., Ventura, A.B., Gilbride, R.M., Lewis, M.S., Xu, G., Kreklywich, C., Whizin, N., Fischer, M., Legasse, A.W., Viswanathan, K., Siess, D., Camp, D.G., Axthelm, M.K., Kahl, C., DeFilippis, V.R., Smith, R.D., Streblow, D.N., Picker, L.J. and Früh, K. 2014. Cytomegalovirus pp65 limits dissemination but is dispensable for persistence. *J Clin Invest*. **124**(5), pp.1928-1944.
- Manicklal, S., Emery, V.C., Lazzarotto, T., Boppana, S.B. and Gupta, R.K. 2013. The "silent" global burden of congenital cytomegalovirus. *Clin Microbiol Rev*. **26**(1), pp.86-102.
- Mantovani, A., Marchesi, F., Malesci, A., Laghi, L. and Allavena, P. 2017. Tumour-associated macrophages as treatment targets in oncology. *Nat Rev Clin Oncol*. **14**(7), pp.399-416.
- Mao, H., Lebrun, D.G., Yang, J., Zhu, V.F. and Li, M. 2012. Deregulated signaling pathways in glioblastoma multiforme: molecular mechanisms and therapeutic targets. *Cancer Invest*. **30**(1), pp.48-56.
- Mar, E.C., Chiou, J.F., Cheng, Y.C. and Huang, E.S. 1985. Inhibition of cellular DNA polymerase alpha and human cytomegalovirus-induced DNA polymerase by the triphosphates of 9-(2-hydroxyethoxymethyl)guanine and 9-(1,3-dihydroxy-2-propoxymethyl)guanine. *J Virol*. **53**(3), pp.776-780.
- Marchini, A., Liu, H. and Zhu, H. 2001. Human cytomegalovirus with IE-2 (UL122) deleted fails to express early lytic genes. *J Virol*. **75**(4), pp.1870-1878.
- Marques, C., Unterkircher, T., Kroon, P., Oldrini, B., Izzo, A., Dramaretska, Y., Ferrarese, R., Kling, E., Schnell, O., Nelander, S., Wagner, E.F., Bakiri, L., Gargiulo, G., Carro, M.S. and Squatrito, M. 2021. NF1 regulates mesenchymal glioblastoma plasticity and aggressiveness through the AP-1 transcription factor FOSL1. *Elife*. **10**.
- Martínez-Cerdeño, V. and Noctor, S.C. 2018. Neural Progenitor Cell Terminology. *Front Neuroanat*. **12**, p104.
- Martinez-Martin, N., Marcandalli, J., Huang, C.S., Arthur, C.P., Perotti, M., Foglierini, M., Ho, H., Dosey, A.M., Shriver, S., Payandeh, J., Leitner, A., Lanzavecchia, A., Perez, L. and Ciferri, C. 2018. An Unbiased Screen for Human Cytomegalovirus Identifies Neuropilin-2 as a Central Viral Receptor. *Cell*. **174**(5), pp.1158-1171.e1119.
- Martini, M., Pallini, R., Luongo, G., Cenci, T., Lucantoni, C. and Larocca, L.M. 2008. Prognostic relevance of SOCS3 hypermethylation in patients with glioblastoma multiforme. *Int J Cancer*. **123**(12), pp.2955-2960.
- Marty, F.M., Ljungman, P., Chemaly, R.F., Maertens, J., Dadwal, S.S., Duarte, R.F., Haider, S., Ullmann, A.J., Katayama, Y., Brown, J., Mullane, K.M., Boeckh, M., Blumberg, E.A., Einsele, H., Snyderman, D.R., Kanda, Y., DiNubile, M.J., Teal, V.L., Wan, H., Murata, Y., Kartsonis, N.A., Leavitt, R.Y. and Badshah, C. 2017. Letermovir Prophylaxis for Cytomegalovirus in Hematopoietic-Cell Transplantation. *N Engl J Med*. **377**(25), pp.2433-2444.
- Masland, R.H. 2004. Neuronal cell types. *Curr Biol*. **14**(13), pp.R497-500.

- Mason, R., Groves, I.J., Wills, M.R., Sinclair, J.H. and Reeves, M.B. 2020. Human cytomegalovirus major immediate early transcripts arise predominantly from the canonical major immediate early promoter in reactivating progenitor-derived dendritic cells. *J Gen Virol.* **101**(6), pp.635-644.
- Masui, S., Nakatake, Y., Toyooka, Y., Shimosato, D., Yagi, R., Takahashi, K., Okochi, H., Okuda, A., Matoba, R., Sharov, A.A., Ko, M.S. and Niwa, H. 2007. Pluripotency governed by Sox2 via regulation of Oct3/4 expression in mouse embryonic stem cells. *Nat Cell Biol.* **9**(6), pp.625-635.
- Mate, J.L., Ariza, A., Muñoz, A., Molinero, J.L., López, D. and Navas-Palacios, J.J. 1998. Induction of proliferating cell nuclear antigen and Ki-67 expression by cytomegalovirus infection. *J Pathol.* **184**(3), pp.279-282.
- Matsuura, H., Kirschner, A.N., Longnecker, R. and Jardetzky, T.S. 2010. Crystal structure of the Epstein-Barr virus (EBV) glycoprotein H/glycoprotein L (gH/gL) complex. *Proceedings of the National Academy of Sciences.* **107**(52), p22641.
- Mauch-Mücke, K., Schön, K., Paulus, C. and Nevels, M.M. 2020. Evidence for Tethering of Human Cytomegalovirus Genomes to Host Chromosomes. *Front Cell Infect Microbiol.* **10**, p577428.
- Maussang, D., Langemeijer, E., Fitzsimons, C.P., Stigter-van Walsum, M., Dijkman, R., Borg, M.K., Slinger, E., Schreiber, A., Michel, D., Tensen, C.P., van Dongen, G.A., Leurs, R. and Smit, M.J. 2009. The human cytomegalovirus-encoded chemokine receptor US28 promotes angiogenesis and tumor formation via cyclooxygenase-2. *Cancer Res.* **69**(7), pp.2861-2869.
- Maussang, D., Verzijl, D., van Walsum, M., Leurs, R., Holl, J., Pleskoff, O., Michel, D., van Dongen, G.A. and Smit, M.J. 2006. Human cytomegalovirus-encoded chemokine receptor US28 promotes tumorigenesis. *Proc Natl Acad Sci U S A.* **103**(35), pp.13068-13073.
- Mawrin, C., Diete, S., Treuheit, T., Kropf, S., Vorwerk, C.K., Boltze, C., Kirches, E., Firsching, R. and Dietzmann, K. 2003. Prognostic relevance of MAPK expression in glioblastoma multiforme. *Int J Oncol.* **23**(3), pp.641-648.
- Mazarakis, N.D., Edwards, A.D. and Mehmet, H. 1997. Apoptosis in neural development and disease. *Arch Dis Child Fetal Neonatal Ed.* **77**(3), pp.F165-170.
- McCarthy, M., Auger, D. and Whittemore, S.R. 2000. Human cytomegalovirus causes productive infection and neuronal injury in differentiating fetal human central nervous system neuroepithelial precursor cells. *J Hum Virol.* **3**(4), pp.215-228.
- McSharry, B.P., Avdic, S. and Slobedman, B. 2012. Human cytomegalovirus encoded homologs of cytokines, chemokines and their receptors: roles in immunomodulation. *Viruses.* **4**(11), pp.2448-2470.
- Melnick, M., Sedghizadeh, P.P., Allen, C.M. and Jaskoll, T. 2012. Human cytomegalovirus and mucoepidermoid carcinoma of salivary glands: cell-specific localization of active viral and oncogenic signaling proteins is confirmatory of a causal relationship. *Exp Mol Pathol.* **92**(1), pp.118-125.
- Mendelson, M., Monard, S., Sissons, P. and Sinclair, J. 1996. Detection of endogenous human cytomegalovirus in CD34+ bone marrow progenitors. *J Gen Virol.* **77** (Pt 12), pp.3099-3102.
- Mendelson, M., Monard, S., Sissons, P. and Sinclair, J. 1996. Detection of endogenous human cytomegalovirus in CD34+ bone marrow progenitors. *J Gen Virol.* **77** (Pt 12), pp.3099-3102.
- Meng, D., Chen, Y., Yun, D., Zhao, Y., Wang, J., Xu, T., Li, X., Wang, Y., Yuan,

- L., Sun, R., Song, X., Huai, C., Hu, L., Yang, S., Min, T., Chen, J., Chen, H. and Lu, D. 2015. High expression of N-myc (and STAT) interactor predicts poor prognosis and promotes tumor growth in human glioblastoma. *Oncotarget*. **6**(7), pp.4901-4919.
- Merkle, F.T., Tramontin, A.D., García-Verdugo, J.M. and Alvarez-Buylla, A. 2004. Radial glia give rise to adult neural stem cells in the subventricular zone. *Proc Natl Acad Sci U S A*. **101**(50), pp.17528-17532.
- Meshesha, M.K., Veksler-Lublinsky, I., Isakov, O., Reichenstein, I., Shomron, N., Kedem, K., Ziv-Ukelson, M., Bentwich, Z. and Avni, Y.S. 2012. The microRNA Transcriptome of Human Cytomegalovirus (HCMV). *Open Virol J*. **6**, pp.38-48.
- Mettenleiter, T.C. 2002. Herpesvirus assembly and egress. *J Virol*. **76**(4), pp.1537-1547.
- Micallef, S. and Galea, R. 2018. CMV encephalitis in an immune-competent patient. *BMJ Case Rep*. **2018**.
- Mikell, I., Crawford, L.B., Hancock, M.H., Mitchell, J., Buehler, J., Goodrum, F. and Nelson, J.A. 2019. HCMV miR-US22 down-regulation of EGR-1 regulates CD34+ hematopoietic progenitor cell proliferation and viral reactivation. *PLoS Pathog*. **15**(11), pe1007854.
- Miller, I., Min, M., Yang, C., Tian, C., Gookin, S., Carter, D. and Spencer, S.L. 2018. Ki67 is a Graded Rather than a Binary Marker of Proliferation versus Quiescence. *Cell Rep*. **24**(5), pp.1105-1112.e1105.
- Mitchell, D.A., Batich, K.A., Gunn, M.D., Huang, M.N., Sanchez-Perez, L., Nair, S.K., Congdon, K.L., Reap, E.A., Archer, G.E., Desjardins, A., Friedman, A.H., Friedman, H.S., Herndon, J.E., Coan, A., McLendon, R.E., Reardon, D.A., Vredenburgh, J.J., Bigner, D.D. and Sampson, J.H. 2015. Tetanus toxoid and CCL3 improve dendritic cell vaccines in mice and glioblastoma patients. *Nature*. **519**(7543), pp.366-369.
- Mitchell, D.A., Xie, W., Schmittling, R., Learn, C., Friedman, A., McLendon, R.E. and Sampson, J.H. 2008. Sensitive detection of human cytomegalovirus in tumors and peripheral blood of patients diagnosed with glioblastoma. *Neuro Oncol*. **10**(1), pp.10-18.
- Miyachi, K., Fritzler, M.J. and Tan, E.M. 1978. Autoantibody to a nuclear antigen in proliferating cells. *J Immunol*. **121**(6), pp.2228-2234.
- Miyamoto, T., Furusawa, C. and Kaneko, K. 2015. Pluripotency, Differentiation, and Reprogramming: A Gene Expression Dynamics Model with Epigenetic Feedback Regulation. *PLoS Comput Biol*. **11**(8), pe1004476.
- Mocarski, E.S., Kemble, G.W., Lyle, J.M. and Greaves, R.F. 1996. A deletion mutant in the human cytomegalovirus gene encoding IE1(491aa) is replication defective due to a failure in autoregulation. *Proc Natl Acad Sci U S A*. **93**(21), pp.11321-11326.
- Molliver, M.E., Kostović, I. and van der Loos, H. 1973. The development of synapses in cerebral cortex of the human fetus. *Brain Res*. **50**(2), pp.403-407.
- Monaco, S.E., Angelastro, J.M., Szabolcs, M. and Greene, L.A. 2007. The transcription factor ATF5 is widely expressed in carcinomas, and interference with its function selectively kills neoplastic, but not nontransformed, breast cell lines. *Int J Cancer*. **120**(9), pp.1883-1890.
- Montgomery, D.L. 1994. Astrocytes: form, functions, and roles in disease. *Vet Pathol*. **31**(2), pp.145-167.
- Moodie, S.A., Willumsen, B.M., Weber, M.J. and Wolfman, A. 1993. Complexes of Ras.GTP with Raf-1 and mitogen-activated protein kinase kinase. *Science*.

260(5114), pp.1658-1661.

Moon, B.S., Yoon, J.Y., Kim, M.Y., Lee, S.H., Choi, T. and Choi, K.Y. 2009. Bone morphogenetic protein 4 stimulates neuronal differentiation of neuronal stem cells through the ERK pathway. *Exp Mol Med.* **41**(2), pp.116-125.

Moorman, N.J., Sharon-Friling, R., Shenk, T. and Cristea, I.M. 2010. A targeted spatial-temporal proteomics approach implicates multiple cellular trafficking pathways in human cytomegalovirus virion maturation. *Mol Cell Proteomics.* **9**(5), pp.851-860.

Morton, C.C. and Nance, W.E. 2006. Newborn hearing screening--a silent revolution. *N Engl J Med.* **354**(20), pp.2151-2164.

Murata, T. and Tsurumi, T. 2014. Switching of EBV cycles between latent and lytic states. *Rev Med Virol.* **24**(3), pp.142-153.

Murphy, E.A., Streblow, D.N., Nelson, J.A. and Stinski, M.F. 2000. The human cytomegalovirus IE86 protein can block cell cycle progression after inducing transition into the S phase of permissive cells. *J Virol.* **74**(15), pp.7108-7118.

Murphy, J.C., Fischle, W., Verdin, E. and Sinclair, J.H. 2002. Control of cytomegalovirus lytic gene expression by histone acetylation. *EMBO J.* **21**(5), pp.1112-1120.

Murrell, I., Bedford, C., Ladell, K., Miners, K.L., Price, D.A., Tomasec, P., Wilkinson, G.W.G. and Stanton, R.J. 2017. The pentameric complex drives immunologically covert cell-cell transmission of wild-type human cytomegalovirus. *Proc Natl Acad Sci U S A.* **114**(23), pp.6104-6109.

Mustakangas, P., Sarna, S., Ammälä, P., Muttillainen, M., Koskela, P. and Koskiniemi, M. 2000. Human cytomegalovirus seroprevalence in three socioeconomically different urban areas during the first trimester: a population-based cohort study. *Int J Epidemiol.* **29**(3), pp.587-591.

Nachtwey, J. and Spencer, J.V. 2008. HCMV IL-10 suppresses cytokine expression in monocytes through inhibition of nuclear factor-kappaB. *Viral Immunol.* **21**(4), pp.477-482.

Nave, K.A. 2010. Myelination and support of axonal integrity by glia. *Nature.* **468**(7321), pp.244-252.

Nedergaard, M., Ransom, B. and Goldman, S.A. 2003. New roles for astrocytes: redefining the functional architecture of the brain. *Trends Neurosci.* **26**(10), pp.523-530.

Nehme, Z., Pasquereau, S., Haidar Ahmad, S., Coaquette, A., Molimard, C., Monnier, F., Algros, M.P., Adotevi, O., Diab Assaf, M., Feugeas, J.P. and Herbein, G. 2021. Polyploid giant cancer cells, stemness and epithelial-mesenchymal plasticity elicited by human cytomegalovirus. *Oncogene.* **40**(17), pp.3030-3046.

Nevels, M., Paulus, C. and Shenk, T. 2004. Human cytomegalovirus immediate-early 1 protein facilitates viral replication by antagonizing histone deacetylation. *Proc Natl Acad Sci U S A.* **101**(49), pp.17234-17239.

Nichols, W.G., Corey, L., Gooley, T., Davis, C. and Boeckh, M. 2002. High risk of death due to bacterial and fungal infection among cytomegalovirus (CMV)-seronegative recipients of stem cell transplants from seropositive donors: evidence for indirect effects of primary CMV infection. *J Infect Dis.* **185**(3), pp.273-282.

Nimchinsky, E.A., Sabatini, B.L. and Svoboda, K. 2002. Structure and function of dendritic spines. *Annu Rev Physiol.* **64**, pp.313-353.

Noctor, S.C., Martínez-Cerdeño, V., Ivic, L. and Kriegstein, A.R. 2004. Cortical neurons arise in symmetric and asymmetric division zones and migrate through

- specific phases. *Nat Neurosci.* **7**(2), pp.136-144.
- Noctor, S.C., Martínez-Cerdeño, V. and Kriegstein, A.R. 2008. Distinct behaviors of neural stem and progenitor cells underlie cortical neurogenesis. *J Comp Neurol.* **508**(1), pp.28-44.
- Oberstein, A. and Shenk, T. 2017. Cellular responses to human cytomegalovirus infection: Induction of a mesenchymal-to-epithelial transition (MET) phenotype. *Proc Natl Acad Sci U S A.* **114**(39), pp.E8244-E8253.
- O'Brien, C.A., Pollett, A., Gallinger, S. and Dick, J.E. 2007. A human colon cancer cell capable of initiating tumour growth in immunodeficient mice. *Nature.* **445**(7123), pp.106-110.
- O'Connor, C.M., Nukui, M., Gurova, K.V. and Murphy, E.A. 2016. Inhibition of the FACT Complex Reduces Transcription from the Human Cytomegalovirus Major Immediate Early Promoter in Models of Lytic and Latent Replication. *J Virol.* **90**(8), pp.4249-4253.
- Odeberg, J., Wolmer, N., Falci, S., Westgren, M., Seiger, A. and Söderberg-Nauclér, C. 2006. Human cytomegalovirus inhibits neuronal differentiation and induces apoptosis in human neural precursor cells. *J Virol.* **80**(18), pp.8929-8939.
- Ogawa-Goto, K., Irie, S., Omori, A., Miura, Y., Katano, H., Hasegawa, H., Kurata, T., Sata, T. and Arao, Y. 2002. An endoplasmic reticulum protein, p180, is highly expressed in human cytomegalovirus-permissive cells and interacts with the tegument protein encoded by UL48. *J Virol.* **76**(5), pp.2350-2362.
- Ogawa-Goto, K., Tanaka, K., Gibson, W., Moriishi, E., Miura, Y., Kurata, T., Irie, S. and Sata, T. 2003. Microtubule network facilitates nuclear targeting of human cytomegalovirus capsid. *J Virol.* **77**(15), pp.8541-8547.
- Ohgaki, H. and Kleihues, P. 2007. Genetic pathways to primary and secondary glioblastoma. *Am J Pathol.* **170**(5), pp.1445-1453.
- Ohgaki, H. and Kleihues, P. 2013. The definition of primary and secondary glioblastoma. *Clin Cancer Res.* **19**(4), pp.764-772.
- O'Rahilly, R. and Müller, F. 1994. Neurulation in the normal human embryo. *Ciba Found Symp.* **181**, pp.70-82; discussion 82-79.
- Ostrom, Q.T., Gittleman, H., Farah, P., Ondracek, A., Chen, Y., Wolinsky, Y., Stroup, N.E., Kruchko, C. and Barnholtz-Sloan, J.S. 2013. CBTRUS statistical report: Primary brain and central nervous system tumors diagnosed in the United States in 2006-2010. *Neuro Oncol.* **15 Suppl 2**, pp.ii1-56.
- Owen, K.L., Brockwell, N.K. and Parker, B.S. 2019. JAK-STAT Signaling: A Double-Edged Sword of Immune Regulation and Cancer Progression. *Cancers (Basel).* **11**(12).
- Paladino, P., Marcon, E., Greenblatt, J. and Frappier, L. 2014. Identification of herpesvirus proteins that contribute to G1/S arrest. *J Virol.* **88**(8), pp.4480-4492.
- Park, J.C., Chang, I.B., Ahn, J.H., Kim, J.H., Song, J.H., Moon, S.M. and Park, Y.H. 2018. Nerve Growth Factor Stimulates Glioblastoma Proliferation through Notch1 Receptor Signaling. *J Korean Neurosurg Soc.* **61**(4), pp.441-449.
- Parsons, W.J., Ramkumar, V. and Stiles, G.L. 1988. Isobutylmethylxanthine stimulates adenylate cyclase by blocking the inhibitory regulatory protein, Gi. *Mol Pharmacol.* **34**(1), pp.37-41.
- Pass, R.F., Fowler, K.B., Boppana, S.B., Britt, W.J. and Stagno, S. 2006. Congenital cytomegalovirus infection following first trimester maternal infection: symptoms at birth and outcome. *J Clin Virol.* **35**(2), pp.216-220.
- Pass, R.F., Stagno, S., Myers, G.J. and Alford, C.A. 1980. Outcome of

- symptomatic congenital cytomegalovirus infection: results of long-term longitudinal follow-up. *Pediatrics*. **66**(5), pp.758-762.
- Patel, M., Vlahava, V.M., Forbes, S.K., Fielding, C.A., Stanton, R.J. and Wang, E.C.Y. 2018. HCMV-Encoded NK Modulators: Lessons From. *Front Immunol*. **9**, p2214.
- Paulus, C. and Nevels, M. 2009. The human cytomegalovirus major immediate-early proteins as antagonists of intrinsic and innate antiviral host responses. *Viruses*. **1**(3), pp.760-779.
- Peckham, C.S., Johnson, C., Ades, A., Pearl, K. and Chin, K.S. 1987. Early acquisition of cytomegalovirus infection. *Arch Dis Child*. **62**(8), pp.780-785.
- Pelloski, C.E., Lin, E., Zhang, L., Yung, W.K., Colman, H., Liu, J.L., Woo, S.Y., Heimberger, A.B., Suki, D., Prados, M., Chang, S., Barker, F.G., Fuller, G.N. and Aldape, K.D. 2006. Prognostic associations of activated mitogen-activated protein kinase and Akt pathways in glioblastoma. *Clin Cancer Res*. **12**(13), pp.3935-3941.
- Pelvig, D.P., Pakkenberg, H., Stark, A.K. and Pakkenberg, B. 2008. Neocortical glial cell numbers in human brains. *Neurobiol Aging*. **29**(11), pp.1754-1762.
- Penfold, M.E., Dairaghi, D.J., Duke, G.M., Saederup, N., Mocarski, E.S., Kemble, G.W. and Schall, T.J. 1999. Cytomegalovirus encodes a potent alpha chemokine. *Proc Natl Acad Sci U S A*. **96**(17), pp.9839-9844.
- Perlman, J.M. and Argyle, C. 1992. Lethal cytomegalovirus infection in preterm infants: clinical, radiological, and neuropathological findings. *Ann Neurol*. **31**(1), pp.64-68.
- Philips, A., Henshaw, D.L., Lamburn, G. and O'Carroll, M.J. 2018. Brain Tumours: Rise in Glioblastoma Multiforme Incidence in England 1995-2015 Suggests an Adverse Environmental or Lifestyle Factor. *J Environ Public Health*. **2018**, p7910754.
- Phillips, S.L., Cygnar, D., Thomas, A. and Bresnahan, W.A. 2012. Interaction between the human cytomegalovirus tegument proteins UL94 and UL99 is essential for virus replication. *J Virol*. **86**(18), pp.9995-10005.
- Piper, K., DePledge, L., Karsy, M. and Cobbs, C. 2021. Glioma Stem Cells as Immunotherapeutic Targets: Advancements and Challenges. *Front Oncol*. **11**, p615704.
- Poland, S.D., Bambrick, L.L., Dekaban, G.A. and Rice, G.P. 1994. The extent of human cytomegalovirus replication in primary neurons is dependent on host cell differentiation. *J Infect Dis*. **170**(5), pp.1267-1271.
- Poland, S.D., Costello, P., Dekaban, G.A. and Rice, G.P. 1990. Cytomegalovirus in the brain: in vitro infection of human brain-derived cells. *J Infect Dis*. **162**(6), pp.1252-1262.
- Port, R.J., Pinheiro-Maia, S., Hu, C., Arrand, J.R., Wei, W., Young, L.S. and Dawson, C.W. 2013. Epstein-Barr virus induction of the Hedgehog signalling pathway imposes a stem cell phenotype on human epithelial cells. *J Pathol*. **231**(3), pp.367-377.
- Portal, D., Zhou, H., Zhao, B., Kharchenko, P.V., Lowry, E., Wong, L., Quackenbush, J., Holloway, D., Jiang, S., Lu, Y. and Kieff, E. 2013. Epstein-Barr virus nuclear antigen leader protein localizes to promoters and enhancers with cell transcription factors and EBNA2. *Proc Natl Acad Sci U S A*. **110**(46), pp.18537-18542.
- Portsmouth, S., Stebbing, J., Gill, J., Mandalia, S., Bower, M., Nelson, M. and Gazzard, B. 2003. A comparison of regimens based on non-nucleoside reverse transcriptase inhibitors or protease inhibitors in preventing Kaposi's sarcoma.

AIDS. **17**(11), pp.F17-22.

Prasad, A., Remick, J. and Zeichner, S.L. 2013. Activation of human herpesvirus replication by apoptosis. *J Virol*. **87**(19), pp.10641-10650.

Prayson, R.A., Castilla, E.A., Vogelbaum, M.A. and Barnett, G.H. 2002. Cyclooxygenase-2 (COX-2) expression by immunohistochemistry in glioblastoma multiforme. *Ann Diagn Pathol*. **6**(3), pp.148-153.

Price, R.L., Song, J., Bingmer, K., Kim, T.H., Yi, J.Y., Nowicki, M.O., Mo, X., Hollon, T., Murnan, E., Alvarez-Breckenridge, C., Fernandez, S., Kaur, B., Rivera, A., Oglesbee, M., Cook, C., Chiocca, E.A. and Kwon, C.H. 2013.

Cytomegalovirus contributes to glioblastoma in the context of tumor suppressor mutations. *Cancer Res*. **73**(11), pp.3441-3450.

Priel, E., Wohl, A., Teperberg, M., Nass, D. and Cohen, Z.R. 2015. Human cytomegalovirus viral load in tumor and peripheral blood samples of patients with malignant gliomas. *J Clin Neurosci*. **22**(2), pp.326-330.

Procter, D.J., Banerjee, A., Nukui, M., Kruse, K., Gaponenko, V., Murphy, E.A., Komarova, Y. and Walsh, D. 2018. The HCMV Assembly Compartment Is a Dynamic Golgi-Derived MTOC that Controls Nuclear Rotation and Virus Spread. *Dev Cell*. **45**(1), pp.83-100.e107.

Pulliam, L., Moore, D. and West, D.C. 1995. Human cytomegalovirus induces IL-6 and TNF alpha from macrophages and microglial cells: possible role in neurotoxicity. *J Neurovirol*. **1**(2), pp.219-227.

Purves, D., Augustine, G. and Fitzpatrick, D. 2001. *Neuroscience. 2nd edition*. [Online]. Sinauer Associates.

Qi, X.T., Li, Y.L., Zhang, Y.Q., Xu, T., Lu, B., Fang, L., Gao, J.Q., Yu, L.S., Zhu, D.F., Yang, B., He, Q.J. and Ying, M.D. 2019. KLF4 functions as an oncogene in promoting cancer stem cell-like characteristics in osteosarcoma cells. *Acta Pharmacol Sin*. **40**(4), pp.546-555.

Qian, Z., Xuan, B., Gualberto, N. and Yu, D. 2011. The human cytomegalovirus protein pUL38 suppresses endoplasmic reticulum stress-mediated cell death independently of its ability to induce mTORC1 activation. *J Virol*. **85**(17), pp.9103-9113.

Rachinger, N., Fischer, S., Böhme, I., Linck-Paulus, L., Kuphal, S., Kappelmann-Fenzl, M. and Bosserhoff, A.K. 2021. Loss of Gene Information: Discrepancies between RNA Sequencing, cDNA Microarray, and qRT-PCR. *Int J Mol Sci*. **22**(17).

Rådestad, A.F., Estekizadeh, A., Cui, H.L., Kostopoulou, O.N., Davoudi, B., Hirschberg, A.L., Carlson, J., Rahbar, A. and Söderberg-Naucler, C. 2018. Impact of Human Cytomegalovirus Infection and its Immune Response on Survival of Patients with Ovarian Cancer. *Transl Oncol*. **11**(6), pp.1292-1300.

Rahman, M., Dastmalchi, F., Karachi, A. and Mitchell, D. 2019. The role of CMV in glioblastoma and implications for immunotherapeutic strategies. *Oncoimmunology*. **8**(1), pe1514921.

Rak, M.A., Buehler, J., Zeltzer, S., Reitsma, J., Molina, B., Terhune, S. and Goodrum, F. 2018. Human Cytomegalovirus UL135 Interacts with Host Adaptor Proteins To Regulate Epidermal Growth Factor Receptor and Reactivation from Latency. *J Virol*. **92**(20).

Ranganathan, P., Clark, P.A., Kuo, J.S., Salamat, M.S. and Kalejta, R.F. 2012. Significant association of multiple human cytomegalovirus genomic Loci with glioblastoma multiforme samples. *J Virol*. **86**(2), pp.854-864.

Rao, X., Huang, X., Zhou, Z. and Lin, X. 2013. An improvement of the 2^{-ΔΔCT} method for quantitative real-time polymerase chain reaction data

analysis. *Biostat Bioinforma Biomath.* **3**(3), pp.71-85.

Raponi, E., Agenes, F., Delphin, C., Assard, N., Baudier, J., Legraverend, C. and Deloulme, J.C. 2007. S100B expression defines a state in which GFAP-expressing cells lose their neural stem cell potential and acquire a more mature developmental stage. *Glia.* **55**(2), pp.165-177.

Ray, S.K. 2016. The Transcription Regulator Krüppel-Like Factor 4 and Its Dual Roles of Oncogene in Glioblastoma and Tumor Suppressor in Neuroblastoma. *For Immunopathol Dis Therap.* **7**(1-2), pp.127-139.

Reap, E.A., Suryadevara, C.M., Batich, K.A., Sanchez-Perez, L., Archer, G.E., Schmittling, R.J., Norberg, P.K., Herndon, J.E., Healy, P., Congdon, K.L., Gedeon, P.C., Campbell, O.C., Swartz, A.M., Riccione, K.A., Yi, J.S., Hossain-Ibrahim, M.K., Saraswathula, A., Nair, S.K., Dunn-Pirio, A.M., Broome, T.M., Weinhold, K.J., Desjardins, A., Vlahovic, G., McLendon, R.E., Friedman, A.H., Friedman, H.S., Bigner, D.D., Fecci, P.E., Mitchell, D.A. and Sampson, J.H. 2018. Dendritic Cells Enhance Polyfunctionality of Adoptively Transferred T Cells That Target Cytomegalovirus in Glioblastoma. *Cancer Res.* **78**(1), pp.256-264.

Reeves, M.B., Breidenstein, A. and Compton, T. 2012. Human cytomegalovirus activation of ERK and myeloid cell leukemia-1 protein correlates with survival of latently infected cells. *Proc Natl Acad Sci U S A.* **109**(2), pp.588-593.

Reeves, M.B., Davies, A.A., McSharry, B.P., Wilkinson, G.W. and Sinclair, J.H. 2007. Complex I binding by a virally encoded RNA regulates mitochondria-induced cell death. *Science.* **316**(5829), pp.1345-1348.

Reeves, M.B., Lehner, P.J., Sissons, J.G.P. and Sinclair, J.H. 2005. An in vitro model for the regulation of human cytomegalovirus latency and reactivation in dendritic cells by chromatin remodelling. *J Gen Virol.* **86**(Pt 11), pp.2949-2954.

Reeves, M.B., MacAry, P.A., Lehner, P.J., Sissons, J.G. and Sinclair, J.H. 2005. Latency, chromatin remodeling, and reactivation of human cytomegalovirus in the dendritic cells of healthy carriers. *Proc Natl Acad Sci U S A.* **102**(11), pp.4140-4145.

Reeves, M.B. and Sinclair, J.H. 2013. Circulating dendritic cells isolated from healthy seropositive donors are sites of human cytomegalovirus reactivation in vivo. *J Virol.* **87**(19), pp.10660-10667.

Reifenberger, G., Szymas, J. and Wechsler, W. 1987. Differential expression of glial- and neuronal-associated antigens in human tumors of the central and peripheral nervous system. *Acta Neuropathol.* **74**(2), pp.105-123.

Reinhardt, J., Smith, G.B., Himmelheber, C.T., Azizkhan-Clifford, J. and Mocarski, E.S. 2005. The carboxyl-terminal region of human cytomegalovirus IE1491aa contains an acidic domain that plays a regulatory role and a chromatin-tethering domain that is dispensable during viral replication. *J Virol.* **79**(1), pp.225-233.

Reuter, J.D., Gomez, D.L., Wilson, J.H. and Van Den Pol, A.N. 2004. Systemic immune deficiency necessary for cytomegalovirus invasion of the mature brain. *J Virol.* **78**(3), pp.1473-1487.

Revello, M.G., Zavattoni, M., Furione, M., Lilleri, D., Gorini, G. and Gerna, G. 2002. Diagnosis and outcome of preconceptional and periconceptional primary human cytomegalovirus infections. *J Infect Dis.* **186**(4), pp.553-557.

Riemenschneider, M.J., Büschges, R., Wolter, M., Reifenberger, J., Boström, J., Kraus, J.A., Schlegel, U. and Reifenberger, G. 1999. Amplification and overexpression of the MDM4 (MDMX) gene from 1q32 in a subset of malignant gliomas without TP53 mutation or MDM2 amplification. *Cancer Res.* **59**(24),

pp.6091-6096.

Rolland, M., Li, X., Sellier, Y., Martin, H., Perez-Berezo, T., Rauwel, B., Benchoua, A., Bessières, B., Aziza, J., Cenac, N., Luo, M., Casper, C., Peschanski, M., Gonzalez-Dunia, D., Leruez-Ville, M., Davrinche, C. and Chavanas, S. 2016. PPAR γ Is Activated during Congenital Cytomegalovirus Infection and Inhibits Neuronogenesis from Human Neural Stem Cells. *PLoS Pathog.* **12**(4), pe1005547.

Rossetto, C.C., Tarrant-Elorza, M. and Pari, G.S. 2013. Cis and trans acting factors involved in human cytomegalovirus experimental and natural latent infection of CD14 (+) monocytes and CD34 (+) cells. *PLoS Pathog.* **9**(5), pe1003366.

Rovetta, A. 2020. Raiders of the Lost Correlation: A Guide on Using Pearson and Spearman Coefficients to Detect Hidden Correlations in Medical Sciences. *Cureus.* **12**(11), pe11794.

Ryckman, B.J., Jarvis, M.A., Drummond, D.D., Nelson, J.A. and Johnson, D.C. 2006. Human cytomegalovirus entry into epithelial and endothelial cells depends on genes UL128 to UL150 and occurs by endocytosis and low-pH fusion. *J Virol.* **80**(2), pp.710-722.

Sadanari, H., Yamada, R., Tanaka, J., Murayama, T., Ohnishi, K., Matsubara, K. and Fukuda, S. 1999. The effect of cyclic AMP on expression of the major immediate-early genes and replication of human cytomegalovirus in human central nervous system cell lines. *Arch Virol.* **144**(5), pp.1015-1025.

Sadler, R., Wu, L., Forghani, B., Renne, R., Zhong, W., Herndier, B. and Ganem, D. 1999. A complex translational program generates multiple novel proteins from the latently expressed kaposin (K12) locus of Kaposi's sarcoma-associated herpesvirus. *J Virol.* **73**(7), pp.5722-5730.

Saha, A. and Robertson, E.S. 2019. Mechanisms of B-Cell Oncogenesis Induced by Epstein-Barr Virus. *J Virol.* **93**(13).

Salvant, B.S., Fortunato, E.A. and Spector, D.H. 1998. Cell cycle dysregulation by human cytomegalovirus: influence of the cell cycle phase at the time of infection and effects on cyclin transcription. *J Virol.* **72**(5), pp.3729-3741.

Samanta, M., Harkins, L., Klemm, K., Britt, W.J. and Cobbs, C.S. 2003. High prevalence of human cytomegalovirus in prostatic intraepithelial neoplasia and prostatic carcinoma. *J Urol.* **170**(3), pp.998-1002.

Sanchez, V., Greis, K.D., Sztul, E. and Britt, W.J. 2000. Accumulation of virion tegument and envelope proteins in a stable cytoplasmic compartment during human cytomegalovirus replication: characterization of a potential site of virus assembly. *J Virol.* **74**(2), pp.975-986.

Sánchez-Alegría, K., Flores-León, M., Avila-Muñoz, E., Rodríguez-Corona, N. and Arias, C. 2018. PI3K Signaling in Neurons: A Central Node for the Control of Multiple Functions. *Int J Mol Sci.* **19**(12).

Sandhu, P.K. and Buchkovich, N.J. 2020. Human Cytomegalovirus Decreases Major Histocompatibility Complex Class II by Regulating Class II Transactivator Transcript Levels in a Myeloid Cell Line. *J Virol.* **94**(7).

Sarisky, R.T. and Hayward, G.S. 1996. Evidence that the UL84 gene product of human cytomegalovirus is essential for promoting oriLyt-dependent DNA replication and formation of replication compartments in cotransfection assays. *J Virol.* **70**(11), pp.7398-7413.

Sathiyamoorthy, K., Hu, Y.X., Möhl, B.S., Chen, J., Longnecker, R. and Jardetzky, T.S. 2016. Structural basis for Epstein-Barr virus host cell tropism mediated by gp42 and gHgL entry glycoproteins. *Nat Commun.* **7**, p13557.

- Sato, Y., Mita, S., Fukushima, N., Fujisawa, H., Saga, Y. and Hirata, T. 2011. Induction of axon growth arrest without growth cone collapse through the N-terminal region of four-transmembrane glycoprotein M6a. *Dev Neurobiol.* **71**(9), pp.733-746.
- Schauflinger, M., Fischer, D., Schreiber, A., Chevillotte, M., Walther, P., Mertens, T. and von Einem, J. 2011. The tegument protein UL71 of human cytomegalovirus is involved in late envelopment and affects multivesicular bodies. *J Virol.* **85**(8), pp.3821-3832.
- Scheurer, M.E., Bondy, M.L., Aldape, K.D., Albrecht, T. and El-Zein, R. 2008. Detection of human cytomegalovirus in different histological types of gliomas. *Acta Neuropathol.* **116**(1), pp.79-86.
- Schleiss, M.R. 2006. Acquisition of human cytomegalovirus infection in infants via breast milk: natural immunization or cause for concern? *Rev Med Virol.* **16**(2), pp.73-82.
- Schmidbauer, M., Budka, H., Ulrich, W. and Ambros, P. 1989. Cytomegalovirus (CMV) disease of the brain in AIDS and congenital infection: a comparative study by histology, immunocytochemistry and in situ DNA hybridization. *Acta Neuropathol.* **79**(3), pp.286-293.
- Schmidt, E.V. 1999. The role of c-myc in cellular growth control. *Oncogene.* **18**(19), pp.2988-2996.
- Schottstedt, V., Blümel, J., Burger, R., Drosten, C., Gröner, A., Gürtler, L., Heiden, M., Hildebrandt, M., Jansen, B., Montag-Lessing, T., Offergeld, R., Pauli, G., Seitz, R., Schlenkrich, U., Strobel, J., Willkommen, H. and von König, C.H. 2010. Human Cytomegalovirus (HCMV) - Revised. *Transfus Med Hemother.* **37**(6), pp.365-375.
- Schuessler, A., Smith, C., Beagley, L., Boyle, G.M., Rehan, S., Matthews, K., Jones, L., Crough, T., Dasari, V., Klein, K., Smalley, A., Alexander, H., Walker, D.G. and Khanna, R. 2014. Autologous T-cell therapy for cytomegalovirus as a consolidative treatment for recurrent glioblastoma. *Cancer Res.* **74**(13), pp.3466-3476.
- Schultz, E.P., Lanchy, J.M., Day, L.Z., Yu, Q., Peterson, C., Preece, J. and Ryckman, B.J. 2020. Specialization for Cell-Free or Cell-to-Cell Spread of BAC-Cloned Human Cytomegalovirus Strains Is Determined by Factors beyond the UL128-131 and RL13 Loci. *J Virol.* **94**(13).
- Schut, R.L., Gekker, G., Hu, S., Chao, C.C., Pomeroy, C., Jordan, M.C. and Peterson, P.K. 1994. Cytomegalovirus replication in murine microglial cell cultures: suppression of permissive infection by interferon-gamma. *J Infect Dis.* **169**(5), pp.1092-1096.
- Schwartz, M. and Stern-Ginossar, N. 2019. The Transcriptome of Latent Human Cytomegalovirus. *J Virol.* **93**(11).
- Setinek, U., Wondrusch, E., Jellinger, K., Steuer, A., Drlicek, M., Grisold, W. and Lintner, F. 1995. Cytomegalovirus infection of the brain in AIDS: a clinicopathological study. *Acta Neuropathol.* **90**(5), pp.511-515.
- Shamay, M., Krithivas, A., Zhang, J. and Hayward, S.D. 2006. Recruitment of the de novo DNA methyltransferase Dnmt3a by Kaposi's sarcoma-associated herpesvirus LANA. *Proc Natl Acad Sci U S A.* **103**(39), pp.14554-14559.
- Shao, F. and Liu, C. 2018. Revisit the Candidacy of Brain Cell Types as the Cell(s) of Origin for Human High-Grade Glioma. *Front Mol Neurosci.* **11**, p48.
- Sharma, M., Kamil, J.P., Coughlin, M., Reim, N.I. and Coen, D.M. 2014. Human cytomegalovirus UL50 and UL53 recruit viral protein kinase UL97, not protein kinase C, for disruption of nuclear lamina and nuclear egress in infected

cells. *J Virol.* **88**(1), pp.249-262.

Sheng, Z., Li, L., Zhu, L.J., Smith, T.W., Demers, A., Ross, A.H., Moser, R.P. and Green, M.R. 2010. A genome-wide RNA interference screen reveals an essential CREB3L2-ATF5-MCL1 survival pathway in malignant glioma with therapeutic implications. *Nat Med.* **16**(6), pp.671-677.

Shibahara, K. and Stillman, B. 1999. Replication-dependent marking of DNA by PCNA facilitates CAF-1-coupled inheritance of chromatin. *Cell.* **96**(4), pp.575-585.

Shitamukai, A., Konno, D. and Matsuzaki, F. 2011. Oblique radial glial divisions in the developing mouse neocortex induce self-renewing progenitors outside the germinal zone that resemble primate outer subventricular zone progenitors. *J Neurosci.* **31**(10), pp.3683-3695.

Shnayder, M., Nachshon, A., Krishna, B., Poole, E., Boshkov, A., Binyamin, A., Maza, I., Sinclair, J., Schwartz, M. and Stern-Ginossar, N. 2018. Defining the Transcriptional Landscape during Cytomegalovirus Latency with Single-Cell RNA Sequencing. *mBio.* **9**(2).

Shnayder, M., Nachshon, A., Rozman, B., Bernshtein, B., Lavi, M., Fein, N., Poole, E., Avdic, S., Blyth, E., Gottlieb, D., Abendroth, A., Slobedman, B., Sinclair, J., Stern-Ginossar, N. and Schwartz, M. 2020. Single cell analysis reveals human cytomegalovirus drives latently infected cells towards an anergic-like monocyte state. *Elife.* **9**.

Sikora, F.J., Dillard, E.F., Copeland, J.P. and Mullins, G.L. 1989. Chemical characterization and bioavailability of phosphorus in water-insoluble fractions of three mono-ammonium phosphate fertilizers. *J Assoc Off Anal Chem.* **72**(5), pp.852-856.

Sin, S.H., Fakhari, F.D. and Dittmer, D.P. 2010. The viral latency-associated nuclear antigen augments the B-cell response to antigen in vivo. *J Virol.* **84**(20), pp.10653-10660.

Singh, S.K., Hawkins, C., Clarke, I.D., Squire, J.A., Bayani, J., Hide, T., Henkelman, R.M., Cusimano, M.D. and Dirks, P.B. 2004. Identification of human brain tumour initiating cells. *Nature.* **432**(7015), pp.396-401.

Sinigalia, E., Alvisi, G., Segré, C.V., Mercorelli, B., Muratore, G., Winkler, M., Hsiao, H.H., Urlaub, H., Ripalti, A., Chiocca, S., Palù, G. and Loregian, A. 2012. The human cytomegalovirus DNA polymerase processivity factor UL44 is modified by SUMO in a DNA-dependent manner. *PLoS One.* **7**(11), pe49630.

Sinzger, C., Digel, M. and Jahn, G. 2008. Cytomegalovirus cell tropism. *Curr Top Microbiol Immunol.* **325**, pp.63-83.

Sison, S.L., O'Brien, B.S., Johnson, A.J., Seminary, E.R., Terhune, S.S. and Ebert, A.D. 2019. Human Cytomegalovirus Disruption of Calcium Signaling in Neural Progenitor Cells and Organoids. *J Virol.* **93**(17).

Skaletskaya, A., Bartle, L.M., Chittenden, T., McCormick, A.L., Mocarski, E.S. and Goldmacher, V.S. 2001. A cytomegalovirus-encoded inhibitor of apoptosis that suppresses caspase-8 activation. *Proc Natl Acad Sci U S A.* **98**(14), pp.7829-7834.

Škubník, J., Pavlíčková, V.S., Ruml, T. and Rimpelová, S. 2021. Vincristine in Combination Therapy of Cancer: Emerging Trends in Clinics. *Biology (Basel).* **10**(9).

Slinger, E., Langemeijer, E., Siderius, M., Vischer, H.F. and Smit, M.J. 2011. Herpesvirus-encoded GPCRs rewire cellular signaling. *Mol Cell Endocrinol.* **331**(2), pp.179-184.

Slinger, E., Maussang, D., Schreiber, A., Siderius, M., Rahbar, A., Fraile-

- Ramos, A., Lira, S.A., Söderberg-Nauclér, C. and Smit, M.J. 2010. HCMV-encoded chemokine receptor US28 mediates proliferative signaling through the IL-6-STAT3 axis. *Sci Signal.* **3**(133), pra58.
- Smart, I. 1961. The subependymal layer of the mouse brain and its cell production as shown by radioautography after thymidine-H3 injection. *Journal of Comparative Neurology.* **116**(3), pp.325-347.
- Smith, J.S., Herrero, R., Bosetti, C., Muñoz, N., Bosch, F.X., Eluf-Neto, J., Castellsagué, X., Meijer, C.J., Van den Brule, A.J., Franceschi, S., Ashley, R. and Group, I.A.f.R.o.C.I.M.C.C.S. 2002. Herpes simplex virus-2 as a human papillomavirus cofactor in the etiology of invasive cervical cancer. *J Natl Cancer Inst.* **94**(21), pp.1604-1613.
- Söderberg-Nauclér, C., Fish, K.N. and Nelson, J.A. 1997. Reactivation of latent human cytomegalovirus by allogeneic stimulation of blood cells from healthy donors. *Cell.* **91**(1), pp.119-126.
- Söderberg-Nauclér, C. and Nelson, J.Y. 1999. Human cytomegalovirus latency and reactivation - a delicate balance between the virus and its host's immune system. *Intervirol.* **42**(5-6), pp.314-321.
- Söderberg-Naucler, C., Peredo, I., Rahbar, A., Hansson, F., Nordlund, A. and Stragliotto, G. 2014. Use of Cox regression with treatment status as a time-dependent covariate to re-analyze survival benefit excludes immortal time bias effect in patients with glioblastoma who received prolonged adjuvant treatment with valganciclovir. *Int J Cancer.* **135**(1), pp.248-249.
- Soroceanu, L., Akhavan, A. and Cobbs, C.S. 2008. Platelet-derived growth factor-alpha receptor activation is required for human cytomegalovirus infection. *Nature.* **455**(7211), pp.391-395.
- Soroceanu, L., Matlaf, L., Khan, S., Akhavan, A., Singer, E., Bezrookove, V., Decker, S., Ghanny, S., Hadaczek, P., Bengtsson, H., Ohlfest, J., Luciani-Torres, M.G., Harkins, L., Perry, A., Guo, H., Soteropoulos, P. and Cobbs, C.S. 2015. Cytomegalovirus Immediate-Early Proteins Promote Stemness Properties in Glioblastoma. *Cancer Res.* **75**(15), pp.3065-3076.
- Spiess, K., Jeppesen, M.G., Malmgaard-Clausen, M., Krzywkowski, K., Dulal, K., Cheng, T., Hjortø, G.M., Larsen, O., Burg, J.S., Jarvis, M.A., Garcia, K.C., Zhu, H., Kledal, T.N. and Rosenkilde, M.M. 2015. Rationally designed chemokine-based toxin targeting the viral G protein-coupled receptor US28 potently inhibits cytomegalovirus infection in vivo. *Proc Natl Acad Sci U S A.* **112**(27), pp.8427-8432.
- Spiller, O.B., Borysiewicz, L.K. and Morgan, B.P. 1997. Development of a model for cytomegalovirus infection of oligodendrocytes. *J Gen Virol.* **78** (Pt **12**), pp.3349-3356.
- Stagno, S., Pass, R.F., Cloud, G., Britt, W.J., Henderson, R.E., Walton, P.D., Veren, D.A., Page, F. and Alford, C.A. 1986. Primary cytomegalovirus infection in pregnancy. Incidence, transmission to fetus, and clinical outcome. *Jama.* **256**(14), pp.1904-1908.
- Stanton, R.J., Baluchova, K., Dargan, D.J., Cunningham, C., Sheehy, O., Seirafian, S., McSharry, B.P., Neale, M.L., Davies, J.A., Tomasec, P., Davison, A.J. and Wilkinson, G.W. 2010. Reconstruction of the complete human cytomegalovirus genome in a BAC reveals RL13 to be a potent inhibitor of replication. *J Clin Invest.* **120**(9), pp.3191-3208.
- Stensjøen, A.L., Berntsen, E.M., Jakola, A.S. and Solheim, O. 2018. When did the glioblastoma start growing, and how much time can be gained from surgical resection? A model based on the pattern of glioblastoma growth in vivo. *Clin*

Neurol Neurosurg. **170**, pp.38-42.

Stergachis, A.B., Pujol-Giménez, J., Gyimesi, G., Fuster, D., Albano, G., Troxler, M., Picker, J., Rosenberg, P.A., Bergin, A., Peters, J., El Achkar, C.M., Harini, C., Manzi, S., Rotenberg, A., Hediger, M.A. and Rodan, L.H. 2019.

Recurrent SLC1A2 variants cause epilepsy via a dominant negative mechanism. *Ann Neurol.* **85**(6), pp.921-926.

Stevenson, E.V., Collins-McMillen, D., Kim, J.H., Cieply, S.J., Bentz, G.L. and Yurochko, A.D. 2014. HCMV reprogramming of infected monocyte survival and differentiation: a Goldilocks phenomenon. *Viruses.* **6**(2), pp.782-807.

Strååt, K., Liu, C., Rahbar, A., Zhu, Q., Liu, L., Wolmer-Solberg, N., Lou, F., Liu, Z., Shen, J., Jia, J., Kyo, S., Björkholm, M., Sjöberg, J., Söderberg-Nauclér, C. and Xu, D. 2009. Activation of telomerase by human cytomegalovirus. *J Natl Cancer Inst.* **101**(7), pp.488-497.

Stragliotto, G., Pantalone, M.R., Rahbar, A. and Söderberg-Nauclér, C. 2020. Valganciclovir as Add-On to Standard Therapy in Secondary Glioblastoma. *Microorganisms.* **8**(10).

Stragliotto, G., Rahbar, A., Solberg, N.W., Lilja, A., Taher, C., Orrego, A., Bjurman, B., Tammik, C., Skarman, P., Peredo, I. and Söderberg-Nauclér, C. 2013. Effects of valganciclovir as an add-on therapy in patients with cytomegalovirus-positive glioblastoma: a randomized, double-blind, hypothesis-generating study. *Int J Cancer.* **133**(5), pp.1204-1213.

Strang, B.L., Boulant, S. and Coen, D.M. 2010. Nucleolin associates with the human cytomegalovirus DNA polymerase accessory subunit UL44 and is necessary for efficient viral replication. *J Virol.* **84**(4), pp.1771-1784.

Streit, W.J., Mrak, R.E. and Griffin, W.S. 2004. Microglia and neuroinflammation: a pathological perspective. *J Neuroinflammation.* **1**(1), p14.

Stupp, R., Mason, W.P., van den Bent, M.J., Weller, M., Fisher, B., Taphoorn, M.J., Belanger, K., Brandes, A.A., Marosi, C., Bogdahn, U., Curschmann, J., Janzer, R.C., Ludwin, S.K., Gorlia, T., Allgeier, A., Lacombe, D., Cairncross, J.G., Eisenhauer, E., Mirimanoff, R.O., Groups, E.O.f.R.a.T.o.C.B.T.a.R. and Group, N.C.I.o.C.C.T. 2005. Radiotherapy plus concomitant and adjuvant temozolomide for glioblastoma. *N Engl J Med.* **352**(10), pp.987-996.

Stupp, R., Taillibert, S., Kanner, A., Read, W., Steinberg, D., Lhermitte, B., Toms, S., Idbaih, A., Ahluwalia, M.S., Fink, K., Di Meco, F., Lieberman, F., Zhu, J.J., Stragliotto, G., Tran, D., Brem, S., Hottinger, A., Kirson, E.D., Lavy-Shahaf, G., Weinberg, U., Kim, C.Y., Paek, S.H., Nicholas, G., Bruna, J., Hirte, H., Weller, M., Palti, Y., Hegi, M.E. and Ram, Z. 2017. Effect of Tumor-Treating Fields Plus Maintenance Temozolomide vs Maintenance Temozolomide Alone on Survival in Patients With Glioblastoma: A Randomized Clinical Trial. *JAMA.* **318**(23), pp.2306-2316.

Stürzl, M., Hohenadl, C., Zietz, C., Castanos-Velez, E., Wunderlich, A., Ascherl, G., Biberfeld, P., Monini, P., Browning, P.J. and Ensoli, B. 1999. Expression of K13/v-FLIP gene of human herpesvirus 8 and apoptosis in Kaposi's sarcoma spindle cells. *J Natl Cancer Inst.* **91**(20), pp.1725-1733.

Sullivan, K.D., Galbraith, M.D., Andrysik, Z. and Espinosa, J.M. 2018. Mechanisms of transcriptional regulation by p53. *Cell Death Differ.* **25**(1), pp.133-143.

Sun, G., Chiappesi, F., Chen, X., Wang, C., Tian, E., Nguyen, J., Kha, M., Trinh, D., Zhang, H., Marchetto, M.C., Song, H., Ming, G.L., Gage, F.H., Diamond, D.J., Wussow, F. and Shi, Y. 2020. Modeling Human Cytomegalovirus-Induced Microcephaly in Human iPSC-Derived Brain

- Organoids. *Cell Rep Med.* **1**(1), p100002.
- Sun, Q., Tsurimoto, T., Juillard, F., Li, L., Li, S., De León Vázquez, E., Chen, S. and Kaye, K. 2014. Kaposi's sarcoma-associated herpesvirus LANA recruits the DNA polymerase clamp loader to mediate efficient replication and virus persistence. *Proc Natl Acad Sci U S A.* **111**(32), pp.11816-11821.
- Sun, R., Liang, D., Gao, Y. and Lan, K. 2014. Kaposi's sarcoma-associated herpesvirus-encoded LANA interacts with host KAP1 to facilitate establishment of viral latency. *J Virol.* **88**(13), pp.7331-7344.
- Sun, Y., Liu, W.Z., Liu, T., Feng, X., Yang, N. and Zhou, H.F. 2015. Signaling pathway of MAPK/ERK in cell proliferation, differentiation, migration, senescence and apoptosis. *J Recept Signal Transduct Res.* **35**(6), pp.600-604.
- Suzich, J.B. and Cliffe, A.R. 2018. Strength in diversity: Understanding the pathways to herpes simplex virus reactivation. *Virology.* **522**, pp.81-91.
- Sylwester, A.W., Mitchell, B.L., Edgar, J.B., Taormina, C., Pelte, C., Ruchti, F., Sleath, P.R., Grabstein, K.H., Hosken, N.A., Kern, F., Nelson, J.A. and Picker, L.J. 2005. Broadly targeted human cytomegalovirus-specific CD4+ and CD8+ T cells dominate the memory compartments of exposed subjects. *J Exp Med.* **202**(5), pp.673-685.
- Tai-Schmiedel, J., Karniely, S., Lau, B., Ezra, A., Eliyahu, E., Nachshon, A., Kerr, K., Suárez, N., Schwartz, M., Davison, A.J. and Stern-Ginossar, N. 2020. Human cytomegalovirus long noncoding RNA4.9 regulates viral DNA replication. *PLoS Pathog.* **16**(4), pe1008390.
- Takahashi, K. and Yamanaka, S. 2006. Induction of pluripotent stem cells from mouse embryonic and adult fibroblast cultures by defined factors. *Cell.* **126**(4), pp.663-676.
- Takahashi, T., Nowakowski, R.S. and Caviness, V.S. 1996. The leaving or Q fraction of the murine cerebral proliferative epithelium: a general model of neocortical neuronogenesis. *J Neurosci.* **16**(19), pp.6183-6196.
- Tan, A.C., Ashley, D.M., López, G.Y., Malinzak, M., Friedman, H.S. and Khasraw, M. 2020. Management of glioblastoma: State of the art and future directions. *CA Cancer J Clin.* **70**(4), pp.299-312.
- Tandon, R. and Mocarski, E.S. 2012. Viral and host control of cytomegalovirus maturation. *Trends Microbiol.* **20**(8), pp.392-401.
- Tarrant-Elorza, M., Rossetto, C.C. and Pari, G.S. 2014. Maintenance and replication of the human cytomegalovirus genome during latency. *Cell Host Microbe.* **16**(1), pp.43-54.
- Tchirkov, A., Rolhion, C., Kémény, J.L., Irthum, B., Puget, S., Khalil, T., Chinot, O., Kwiatkowski, F., Périssel, B., Vago, P. and Verrelle, P. 2003. Clinical implications of quantitative real-time RT-PCR analysis of hTERT gene expression in human gliomas. *Br J Cancer.* **88**(4), pp.516-520.
- Teissier, N., Fallet-Bianco, C., Delezoide, A.L., Laquerrière, A., Marcorelles, P., Khung-Savatovsky, S., Nardelli, J., Cipriani, S., Csaba, Z., Picone, O., Golden, J.A., Van Den Abbeele, T., Gressens, P. and Adle-Biassette, H. 2014. Cytomegalovirus-induced brain malformations in fetuses. *J Neuropathol Exp Neurol.* **73**(2), pp.143-158.
- Terhune, S., Torigo, E., Moorman, N., Silva, M., Qian, Z., Shenk, T. and Yu, D. 2007. Human cytomegalovirus UL38 protein blocks apoptosis. *J Virol.* **81**(7), pp.3109-3123.
- Thomas, S.J., Snowden, J.A., Zeidler, M.P. and Danson, S.J. 2015. The role of JAK/STAT signalling in the pathogenesis, prognosis and treatment of solid tumours. *Br J Cancer.* **113**(3), pp.365-371.

- Thota, B., Arimappamagan, A., Kandavel, T., Shastry, A.H., Pandey, P., Chandramouli, B.A., Hegde, A.S., Kondaiah, P. and Santosh, V. 2014. STAT-1 expression is regulated by IGF1BP-3 in malignant glioma cells and is a strong predictor of poor survival in patients with glioblastoma. *J Neurosurg.* **121**(2), pp.374-383.
- Tomlinson, C.C. and Damania, B. 2004. The K1 protein of Kaposi's sarcoma-associated herpesvirus activates the Akt signaling pathway. *J Virol.* **78**(4), pp.1918-1927.
- Tomtishen, J.P. 2012. Human cytomegalovirus tegument proteins (pp65, pp71, pp150, pp28). *Virol J.* **9**, p22.
- Tong, H., Yu, X., Lu, X. and Wang, P. 2015. Downregulation of solute carriers of glutamate in gliosomes and synaptosomes may explain local brain metastasis in anaplastic glioblastoma. *IUBMB Life.* **67**(4), pp.306-311.
- Toth, A.B., Shum, A.K. and Prakriya, M. 2016. Regulation of neurogenesis by calcium signaling. *Cell Calcium.* **59**(2-3), pp.124-134.
- Tramontin, A.D., García-Verdugo, J.M., Lim, D.A. and Alvarez-Buylla, A. 2003. Postnatal development of radial glia and the ventricular zone (VZ): a continuum of the neural stem cell compartment. *Cereb Cortex.* **13**(6), pp.580-587.
- Trépant, A.L., Bouchart, C., Rorive, S., Sauvage, S., Decaestecker, C., Demetter, P. and Salmon, I. 2015. Identification of OLIG2 as the most specific glioblastoma stem cell marker starting from comparative analysis of data from similar DNA chip microarray platforms. *Tumour Biol.* **36**(3), pp.1943-1953.
- Tsai, H.L., Kou, G.H., Chen, S.C., Wu, C.W. and Lin, Y.S. 1996. Human cytomegalovirus immediate-early protein IE2 tethers a transcriptional repression domain to p53. *J Biol Chem.* **271**(7), pp.3534-3540.
- Tsutsui, Y., Kawasaki, H. and Kosugi, I. 2002. Reactivation of latent cytomegalovirus infection in mouse brain cells detected after transfer to brain slice cultures. *J Virol.* **76**(14), pp.7247-7254.
- Uckun, F.M., Sather, H., Reaman, G., Shuster, J., Land, V., Trigg, M., Gunther, R., Chelstrom, L., Bleyer, A. and Gaynon, P. 1995. Leukemic cell growth in SCID mice as a predictor of relapse in high-risk B-lineage acute lymphoblastic leukemia. *Blood.* **85**(4), pp.873-878.
- Umashankar, M., Rak, M., Bughio, F., Zagallo, P., Caviness, K. and Goodrum, F.D. 2014. Antagonistic determinants controlling replicative and latent states of human cytomegalovirus infection. *J Virol.* **88**(11), pp.5987-6002.
- Vanarsdall, A.L. and Johnson, D.C. 2012. Human cytomegalovirus entry into cells. *Curr Opin Virol.* **2**(1), pp.37-42.
- Veeriah, S., Brennan, C., Meng, S., Singh, B., Fagin, J.A., Solit, D.B., Paty, P.B., Rohle, D., Vivanco, I., Chmielecki, J., Pao, W., Ladanyi, M., Gerald, W.L., Liao, L., Cloughesy, T.C., Mischel, P.S., Sander, C., Taylor, B., Schultz, N., Major, J., Heguy, A., Fang, F., Mellinghoff, I.K. and Chan, T.A. 2009. The tyrosine phosphatase PTPRD is a tumor suppressor that is frequently inactivated and mutated in glioblastoma and other human cancers. *Proc Natl Acad Sci U S A.* **106**(23), pp.9435-9440.
- Verhaak, R.G., Hoadley, K.A., Purdom, E., Wang, V., Qi, Y., Wilkerson, M.D., Miller, C.R., Ding, L., Golub, T., Mesirov, J.P., Alexe, G., Lawrence, M., O'Kelly, M., Tamayo, P., Weir, B.A., Gabriel, S., Winckler, W., Gupta, S., Jakkula, L., Feiler, H.S., Hodgson, J.G., James, C.D., Sarkaria, J.N., Brennan, C., Kahn, A., Spellman, P.T., Wilson, R.K., Speed, T.P., Gray, J.W., Meyerson, M., Getz, G., Perou, C.M., Hayes, D.N. and Network, C.G.A.R. 2010. Integrated genomic analysis identifies clinically relevant subtypes of glioblastoma characterized by

- abnormalities in PDGFRA, IDH1, EGFR, and NF1. *Cancer Cell*. **17**(1), pp.98-110.
- Viswanathan, K., Smith, M.S., Malouli, D., Mansouri, M., Nelson, J.A. and Fröh, K. 2011. BST2/Tetherin enhances entry of human cytomegalovirus. *PLoS Pathog*. **7**(11), pe1002332.
- Vitucci, M., Irvin, D.M., McNeill, R.S., Schmid, R.S., Simon, J.M., Dhruv, H.D., Siegel, M.B., Werneke, A.M., Bash, R.E., Kim, S., Berens, M.E. and Miller, C.R. 2017. Genomic profiles of low-grade murine gliomas evolve during progression to glioblastoma. *Neuro Oncol*. **19**(9), pp.1237-1247.
- von Laer, D., Meyer-Koenig, U., Serr, A., Finke, J., Kanz, L., Fauser, A.A., Neumann-Haefelin, D., Brugger, W. and Hufert, F.T. 1995. Detection of cytomegalovirus DNA in CD34+ cells from blood and bone marrow. *Blood*. **86**(11), pp.4086-4090.
- Vossen, M.T., Westerhout, E.M., Söderberg-Nauclér, C. and Wiertz, E.J. 2002. Viral immune evasion: a masterpiece of evolution. *Immunogenetics*. **54**(8), pp.527-542.
- Walker, F., Kato, A., Gonez, L.J., Hibbs, M.L., Pouliot, N., Levitzki, A. and Burgess, A.W. 1998. Activation of the Ras/mitogen-activated protein kinase pathway by kinase-defective epidermal growth factor receptors results in cell survival but not proliferation. *Mol Cell Biol*. **18**(12), pp.7192-7204.
- Walton, N.M., Sutter, B.M., Chen, H.X., Chang, L.J., Roper, S.N., Scheffler, B. and Steindler, D.A. 2006. Derivation and large-scale expansion of multipotent astroglial neural progenitors from adult human brain. *Development*. **133**(18), pp.3671-3681.
- Wang, D. and Shenk, T. 2005a. Human Cytomegalovirus UL131 Open Reading Frame Is Required for Epithelial Cell Tropism. *Journal of Virology*. **79**(16), p10330.
- Wang, D. and Shenk, T. 2005b. Human cytomegalovirus virion protein complex required for epithelial and endothelial cell tropism. *Proceedings of the National Academy of Sciences of the United States of America*. **102**(50), p18153.
- Wang, D., Zhang, J., Li, Z., Han, J., Gao, Y., Chen, M. and Li, Y. 2019. Upregulation of Fibroblast Growth Factor 19 Is Associated with the Initiation of Colorectal Adenoma. *Dig Dis*. **37**(3), pp.214-225.
- Wang, J., Cazzato, E., Ladewig, E., Frattini, V., Rosenbloom, D.I., Zairis, S., Abate, F., Liu, Z., Elliott, O., Shin, Y.J., Lee, J.K., Lee, I.H., Park, W.Y., Eoli, M., Blumberg, A.J., Lasorella, A., Nam, D.H., Finocchiaro, G., Iavarone, A. and Rabadan, R. 2016. Clonal evolution of glioblastoma under therapy. *Nat Genet*. **48**(7), pp.768-776.
- Wang, L., Wang, Z., Li, J., Zhang, W., Ren, F. and Yue, W. 2015. NFATc1 activation promotes the invasion of U251 human glioblastoma multiforme cells through COX-2. *Int J Mol Med*. **35**(5), pp.1333-1340.
- Wang, T., Qian, D., Hu, M., Li, L., Zhang, L., Chen, H., Yang, R. and Wang, B. 2014. Human cytomegalovirus inhibits apoptosis by regulating the activating transcription factor 5 signaling pathway in human malignant glioma cells. *Oncol Lett*. **8**(3), pp.1051-1057.
- Wang, X., Huong, S.M., Chiu, M.L., Raab-Traub, N. and Huang, E.S. 2003. Epidermal growth factor receptor is a cellular receptor for human cytomegalovirus. *Nature*. **424**(6947), pp.456-461.
- Wang, X., Zhou, R., Xiong, Y., Zhou, L., Yan, X., Wang, M., Li, F., Xie, C., Zhang, Y., Huang, Z., Ding, C., Shi, K., Li, W., Liu, Y., Cao, Z., Zhang, Z.N., Zhou, S., Chen, C., Chen, L. and Wang, Y. 2021. Sequential fate-switches in

- stem-like cells drive the tumorigenic trajectory from human neural stem cells to malignant glioma. *Cell Res.* **31**(6), pp.684-702.
- Wang, Y.D., Cai, N., Wu, X.L., Cao, H.Z., Xie, L.L. and Zheng, P.S. 2013. OCT4 promotes tumorigenesis and inhibits apoptosis of cervical cancer cells by miR-125b/BAK1 pathway. *Cell Death Dis.* **4**, pe760.
- Wang, Y.J. and Herlyn, M. 2015. The emerging roles of Oct4 in tumor-initiating cells. *Am J Physiol Cell Physiol.* **309**(11), pp.C709-718.
- Wang, Y.Q. and Zhao, X.Y. 2020. Human Cytomegalovirus Primary Infection and Reactivation: Insights From Virion-Carried Molecules. *Front Microbiol.* **11**, p1511.
- Wang, Z., Zhang, H., Xu, S., Liu, Z. and Cheng, Q. 2021. The adaptive transition of glioblastoma stem cells and its implications on treatments. *Signal Transduct Target Ther.* **6**(1), p124.
- Wathen, M.W. and Stinski, M.F. 1982. Temporal patterns of human cytomegalovirus transcription: mapping the viral RNAs synthesized at immediate early, early, and late times after infection. *J Virol.* **41**(2), pp.462-477.
- Weekes, M.P., Tan, S.Y., Poole, E., Talbot, S., Antrobus, R., Smith, D.L., Montag, C., Gygi, S.P., Sinclair, J.H. and Lehner, P.J. 2013. Latency-associated degradation of the MRP1 drug transporter during latent human cytomegalovirus infection. *Science.* **340**(6129), pp.199-202.
- Wei, F., Gan, J., Wang, C., Zhu, C. and Cai, Q. 2016. Cell Cycle Regulatory Functions of the KSHV Oncoprotein LANA. *Front Microbiol.* **7**, p334.
- Weidner-Glunde, M., Kruminis-Kaszkiel, E. and Savanagouder, M. 2020. Herpesviral Latency-Common Themes. *Pathogens.* **9**(2).
- Weiland, K.L., Oien, N.L., Homa, F. and Wathen, M.W. 1994. Functional analysis of human cytomegalovirus polymerase accessory protein. *Virus Res.* **34**(3), pp.191-206.
- Wiebusch, L. and Hagemeyer, C. 2001. The human cytomegalovirus immediate early 2 protein dissociates cellular DNA synthesis from cyclin-dependent kinase activation. *EMBO J.* **20**(5), pp.1086-1098.
- Wilhelmsson, U., Bushong, E.A., Price, D.L., Smarr, B.L., Phung, V., Terada, M., Ellisman, M.H. and Pekny, M. 2006. Redefining the concept of reactive astrocytes as cells that remain within their unique domains upon reaction to injury. *Proc Natl Acad Sci U S A.* **103**(46), pp.17513-17518.
- Wilkinson, G.W.G., Davison, A.J., Tomasec, P., Fielding, C.A., Aicheler, R., Murrell, I., Seirafian, S., Wang, E.C.Y., Weekes, M., Lehner, P.J., Wilkie, G.S. and Stanton, R.J. 2015. Human cytomegalovirus: taking the strain. *Medical microbiology and immunology.* **204**(3), pp.273-284.
- Wille, P.T., Wisner, T.W., Ryckman, B. and Johnson, D.C. 2013. Human cytomegalovirus (HCMV) glycoprotein gB promotes virus entry in trans acting as the viral fusion protein rather than as a receptor-binding protein. *mBio.* **4**(3), pp.e00332-00313.
- Wills, M.R., Carmichael, A.J., Mynard, K., Jin, X., Weekes, M.P., Plachter, B. and Sissons, J.G. 1996. The human cytotoxic T-lymphocyte (CTL) response to cytomegalovirus is dominated by structural protein pp65: frequency, specificity, and T-cell receptor usage of pp65-specific CTL. *J Virol.* **70**(11), pp.7569-7579.
- Wilson, A.C. and Mohr, I. 2012. A cultured affair: HSV latency and reactivation in neurons. *Trends Microbiol.* **20**(12), pp.604-611.
- Wolmer-Solberg, N., Baryawno, N., Rahbar, A., Fuchs, D., Odeberg, J., Taher, C., Wilhelmi, V., Milosevic, J., Mohammad, A.A., Martinsson, T., Sveinbjörnsson, B., Johnsen, J.I., Kogner, P. and Söderberg-Nauclér, C. 2013.

- Frequent detection of human cytomegalovirus in neuroblastoma: a novel therapeutic target? *Int J Cancer*. **133**(10), pp.2351-2361.
- Wu, X., Ge, H., Lemon, B., Vonderfecht, S., Weiszmann, J., Hecht, R., Gupte, J., Hager, T., Wang, Z., Lindberg, R. and Li, Y. 2010. FGF19-induced hepatocyte proliferation is mediated through FGFR4 activation. *J Biol Chem*. **285**(8), pp.5165-5170.
- Wurdak, H., Zhu, S., Romero, A., Loriger, M., Watson, J., Chiang, C.Y., Zhang, J., Natu, V.S., Lairson, L.L., Walker, J.R., Trussell, C.M., Harsh, G.R., Vogel, H., Felding-Habermann, B., Orth, A.P., Miraglia, L.J., Rines, D.R., Skirboll, S.L. and Schultz, P.G. 2010. An RNAi screen identifies TRRAP as a regulator of brain tumor-initiating cell differentiation. *Cell Stem Cell*. **6**(1), pp.37-47.
- Wylie, K.M., Mihindukulasuriya, K.A., Zhou, Y., Sodergren, E., Storch, G.A. and Weinstock, G.M. 2014. Metagenomic analysis of double-stranded DNA viruses in healthy adults. *BMC Biol*. **12**, p71.
- Xie, J., Wang, Z., Fan, W., Liu, Y., Liu, F., Wan, X., Liu, M., Wang, X., Zeng, D., Wang, Y., He, B., Yan, M., Zhang, Z., Zhang, M., Hou, Z., Wang, C., Kang, Z., Fang, W., Zhang, L., Lam, E.W., Guo, X., Yan, J., Zeng, Y., Chen, M. and Liu, Q. 2021. Targeting cancer cell plasticity by HDAC inhibition to reverse EBV-induced dedifferentiation in nasopharyngeal carcinoma. *Signal Transduct Target Ther*. **6**(1), p333.
- Xie, Z., Bailey, A., Kuleshov, M.V., Clarke, D.J.B., Evangelista, J.E., Jenkins, S.L., Lachmann, A., Wojciechowicz, M.L., Kropiwnicki, E., Jagodnik, K.M., Jeon, M. and Ma'ayan, A. 2021. Gene Set Knowledge Discovery with Enrichr. *Curr Protoc*. **1**(3), pe90.
- Yan, L., Majerciak, V., Zheng, Z.M. and Lan, K. 2019. Towards Better Understanding of KSHV Life Cycle: from Transcription and Posttranscriptional Regulations to Pathogenesis. *Virology*. **34**(2), pp.135-161.
- Yi, F., Saha, A., Murakami, M., Kumar, P., Knight, J.S., Cai, Q., Choudhuri, T. and Robertson, E.S. 2009. Epstein-Barr virus nuclear antigen 3C targets p53 and modulates its transcriptional and apoptotic activities. *Virology*. **388**(2), pp.236-247.
- Yin, H., Qu, J., Peng, Q. and Gan, R. 2019. Molecular mechanisms of EBV-driven cell cycle progression and oncogenesis. *Med Microbiol Immunol*. **208**(5), pp.573-583.
- Yu, Y. and Alwine, J.C. 2002. Human cytomegalovirus major immediate-early proteins and simian virus 40 large T antigen can inhibit apoptosis through activation of the phosphatidylinositide 3'-OH kinase pathway and the cellular kinase Akt. *J Virol*. **76**(8), pp.3731-3738.
- Yu, Y., Cai, J.P., Tu, B., Wu, L., Zhao, Y., Liu, X., Li, L., McNutt, M.A., Feng, J., He, Q., Yang, Y., Wang, H., Sekiguchi, M. and Zhu, W.G. 2009. Proliferating cell nuclear antigen is protected from degradation by forming a complex with MutT Homolog2. *J Biol Chem*. **284**(29), pp.19310-19320.
- Yuan, J., Li, M., Torres, Y.R., Galle, C.S. and Meier, J.L. 2015. Differentiation-Coupled Induction of Human Cytomegalovirus Replication by Union of the Major Enhancer Retinoic Acid, Cyclic AMP, and NF- κ B Response Elements. *J Virol*. **89**(24), pp.12284-12298.
- Zhang, S., Mercado-Urbe, I., Xing, Z., Sun, B., Kuang, J. and Liu, J. 2014. Generation of cancer stem-like cells through the formation of polyploid giant cancer cells. *Oncogene*. **33**(1), pp.116-128.
- Zhang, Y., Pan, C., Wang, J., Cao, J., Liu, Y., Wang, Y. and Zhang, L. 2017. Genetic and immune features of resectable malignant brainstem gliomas.

Oncotarget. **8**(47), pp.82571-82582.

Zhang, Y., Peng, X., Tang, Y., Gan, X., Wang, C., Xie, L., Xie, X., Gan, R. and Wu, Y. 2016. Identification of IgH gene rearrangement and immunophenotype in an animal model of Epstein-Barr virus-associated lymphomas. *J Med Virol*. **88**(10), pp.1804-1813.

Zhang, Z., Huang, X., Li, J., Fan, H., Yang, F., Zhang, R., Yang, Y., Feng, S., He, D., Sun, W. and Xin, T. 2019. Interleukin 10 promotes growth and invasion of glioma cells by up-regulating KPNA 2. *J Cancer Res Ther*. **15**(4), pp.927-932.

Zhou, X., Hao, Q., Liao, P., Luo, S., Zhang, M., Hu, G., Liu, H., Zhang, Y., Cao, B., Baddoo, M., Flemington, E.K., Zeng, S.X. and Lu, H. 2016. Nerve growth factor receptor negates the tumor suppressor p53 as a feedback regulator. *Elife*. **5**.

Zhu, X., Gleiberman, A.S. and Rosenfeld, M.G. 2007. Molecular physiology of pituitary development: signaling and transcriptional networks. *Physiol Rev*. **87**(3), pp.933-963.

Zhu, X., Hu, B., Hu, M., Qian, D. and Wang, B. 2020. Human cytomegalovirus infection enhances invasiveness and migration of glioblastoma cells by epithelial-to-mesenchymal transition. *Int J Clin Exp Pathol*. **13**(10), pp.2637-2647.

Zoncu, R., Efeyan, A. and Sabatini, D.M. 2011. mTOR: from growth signal integration to cancer, diabetes and ageing. *Nat Rev Mol Cell Biol*. **12**(1), pp.21-35.

Zuhair, M., Smit, G.S.A., Wallis, G., Jabbar, F., Smith, C., Devleesschauwer, B. and Griffiths, P. 2019. Estimation of the worldwide seroprevalence of cytomegalovirus: A systematic review and meta-analysis. *Rev Med Virol*. **29**(3), pe2034.

Zuhair, M., Smit, G.S.A., Wallis, G., Jabbar, F., Smith, C., Devleesschauwer, B. and Griffiths, P. 2019. Estimation of the worldwide seroprevalence of cytomegalovirus: A systematic review and meta-analysis. *Rev Med Virol*. **29**(3), pe2034.